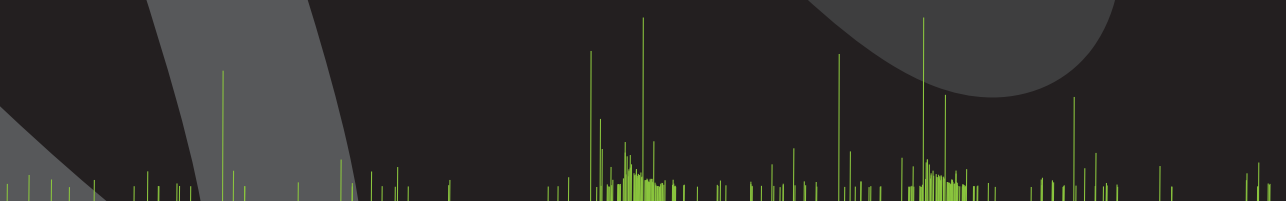


Biosensing Bioactive Contaminants

*Assay Development and Hyphenation
with Mass Spectrometry*

Gerardo R. Marchesini



Biosensing Bioactive Contaminants

Assay Development and Hyphenation with
Mass Spectrometry

Biosensing Bioactive Contaminants.

Assay Development and Hyphenation with
Mass Spectrometry

Gerardo R. Marchesini



The financial support for the publication of this thesis is gratefully acknowledged to Rikilt Institute of Food Safety, the Vrije Universiteit, GE Healthcare and Elti Support VOF.

Printed by Ponsen and Looijen b.v.

The cover was designed by Diego Camiletti and Gerardo Marchesini

VRIJE UNIVERSITEIT

Biosensing Bioactive Contaminants

Assay Development and Hyphenation with
Mass Spectrometry

ACADEMISCH PROEFSCHRIFT

ter verkrijging van de graad Doctor aan
de Vrije Universiteit Amsterdam,
op gezag van de rector magnificus
prof.dr. L.M. Bouter,
in het openbaar te verdedigen
ten overstaan van de promotiecommissie
van de faculteit der Exacte Wetenschappen
op woensdag 29 oktober 2008 om 10.45 uur
in de aula van de universiteit,
De Boelelaan 1105

door
Gerardo Raul Marchesini
geboren te Villa Allende, Cordoba, Argentinië

promotoren: prof.dr. H. Irth
prof.dr. M.W.F. Nielen

copromotor: dr. E.P. Meulenberg

Leescommissie:

prof.dr. A.A. Bergwerff

prof.dr. J. de Boer

prof.dr. C. Elliot

W. Haasnoot

dr. M. Honing

The research described in this thesis was carried out in the Biomolecular Detection Group of the RIKILT Institute of Food Safety, Wageningen UR.

Contents

Chapter 1. General Introduction p. 9

Part I. Surface Plasmon Resonance (SPR)-based Biosensor Screening Assays

Chapter 2. Biosensor immunoassays for the detection of bisphenol A p. 51

Chapter 3. Biosensor recognition of thyroid-disrupting chemicals using transport proteins p. 73

Chapter 4. Biosensor discovery of thyroxine transport disrupting chemicals p. 97

Part II. Towards Simple and Portable SPR Biosensor Screening

Chapter 5. Spreeta-based biosensor assays for endocrine disruptors p. 131

Part III. Strategies for Coupling SPR Biosensor Screening with Liquid Chromatography Electrospray Time-of-Flight Mass Spectrometry Identification

Chapter 6. Dual biosensor immunoassay-directed identification of fluoroquinolones in chicken muscle by liquid chromatography electrospray time-of-flight mass spectrometry. p. 153

Chapter 7.	Nanoscale affinity chip interface for coupling inhibition SPR immunosensor screening with nano-LC TOF MS	p. 178
------------	--	--------

Part IV. Summary, Conclusions and Future Perspectives

Chapter 8.	Summary, Conclusions and Future Perspectives	p. 207
------------	--	--------

	Samenvatting	p. 219
--	--------------	--------

Appendices

List of Publications	p. 225
----------------------	--------

About the Author	p. 227
------------------	--------

Acknowledgments	p. 229
-----------------	--------

Chapter 1

General Introduction



Part I. Bioactive Contaminants

The analytes researched in this study can all be considered as environmental and/or food contaminants and are divided in groups based on their origin. The first group of analytes consists of chemicals derived from an industrial source (industrial contaminants) that enter the food chain through the environment or from their use in household products. The second group includes chemicals used for pharmacological purposes (pharmaceutical contaminants) entering the food chain through contaminated drinking water or as drug residues in treated livestock.

Industrial Contaminants

The chemical industry produces an ever-increasing variety and quantity of chemical substances to satisfy the needs of our society. Either accidentally or deliberately, some of these chemicals might wind up in the wrong compartment of the ecosystem contaminating the soil, the surface water or the atmosphere with detrimental effects to the organisms living in these compartments. The concentration of some of these chemicals in living organisms might be biomagnified downstream the food chain in species of higher hierarchy, depending on their toxicity and persistence.

Xenobiotics are considered those man-made chemical contaminants that are present in an organism as a consequence of an external agent but which are not normally produced by the organism, or expected to be present. A source of human exposure to xenobiotics is the leaking of chemicals present in household products. For instance, bisphenol A (BPA), a monomer used for the production of epoxy coatings and polycarbonate applied in plastic containers, migrates to food [1, 2]. Due to the widespread use of BPA, its global production reached 2.7 million tons/year in 2003 [3]. In consequence, BPA is an ubiquitous environmental contaminant mainly present in raw sewage or wastewater effluents up to ppb ($\mu\text{g L}^{-1}$) concentrations [4], and at ppt (ng L^{-1}) levels in surface water and sediments [5-8]

Many industrial xenobiotics are bioactive by having hormonal activity and might disrupt the normal functioning of the endocrine system of wildlife or humans. These compounds are considered "endocrine disrupting chemicals" (EDCs) if they mimic or antagonize the effects of endogenous hormones or if they are able to disrupt the synthesis or

metabolism of endogenous hormones and hormone receptors [9]. The “endocrine disruptor hypothesis” surged in the late 1980’s from observations of Colborn et. al, of environmental contaminants affecting the endocrine system of wildlife and laboratory animals [10]. These observations were a continuation of the environmental awareness that arose from the work of Dr. Carson about the danger of pesticides and pollution of the environment by chemical industries [11].

EDCs are not exclusively industrial contaminants, but also some pharmaceuticals or agrochemicals, nevertheless, all the EDCs analyzed in this thesis are of industrial sources and their mechanism of action will be discussed in this section. EDCs can be classified according to the system they disrupt (the endocrine homeostasis system), i.e. the estrogen (structure of the 17 β -estradiol hormone in Figure 1A), the androgen or the thyroid system (structure of Thyroxine (T4) and Triiodothyronine (T3) in Figure 1A).

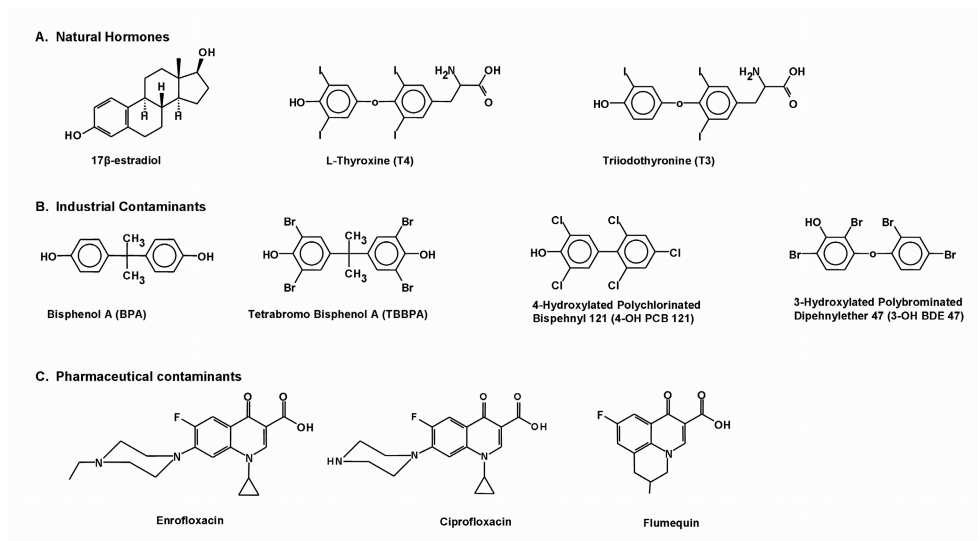


Figure 1. Chemical structures of: (A) Natural hormones of the endocrine system. (B) Industrial contaminants disrupting the endocrine system. (C) Fluoroquinolone antibiotics considered pharmaceutical contaminants.

Within each system, the EDCs might interfere at different levels of the hormone’s pathway, i.e. at the nuclear receptor, at the transport during cellular uptake, at the transport from the gland to the tissues (transport protein) and the metabolism. However, EDCs can be promiscuous across

levels within a system and even between distinct systems [12]. One example is again BPA (Structure in Figure 1B), which is considered a weak estrogenic substance linked to effects on the reproductive system because it binds to the estrogen receptor similar to 17 β -estradiol and may induce a decrease of sperm quality in humans [13-16]. BPA not only mimics estrogens it also mimics thyroid hormone action as an antagonist in some organisms [17-20].

Many polyhalogenated aromatic hydrocarbons (PHAHs) are industrial contaminants considered as EDCs (structures shown in Figure 1B). PHAHs can become hydroxylated in vivo by the cytochrome P450 monooxygenase system [21]. Polychlorinated biphenyls (PCBs) are a group of PHAHs that are highly persistent and bioaccumulate in lipid tissues. The hydroxylated metabolites of PCBs (Figure 1B) display a high degree of structural resemblance to the thyroid hormone, thyroxine (T4) (Figure 1A). An even closer structural resemblance to T4 is shown by metabolites of the flame retardants (Figure 1B), widely used in household. Flame retardants such as tetrabromobisphenol A (TBBPA) (Figure 1B) and polybrominated diphenyl ethers (PBDEs) are extensively used in plastics, electrical components and synthetic textiles. Therefore humans are in continuous contact with compounds that structurally resemble T4. For instance, PBDEs have been measured in human adipose tissues from New York City inhabitants at concentrations up to two orders of magnitude greater than those reported in European countries [22, 23].

T4 and its biologically active metabolite, triiodothyronine (T3), are essential for the modulation of the cellular metabolic rate and for the development and differentiation of several organs, especially the brain [24, 25]. The thyroid gland produces and releases T4 in response to the thyroid-stimulating hormone (TSH) released by the pituitary. Once T4 enters the blood stream it is bound to transport proteins (TP) and distributed to the target tissues. Thyroxine binding globulin (TBG) is the major T4 TP in human plasma and is responsible for 75% of the specific T4 binding activity. TBG has been linked to facilitate the iodine supply to the fetus that initially has no iodine reserve [26]. Transthyretin (TTR) is the second TP carrying about 20% of T4 and is important for maternal to fetal transport of thyroid hormones and for delivery of T4 across the brain barrier [27]. Finally, human serum albumin (HSA) is the third TP carrying about 5% of the total T4. These three TPs form a comprehensive T4 buffer system because they circulate in the blood stream differing more than three orders of magnitude in concentration

(TBG 0.27 μM , TTR 4.6 μM and HSA 640 μM) and have an even larger difference in affinity for T4 [26]. When T4 reaches a target tissue in the T4-TP complex, it is specifically transported through the cell membrane into the intracellular compartment and deiodinated to the biologically active T3 metabolite in different tissues [28]. Once inside the cell, T3 is non-specifically transported to the nucleus where it exerts its action by binding to the nuclear thyroid receptors.

Several industrial contaminants resembling T4 have been shown to interfere at different levels with the thyroid pathway (for review see [29]). Hydroxylated PHAHs interact at the T4 transport level binding TTR with high affinity [30, 31] and some of them, albeit with much lower affinity, interact with TBG [32, 33]. Displacement of T4 from its TP complex during the developmental stage could have consequences in fetal development and later in adulthood [34-36]. Therefore, the presence and bioaccumulation of these bioactive chemicals in the food chain and consequently in humans is a cause of health concern and there is a rising need for high throughput screening methods for chemicals affecting the thyroid system at different levels.

Pharmaceutical Contaminants

The pharmaceutical xenobiotics, are chemicals of concern because they might either be EDCs (i.e. from hormonal replacement therapies), like the industrial xenobiotics, or because they might cause adverse health effects when consumed without a specific need. Pharmaceuticals might contaminate surface waters and affect wildlife as a consequence of the treatment of humans and livestock and a poor or inefficient drug residues removal by sewage water treatment plants [37, 38]. Wildlife might be directly contaminated with pharmaceuticals at measurable levels if it feeds from treated livestock [39].

A specific example of pharmaceutical contaminants affecting humans are the antibiotics. Antibiotics are considered xenobiotics, but are essential to cure bacterial-related diseases. Farmers often apply antibiotics to livestock to handle specific diseases or as growth promoters [40, 41]. Unfortunately, the continuous exposure of bacteria to antibiotics generates antibiotic-resistant strains that might cause bacterial infections to the consumers exposed [40]. Because the profitability of livestock is often hampered by infectious diseases, the use of veterinary antibacterial drugs is expected, not only for treatment, but also for prophylaxis. This practice might lead to the acquisition of methicillin-

resistant *Staphylococcus aureus* (MRSA) by farmers and their communities [42]. As a matter of fact, the presence of antibiotics in livestock not only raises the concern of antibiotic resistant bacterial strains [43-45], but also, about the occurrence of allergic reactions in consumers [46].

Fluoroquinolones (FQs) (structures shown in Figure 1C) one group of antibiotics that target the DNA gyrase in gram-negative bacteria and probably topoisomerase IV in gram-positive bacteria leading to inhibition of DNA replication and cell death [47]. FQs have widespread use for infection treatment, as well as a prophylactic and as growth promoters in farmed fish, turkeys, pigs, calves and poultry [48, 49].

Consequently, there is a rising need for rapid, robust, multi residue screening methods complying with EC Council Directive 96/23/EC that establishes the need of a residue monitoring plan for these and other groups of substances by the EU member countries for these pharmaceuticals and their metabolites [43]. The diversity of commonly used pharmaceuticals poses a great analytical challenge to their detection due to the different matrices in which they are usually present.

Part II. Biosensor Screening

Classical analytical chemistry separation methods like liquid or gas chromatography (LC or GC) coupled with a spectrometric detector like ultra violet (UV) absorbance, fluorescence emission or mass spectrometry (MS) provide information about the presence and the structure of the bioactive contaminants described above. Nevertheless, the detection is based only on the chemical and physical properties of the analyte(s). Hence, these methods are usually unable to generate information about on the biological effects of the analytes. Furthermore, analyzing the diversity of chemicals in complex food and environmental samples with classical analytical techniques requires considerable time and specialized human resources. These issues not only limit the number of samples that can be analyzed with classical analytical techniques, they also restrict the possibility of making cost-effective monitoring programmes and are slow to adapt to the market-driven evolution of the analytes if compared with other bioassays featuring a selectivity based on the biological activity of the analyte(s).

An interesting alternative is the use of low-cost biosensors for the screening process and subsequently, to focus the analytical efforts only

on the suspected non compliant samples. The specificity of the biosensor assays for the bioactive contaminants can be tailored depending on the biomolecule used as biorecognition element. The incorporation of effect-related biomolecules (i.e. receptors, transport proteins, etc) provides a further advantage, since it allows the screening of known bioactive compounds and the detection of emerging ones sharing a similar biological endpoint. In this study, the application of biosensors for the screening of different bioactive contaminants is evaluated and the following section describes background information of the biosensor screening technology.

History of Screening Methods

One of the first biomolecule-based screening methods was a radioimmunoassay (RIA) for the detection of insulin which was published in 1960 by R.S. Yalow [50] and was awarded in 1977 with the Nobel Prize of Physiology. In this RIA, a known amount of free radiolabeled analyte is mixed with the sample and an antibody previously raised against the analyte (the antigen). The analyte in the sample and the radiolabeled analyte compete for binding to the antibody, the bound and unbound fractions are separated and the amount of free radiolabeled analyte is proportional to the amount of analyte in the sample. Although this method is still used and is very sensitive, the handling of radioisotopes requires strict safety conditions and an alternative method was sought. The radioisotope label was replaced by an enzyme catalyzing a reaction that can be monitored using simple colorimetric techniques leading to the widely used enzyme-linked immunosorbent assay (ELISA) [51, 52]. The relative simplicity with which an antibody can be raised against virtually any type of antigen has made ELISAs the most commonly used screening method.

Further developments of immunochemical screening methods led to the use of fluorescent [53], electrochemical and chemiluminescent [54] labels to amplify the signal and obtain a higher sensitivity. The binding partners in these methods are not restricted to antibody-antigen interactions, any other couple of binding partners is feasible, like receptor-ligand, binding protein-ligand, DNA-DNA, RNA-DNA, DNA-receptor, etc. The forces governing the interactions of binding partners will be discussed in detail in the next section. Biosensor technology is based on these biological molecules integrated with a transducer that is sensitive to the generation of a signal in response to a biochemical

reaction or a binding event. The different components and types of biosensors will be presented later in this introduction.

Biomolecular Binding Forces

An antibody binds to an antigen or a receptor to a ligand forming a supramolecular complex driven by non-covalent intermolecular forces. These forces are individually weak, but given the large number of possible interactions with a biomolecule, they are collectively strong. Intermolecular forces include electrostatic interactions (like dipole-dipole interactions, hydrogen bonds and ionic interactions), hydrophobic interactions as well as van der Waals forces. The first subset of electrostatic interactions are forces between dipoles. Highly polar molecules, like the polar amine and carbonyl groups of the polypeptide backbone of proteins, lead to permanent dipoles. Dipoles can either attract or repel each other and they play an important role in protein structure. The hydrogen bonds are a type of dipole-dipole interactions that occur between a hydrogen atom bonded to an electronegative atom and an unbound pair of electrons in a highly electronegative atom like an amine and a carbonyl group. The sharing of the electrons is unequal for the hydrogen and creates a partially positive charge that is attracted to the partially negative charge in the carbonyl group. Electrostatic interactions in an aqueous solution contribute to the binding strength and intermolecular stabilization [55, 56]. The ionic interaction or ionic bonds are based on the electrostatic attraction between charged molecules of opposite sign (ions).

Hydrophobic interactions are repulsive forces that occur between non-polar molecules and polar molecules like water. The non-polar regions of the molecule interfere with the hydrogen bonding of the solvent and tend to cluster together repelling the polar solvent (usually water) to attain a more favorable energy level. The strength of the hydrophobic interactions results from the system achieving thermodynamic stability by minimizing the number of ordered water molecules required to surround the hydrophobic portions. Hydrophobic interactions at the binding site play an important role in the binding strength and stabilize the intermolecular complex [57].

Van der Waals forces are weaker than the dipole-dipole interactions and are the consequence of random variations in the positions of electrons around one nucleus. This creates a transient electric dipole that induces an equally transient but opposite dipole in a nearby atom. These

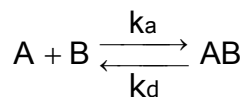
transient dipoles attract each other until their electron clouds start to repel.

The interaction of an antigen with an antibody, an enzyme with its substrate or a receptor with its ligand may involve several hydrogen bonds, one or more ionic, hydrophobic and van der Waals interactions. The cumulative effect of all these weak interactions is enormous and is responsible for the high affinity, complementarity, flexibility and reversibility that interacting biomolecules exhibit. A characteristic binding site contains a hydrophobic pocket lined with charged groups and hydrogen bond donors and acceptors. Upon collision, mainly the electrostatic forces of the binding site interact with the dipoles of the antigen aligning and pulling both molecules together. The other forces provide supplementary attraction and stabilization of the complex [57, 58]. Opposed to the attraction forces, are the repulsive forces due to steric hindrance. These forces are minimized as the complementation between interactants increases.

Binding Kinetics

The kinetics of the biomolecular binding interactions in solution can be described by:

(1)



Where the equilibrium constant or affinity K , between reactant A and B for the formation of the supramolecular structure AB is given by:

(2)

$$K = \frac{[AB]}{[A][B]} = \frac{k_a}{k_d}$$

Being k_a and k_d respectively the association and dissociation rate constants. The equilibrium dissociation constant or K_D , is the inverse of K . In solution, k_a is affected by the diffusion of reactants and the collision probability. k_d is influenced by the strength and stability of the binding interaction, as well as the thermal energy available compared to the activation energy needed to break the interactions.

Biosensors

The beginning of the biosensor technology dates back to 1956 when Clark and Lyons invented the oxygen electrode. In 1962 they presented their work on the integration of the oxygen electrode with the enzyme glucose oxidase using a dialysis membrane [59]. The decrease in measured oxygen concentration was proportional to the glucose concentration in solution. This was the beginning of the successful in-home glucose biosensor still used nowadays for monitoring blood glucose levels [60].

Biosensors are classified based on the biological sensing element used, such as antibody, enzyme, receptor or cell and based on the transducer in contact with the biological element such as an electrode (electrochemical potentiometric and amperometric sensors), piezoelectric acoustic, and optical sensors. The sensitivity of the transducer to selectively transform a parameter of the biological element-analyte reaction into a quantifiable electrical signal is crucial for the biosensor performance. The specificity of a biosensor is given by the properties of the biological sensing element per se. A short description of the various types of biosensors will be presented below. Special emphasis will be given to surface plasmon resonance-based optical biosensors since they are the focus of the present study.

Electrochemical biosensors are usually based on the detection of an ion product of the specific catalytic power given by an enzyme immobilized at a working electrode. There are potentiometric and amperometric biosensors. The potentiometric sensors measure a change in potential between an ion selective electrode and a reference electrode with no current flow. The amperometric biosensors measure the current produced by the oxidation or reduction of an electro active compound at an electrode when a potential is constantly applied with respect to a counter electrode. The oxidation or reduction of the analyte (or an enzymatic product) proceeds at the working electrode. The current generated is proportional to the oxidation or reduction rate, which is proportional to the analyte concentration [61]. The glucose biosensor mentioned before is amperometric and measures either the hydrogen peroxide produced or the oxygen consumed by the glucose oxidase immobilized on the electrode surface. When the analyte is not susceptible to enzymatic breakdown into electroactive species, an enzyme label like horseradish peroxidase or alkaline phosphatase can be used in combination with a specific biorecognition molecule [62].

Piezoelectric biosensors are based on the principle that a crystal oscillates at a specific frequency upon the application of an alternating electric field. A change in mass on the surface of the crystal (i.e. when an antibody binds to a derivatized surface) is measured from the shift of the resonating frequency, wave velocity or amplitude of the oscillating crystal [63].

Optical Biosensors

Optical biosensors are popular devices used for bioanalysis and offer the largest group of transducers. Numerous applications are described in literature using either fluorescent, bioluminescent or chemiluminescent labels for detection, as well as the direct (label-free) detection of analytes on a surface using ellipsometric biosensors, total internal reflection spectroscopy (TIRS) and surface plasmon resonance (SPR)-based biosensors. If linearly polarized light is reflected from a planar surface, the light is elliptically polarized. This principle is exploited by the ellipsometric optical biosensors that are able to monitor adsorption of biomolecules to a planar surface (as changes in refractive index and biomolecular layer thickness) by measuring a change in phase and amplitude of the reflected light [64]. A drawback of this configuration is that the light has to penetrate the liquid carrying the sample and the reagents, making the sensitivity of this configuration very susceptible to scattering by particles or air bubbles. On the contrary, evanescent wave (EW)-based biosensors only probe a small volume of liquid around the sensing area and the light path can be outside the bulk sample [64]. To better clarify the principle of EW-based biosensors, some optical properties will be discussed. When light travels from a medium with a high refractive index (n_1) to one with a lower refractive index (n_2), the light beam will be partially reflected at the boundary surface, and partially refracted according to Snell's law (see Figure 2.).

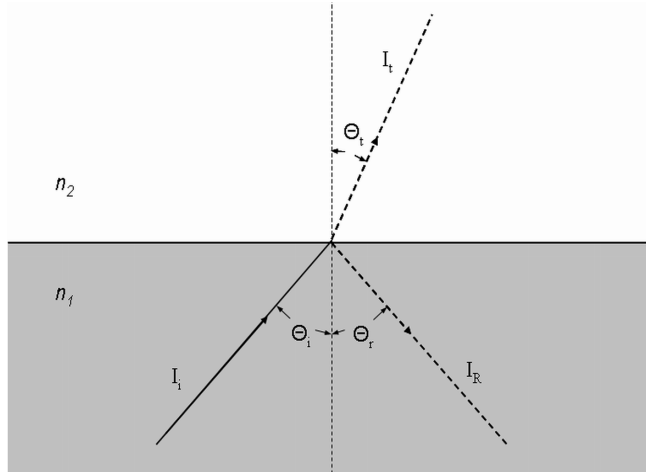


Figure 2. Refraction and reflection of light at the surface of two dielectrics. (I , n , Θ are explained in the text)

An incident light beam of intensity I_i striking the interface of two dielectric materials with different refractive index (n) is reflected or refracted with an angle (Θ)

(3)

$$n_1 \sin\Theta_i = n_2 \sin\Theta_t$$

n_1 and n_2 being the refractive indices of the materials, Θ_i the angle of the incident light and Θ_t , the angle of the refracted light. Total internal reflection (TIR) of the incident light occurs if Θ_i is above the critical angle (Θ_{iCr}) and according to Snell's law for Θ_t of 90° (4).

(4)

$$\Theta_{iCr} = \sin^{-1}\left(\frac{n_2}{n_1}\right)$$

Interestingly, when TIR occurs, an electromagnetic field component called the evanescent wave (EW) penetrates into the medium with a lower refractive index and it decays exponentially with the penetration depth.

The penetration depth of the EW is defined as the distance from the interface where it decays to 1/e of its value at the interface [65]. The penetration depth is described by:

(5)

$$d_p = \frac{\lambda}{2\pi\sqrt{(n_1^2 \sin^2 \theta_i - n_2^2)}}$$

where, λ is the wavelength of light, θ_i the angle of incidence and n_1 and n_2 the refractive indices of the materials [66]. The penetration depth is strongly dependent on the wavelength that can range from 50 nm to 1000 nm for visible light.

Different features of the EW phenomenon can be measured to exploit it in a biosensor setup. First, when a UV-visible chromophore absorbs light within the EW, the change in UV light intensity passed through a waveguide or optical fibre can be monitored. Although simple, this setup lacks sensitivity due to the small percentage of the light beam that actually interacts with the chromophore in the form of EW [67]. Another option is the utilization of the EW for exciting fluorophores. By monitoring the fluorescence generated at the waveguide interface, powerful total internal reflection fluorescence (TIRF) biosensors were developed [67-69] reaching femtomolar sensitivity [70]. The common limitations of TIRF-based biosensors are the difficulty of labeling the reagents and fluorescence quenching due to matrix effects. The third possibility is to excite surface plasmons to measure refractive index changes at a dielectric-metal interface. The latter phenomenon is called surface plasmon resonance and, because of its application throughout this study, it will be discussed in detail.

Surface Plasmon Resonance Biosensors

The beginning of SPR-based biosensors goes back to 1902, when Wood observed an anomaly in the absorption bands of polarized light reflected from a metal grating [71]. In 1941, Fano concluded that these anomalies were linked to surface plasma waves (SPW) of the grating [72]. SPW are electromagnetic waves propagating at the surface through the collective motion of large numbers of excited metal electrons. In 1968 Otto [73], Kretschman and Raether [74] pioneered with the configurations used to excite SPW. When a metal film is placed

at the dielectric interface, light in the form of EW arising from TIR can be coupled to a SPW. In the Otto configuration, the light goes through the high refractive index prism and TIR occurs at the prism-dielectric interface generating an EW. A metal layer, separated from the prism by a dielectric layer of correct thickness, contains surface plasmons that can couple to the EW [73] to generate SPR.

The outcome of such coupling is the reduction of the intensity of the reflected light. The incident light angle at which this reduction ("shadow") occurs is called the SPR angle. Since the waves are on the boundary of the metal and the external medium (air or water), the plasmon oscillations, and as a consequence the SPR angle, are very sensitive to any change of this boundary, such as the adsorption of molecules to the metal surface. A plot of the SPR angle against time (the sensorgram) displays the progress of the interaction at the sensor surface.

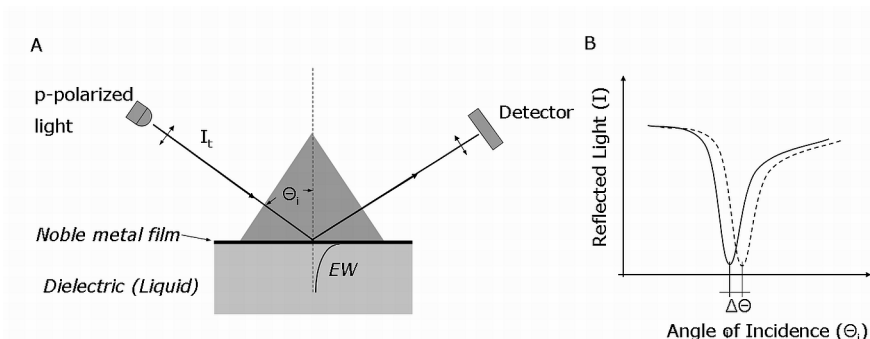


Figure 3. (A) Kretschmann configuration used in surface plasmon resonance spectrometry (B) Shift in the optimum angle of incidence to generate SPR (SPR dip minimum shift).

Most of the commercially available SPR biosensors are based on the Kretschmann configuration (Figure 3A). Where the EW penetrates through a thin gold film (≈ 50 nm) and couples with the surface plasmons at the outer boundary of the gold film, at the metal-dielectric interface [75, 76].

A metal surface contains free electrons (surface plasmons) that collectively oscillate creating an SPW. The SPW propagates along a metal dielectric interface and generates an asymmetric electromagnetic field that extends into both the metal and mostly in to the dielectric

medium ($\approx 90\%$) that decays exponentially and perpendicular to the propagation direction. The permittivity (ϵ) of a material describes how it is affected or affects an electric field and is expressed in complex numbers. A SPW propagates if the real part of the metal permittivity (ϵ_m) is negative and its absolute value is smaller than the permittivity of the dielectric (ϵ_d) [65]. Several metals fulfill this condition; however gold and silver are commonly used in SPR sensors.

The propagation constant (β) of a SPW along a thin metal film is described by

(6)

$$\beta^{\text{SPW}} = \frac{\omega}{c} \sqrt{\frac{\epsilon_d \epsilon_m}{\epsilon_d + \epsilon_m}} + \Delta\beta$$

where, ω is the angular frequency, c is the velocity of light in vacuum and $\Delta\beta$ accounts for finite thickness of the metal film and the presence of the prism. From Eq. 6, we observe that β^{SPW} is influenced by the dielectric present on the opposite side of the metal film and β^{SPW} changes if ϵ_d is perturbed.

The propagation constant of light in the form of EW at the dielectric-metal interface is defined as

(7)

$$\beta^{\text{EW}} = \frac{\omega}{c} n_p \sin\theta_i$$

where, n_p is the refractive index of the prism. Surface plasmon resonance occurs when a metal surface at a dielectric interface is illuminated with p-polarized light (or transverse magnetic (TM)-polarized light) through a prism and the light's wave vector parallel to the interface (or β^{EW}) matches that of the SPW. The prism, of high refractive index, is used as a coupler to enhance the light's wave vector [65].

In other words, surface plasmon resonance occurs when:

(8)

$$\beta^{\text{EW}} = \beta^{\text{SPW}}$$

Hence, from Eq. 6 and 7:

(9)

$$n_p \sin \theta_i = \sqrt{\frac{\epsilon_d \epsilon_m}{\epsilon_d + \epsilon_m}} + \Delta\beta$$

If this pre-requisite is fulfilled, at a certain angle of incident light the energy is transferred to the metal in the form of resonating plasmons (when the light's wave vector couples with the SPW) and is not reflected. From eq 8. it is obvious that if the permittivity of the dielectric is perturbed (i.e. due to a change in refractive index) on the right side of the equation, then a new angle of incident light will be required to generate SPR. An increase of the concentration of biomolecules within the EW influences the refractive index of the dielectric and hence its permittivity (see Eq. 8.)

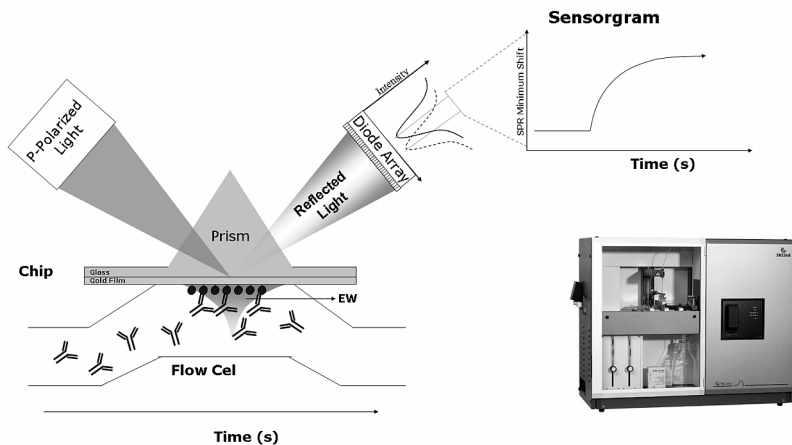


Figure 4. Schematic view of a Biacore system setup.

When the reflected light intensity is plotted against the angle of incidence, SPR is evidenced as a sharp dip when the reflected light intensity shows a minimum at a certain angle of incidence (Figure 3B). If a change in refractive index within the EW occurs within the small volume of the dielectric probed by the EW volume, it is observed in the

attenuated total reflection (ATR) method described here as a shift in the SPR dip minimum (Figure 3B, dotted line). Tracking the change in the incident angle of light ($\Delta\theta$) by means of the SPR dip minimum over time, provides a parameter that is linearly correlated to changes in refractive index of the dielectric (usually a fluid) within the EW. The width and depth of the SPR dip depends on the type and thickness of the metal film used and the incident light wavelength. Silver yields narrower dips than gold increasing the signal to noise ratio but is easily oxidized. Therefore, most biosensors use a thin gold film. The use of stacked heterogeneous metallic layers is a promising technique to improve the signal to noise ratio and the sensitivity [77].

SPR sensors where the angle of incident light is modulated are classified as SPR sensors with angular modulation. Other SPR sensor setups use the light's wavelength, intensity and phase modulation to generate SPR. Three SPR biosensor systems based on prism couplers and angular modulation will be used throughout this thesis, two Biacore systems (models 3000 and Q) based on the same setup and a Spreeta 2K optical integrated SPR unit from Texas Instruments.

The Biacore systems were first introduced in 1991 [78]. These systems are based on collimated and focused, wedge-shaped, beams of p-polarized light that strike a gold film through a prism in four sensing areas (Figure 4). The angular spectrum of each sensing area is reflected on a linear diode array where the light intensity is measured.

The biosensor signal output is calculated from the shift of the angle of incident light at which the SPR dip occurs. This shift plotted against time provides a real time sensorgram of the refractive index in the area probed by the EW. When biomolecules like antibodies interact with antigens immobilized on the sensor surface, there is change in local refractive index of the area probed by the EW.

On the opposite side of the gold film, the microfluidic system features four serially connected flow cells (or channels). These flow channels (Fc) allow the system to run spatially-resolved immobilizations and assays (only in Biacore 3000) on the same sensor chip. Each Fc has an area of 1.2 mm^2 , heights of $20 \text{ }\mu\text{m}$ (Biacore 3000) or $50 \text{ }\mu\text{m}$ (Biacore Q) and volumes of 0.02 (Biacore 3000) and $0.06 \text{ }\mu\text{L}$ (Biacore Q).

The Spreeta SPR sensor (Figure 5) is an integrated optical unit [79]. The light from a LED is p-polarized and strikes a tilted gold film through a prism. The tilting of the gold film relative to the light source provides a continuous change in the angle of incident light. The angular spectrum of light is reflected to a mirror and finally to a photodiode array where

General Introduction

the light intensity is measured. The biosensor signal output is also calculated from the shift in the SPR angle and resembles the Biacore systems.

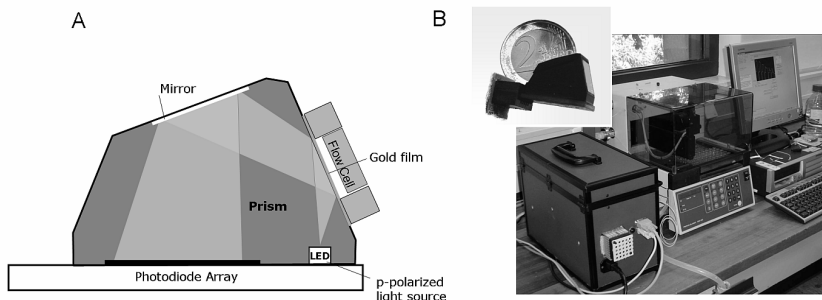


Figure 5. Cross section of the Spreeta 2K integrated optical unit with a flow cell. (B) Experimental Spreeta SPR biosensor system (portable box) connected to an autoinjector. The size of the optical unit is comparable to a medium size coin (insert).

The sensitivity of SPR sensors with angular modulation depends on the magnitude of the incident angle shift, elicited by a change in refractive index within the EW, usually in the order of 50-100 degrees/refractive index unit (RIU). It also depends on the optical properties of the prism, the properties of the metal film containing the SPW and the wavelength used [80].

The resolution is defined as the smallest change in refractive index that produces a detectable sensor output [76]. Therefore it is highly influenced by the level of noise that originates mainly from the intensity of the light emitted in the optical system and the electronics. The angular spectrum of light intensities obtained by the diode array is mathematically processed to reduce noise. Usually, the spectra are normalized and time-averaged. The algorithm used to calculate the sensor output also influences the noise. The maximum resolution achieved with SPR biosensors based on angular modulation is in the order of 3×10^{-7} RIU [81]. Finally, the presence of reference channels (in Biacore 3000) and a post-measurement subtraction of the specific and non specific signals (i.e. bulk refractive index changes during measurement) further reduces the noise and increases the resolution allowing the direct measurement of small molecules (i.e. below 1 KDa) [82].

Sensor Chips

A crucial part of SPR biosensors is the surface chemistry on the sensor chip for covalent attachment of either the biorecognition element or its ligand, depending on the assay format required. The highly hydrophobic gold film is usually derivatized with a self-assembled monolayer of alkanethiols with suitable reactive groups for immobilizing a monolayer of one of the binding partners [83]. This layer yields a limited amount of molecules within the EW resulting in a limited biosensor signal output. A recent application of this type of chip surface is for the capture of lipid monolayers and the study of the interaction between molecules and membrane surfaces (for review see [84]). A hydrogel matrix can be immobilized on the gold surface, in order to increase the volumetric density of the binding partners within the EW. Usually a layer of carboxymethylated dextran (CMD) is immobilized on the chip by means of a previously covalently linked monolayer of long-chain hydroxyalkyl thiols to the gold surface [85]. The CMD forms a thin layer of about 100-200 nm thick [86]. Variations in the length, number of carboxyl groups (charge) and porosity (crosslinking degree) of the CMD are commercially available [87, 88]. Alternatively, there are nitriloacetic acid chips based on metal chelation for the capture of polyhistidine tagged proteins and chips with streptavidin for the capture of biotinylated biomolecules [88]. The chip surface properties should also be considered when designing a biosensor assay since its non-specific affinity towards components of the sample matrix will influence the assays performance and determine the applicability of the assay. Molecules containing an amine group can be covalently immobilized to CMD chip surfaces. In these cases the carboxyl groups on the surface are activated using a mixture of 1-ethyl-3-(3-dimethylaminopropyl) carbodiimide (EDC) and N-hydroxysuccinimide (NHS) followed by an exposure of the activated CMD surface to the molecule at the appropriate pH. The coupling reaction requires uncharged amino groups on the ligand and is therefore favored by high pH. A bifunctional linker (ethylenediamine) is typically used to immobilize molecules bearing a carboxyl group. More coupling chemistries are available (for instance the thiol-disulphide exchange or the aldehyde coupling) which are not within the scope of this study.

Biorecognition Elements

The biorecognition molecules in SPR biosensor assays are usually biomacromolecules varying from a few kDa to 800 kDa depending on their nature. Antibodies are the most common biorecognition molecules in SPR biosensor assays.

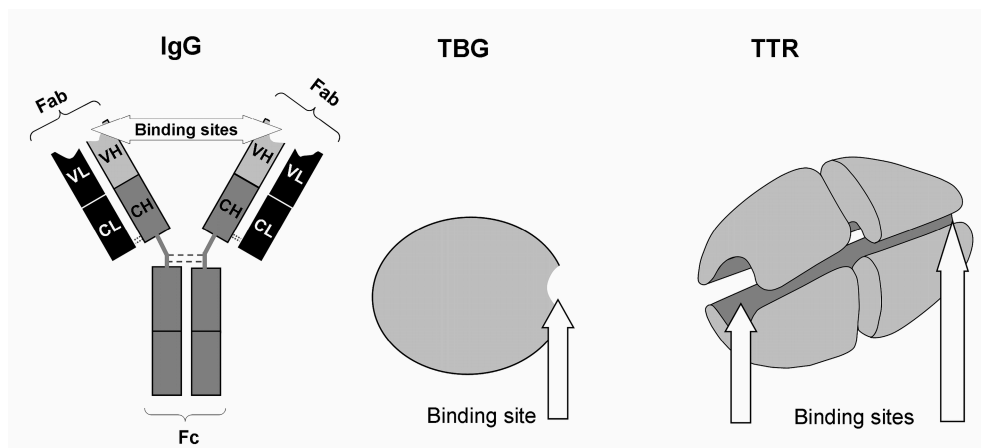


Figure 6. Biorecognition elements used in this study. Immunoglobulin G (IgG), Thyroxine Binding Globulin (TBG) and Transthyretin (TTR).

Antibodies belong to the family of macromolecules known as immunoglobulins which are present at $12\text{--}15\text{ mg ml}^{-1}$ in blood serum, amounting to nearly one fifth of its total protein content. There are five immunoglobulin classes known in mammals, IgG, IgM, IgA, IgD and IgE with molecular masses ranging from 150,000 to 970,000 Da. IgG represents 70% of the serum immunoglobulins and constitutes the majority of the secondary immunological response to most antigens. IgG molecules have three domains (two Fab domains and one Fc domain) (Figure 6). The Fab domains (fragment that carries the antigen binding site) form the arms of the Y shape and are identical which makes IgG molecules bivalent. The domain that is involved in immune regulation is termed Fc fragment (for the fragment that crystallizes) and forms the base of the Y structure. The two heavy (H)-chain polypeptides (each 440 amino acids [approximately 55,000 Da]) and the two light (L)-chains (each about 220 amino acids [about 25,000 Da]) are identical. One L-chain associates with the amino-terminal region of one H-chain to form an antigen-binding site. The carboxy-terminal regions of the two H-

chains fold together to form the Fc domain. The four polypeptide chains are held together by disulphide bridges and noncovalent bonds. L-chains can be divided into two regions, the variable (VL) and the constant (CL) region (each about 110 amino acids in length). H-chains can be divided in two regions, a variable (VH) and a constant (CH) region. The V regions (located at the amino end) of one H-chain and one L-chain combine to form one antigen binding site. The heterogeneity in the V regions of both L- and H-chains confer the capability to respond to a very large number of antigens [89], allowing mammals to generate an immune response with a diversity of up to 10^5 - 10^6 different antibodies.

Small molecules of less than a few thousand Da, such as most of the bioactive contaminants relevant in the present study, are not immunogenic. Hence, for the production of antibodies the analyte must be covalently conjugated to a large carrier protein. The nature and position of this conjugation has a direct effect on the properties of the resulting antibodies. In general, the best chances of producing high quality antibodies result from a linkage of the analyte producing the minimum perturbation of the three dimensional structural conformation and the electric properties [90]. In principle, the specificity of antibodies against substances of low molecular mass is mainly determined by the choice of the coupling site. Usually the part of the molecule that is opposite to the coupling site acts as the immunodominant portion of the hapten-protein conjugate. Structural changes in the vicinity of the coupling site cannot be readily recognized by the antibody and will show less influence on the immunoreactivity.

Polyclonal (PABs), monoclonal (MAbs) and occasionally recombinant antibodies (RABs) derived from libraries are used in immunoassays [91]. RABs are a very interesting alternative that can be derived from present MAbs. RABs can be mutated to generate a library, and later selected, thus tailoring the biorecognition element for a required selectivity or resistance to specific conditions [92, 93].

In this study we have used MAbs and PABs. PABs are applied most frequently because they are cheap to prepare in host animals. However, the main drawback of using PABs is the serum batch quantity and the batch to batch variation. MAbs, in turn, are homogeneous, specific and can be produced in unlimited quantities using the hybridoma technology [94]. During the production, a specific MAb can be isolated for a unique and chosen specificity. A further advantage of hybridoma production is that impure antigens can be used to produce specific antibodies. The

limitations of hybridoma technology include the specialized cell culture facilities, extensive time, labor, expenses, as well as expertise needed to prepare and screen large numbers of hybridomas in order to select the most suitable ones. PABs as well as MABs have been shown to be sensitive, robust and specific biorecognition elements in biosensor assays. Furthermore, antibodies can even be raised to be group-specific biorecognition elements when a group of structurally related compounds has to be detected.

However, antibodies fail when a group of structurally varied chemicals like the EDCs described in Part I has to be targeted in a single assay. In this case, if the chemicals share a common biological endpoint like the binding to a receptor or a transport protein, these biomolecules can be used as biorecognition elements. These natural biorecognition elements can either be purified from their containing organism like the thyroxine binding globulin (TBG) used in this study (Figure 6) that is purified from human serum. TBG is a 54 KDa acidic glycoprotein with one external T4 binding pocket responsible for transporting 75% of serum T4 [95]. TBG is synthesized in the liver as single polypeptide chain of 415 amino acids. Alternatively, the biorecognition element can be recombinantly produced in to a foreign organism by cloning the coding DNA into a vector and transforming the most suitable organism for overexpressing the protein. Using this approach the supply of the biorecognition element is virtually unlimited and it was used by our collaborators for the production of recombinant transthyretin (TTR), a human thyroxine transport protein, used in this study [96]. TTR is a 55 KDa tetramer of identical subunits, each containing 127 amino acids [97]. The four subunits form a symmetrical β -barrel structure with a double trumpeted hydrophobic channel that traverses the molecule forming the two allosteric iodothyronine binding sites (Figure 6). Although TTR is bivalent, only one T4 molecule is usually bound because the binding affinity of the second site is greatly reduced through a negative cooperative effect [98].

Biosensor Assay Formats

Various assay formats are possible in SPR biosensors. In the direct binding assay (DBA) format, the biorecognition molecule is immobilized or captured on the chip surface and is brought into contact with the sample containing the analytes and the binding increases the refractive index at the sensor surface. The DBA format is in theory the most

sensitive [99, 100] and is widely used for fishing high molecular weight biomolecules out of complex biological matrices because the biosensor signal output depends directly on the mass of the interacting analyte. The smaller the analyte to be detected in a DBA format, the more biosensor resolution is required to detect it. Additionally, an in-line SPR referencing surface is needed to be able to subtract noise and signals from bulk responses due to minor refractive index dissimilarities of the solutions injected. If these conditions are fulfilled and with the proper experimental forethought, the DBA format is effective for the determination of kinetic parameters of low molecular weight molecules binding to antibodies or receptors [101, 102]. The DBA format has the advantage of yielding information about the analyte-biorecognition element interaction strength and kinetics. Association and dissociation rates are of special interest when dealing with non conventional biorecognition elements like receptors or transport proteins. The sandwich assay is a variation of the DBA, where secondary biorecognition molecules are introduced to enhance the signal of the bound analyte. However, sandwich assays do not work with small molecules due to the relatively large binding sites of the biomolecules.

For low molecular weight compounds the inhibition assay format is generally preferred in biosensor immunoassays (BIAs) because of its flexibility, higher response and robustness [103, 104]. In the inhibition BIA (iBIA) format the analyte, or a structural analogue, is immobilized on the sensor surface preserving its affinity for the biorecognition molecule. The sample containing the analyte is mixed with the biorecognition molecule and brought into contact with the analyte derivative or structural analogue immobilized on the sensor chip surface. The higher the concentration of analyte in the sample, the lower the number of biorecognition molecules bound to the chip surface. The signal drop due to the inhibition of the binding of the biomolecule to the immobilized analyte on the chip surface will be proportional to the analyte concentration in the sample.

The molecular mass of the analyte in this case does not influence the detection capabilities of the biosensor assay, because the refractive index change at the chip surface is generated by the biorecognition molecule. The concentration and affinity of the biorecognition molecule used in the inhibition assay ultimately influences the sensitivity of the assay.

Part III. Interfacing SPR Biosensors with MS

The SPR biosensors presented in Part II have been proposed as an alternative to traditional analytical methods on the basis of the analysis time required by analytical techniques, the cost of the equipment and the specialized human resources required for operation. Although biosensors are indeed useful tools for the biospecific determination of analytes in various matrices, the information provides no data about the analyte structure or identity. On the contrary, analytical techniques like liquid chromatography (LC), gas chromatography (GC) and capillary electrophoresis (CE) are able to separate the analytes based on their physico-chemical properties. Unequivocal structural information can be obtained if these high performance separation techniques are hyphenated with a spectrometric detection method like mass spectrometry (MS). Hence, a synergistic complement can be obtained by combining SPR biosensor technology based on molecular biorecognition events with analytical techniques based on physico-chemical properties of the analytes. The pioneering work of Moorhouse *et al.* in 1969, who added a new dimension to his GC- flame ionization detector by hyphenating the antenna of an insect as a parallel detector for the discovery of insect pheromones, marked the beginning of several successful studies coupling biosensor or other bioassay technologies with analytical techniques in the last years [105-108]. SPR biosensors in particular have been combined offline with micro preparative HPLC [109], online as a detector for IgG when using CE for separation [110], in parallel with LC-diode array detector (DAD)-MS for drug screening [111] and offline and online with MS [112].

The choice of ionization technique amenable for hyphenating with SPR biosensor technology with MS greatly depends on the characteristics of the molecule to be analyzed and on the assay format chosen to detect it. When the DBA format is chosen, the analyte is captured on the chip surface and can be eluted for further offline or online analysis. In contrast, the iBIA format the analyte interacting with the biorecognition element is usually discarded to the waste. In this case, a split flow strategy for parallel coupling of the technologies has to be implemented, or alternatively, an online strategy to purify and recover the analytes for further analysis. These two strategies are investigated in Part III of this thesis.

One common problem when coupling biosensor or bioassay technology with MS is the mobile phase compatibility. To preserve biomolecular interactions, the biorecognition element in the biosensor usually needs a suitable buffer containing salts that might interfere with the MS analysis. Additionally, nonionic detergents, also incompatible with MS analysis, are generally used in the mobile phase of biosensors to avoid nonspecific adsorption of matrix or analytes to the fluidic system. Hence, the mobile phase used in the biosensor analysis has to be carefully optimized and considered in the context of the type of hyphenation chosen [113].

Interfacing SPR-MS Using a DBA Format

Matrix-assisted laser desorption ionization - time-of-flight mass spectrometry (MALDI-TOF MS) is the most commonly used technology in combination with SPR biosensor assays. MALDI has the advantage of generating intact vapor phase ions from a solid of large molecules co-crystallized with small volatile molecules (matrix). A laser pulse initiates the desorption/ionization of the matrix simultaneously generating a packet of analyte ions. The matrix absorbs most of the laser energy, co-ionizes the analyte upon desorption and prevents its fragmentation. This gentle ionization technique allowed the mass spectrometric analysis of large macromolecules like proteins and protein complexes of megadalton masses [114, 115]. MALDI in combination with TOF MS has achieved fmol sensitivity. In a TOF MS system, the ions are accelerated at the same electrostatic potential, allowed to drift a known distance and strike a detector. The flight time of the ions will depend on their mass/charge ratio (m/z) that can be related to their masses based on the kinetic energy equation. Regardless of the sensitivity, the mass accuracy of MALDI TOF MS is in the range of 0.1-0.01% for proteins above 30 KDa, hence it cannot be considered a general method for protein identification [114]. On the other hand, the 10-50 ppm mass accuracy of MALDI TOF MS for small polypeptides, enables the identification of enzymatically digested proteins by peptide mass fingerprinting based on database search [116].

The use of MALDI TOF MS in combination with SPR has evolved from the direct on-chip analysis, yielding the chip unusable after one binding cycle [117, 118], to the elution of the analytes in a small volume between two air bubbles that is respotted onto a MALDI plate [119-122]. Further, the interfacing was improved with completely automated

commands, including those for sample preparation needed prior to MALDI [123]. The developments of imaging SPR have enabled SPR-MS array platforms for the high throughput screening of large numbers of interactants in the field of proteomics [124].

Although MALDI TOF MS has greatly improved, it is still considered unreliable for analysis of small molecular weight analytes such as the bioactive contaminants described in Part I. The main shortcoming of MALDI was its mass resolution and accuracy, with the advent of newer instrumentation the main concerns are signal reproducibility and sample preparation. The latter aspect concerns the matrix interfering with the ionization and detection of small molecules [125].

A different approach for SPR-MS analysis in a DBA format, is the elution of the captured analytes and their offline or online analysis using electrospray ionization (ESI) coupled to MS. ESI is a gentle ionization technique that produces singly or multiply charged ions in a gaseous phase directly from a liquid phase (either organic or aqueous). This makes ESI amenable for online hyphenation with other continuous-flow liquid-phase analytical techniques like liquid chromatography and biosensor technology. ESI solves in one step the transition of ions to gas phase needed for MS analysis, simplifying the interfacing if compared to MALDI, where the analytes are first brought in to a solid phase and later gasified. ESI creates a fine spray of highly charged droplets in the presence of a strong electric field. As the droplets evaporate due to the dry gas and heat, they are reduced in size increasing the surface to charge density and finally expelling the ions in to the MS. ESI overcomes the use of an interfering matrix, making it more suitable for small molecules in combination with TOF MS instrumentation that allows the acquisition of accurate masses within 5 ppm. The high resolving power of typical TOF MS instruments provides the unambiguous verification of their elemental composition for further confirmation of identity through structure search in databases [126].

Previous research attempted the offline ESI-MS analysis of SPR eluates containing small molecules by a direct infusion into a nano-ESI- ion trap MS. However, it was not satisfactory due to the chemical noise arising from the lack of an analytical chromatographic step [127]. Recently, a similar off-line approach addressed the lack of chromatographic step and successfully achieved the identification of proteins using a larger chip surface and nano ESI LC MS/MS analysis of tryptic digests of the eluates [128]. An alternative to the laborious handling of the eluates is to hyphenate the fluidic system of the biosensor directly with a reverse

phase trapping column that is subsequently coupled to LC- electrospray ionization (ESI) - MS analysis. This strategy has been successfully tested for MS-based amino acid sequencing after on-chip digestion of proteins using a simple Biacore X instrument [129]. Bouffartigues *et al.* attempted a similar system setup using a Biacore 2000 instrument for the analysis of nucleoproteins. Unfortunately the ion suppression caused by a buffer detergent prevented MS identification. The advantage of the online strategy is that it prevents sample loss that might be of critical importance for some applications where sample volumes are limited.

Interfacing SPR-MS Using an iBIA Format

Although the strategies presented above are all suited for SPR-MS analysis of macromolecules usually detected in the DBA format, they are not suited for small molecules when using the iBIA format because the analytes are not retained on the chip surface. Hence, a different strategy is required for coupling SPR iBIA with MS.

When the amount of sample is not limited, one option is to use a split flow strategy for the parallel coupling of the screening and MS. Such an approach was proven using a yeast bioassay for the screening of androgens and estrogens in combination with LC ESI quadrupole (Q) TOF MS [130, 131]. In this thesis, iBIAs for the detection of fluoroquinolones (FQs) replace the yeast bioassay and are able to perform a fast screening among a large number of samples and only the relevant samples are analyzed with MS. When a sample is considered non-compliant during screening for FQs it is fractionated by LC and the effluent is splitted toward two 96-well fraction collectors. The immunoactive LC fractions in one of the 96-well plates are immuno-discriminated using the biosensor immunoassay creating an immunogram and the positive well's positions are used in the second 96-well plate for immunoactive oriented identification with ESI TOF MS (Chapter 6 of this thesis).

Although succesful, the iBIA screening-MS offline strategy has some limitations. First, it requires a relatively large sample volume. Second, due to the amount of sample handling required, the chances of sample contamination are high. Third, the fractionation resolution is limited and this might hamper the identification given that complex samples may contain hundreds of peaks separated during the chromatographic step, but pooled back together in the same fraction. Fourth, the fractionation process is unfeasible when screening for bioactive compounds whose

half life is short or unknown. Considering these limitations, a fast, online system, requiring minimum sample volume and handling was studied. Such an iBIA-online affinity chip recovery-MS was tested. The SPR-MS interface recovers the analyte in a nanoscale affinity chip that features a mirroring immunochemistry to the iBIA screening. The samples suspected non-compliant during the SPR immunoassay screening are reinjected onto a recovery chip with similar, but reversed, immunochemistry. The antibiotic Enrofloxacin (Enro) was used as a model analyte with anti-Enro antibodies as the biorecognition element. The antibodies in the biosorbent specifically capture the analyte while the sample matrix flows through. The analyte captured in the recovery chip is eluted into loop-type interface using an MS-compatible buffer. The loop-type interface solves the pressure incompatibility between the microfluidic system of the biosensor operating at low pressure and the nano LC ESI TOF MS system operating at high pressure. Once in the loop type interface, the analytes enter the nano-LC system and are retained in a trapping column followed by an analytical column connected to the nano-ESI TOF MS for mass analysis. Two main advantages are found in the online strategy. First, that it uses a minimum sample volume and second that the recovery chip interface enables the acquisition of in depth information about the performance of the biosorbent prior to use and for periodical quality control with SPR (Chapter 7 of this thesis).

Part IV. Aims and Scope

SPR biosensors are increasingly used for the detection of xenobiotics of biomedical, food and environmental interest [102, 103, 132, 133]. In the present study various immuno- and transport protein-based assays were developed and tested for xenobiotics in different matrices. These include: Immunoassays for the specific detection of BPA (Chapter 2) and two thyroxine transport protein (TP)-based iBIAs for the bioeffect-related detection and discovery of EDCs interfering with the thyroid system (Chapter 3). The application of the developed TP-based iBIAs for the discovery of new bioactive substances (Chapter 4) is followed by a performance evaluation of a low-cost SPR system (Spreeta) (Chapter 5). The implementation of combined specific immunoassays for fluoroquinolones (Chapter 6) is followed by two strategies for the coupling of the biosensor screening to mass spectrometric confirmation (Chapters 6 and 7).

References

1. Krishnan AV, Stathis P, Permuth SF, Tokes L, Feldman D (1993) Bisphenol-A: an estrogenic substance is released from polycarbonate flasks during autoclaving *Endocrinology* 132, 2279-86
2. Ash M, Ash I (1995) Handbook of Plastic and Rubber Additives: An International Guide to More Than 12, 000 Products by Trade Name, Composition, Function and Manufacturer, Gower Publishing Ltd, Hampshire
3. Burridge E (2003) Bisphenol A product profile *Eur. Chem. News* 17, 14-20
4. Furhacker M, Scharf S, Weber H (2000) Bisphenol A: emissions from point sources *Chemosphere* 41, 751-6
5. Vethaak AD, Rijs GBJ, Schrap SM, Ruiter H, Gerritsen A, Lahr J (2002) Estrogens and xeno-estrogens in the aquatic environment of the Netherlands: occurrence, potency and biological effects., RIZA/RIKZ.,
6. Bolz U, Hagenmaier H, Korner W (2001) Phenolic xenoestrogens in surface water, sediments, and sewage sludge from Baden-Wurttemberg, south-west Germany *Environ. Pollut.* 115, 291-301
7. Heemken OP, Reincke H, Stachel B, Theobald N (2001) The occurrence of xenoestrogens in the Elbe river and the North Sea *Chemosphere* 45, 245-59
8. Belfroid A, van Velzen M, van der Horst B, Vethaak D (2002) Occurrence of bisphenol A in surface water and uptake in fish: evaluation of field measurements *Chemosphere* 49, 97-103
9. Brouwer A (1991) Role of biotransformation in PCB-induced alterations in vitamin A and thyroid hormone metabolism in laboratory and wildlife species *Biochem. Soc. Trans.* 19, 731-8
10. Colborn T, Dumanoski D, Meyers JP (1996) Our Stolen Future: Are We Threatening Our Fertility, Intelligence and Survival? A Scientific Detective Story, Ed. I, Dutton Press, New York
11. Carson R (1962) Silent Spring, Fawcett Crest, New York
12. Kitamura S, Suzuki T, Sanoh S, Kohta R, Jinno N, Sugihara K, Yoshihara Si, Fujimoto N, Watanabe H, Ohta S (2005) Comparative Study of the Endocrine-Disrupting Activity of Bisphenol A and 19 Related Compounds *Toxicol. Sci.* 84, 249-59

13. Vidaeff AC, Sever LE (2005) In utero exposure to environmental estrogens and male reproductive health: a systematic review of biological and epidemiologic evidence *Reprod. Toxicol.* 20, 5-20
14. Carlsen E, Giwercman A, Keiding N, Skakkebaek NE (1995) Declining semen quality and increasing incidence of testicular cancer: is there a common cause? *Environ. Health Perspect.* 103 Suppl 7, 137-9
15. Matthews JB, Twomey K, Zacharewski TR (2001) In vitro and in vivo interactions of bisphenol A and its metabolite, bisphenol A glucuronide, with estrogen receptors alpha and beta *Chem. Res. Toxicol.* 14, 149-57
16. Vandenberg LN, Hauser R, Marcus M, Olea N, Welshons WV (2007) Human exposure to bisphenol A (BPA) *Reprod. Toxicol.* 24, 139-77
17. Moriyama K, Tagami T, Akamizu T, Usui T, Saijo M, Kanamoto N, Hataya Y, Shimatsu A, Kuzuya H, Nakao K (2002) Thyroid hormone action is disrupted by bisphenol A as an antagonist *J. Clin. Endocrinol. Metab.* 87, 5185-90
18. Tan BL, Kassim NM, Mohd MA (2003) Assessment of pubertal development in juvenile male rats after sub-acute exposure to bisphenol A and nonylphenol *Toxicol. Lett.* 143, 261-70
19. Iwamuro S, Yamada M, Kato M, Kikuyama S (2006) Effects of bisphenol A on thyroid hormone-dependent up-regulation of thyroid hormone receptor [alpha] and [beta] and down-regulation of retinoid X receptor [gamma] in *Xenopus* tail culture *Life Sci.* 79, 2165-71
20. Zoeller RT, Bansal R, Parris C (2005) Bisphenol-A, an Environmental Contaminant that Acts as a Thyroid Hormone Receptor Antagonist in Vitro, Increases Serum Thyroxine, and Alters RC3/Neurogranin Expression in the Developing Rat Brain *Endocrinology* 146, 607-12
21. Hakk H, Letcher RJ (2003) Metabolism in the toxicokinetics and fate of brominated flame retardants-A review *Environ. Int.* 29, 801-28
22. Hites RA (2004) Polybrominated Diphenyl Ethers in the Environment and in People: A Meta-Analysis of Concentrations *Environ. Sci. Technol.* 38, 945-56
23. Sjodin A, Jones RS, Focant JF, Lapeza C, Wang RY, McGahee EE, 3rd, Zhang Y, Turner WE, Slazyk B, Needham LL, Patterson DG, Jr. (2004) Retrospective time-trend study of polybrominated diphenyl ether and polybrominated and polychlorinated biphenyl levels in human serum from the United States *Environ. Health Perspect.* 112, 654-8

General Introduction

24. Yen PM (2001) Physiological and Molecular Basis of Thyroid Hormone Action *Physiol. Rev.* 81, 1097-142
25. Bernal J, Guadano-Ferraz A, Morte B (2003) Perspectives in the study of thyroid hormone action on brain development and function *Thyroid* 13, 1005-12
26. Schussler GC (2000) The thyroxine-binding proteins *Thyroid* 10, 141
27. Schreiber G (2002) The evolutionary and integrative roles of transthyretin in thyroid hormone homeostasis *J. Endocrinol.* 175, 61-73
28. Friesema EC, Jansen J, Visser TJ (2005) Thyroid hormone transporters *Biochem. Soc. Trans.* 33, 228-32
29. Boas M, Feldt-Rasmussen U, Skakkebaek NE, Main KM (2006) Environmental chemicals and thyroid function *Eur. J. Endocrinol.* 154, 599-611
30. Hallgren S, Darnerud PO (2002) Polybrominated diphenyl ethers (PBDEs), polychlorinated biphenyls (PCBs) and chlorinated paraffins (CPs) in rats--testing interactions and mechanisms for thyroid hormone effects *Toxicology* 177, 227-43
31. Lans MC, Klasson-Wehler E, Willemsen M, Meussen E, Safe S, Brouwer A (1993) Structure-dependent, competitive interaction of hydroxy-polychlorobiphenyls, -dibenzo-p-dioxins and -dibenzofurans with human transthyretin *Chem.-Biol. Interact.* 88, 7-21
32. Lans MC, Spiertz C, Brouwer A, Koeman JH (1994) Different competition of thyroxine binding to transthyretin and thyroxine-binding globulin by hydroxy-PCBs, PCDDs and PCDFs *Eur. J. Pharmacol.* 270, 129-36
33. Cheek AO, Kow K, Chen J, McLachlan JA (1993) Potential mechanisms of thyroid disruption in humans: interaction of organochlorine compounds with thyroid receptor, transthyretin, and thyroid-binding globulin. PG - 273-8 *Environ. Health Perspect.* 107, 273-8
34. Porterfield SP (2000) Thyroidal dysfunction and environmental chemicals--potential impact on brain development *Environ. Health Perspect.* 108 Suppl 3, 433-8
35. Fritsche E, Cline JE, Nguyen NH, Scanlan TS, Abel J (2005) Polychlorinated biphenyls disturb differentiation of normal human neural progenitor cells: clue for involvement of thyroid hormone receptors *Environ. Health Perspect.* 113, 871-6

36. Palha JA, Goodman AB (2006) Thyroid hormones and retinoids: A possible link between genes and environment in schizophrenia *Brain Res. Rev.* 51, 61
37. Hernando MD, Heath E, Petrovic M, Barcelo D (2006) Trace-level determination of pharmaceutical residues by LC-MS/MS in natural and treated waters. A pilot-survey study *Anal. Bioanal. Chem.* 385, 985-91
38. Stackelberg PE, Furlong ET, Meyer MT, Zaugg SD, Henderson AK, Reissman DB (2004) Persistence of pharmaceutical compounds and other organic wastewater contaminants in a conventional drinking-water-treatment plant *Sci. Total Environ.* 329, 99-113
39. Lemus JA, Blanco G, Grande J, Arroyo B, Garcia-Montijano M, Martinez F (2008) Antibiotics threaten wildlife: circulating quinolone residues and disease in avian scavengers *PLoS ONE* 3, e1444
40. Sapkota AR, Lefferts LY, McKenzie S, Walker P (2007) What do we feed to food-production animals? A review of animal feed ingredients and their potential impacts on human health *Environ. Health Perspect.* 115, 663-70
41. Sarmah AK, Meyer MT, Boxall AB (2006) A global perspective on the use, sales, exposure pathways, occurrence, fate and effects of veterinary antibiotics (VAs) in the environment *Chemosphere* 65, 725-59
42. Huijsdens XW, van Dijke BJ, Spalburg E, van Santen-Verheuve MG, Heck ME, Pluister GN, Voss A, Wannet WJ, de Neeling AJ (2006) Community-acquired MRSA and pig-farming *Ann. Clin. Lab. Microbiol.* 5, 26
43. EEC (1996) Council Directive 96/23/EC On measures to monitor certain substances and residues thereof in live animals and animal products and repealing Directives 85/358/EEC and 86/469/EEC and Decisions 89/187/EEC and 91/664/EEC *OJEC* L125, 10-31
44. Bower CK, Daeschel MA (1999) Resistance responses of microorganisms in food environments *Int. J. Food Microbiol.* 50, 33-44
45. Price LB, Lackey LG, Vailes R, Silbergeld E (2007) The persistence of fluoroquinolone-resistant *Campylobacter* in poultry production *Environ. Health Perspect.* 115, 1035-9
46. Doyle ME (2006) Veterinary Drug Residues in Processed Meats — Potential Health Risk, Food Research Institute, University of Wisconsin–Madison, http://www.wisc.edu/fri/briefs/FRIBrief_VetDrqRes.pdf
47. Hooper DC (1999) Mode of action of fluoroquinolones *Drugs* 58, 6-10

General Introduction

48. Wolfson JS, Hooper DC (1991) Overview of fluoroquinolone safety *Am. J. Med.* 91, 153-61
49. Steffenak I, Hormazabal V, Yndestad M (1991) Reservoir of quinolone residues in fish *Food Addit. Contam.* 8, 777-80
50. Yalow RS, Berson SA (1960) Immunoassay of endogenous plasma insulin in man *J. Clin. Invest.* 39, 1157-75
51. Engvall E, Perlman P (1971) Enzyme-linked immunosorbent assay (ELISA). Quantitative assay of immunoglobulin G *Immunochemistry* 8, 871-4
52. Van Weemen BK, Schuurs AH (1971) Immunoassay using antigen-enzyme conjugates *FEBS Lett.* 15, 232-36
53. Christopoulos TK, Diamandis EP, Eleftherios PD, Theodore KC (1996) In *Immunoassay*; Academic Press: San Diego, 309-35
54. Kricka LJ, Eleftherios PD, Theodore KC (1996) In *Immunoassay*; Academic Press: San Diego, 337-53
55. Buckingham AD (1993) In *Principles of Molecular Recognition*; Blackie Academic and Professional: New York, 1-17
56. Wilchek M, Bayer EA, Livnah O (2006) Essentials of biorecognition: the (strept)avidin-biotin system as a model for protein-protein and protein-ligand interaction *Immunol. Lett.* 103, 27-32
57. Leckband D (2000) Measuring the Forces that Control Protein Interactions *Annu. Rev. Biophys. Biomol. Struct.* 29, 1-26
58. Rabbany SY, Donner BL, Ligler FS (1994) Optical immunosensors *Crit. Rev. Biomed. Eng.* 22, 307-46
59. Clark LC, Jr., Lyons C (1962) Electrode systems for continuous monitoring in cardiovascular surgery *Ann. N. Y. Acad. Sci.* 102, 29-45
60. Newman JD, Turner AP (2005) Home blood glucose biosensors: a commercial perspective *Biosens. Bioelectron.* 20, 2435-53
61. Schalkammer TGM (2002) In *Analytical Biotechnology*, I ed.; Schalkammer, TGM, Ed.; Birkhäuser Verlag: Basel, 168-217
62. D'Orazio P (2003) Biosensors in clinical chemistry *Clin. Chim. Acta* 334, 41-69

63. Bunde RL, Jarvi EJ, Rosentreter JJ (1998) Piezoelectric quartz crystal biosensors *Talanta* 46, 1223-36
64. Luppia PB, Sokoll LJ, Chan DW (2001) Immunosensors--principles and applications to clinical chemistry *Clin. Chim. Acta* 314, 1-26
65. Homola J, Yee SS, Myszka D, Frances SL, Chris ART (2002) In *Optical Biosensors*; Elsevier Science: Amsterdam, 207-51
66. Place JF, Sutherland RM, Dahne C (1985) Opto-electronic immunosensors: a review of optical immunoassay at continuous surfaces *Biosensors* 1, 321-53
67. Byfield MP, Abuknesha RA (1994) Biochemical aspects of biosensors *Biosens. Bioelectron.* 9, 373-99
68. Asanov AN, Wilson WW, Oldham PB (1998) Regenerable biosensor platform: a total internal reflection fluorescence cell with electrochemical control *Anal. Chem.* 70, 1156-63
69. Taitt CR, Anderson GP, Ligler FS (2005) Evanescent wave fluorescence biosensors *Biosens. Bioelectron.* 20, 2470-87
70. Plowman TE, Reichert WM, Peters CR, Wang HK, Christensen DA, Herron JN (1996) Femtomolar sensitivity using a channel-etched thin film waveguide fluoroimmunosensor *Biosens. Bioelectron.* 11, 149-60
71. Wood RW (1902) On a Remarkable Case of Uneven Distribution of Light in a Diffraction Grating Spectrum *Proc. Phys. Soc. London*, 269
72. Fano U (1941) The theory of anomalous diffraction gratings and of quasi-stationary waves on metallic surfaces (Sommerfeld's waves) *J. Opt. Soc. Am.* 31, 213
73. Otto A (1968) Excitation of nonradiative surface plasma waves in silver by the method of frustrated total reflection *Zeitschrift für Physik A Hadrons and Nuclei* 216, 398-410
74. Kretschmann E, Raether H (1968) Radiative decay of nonradiative surface plasmons excited by light *Zeitschrift für Naturforschung A* 23, 2135-36
75. Kretschmann E (1971) Die Bestimmung optischer Konstanten von Metallen durch Anregung von Oberflächenplasmaschwingungen *Zeitschrift für Physik A Hadrons and Nuclei* 241, 313-24

General Introduction

76. Homola J (2006) *Surface Plasmon Resonance Based Sensors*, Springer-Verlag Berlin Heidelberg, Berlin, Heidelberg

77. Zynio SA, Samoylov AV, Surovtseva ER, Mirsky VM, Shirshov YM (2002) Bimetallic layers increase sensitivity of affinity sensors based on surface plasmon resonance *Sensors* 2, 62-70

78. Jonsson U, Fagerstam L, Ivarsson B, Johnsson B, Karlsson R, Lundh K, Lofas S, Persson B, Roos H, Ronnberg I, Sjölander S, Stenberg E, Stahlberg R, Urbaniczky C, Ostlin H, Malmqvist M (1991) Real-time biospecific interaction analysis using surface plasmon resonance and a sensor chip technology *BioTechniques* 11, 620-7

79. Melendez J, Carr R, Bartholomew DU, Kukanskis K, Elkind J, Woodbury R, Furlong C, Yee S (1996) A commercial solution for surface plasmon sensing *Sens. Actuators B: Chem.* 35, 212

80. Homola J, Koudela I, Yee SS (1999) Surface plasmon resonance sensors based on diffraction gratings and prism couplers: sensitivity comparison *Sens. Actuators B: Chem.* 54, 16

81. Karlsson R, Stahlberg R (1995) Surface plasmon resonance detection and multispot sensing for direct monitoring of interactions involving low-molecular-weight analytes and for determination of low affinities *Anal. Biochem.* 228, 274-80

82. Myszka DG (1999) Improving biosensor analysis *J. Mol. Recognit.* 12, 279-84

83. Duschl C, Sevin-Landais AF, Vogel H (1996) Surface engineering: optimization of antigen presentation in self-assembled monolayers *Biophys. J.* 70, 1985-95

84. Besenicar M, Macek P, Lakey JH, Anderluh G (2006) Surface plasmon resonance in protein-membrane interactions *Chem. Phys. Lipids* 141, 169-78

85. Lofas S, Johnsson B (1990) A Novel Hydrogel Matrix on Gold Surfaces in Surface Plasmon Resonance Sensors for Fast and Efficient Covalent Immobilization of Ligands *J. Chem. Soc., Chem. Commun.*, 1526

86. Lofas S, Malmqvist M, Ronnberg I, Stenberg E, Liedberg B, Lundstrom I (1991) Bioanalysis with surface plasmon resonance *Sensors and Actuators B: Chemical* 5, 79-84

87. Xantec; www.xantec.com

88. Biacore; www.biacore.com
89. Harlow E, Lane D (1988) *Antibodies: A Laboratory Manual*, Cold Spring Harbour Laboratory, New York
90. Stanker LH, Beier RC (1996) In *ACS Symp. Ser.*; Beier, RC, Stanker, LH, Eds.; ACS, 16-27
91. Winter G, Milstein C (1991) Man-made antibodies *Nature* 349, 293-99
92. Korpimäki T, Rosenberg J, Virtanen P, Lamminmäki U, Tuomola M, Saviranta P (2003) Further improvement of broad specificity hapten recognition with protein engineering *Protein Eng.* 16, 37-46
93. Korpimäki T, Brockmann EC, Kuronen O, Saraste M, Lamminmäki U, Tuomola M (2004) Engineering of a broad specificity antibody for simultaneous detection of 13 sulfonamides at the maximum residue level *J. Agric. Food Chem.* 52, 40-7
94. Kohler G, Milstein C (1975) Continuous cultures of fused cells secreting antibody of predefined specificity *Nature* 256, 495-97
95. Zhou A, Wei Z, Read RJ, Carrell RW (2006) Structural mechanism for the carriage and release of thyroxine in the blood *Proc. Natl. Acad. Sci.* 103, 13321-26
96. Matsubara K, Mizuguchi M, Kawano K (2003) Expression of a synthetic gene encoding human transthyretin in *Escherichia coli* *Protein Expr. Purif.* 30, 55-61
97. Tsuzuki T, Mita S, Maeda S, Araki S, Shimada K (1985) Structure of the human prealbumin gene *J. Biol. Chem.* 260, 12224-27
98. Neumann P, Cody V, Wojtczak A (2001) Structural basis of negative cooperativity in transthyretin *Acta Biochim. Pol.* 48, 867-75
99. Jackson TM, Ekins RP (1986) Theoretical limitations on immunoassay sensitivity: Current practice and potential advantages of fluorescent Eu³⁺ chelates as non-radioisotopic tracers *J. Immunol. Methods* 87, 13-20
100. Ekins R (1994) Immunoassay: recent developments and future directions *Nucl. Med. Biol.* 21, 495-521
101. Rich RL, Hoth LR, Geoghegan KF, Brown TA, LeMotte PK, Simons SP, Hensley P, Myszka DG (2002) Kinetic analysis of estrogen receptor/ligand interactions *Proc. Natl. Acad. Sci.* 99, 8562-67

General Introduction

102. Rich RL, Myszka DG (2006) Survey of the year 2005 commercial optical biosensor literature *J. Mol. Recognit.* 19, 478-534
103. Shankaran DR, Gobi KV, Miura N (2007) Recent advancements in surface plasmon resonance immunosensors for detection of small molecules of biomedical, food and environmental interest *Sens. Actuators B: Chem.* 121, 158-77
104. Haasnoot W, Loomans EEMG, Cazemier G, Dietrich R, Verheijen R, Bergwerff AA, Stephany RW (2002) Direct Versus Competitive Biosensor Immunoassays for the Detection of (Dihydro)Streptomycin Residues in Milk *Food Agr. Immun.* 14, 15
105. Moorhouse JE, Yeadon R, Beevor PS, Nesbitt BF (1969) Method for Use in Studies of Insect Chemical Communication *Nature* 223, 1174-75
106. Fishman HA, Greenwald DR, Zare RN (1998) Biosensors in Chemical Separations *Annu. Rev. Biophys. Biomol. Struct.* 27, 165-98
107. Queiroz EF, Wolfender JL, Atindehou KK, Traore D, Hostettmann K (2002) On-line identification of the antifungal constituents of *Erythrina vogelii* by liquid chromatography with tandem mass spectrometry, ultraviolet absorbance detection and nuclear magnetic resonance spectrometry combined with liquid chromatographic micro-fractionation *J. Chromatogr. A* 974, 123-34
108. Trojanowicz M, SzewczyImageskac M (2005) Biosensing in high-performance chemical separations *Trends Anal. Chem.* 24, 92-106
109. Nice E, Lackmann M, Smyth F, Fabri L, Burgess AW (1994) Synergies between micropreparative high-performance liquid chromatography and an instrumental optical biosensor *J. Chromatogr. A* 660, 169-85
110. Whelan RJ, Zare RN (2003) Surface plasmon resonance detection for capillary electrophoresis separations *Anal. Chem.* 75, 1542-7
111. Minunni M, Tombellia S, Mascini Ma, Biliab A, Bergonzi CM, Vincieri FF (2005) An optical DNA-based biosensor for the analysis of bioactive constituents with application in drug and herbal drug screening *Talanta* 65, 578-85
112. Nedelkov D, Nelson RW (2003) Surface plasmon resonance mass spectrometry: recent progress and outlooks *Trends Biotechnol.* 21, 301
113. Larsericdotter H, Jansson O, Zhukov A, Areskoug D, Oscarsson S, Buijs J (2006) Optimizing the surface plasmon resonance/mass spectrometry interface

for functional proteomics applications: how to avoid and utilize nonspecific adsorption *Proteomics* 6, 2355-64

114. Fenselau C (1997) MALDI MS and strategies for protein analysis *Anal. Chem.* 69, 661A-65A

115. Wenzel RJ, Matter U, Schultheis L, Zenobi R (2005) Analysis of megadalton ions using cryodetection MALDI time-of-flight mass spectrometry *Anal. Chem.* 77, 4329-37

116. Yates JR, 3rd (1998) Mass spectrometry and the age of the proteome *J. Mass Spectrom.* 33, 1-19

117. Krone JR, Nelson RW, Dogruel D, Williams P, Granzow R (1997) BIA/MS: interfacing biomolecular interaction analysis with mass spectrometry *Anal. Biochem.* 244, 124-32

118. Nelson RW, Krone JR, Jansson O (1997) Surface Plasmon Resonance Biomolecular Interaction Analysis Mass Spectrometry. 1. Chip-Based Analysis *Anal. Chem.* 69, 4363-68

119. Sönksen CP, Nordhoff E, Jansson O, Malmqvist M, Roepstorff P (1998) Combining MALDI Mass Spectrometry and Biomolecular Interaction Analysis Using a Biomolecular Interaction Analysis Instrument *Anal. Chem.* 70, 2731-36

120. Nedelkov D, Nelson RW (2001) Analysis of native proteins from biological fluids by biomolecular interaction analysis mass spectrometry (BIA/MS): exploring the limit of detection, identification of non-specific binding and detection of multi-protein complexes *Biosens. Bioelectron.* 16, 1071

121. Borch J, Roepstorff P (2004) Screening for Enzyme Inhibitors by Surface Plasmon Resonance Combined with Mass Spectrometry *Anal. Chem.* 76, 5243-48

122. Lopez F, Pichereaux C, Burlet-Schiltz O, Pradayrol L, Monsarrat B, Estève J-P (2003) Improved sensitivity of biomolecular interaction analysis mass spectrometry for the identification of interacting molecules *Proteomics* 3, 402-12

123. Zhukov A, Schurenberg M, Jansson O, Areskoug D, Buijs J (2004) Integration of Surface Plasmon Resonance with Mass Spectrometry: Automated Ligand Fishing and Sample Preparation for MALDI MS Using a Biacore 3000 Biosensor *J. Biom. Tech.* 15, 112-19

124. Nedelkov D (2007) Development of Surface Plasmon Resonance Mass Spectrometry Array Platform *Anal. Chem.*

General Introduction

125. Cohen LH, Gusev AI (2002) Small molecule analysis by MALDI mass spectrometry *Anal. Bioanal. Chem.* 373, 571-86

126. Ferrer I, Thurman EM (2003) Liquid chromatography/time-of-flight/mass spectrometry (LC/TOF/MS) for the analysis of emerging contaminants *Trends Anal. Chem.* 22, 750

127. Sönksen C, Roepstorff P, Markgren PU, Danielson H, Hämäläinen MD, Jansson Ö (2001) Capture and analysis of low molecular weight ligands by surface plasmon resonance combined with mass spectrometry *Eur. J. Mass Spectrom.* 7, 385-91

128. Visser NFC, Scholten A, van den Heuvel RHH, Heck AJR (2007) Surface-Plasmon-Resonance-Based Chemical Proteomics: Efficient Specific Extraction and Semiquantitative Identification of Cyclic Nucleotide-Binding Proteins from Cellular Lysates by Using a Combination of Surface Plasmon Resonance, Sequential Elution and Liquid Chromatography-Tandem Mass Spectrometry *ChemBioChem* 8, 298-305

129. Natsume T, Nakayama H, Jansson O, Isobe T, Takio K, Mikoshiba K (2000) Combination of biomolecular interaction analysis and mass spectrometric amino acid sequencing *Anal. Chem.* 72, 4193-8

130. Nielen MWF, Bovee TFH, vanEngelen MC, Rutgers P, Hamers ARM, vanRhijn JA, Hoogenboom LAP (2006) Urine Testing for Designer Steroids by Liquid Chromatography with Androgen Bioassay Detection and Electrospray Quadrupole Time-of-Flight Mass Spectrometry Identification *Anal. Chem.* 78, 424-31

131. Nielen MWF, van Bennekom EO, Heskamp HH, van Rhijn JA, Bovee TH, Hoogenboom LAP (2004) Bioassay-directed identification of estrogen residues in urine by liquid chromatography electrospray quadrupole time-of-flight mass spectrometry *Anal. Chem.* 76, 6600-08

132. Rogers KR (2006) Recent advances in biosensor techniques for environmental monitoring *Anal. Chim. Acta* 568, 222-31

133. Patel PD (2002) (Bio)sensors for measurement of analytes implicated in food safety: a review *Trends Anal. Chem.* 21, 96-115

**Part I. Surface Plasmon Resonance
(SPR)-based Biosensor Screening
Assays**

Chapter 2

Biosensor Immunoassays for the Detection of Bisphenol A

Published in: *Analytica Chimica Acta* 528 (2005) 37-45

Abstract

Bisphenol A (BPA) is a xenoestrogen found in the environment. In consequence, for the biosensor detection of BPA we raised antibodies (polyclonal (PABs) and monoclonal (MABs)) against a structural analogue of BPA, 4,4 bis (4-hydroxyphenyl) valeric acid (BVA). The kinetics of the MAb-BPA interaction were evaluated and the MAb providing the highest affinity was directly immobilized onto the sensor chip surface to evaluate a direct assay. Afterwards, the performance of the MABs and the PABs was compared in an inhibition assay using a BVA coated chip.

The highest sensitivity (limit of detection (LOD) of $0.4 \mu\text{g L}^{-1}$) was obtained with MAb 12 in the direct assay. However, the inhibition assay was the most robust and the PABs showed the highest sensitivity (LOD of $0.5 - 1 \mu\text{g L}^{-1}$). The antibodies were specific for BVA and BPA as only minor cross-reactivities were found toward structurally related compounds or other endocrine disruptors. In the inhibition assay (with a run time of 6 min), water samples spiked with BPA at different levels ($0.5-50 \mu\text{g L}^{-1}$) resulted in recoveries varying between 68 and 121%. The sensitivity of the inhibition assay could be improved 40 times (LOD of $0.03 \mu\text{g L}^{-1}$ with the Mab 12-based assay) using solid phase extraction (SPE).

Introduction

Endocrine disruptors (EDC's) have concern in human health and wildlife. When chemicals with endocrine activity are present in the environment, they might affect the development of any organism and the later functioning in adult life of an individual, a population and even a community [1]. Some of these compounds, called xeno-estrogens, have estrogenic activity. One of these compounds, bisphenol A (BPA), is an important monomer for the production of epoxy coatings and polycarbonate. It is used as a stabilizer or antioxidant in polyvinyl chloride (PVC) [2] and as an intermediate in a wide variety of plastics for industry and household. Some of these materials are used in food and water containers from which BPA migrates [3-5].

Due to the widespread use of BPA, with a global production of over 1 million tons/year [6] it is also an environmental contaminant mainly present in raw sewage or wastewater effluents at up to ppb ($\mu\text{g L}^{-1}$) concentrations [7], and at ppt (ng L^{-1}) concentrations in river water and sediments [8-11].

There is a wide variety of studies available supporting the endocrine activity of BPA. First, BPA binds to the estrogen receptor [12], produces meiotic aneuploidy in the female mouse [13] and increases cell proliferation of the male and female sexual organs [14]. Moreover, several cases of reproductive abnormalities have been reported in wildlife exposed to estrogenic environmental contaminants [15]. Additionally, though still controversial, BPA may even induce a decrease of sperm quality in humans [16]. Finally, it seems that BPA would not only mimic estrogens, but also the thyroid hormone action as an antagonist [17], which might be supported by recent studies where rats exposed to BPA evidenced an increase in thyroid gland size [18].

The studies mentioned above evidence the necessity to detect BPA in the high ppt to low ppb range. This is currently done using classic instrumental analytical techniques such as gas chromatography (GC) and high-performance liquid chromatography (HPLC) [19-21]. Immunochemical techniques were recently reported using monoclonal [22] and polyclonal mammalian [23] and chicken [24] antibodies in enzyme-linked immunosorbent assays (ELISA's) with different limits of detection (ranging from 0.05 to $500 \mu\text{g L}^{-1}$) depending on the immunogen and the type of antibody produced). The aim of the present study was to evaluate a different approach using a commercially available Surface Plasmon Resonance (SPR)-based biosensor (Biacore

3000) as a novel method for the detection of BPA. This biosensor is able to measure the antigen-antibody binding in real time and without labeling the reagents [25]. The results can be obtained within minutes and the procedure is fully automated making this system suitable for high-throughput screening. Therefore, such an assay might be a useful tool for water screening. Because of a lack of functional groups in BPA for coupling to carrier proteins, polyclonal and monoclonal antibodies were raised against 4,4 bis (4-hydroxyphenyl) valeric acid (BVA), a structural analogue of BPA containing a carboxyl group (Figure 1).

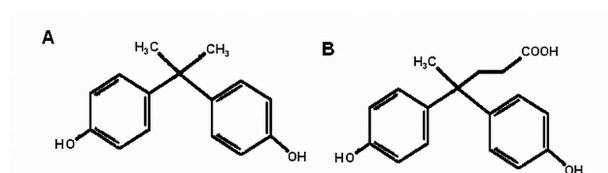


Figure 1. Structures of (A) bisphenol A (BPA) and (B) the analogue 4,4 bis (4-hydroxyphenyl) valeric acid (BVA) used as hapten in the immunogen.

As the affinity of the antibodies is determinant for the further assay performance [26], we selected our best monoclonal antibody in the biosensor by means of its kinetic parameters. Subsequently different assay formats were evaluated and the results were compared with those obtained using the polyclonal antibodies. Finally, the selected best monoclonal and polyclonal antibodies were compared for their performances using water samples with and without the addition of BPA. The possibility of improving the LOD of the assay was also evaluated in combination with a solid phase extraction (SPE) procedure.

Experimental

Materials

Sensor chips (CM5), HBS-EP buffer [pH 7.4, consisting of 10 mM 4-(2-hydroxyethyl) piperazine-1-ethanesulfonic acid, 150 mM sodium chloride, 3 mM EDTA, 0.005% (v/v) surfactant polysorbate (P20)] and an amine coupling kit [containing 0.1 M N-hydroxysuccinimide (NHS), 0.4 M N-ethyl-N'-(3-dimethylaminopropyl) carbodiimide hydrochloride (EDC), and 1 M ethanolamine hydrochloride-NaOH (pH 8.5)] were

supplied by Biacore AB (Uppsala, Sweden). ELISA microtiter plates were supplied by Greiner (Frickenhausen, Germany). Rabbit anti-mouse (RAM) and RAM-immunoglobulin-horseradish peroxidase (RAM-HRP) were purchased from DAKO (Denmark) and solutions of tetramethylbenzidine (TMB) peroxidase substrate and peroxide from Kirkegaard and Perry Labs (Gaithersburg, MD, USA). Specol was obtained from the Animal Sciences Group (Lelystad, The Netherlands) and the BCA protein assay reagents from Pierce (Rockford, IL, USA). Murine myeloma P3/NS-1/1-Ag4-1 (NS-1) were supplied by American Type Culture Collection, Rockville, MA, USA) and iso-propanol by Merck (Darmstadt, Germany). Bovine serum albumin (BSA), ovalbumin (OVAL), antifoam A [A5758], bisphenol A (BPA; 2,2-bis-(4-hydroxyphenyl) propane), BVA (4,4-bis (4-hydroxyphenyl) valeric acid), NHS, EDC and all other cross-reactants were obtained from Sigma-Aldrich Chemie (Zwijndrecht, The Netherlands) unless otherwise stated.

Equipment

The Biacore 3000 was supplied by Biacore AB (Uppsala, Sweden), the ÄKTA purifier and HiTrap protein G columns (5 mL) by Amersham Biosciences (Uppsala, Sweden) and the Argus 400 microplate reader by Canberra Packard (Downers Grove, IL, USA).

Preparation of the BVA Conjugates

BVA was coupled to BSA for the immunization of rabbits and mice and to OVAL for evaluation purposes in ELISA and in the biosensor. The coupling reactions were performed at pH 7 according to the following procedure. NHS (23 mg in 2 mL DMF) was mixed with EDC (156 mg in 2 mL DMF) and BVA (28 mg in 1 mL of DMF) for 30 min at 25 °C. Of this mixture, 2.5 mL were added drop wise to 5 mL of a BSA or OVAL solution (40 mg mL⁻¹ in 0.1 M borate buffer at pH 7). After 1 h incubation at 25 °C, the products were dialyzed against PBS and the end volumes were adjusted to 15 mL with PBS, reaching a final protein concentration of 13 mg mL⁻¹ as determined with the BCA test.

Production of MAbs

Immunization of Mice

Two 10-12 weeks old female Swiss-mice were immunized subcutaneously with 100 μL of BVA-BSA (0.2 mg mL^{-1} in PBS) emulsified with Specol (1:1; v/v). Booster injections were given every 2 weeks. Blood was taken from each mouse prior to the first immunization (pre-immune) and 1 week after each booster injection. The sera were tested for antibodies against BVA using the BVA-OVAL conjugate in an indirect ELISA.

Fusion and Cloning

The mice were primed intraperitoneally with 0.02 mg BVA-BSA in 200 μL of PBS 4-5 days before spleen cell isolation.

Hybridoma cells were prepared using murine myeloma (NS-1) as the fusion partner following a previously described procedure [27]. The MAbs immunoglobulin subclasses were determined by the Mouse Monoclonal Antibody Isotyping Kit (IsoStrip) of Roche (Mannheim, Germany).

MAbs were isolated from one liter of raw cell culture medium by ammonium sulphate precipitation [28] followed by affinity chromatography using a HiTrap Protein G column in accordance with the manufacturer's instructions.

Production of PAb

Two New Zealand White rabbits were immunized by injecting 250 μL of a mixture of Freund's complete adjuvant and BVA-BSA (0.5 mg mL^{-1} in PBS) (1:1; v/v). Booster injections with Freund's incomplete adjuvant were given every 3 weeks. After the 22nd week, the boosters were administered every 6 weeks and 40 mL of blood were obtained each time. Serum was extracted from each bleeding and pooled prior to the experiments.

ELISA

The ELISA was performed as previously described [27] with the exception that the microtiter plates were coated with an OVAL-BVA solution (100 ng/100 μL /well) in coating buffer.

Biosensor Immunoassays (BIAs)

Capture Assay for Kinetic Evaluation of MABs

The surface of a CM5 sensor chip in flow channel 4 (Fc4) of the Biacore 3000 was coated with polyclonal rabbit anti-mouse antibodies (15000 Response Units (RU)) using the amine coupling kit and following manufacturer's instructions. Fc3 was left unmodified for referencing.

Each MAb was injected at equivalent concentrations at a flow rate of 5 $\mu\text{L min}^{-1}$ for five minutes or until at least 1300 RU of MAb was captured. The integrated μ -fluidic cartridge (IFC) was washed with HBS-EP buffer during 1 min to remove unbound antibodies. The Ab/Ab complex was stable within the cycle and it was fully regenerated only after two subsequent injections (a mixture of H_3PO_4 (100 mM) and HCl (100 mM) (1:1; v/v) for 30 s followed by NaOH (100 mM) for 10 s) (Figure 2).

In order to collect detailed kinetic data of BPA binding to the captured MABs, we used a modification of an existent protocol [29]; 100 μL of BPA (6.6 $\mu\text{g L}^{-1}$ (29 nM)) in HBS-EP buffer were injected in triplicate at a flow rate of 100 $\mu\text{L min}^{-1}$. At least triplicate injections of HBS-EP buffer (blanks) for each MAb were used for further double referencing [30]. The measured dissociation time was 300 s and the data were collected at a rate of 5 Hz.

The sensorgrams obtained during the binding of BPA were normalized to the response of the corresponding maximum response of captured MAB; multiplied by the mean of the maximum response of captured MAB in all the cycles using $\text{NS} = ((\text{SR}/R_{\text{MABc}}) \times R_{\text{maxAvg}})$. NS being the normalized sensorgram, SR the response of each point of the BPA binding sensorgrams, R_{MAB} the maximum response of captured MAB in that cycle and R_{maxAvg} the average maximum response obtained from all the cycles using the four MABs.

Data were processed as described before [30] with Scrubber software and used to obtain kinetic rate constants by fitting to a 1:1 bimolecular interaction model using CLAMP software [31]. The equilibrium

dissociation constants (K_D) shown in Table 1, are the quotients K_d/K_a of the constants obtained with CLAMP.

Non-Competitive (Direct) Immunoassay Format

The MAb with the highest affinity (as determined in the previous section) was immobilized (yielding approx. 10,000 RU) on the surface of a CM5 sensor chip in Fc2 using the amine coupling kit following manufacturer's instructions. Fc1 was left unmodified for further referencing. To obtain a calibration graph, standard solutions of BPA in HBS-EP buffer (50 - 0.39 $\mu\text{g L}^{-1}$) were injected (100 μL , at a flow rate of 20 $\mu\text{L min}^{-1}$). At the end of each cycle the surface was regenerated with HCL (50 mM) for 20 s. The data was double referenced as described before [30]. The maximum response was recorded 20 s before the injection ended.

Competitive Inhibition (Indirect) Immunoassay Format

BVA was directly immobilized onto a CM5 chip surface. The surface was activated by injecting 120 μL of a mixture of 0.4 M EDC and 0.1 M NHS (1:1; v/v) at a flow rate of 2 $\mu\text{L min}^{-1}$. Ethylenediamine (120 μL of a 2 M solution with pH 10) was injected at a flow rate of 2 $\mu\text{L min}^{-1}$ over the activated surface and was used as a linker between the activated surface and the BVA carboxylic groups. A solution of activated BVA was prepared by adding 3 mg NHS and 7.5 mg EDC to a solution of BVA (3 mg BVA in 0.5 mL ethanol and 0.9 mL 10 mM sodium acetate coupling buffer (pH 4.5)). The chip surface was incubated for 60 min outside the Biacore with the activated BVA solution by directly pipeting 100 μL of the solution on the CM5 chip surface. The activated BVA solution on the chip surface was changed every 10 min or when a white deposit was observed. Before the chip was docked into the Biacore, the surface was washed with methanol and dried under a stream of nitrogen gas.

In the Biacore 3000 the antibody solutions (dilution factor of 1/1000 for the MAbs, 1/1500 for the PABs) were mixed with the sample (1:5; v/v) and 50 μL were injected over the sensor surface at a flow rate of 25 $\mu\text{L min}^{-1}$. Triplicate injections were performed for each concentration within each cycle. The surface was regenerated by injecting 20 μL NaOH (0.2 M) containing 20% acetonitrile. The total run time between samples was 11 min. Maximum responses were recorded 10 s after the injections ended. The LODs were measured as the concentration of BPA

corresponding with the average of the blank's average response minus three times its standard deviation.

Determination of Inter- and Intra-Assay Variation

Water samples were obtained in the city of Wageningen from the laboratory tap, the river Rhine, the city canal and an irrigation lagoon. The samples were spiked to a final concentration of 1, 5, 10, 25 and 50 $\mu\text{g L}^{-1}$ and were centrifuged for 5 min at 10,000 rpm prior to the measurements for a fast and easy clean up of the material in suspension. To reduce the run time between samples, each supernatant was pre-mixed (5:1; v/v) with antibody solutions in five times concentrated HBS-EP buffer and 50 μL were injected at a flow rate of 25 $\mu\text{L min}^{-1}$. The total run time of a cycle was 6 min. Recoveries were determined from a standard calibration graph in millipore water which was mixed like the other water samples. The calibration graphs were fitted to a four-parameter logistic equation using Biacore BIAevaluation software. Intra-assay variation was calculated from the analysis of three replicates of each dilution on a single day. Inter-assay variation was calculated from the analysis of three replicates of each dilution carried out on three different days. Intra- and inter-assay variation, as well as recoveries at all spiked concentrations, were averaged for each water sample source as shown in Table 3.

Solid Phase Extraction

Tap Water samples were spiked with BPA (0.03, 0.1, 0.3, 0.9 $\mu\text{g L}^{-1}$) in duplicate, acidified to pH 3 with HCL and extracted using OASIS cartridges (20 mg N-vinylpyrrolidone/divinylbenzene-based sorbent; Waters – Milford, MA, USA) and according to the manufacturer's protocol for phenols in tap water [32]. Briefly, 50 mL of water were passed through the cartridge after proper condition and equilibration steps, the cartridge was washed, dried and eluted (methanol/methyl t-butyl ether (1:10; v/v)). The eluate was evaporated to dryness under a gentle nitrogen stream and the residue was resuspended in 500 μL of HBS-EP buffer for further measurement.

Results and Discussion

Development of Antibodies

Antisera from two mice and two rabbits were tested in the ELISA and all four animals developed antibodies reacting with the OVAL-BVA coated plates.

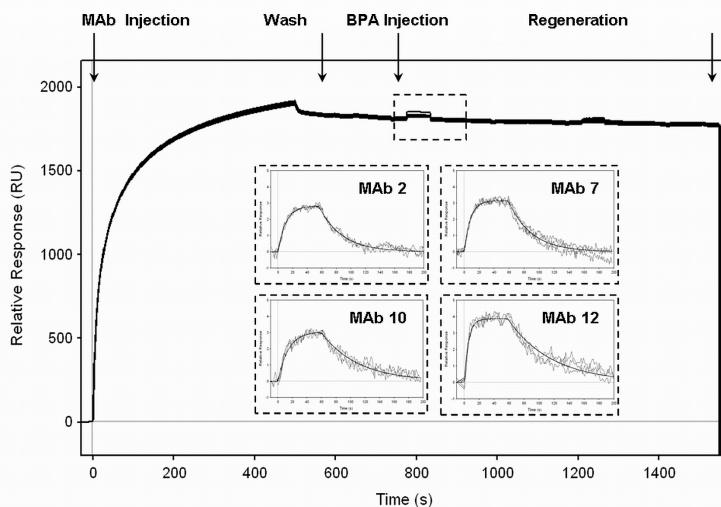


Figure 2. Six overlaid sensorgrams of complete antibody/antibody/ligand binding cycles obtained in the capture assay format. The different MABs were captured by the rabbit anti-mouse surface yielding a response of approx. 1700 RU, the surface was washed for 60 s, the ligand was injected yielding approx. 4-6 RU depending on the captured MAB. The insert is a view in larger scale of the area inside the dashed square. It shows the sensorgrams of the MAB-BPA interactions of triplicate injections of BPA ($6.6 \mu\text{g L}^{-1}$) over the captured MAB surface. Black lines depict the global fit of the data to a simple 1:1 bimolecular interaction model. The four MABs were globally fitted.

After spleen cells fusion of the two mice with myeloma cells, the screening of 872 hybridoma-containing wells in the ELISA resulted in 101 wells with culture supernatants reactive to the BVA-OVAL coated plate. Finally, limiting dilutions of the hybridoma cells resulted in 15 stable clones. The 15 supernatants were screened in the Biacore with the competitive inhibition assay. Inhibition with BPA ($10 \mu\text{g L}^{-1}$) was found with 9 of these supernatants and 4 of them (MABs 2, 7, 10 and 12) were selected based on the best inhibition values. These MABs were

further isolated from the culture supernatants by affinity chromatography. The total amounts of IgG isolated from 1 L portions of medium, as determined with the BCA protein test, were: 6.5 mg (MAb 12), 12 mg (MAb10), 6.6 mg (MAb 7) and 3.8 mg (MAb 2). The subclasses of these MAbs were identified as IgG1 with kappa light chain.

Capture Assay and the Binding Kinetics of Bisphenol A

A capture assay was used to compare binding kinetics of the MAbs to BPA (228 Da) in the Biacore. Each cycle (Figure 2) was started by injecting the MAb onto the chip surface containing the immobilized anti-mouse antibody. Once captured, the surface was washed to remove any unbound antibodies. The flow was set to $100 \mu\text{l min}^{-1}$, BPA was injected for 60 s and the BPA dissociation was monitored for 300 s, followed by the regeneration of the surface. All capture experiments were performed on the same chip with no significant reduction in binding capacity. Six cycles were run for each MAb, three of them were running buffer injections for further referencing.

The sensorgrams were double referenced by subtracting the sensorgram of the reference channel and an average of the running buffer injections (blanks). Furthermore, the sensorgrams were normalized to the captured antibody response, although differences among the cycles were small ($< 5\%$), and fitted to a 1:1 bimolecular model, using CLAMP software [30].

Table 1. Affinity and rate constants for MAb/BPA interactions as determined in the capture assay.

Interaction	K_a ($\text{M}^{-1} \text{s}^{-1}$)	K_d (s^{-1})	KD (nM)
MAb 2	3.1×10^{06}	3.3×10^{-02}	10.5
MAb 7	2.1×10^{06}	3.2×10^{-02}	15.1
MAb 10	1.7×10^{06}	2.0×10^{-02}	11.5
MAb 12	5.5×10^{06}	1.7×10^{-02}	3.1

The BPA-MAb interactions were successfully monitored as can be observed in Figure 2 insert, binding responses were reproducible among the different cycles. From the affinity parameters shown in Table 1, it can be observed that MAb 12 showed the highest association constant ($K_a = 5.5 \times 10^{06}$) and the lowest dissociation constant ($K_d = 1.71 \times 10^{-02}$).

⁰²⁾ in comparison with the other MABs. Therefore, MAb 12 was considered as the most appropriate MAB for further evaluation in the different BIAs.

Non Competitive (Direct) Immunoassay

As MAb 12 showed the highest affinity for BPA, which is essential for the future assay sensitivity [26], MAb 12 was immobilized onto a CM5 sensor chip surface for its evaluation in a non-competitive (direct) immunoassay. Figure 3A shows the overlaid sensorgrams of injections with different concentrations of BPA in HBS-EP buffer (45.6, 22.8, 11.4, 5.7, 2.9, 1.4, 0.7, 0.4, 0.2 $\mu\text{g L}^{-1}$) over the MAB surface. Figure 3B is the correspondent calibration graph, using the responses obtained 20 s before injections ended. The sensitivity of this immunoassay, the concentration corresponding to 50% of the maximum binding response (B_{50}), was 1.6 $\mu\text{g L}^{-1}$. The limit of detection (LOD) was 0.4 $\mu\text{g L}^{-1}$.

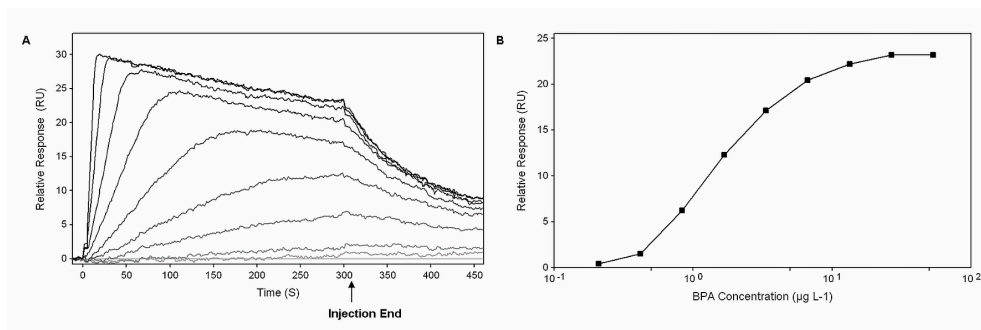


Figure 3. (A) Overlaid sensorgrams of BPA standard solutions (200, 100, 50, 25, 12.5, 6.25, 3.12, 1.56, 0.79 $\text{nM } \mu\text{g L}^{-1}$) obtained in the direct assay format. (B) Calibration graph of BPA, using the relative responses measured 20 s before injections ended.

As the direct assay format is in theory the most sensitive [26], this sensitivity is probably close to the best that MAB 12 can achieve in this biosensor immunoassay. However, in this direct format we encountered losses of binding sites after regeneration and after storage of the chip. These problems together with the low responses obtained (max. 23 RU) due to the low molecular mass of BPA did not make this format suitable for routine analysis.

Evaluation of Inhibition Immunoassays

To obtain a more robust assay, a competitive inhibition assay format was evaluated using a chip with immobilized BVA (see Experimental section). A response of around 700 RU was obtained after the injection of 50 μL of PAB K66 (d.f. 1/1500 in HBS-EP) buffer at a flow rate of 25 μLmin^{-1} .

Proper AB dilutions were mixed with BPA standard solutions (100, 33.3, 11.1, 3.7, 1.1 $\mu\text{g L}^{-1}$) (1:5; v/v) in the Biacore. The mixtures were injected in triplicate and at random to check for possible cross-contamination. Calibration graphs are shown in Figure 4 comparing the most sensitive PAb and MAb-based BIAs. From these graphs and Table 2 a rather small difference between the MAb-based BIAs can be noted. Although the LODs of the MAbs were comparable, MAb 12 shows the lowest IC_{50} value (9.1 $\mu\text{g L}^{-1}$) and the highest inhibition at the maximum concentration of BPA (100 $\mu\text{g L}^{-1}$), as would be expected based on the affinity parameters.

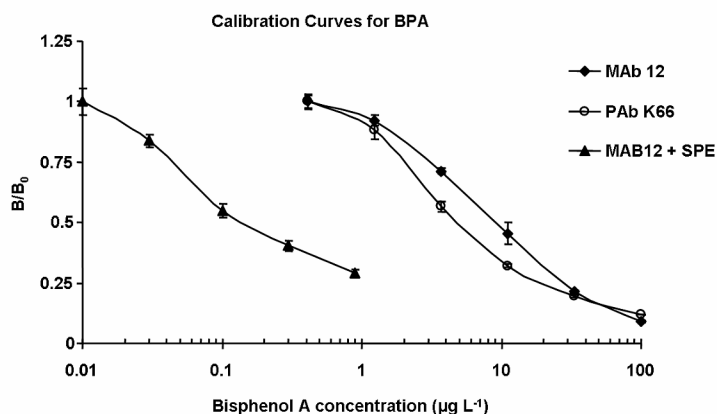


Figure 4. Normalized BPA calibration graphs obtained with the most sensitive antibodies (PAb K66 and MAb 12) in the competitive inhibition format and after a pre-concentration with SPE in combination with the Mab 12-based assay.

There was no significant difference in IC_{50} values between the two PABs evaluated (Table 2), but PAb K66 showed a higher inhibition at the maximum concentration of BPA as well as a steeper slope of the

calibration graph. The PAb K66-based BIA was twice as sensitive when compared with the MAb 12-based BIA. The BVA-coated chip was used for over 1000 cycles with no evident decrease in binding capacity.

Table 2. Sensitivity of the biosensor inhibition immunoassays with different antibodies.

Antibody	LOD (ppb)	IC ₅₀ (ppb)
MAb 2	1.1	13.6
MAb 7	0.9	18.0
MAb 10	1.6	11.8
MAb 12	1.2	9.1
PAb K66	1.0	4.9
PAb K67	0.5	4.8

Competitive Inhibition Immunoassays Performance with Water

Samples

The level of BPA found in surface waters is generally in the level of parts per trillion (ng L^{-1}), however, levels of BPA above $1 \mu\text{g L}^{-1}$ have been found in 7% of the samples out of a whole-country survey of 135 samples [33] in the surrounding of industrialized areas or near discharge points of sewage treatment plants. Consequently, we decided to conduct a small spike and recovery experiment using the inhibition immunoassays previously described to evaluate the possible use of the assays for the screening of BPA in water samples at levels of concern to the aquatic wildlife [33, 34].

Real water samples were spiked and correspondent calibration graphs were performed in millipore water. Assay performance parameters were comparable to those obtained in HBS-EP buffer. The inter and intra-assay variation for real water samples are shown in Table 3. The average recoveries and variation were acceptable even though the samples spiked at $1 \mu\text{g L}^{-1}$ were included in the average, this concentration is in the lower end of the calibration curve where greater variance is commonly found. Recoveries ranged from 68 to 118% depending on the matrix, these values were considered acceptable as almost no pre-treatment was performed except for the centrifugation step.

Intra-assay variation values were all below 5% for both immunoassays, inter-assay variation values were below 25% in all cases with the exception of the PAb K66-based immunoassay in lagoon water, where a 40% inter-assay variation was found.

The throughput of the system was 10 samples per hour and up to 425 samples were measured in a single experiment.

Evaluation of SPE Extraction in Combination with BIA

To be able to measure lower concentrations of BPA in water, we evaluated the possibility of combining the MAb 12-based inhibition assay with a fast extraction procedure like solid phase extraction.

Table 3. Intra- and inter-assay variations obtained in the inhibition assay format with water samples from four different sources fortified with BPA (1, 5, 10, 25, 50 ppb)^a.

Water Source	Intra-assay				Inter-assay			
	Recovery (%)		CV (%)		Recovery (%)		CV (%)	
	MAb 12	PAb K66	MAb 12	PAb K66	MAb 12	PAb K66	MAb 12	PAb K66
Tap	91	85	3	2	81	80	16	14
Rhine	102	68	1	2	85	78	21	7
Canal	118	118	4	1	98	97	18	19
Lagoon	92	121	5	2	77	109	21	40

^a Recovery (%) and CV (%) values at all concentrations were averaged for each water source.

A calibration curve was performed extracting BPA spiked tap water samples (0.03, 0.1, 0.3, 0.9 $\mu\text{g L}^{-1}$) (see experimental Section 2.7.4. and Figure 4) and the eluates were measured with the MAb 12 competitive inhibition immunoassay described in the previous section. The samples were concentrated 100 times with the SPE procedure and the calibration curve reached an IC_{50} of 0.14 $\mu\text{g L}^{-1}$ and an LOD of 0.03 $\mu\text{g L}^{-1}$. Although the throughput of the system decreased to 4 samples per hour in combination with this manual SPE procedure, this could be improved in the future by an off-line coupling of an automated SPE system [35] with the BIA.

Specificity of the Assays

Cross-reactivities of various structurally related compounds were evaluated for PAb K66 and for MAb 12-based BIAs (see Table 4) and were calculated as $CR (\%) = (BPA IC_{50}) / (Cross\ reactant\ IC_{50}) \times 100$.

Table 4. Cross-reactivities of the inhibition assays with selected endocrine disruptors.

Compound	Cross-Reactivity (%)	
	MAb 12	PAb K66
Bisphenol A	100	100
BVA	73	118
Bis-(4-hydroxyphenyl)-methane	2.3	1.5
4-Cumylphenol	1.3	1
4,4'-(ethylidene)bisphenol	12	2
17- β -Estradiol	<0.1	<0.1
17- α -Ethinylestradiol	<0.1	<0.1
Bisphenol A diglycidyl ether (BADGE)	<0.1	<0.1
Zearalanone	<0.1	<0.1
Estrone	<0.1	<0.1
Estriol	0.2	0.15
Dienestrol	<0.1	<0.1
Nonylphenol	1.5	0.7
Diethylstilbestrol	<0.1	<0.1
Hexestrol	<0.1	<0.1
Coumestrol	<0.1	<0.1
Genistein	<0.1	<0.1
4,4'-Cyclohexylidenebisphenol	<0.1	2.21

Calibration graphs of the compounds were prepared in running buffer. Both, MAb 12- and PAb K66-based BIAs showed high cross-reactivity towards BVA (73% and 118%, respectively), as expected, because it was used as immunogen. Interestingly MAb 12 showed an even higher affinity for BPA than for BVA. MAb 12 also showed a high cross-reactivity (< 10%) with 4,4'-(ethylidene) bisphenol and a small cross-

reactivity (< 2.5%) with nonylphenol, bis-(4-hydroxyphenyl)-methane and 4-cumylphenol. On the other hand, PAb K66 showed an overall lower (< 2%) cross-reactivity than MAb 12 with 4,4' (ethylidene) bisphenol. PAb K66 cross-reacted (2.2%) with 4,4' cyclohexylidenebisphenol. Cross-reactivities of both BIAs towards most of the estrogenic compounds were very low (<0.1%) making these BIAs very specific.

Conclusions

It was possible to raise MAbs and PAbS against a BVA conjugate that showed strong cross-reactions towards the target compound, BPA. The kinetic parameters of the MAb-BPA interaction were useful and reliable for predicting assay performance. The direct (non-competitive) assay proved that a small analyte like BPA (228 g/mol) can be directly detected and it was also shown that this is the most sensitive format, something which is in accordance to the theory [26]. However, the direct assay was also the least robust due to the fast decrease in binding capacity of the immobilized MAbs. Future research using techniques of protein engineering which can potentially provide more robust biorecognition molecules would significantly improve this assay.

The inhibition immunoassay with BVA immobilized directly on the chip was very robust due to a stable chip (>1500 cycles were run under the mentioned conditions) and high maximum responses (700 RU).

Both MAb 12- and PAb K66-based BIAs were fast (6 min/sample), specific as well as accurate and repeatable for the screening of BPA in real water samples at low $\mu\text{g L}^{-1}$ levels.

We have shown that if lower concentrations, in the order of ng L^{-1} , are to be measured, the sensitivity of the assays can be improved by using solid phase extraction (SPE) to obtain a pre-concentration of the samples. This approach proved to be useful at the expenses of the throughput of the system. The validation of the system and measurements of environmental samples are issues which will require further attention.

Acknowledgements

This study is part of a PhD project supported by a Marie Curie Host Industry Fellowship from the EU funded Marie Curie foundation. The authors thank Dr Kees Koopal who kindly suggested the use of BVA as an analogue for BPA, Nathalie Smits and Jolanda du Pré of RIKILT for the production of the MAbs and Gijsbert Peelen of ELTI-Support for organizing the immunizations.

References

1. Hock B, Barcelo D, Cammann K In Teubner-Reihe Umwelt; Hock, B, Barceló, D, Camman, K, Hansen, PD, Turner, APF, Eds.; Teubner, B.G.: Stuttgart-Leipzig, 1998
2. Ash M, Ash I (1995) Handbook of Plastic and Rubber Additives: An International Guide to More Than 12, 000 Products by Trade Name, Composition, Function and Manufacturer, Gower Publishing Ltd, Hampshire
3. Krishnan AV, Stathis P, Permuth SF, Tokes L, Feldman D (1993) Bisphenol-A: an estrogenic substance is released from polycarbonate flasks during autoclaving *Endocrinology* 132, 2279-86
4. Biles JE, McNeal TP, Begley TH, Hollifield HC (1997) Determination of Bisphenol-A in Reusable Polycarbonate Food-Contact Plastics and Migration to Food-Simulating Liquids *J. Agric. Food Chem.* 45, 3541-44
5. Brede C, Fjeldal P, Skjevraak I, Herikstad H (2003) Increased migration levels of bisphenol A from polycarbonate baby bottles after dishwashing, boiling and brushing *Food Addit. Contam.* 20, 684-9
6. Staples CA, Dorn PB, Klecka GM, O'Block ST, Harris LR (1998) A review of the environmental fate, effects, and exposures of bisphenol A *Chemosphere* 36, 2149-73
7. Furhacker M, Scharf S, Weber H (2000) Bisphenol A: emissions from point sources *Chemosphere* 41, 751-6
8. Bolz U, Hagenmaier H, Korner W (2001) Phenolic xenoestrogens in surface water, sediments, and sewage sludge from Baden-Wurtemberg, south-west Germany *Environ. Pollut.* 115, 291-301
9. Heemken OP, Reincke H, Stachel B, Theobald N (2001) The occurrence of xenoestrogens in the Elbe river and the North Sea *Chemosphere* 45, 245-59
10. Fromme H, Küchler T, Otto T, Pilz K, Müller J, Wenzel A (2002) Occurrence of phthalates and bisphenol A and F in the environment *Water Res.* 36, 1429-38
11. Vethaak AD, Rijs GBJ, Schrap SM, Ruiter H, Gerritsen A, Lahr J; RIZA/RIKZ.: Lelystad, 2002, 292

12. Matthews JB, Twomey K, Zacharewski TR (2001) In vitro and in vivo interactions of bisphenol A and its metabolite, bisphenol A glucuronide, with estrogen receptors alpha and beta *Chem. Res. Toxicol.* 14, 149-57
13. Hunt PA, Koehler KE, Susiarjo M, Hodges CA, Llagan A, Voigt RC, Thomas S, Thomas BF, Hassold TJ (2003) Bisphenol a exposure causes meiotic aneuploidy in the female mouse *Curr. Biol.* 13, 546-53
14. Wetherill YB, Petre CE, Monk KR, Puga A, Knudsen KE (2002) The xenoestrogen bisphenol A induces inappropriate androgen receptor activation and mitogenesis in prostatic adenocarcinoma cells *Mol. Cancer Ther.* 1, 515-24
15. Segner H, Carroll K, Fenske M, Janssen CR, Maack G, Pascoe D, Schafers C, Vandenberg GF, Watts M, Wenzel A (2003) Identification of endocrine-disrupting effects in aquatic vertebrates and invertebrates: report from the European IDEA project *Ecotoxicol. Environ. Saf.* 54, 302-14
16. Carlsen E, Giwercman A, Keiding N, Skakkebaek NE (1995) Declining semen quality and increasing incidence of testicular cancer: is there a common cause? *Environ. Health Perspect.* 103 Suppl 7, 137-9
17. Moriyama K, Tagami T, Akamizu T, Usui T, Saijo M, Kanamoto N, Hataya Y, Shimatsu A, Kuzuya H, Nakao K (2002) Thyroid hormone action is disrupted by bisphenol A as an antagonist *J. Clin. Endocrinol. Metab.* 87, 5185-90
18. Tan BL, Kassim NM, Mohd MA (2003) Assessment of pubertal development in juvenile male rats after sub-acute exposure to bisphenol A and nonylphenol *Toxicol. Lett.* 143, 261-70
19. Paseiro Losada P, PerezLamela C, LopezFabal MF, SanmartinFenollera P, Simal Lozano J (1997) Two RP-HPLC Sensitive Methods To Quantify and Identify Bisphenol A Diglycidyl Ether and Its Hydrolysis Products. 1. European Union Aqueous Food Simulants *J. Agric. Food Chem.* 45, 3493-500
20. Inoue K, Yoshie Y, Kondo S, Yoshimura Y, Nakazawa H (2002) Determination of phenolic xenoestrogens in water by liquid chromatography with coulometric-array detection *J. Chromatogr. A* 946, 291-4
21. Zafra A, del Olmo M, Suarez B, Hontoria E, Navalon A, Vilchez JL (2003) Gas chromatographic-mass spectrometric method for the determination of bisphenol A and its chlorinated derivatives in urban wastewater *Water Res.* 37, 735-42
22. Fujimoto S, Goda Y (2000) Development of ELISAs for endocrine disrupting chemicals *Nippon Rinsho* 58, 2491-4

23. Ohkuma H, Abe K, Ito M, Kokado A, Kambegawa A, Maeda M (2002) Development of a highly sensitive enzyme-linked immunosorbent assay for bisphenol A in serum *The Analyst* 127, 93-7
24. De Meulenaer B, Baert K, Lanckriet H, Van Hoed V, Huyghebaert A (2002) Development of an enzyme-linked immunosorbent assay for bisphenol a using chicken immunoglobulins *J. Agric. Food Chem.* 50, 5273-82
25. Quinn J, Patel P, Fitzpatrick B, Manning B, Dillon P, Daly S, Okennedy R, Alcocer M, Lee H, Morgan M, Lang K (1999) The use of regenerable, affinity ligand-based surfaces for immunosensor applications *Biosens. Bioelectron.* 14, 587-95
26. Ekins R (1994) Immunoassay: recent developments and future directions *Nucl. Med. Biol.* 21, 495-521
27. Haasnoot W, Pre JD, Cazemier G, Kemmers-Voncken A, Verheijen R, Jansen BJM (2000) Monoclonal Antibodies Against a Sulfathiazole Derivative for the Immunochemical Detection of Sulfonamides *Food Agr. Immun.* 12, 127
28. Verheijen R, Osswald IK, Dietrich R, Haasnoot W (2000) Development of a One Step Strip Test for the Detection of (Dihydro)streptomycin Residues in Raw Milk *Food Agr. Immun.* 12, 31
29. Canziani GA, Klakamp S, Myszka DG (2004) Kinetic screening of antibodies from crude hybridoma samples using Biacore *Anal. Biochem.* 325, 301-7
30. Myszka DG (1999) Improving biosensor analysis *J. Mol. Recognit.* 12, 279-84
31. Myszka DG, Morton TA (1998) CLAMP: a biosensor kinetic data analysis program *Trends Biochem. Sci.* 23, 149-50
32. Waters (2002) Environmental and Agrochemical Applications WA20252 *Waters Corporation*, 26-27
33. Azevedo DA, Lacorte S, Viana P, Barceló D (2001) Occurrence of nonylphenol and bisphenol-A in surface waters from Portugal *J. Braz. Chem. Soc.* 12, 532-37
34. Jobling S, Casey D, Rogers-Gray T, Oehlmann J, Schulte-Oehlmann U, Pawlowski S, Baunbeck T, Turner AP, Tyler CR (2004) Comparative responses of molluscs and fish to environmental estrogens and an estrogenic effluent *Aquat. Toxicol.* 66, 207-22
35. Rossi DT, Zhang N (2000) Automating solid-phase extraction: current aspects and future prospects *J. Chromatogr. A* 885, 97-113

Chapter 3

Biosensor Recognition of Thyroid Disrupting Chemicals Using Transport Proteins

Abstract

Novel surface plasmon resonance-based biosensor assays for the bioeffect-related screening of chemicals with thyroid disrupting activity are described. Two thyroid transport proteins (TPs), thyroxine binding globulin (TBG) and recombinant transthyretin (rTTR), were applied in an inhibition assay format in a Biacore 3000 using CM5 biosensor chips coated with L-thyroxine (T4), the main hormone of the thyroid system. Assay conditions were optimized for the natural thyroid hormones and known thyroid disruptors and structurally related compounds were selected as model compounds to be tested in both assays for their relative potency (RP) compared to T4. The chosen compounds were halogenated phenols, halogenated bisphenols, bisphenol A and 3,5-dichlorobiphenyl and its hydroxylated metabolite 4-hydroxy-3,5-dichlorobiphenyl (4-OH PCB 14). The TBG-based assay was highly specific for T4 and the rTTR-based assay was sensitive toward several compounds, the highest sensitivity (RP = 4.4) being obtained with 4-OH PCB 14, followed by tetrabromobisphenol A (RP = 1.5) and tetrachlorobisphenol A (RP = 0.75).

For the bioeffect-related screening of known and identification of possible new thyroid disruptors, the TPs-based biosensor assays were more sensitive (IC_{50} of 13.7 ± 1.3 nM and 8.6 ± 0.7 nM for the rTTR and the TBG-based assay respectively), easier to perform and faster alternatives (10 min per sample) compared to the currently used methods such as radioligand binding assays and immunoprecipitation-HPLC.

Introduction

Diverse groups of chemical compounds are released in to the environment and some of these are considered endocrine disrupting chemicals (EDCs). A chemical is considered an EDC if it mimics or antagonizes the effects of endogenous hormones or if it is able to disrupt the synthesis or metabolism of endogenous hormones and hormone receptors [1]. The different EDCs can be roughly grouped by their biological effect. One of these compound classes is the thoroughly studied group of estrogenic compounds [1, 2]. Another group of compounds, which has received less attention, are the compounds with thyroid activity. Previous investigations show that organohalogen compounds can affect thyroid gland morphology and hormonal status in rats [3]. These compounds can disrupt the thyroid hormone system at least at three different levels; at the thyroid gland, at the thyroid hormone transport proteins and at the thyroid hormone metabolism [4]. The polyhalogenated aromatic hydrocarbons (PHAHs) are lipophilic compounds present in the environment and known to bioaccumulate in the trophic chain [3]. PHAHs are hydroxylated in vivo by the cytochrome P450 monooxygenase system [5]. Some hydroxylated polychlorinated biphenyls, hydroxylated polychlorinated p-dioxins and hydroxylated polybrominated diphenyl ethers strongly resemble the structure of thyroxine (T4), the natural hormone of the thyroid system.

Some of the PHAHs and several hydroxylated metabolites interact with high affinity with transthyretin (TTR) [6, 7], one of the three thyroxine transport proteins (TPs) which carries ~20% of the total T4 in humans and larger eutherians. Likewise, although with a lower affinity, hydroxylated PHAHs bind to thyroxine binding globulin (TBG) [8, 9]. TBG is the major T4 TP in human plasma responsible for 75% of the T4 binding activity. Human serum albumin (HSA) is the third TP (carrying about 5% of the total T4).

Even though TTR carries only a minor part of the T4 pool in plasma in large eutherians, it is important for maternal to fetal transport of thyroid hormones and for delivery of T4 across the brain barrier [10]. TTR binding has also been suggested as predictive of interactions with other proteins involved in the T4 pathway [11].

It is hypothesized that one of the thyroid disruption mechanisms is through the displacement of the natural ligand T4 from TTR by the endocrine disruptors with a consequent increase in T4 clearance which induces hypothyroidism [12]. In smaller eutherians and vertebrates,

TTR is the major T4 transport protein, hence, in some wildlife like birds, amphibians, fish and rodents, the impact of EDCs binding to TTR would have greater effects than in humans [13]. Thyroid hormone transport is therefore a true pathway for thyroid disruption and T4 displacement from thyroid transport proteins is one biochemical marker for the screening of potential endocrine disruptors. Based on this concept, radioligand binding assays (RLBA), using [I^{125}] T4 as label, were employed to demonstrate the affinity of xenobiotics for these purified human and rat TTR and TBG [8, 14, 15]. Additionally, purified chicken and bullfrog TTR have been successfully used as the biorecognition elements in RLBA to obtain the average thyroid activity of a complex environmental sample using [I^{125}] T3 as label [16].

Although these widely used techniques have been shown to be sensitive and reliable, they involve the use of isotopes of which the handling and disposal are subjected to stringent regulations. Furthermore, a separation or wash procedure is involved to separate the free radioactive T4 fraction from the fraction bound to TTR or TBG. This separation step not only lowers the throughput but might also cause a deviation in the reaction equilibrium between the TPs and the ligands.

An alternative to these methods is the biosensor-based approach in which the same biochemical entities could be used for the bioeffect-related recognition of endocrine disruptors. Advantages of the biosensor-based approach and in particular of the surface plasmon resonance (SPR) technique are the speed of automated analysis, simplicity, quantitative and label-free analysis in real time as well as the possibility of kinetic and affinity analysis [17].

We investigated the use of human TPs, TBG and recombinant TTR (rTTR), as recognition elements using the SPR-based biosensor (Biacore 3000) in the inhibition assay format. To obtain a successful assay, the ligand (T4) linking chemistry to the chip surface was optimized to preserve its biochemical properties. The nature of the rTTR-T4 interaction was compared to that of the purified human TTR (pTTR) and to that of rTTR-T4 analogue immobilized on the sensor chip.

The assays were optimized to obtain the highest sensitivity and robustness by evaluating the optimum binding pH, ionic strength and buffer composition. Seven endocrine disruptors, belonging to three different structural groups were evaluated for inhibition in these assays and their relative potencies (RP) to T4 were measured.

Experimental Section

Chemicals and Equipment

Sensor chips (CM5 and NTA), the amine coupling kit [containing 0.1 M N-hydroxysuccinimide (NHS), 0.4 M 1-ethyl-3-(3-dimethylaminopropyl) carbodiimide hydrochloride (EDC) and 1 M ethanolamine hydrochloride (pH 8.5)] and the Biacore 3000 were supplied by Biacore AB (Uppsala, Sweden). The PCB 3,5-dichlorobiphenyl (PCB 14) and 4-hydroxylated-3,5-dichlorobiphenyl (4-OH PCB 14) were purchased from Accu Standard (New Haven, CT). L-Thyroxine ((T4) 3,3',5,5'-tetraiodo-L-thyronine), 3,3',5-triiodothyronine (T3), bisphenol A (BPA; 2, 2-bis (4-hydroxyphenyl) propane), tetrabromo-BPA, tetrachloro-BPA, pentachlorophenol, pentabromophenol, 5-aminovaleric acid (AVA), glycine, purified TTR (pTTR) and all other reagents were obtained from Sigma-Aldrich Chemie (Zwijndrecht, The Netherlands) unless otherwise stated.

The recombinant His-tagged transthyretin (rTTR) was a kind gift from the Toyama Medical and Pharmaceutical University (Toyama, Japan). Thyroxine Binding Globulin (TBG) was a kind gift from Scipac (Kent, UK).

Biosensor Chip Immobilization Procedures

Five different spacers and two different chemistries were evaluated for the immobilization of T4 to the carboxymethylated dextran surface of the CM5 sensor chip. The spacer structures and immobilization chemistries are depicted in Figure 1. First, we evaluated the immobilization of T4 via the carboxyl group of the alanyl side chain (Figure 1B) using ethylenediamine (EDA) as we previously described for bisphenol A [18].

In the other four immobilization procedures, T4 was immobilized via the amino group of the alanyl side chain using spacers of different length: (1) no spacer, creating a direct amide bond between the amino group and the carboxymethylated dextran (Figure 1C), (2) with glycine (Gly) as the bifunctional spacer (Figure 1D), (3) with 5-aminovaleric acid (AVA) as spacer (Figure 1E) and (4) with two molecules of AVA as spacer (Figure 1F). Figure 1G shows the binding of rTTR (18.2 nM) to the different immobilized conjugates.

The CM5 sensor chip surface was activated by injecting 140 μL of a mixture of 0.4 M EDC and 0.1 M NHS (1:1; v/v) at a flow rate of 5 $\mu\text{L min}^{-1}$. The activation was followed by 140 μL injections, at a flow rate of 5 $\mu\text{L min}^{-1}$, of either the T4 (2 mM in 10 mM borate buffer pH 8.5) or the spacer (2 mM in 10 mM borate buffer pH 8.5) depending on the applied immobilization procedure.

The double AVA spacer was constructed on the sensor chip surface by the immobilization of AVA followed by a new AVA immobilization procedure on the AVA surface. After the immobilization of the proper spacer and activation with EDC/NHS, T4 was immobilized as described above.

The T4 stock solution (10 mM) was prepared by dissolving T4 in a solution containing DMSO (94%) chloroform (5%) and 1 M NaOH (1%).

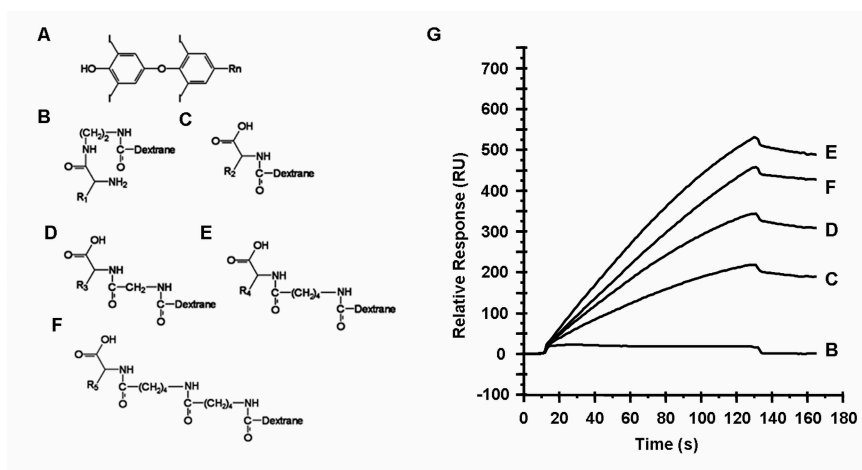


Figure 1. Conjugation position and structures of the different spacers used to immobilize L-thyroxine (T4) to the carboxymethylated dextran surface of the CM5 biosensor chip. (A) Structure of T4 without the terminal alanine group (Rn). (B) Immobilization of T4 via the alanine's carboxyl group using ethylenediamine (EDA) as spacer. (C-F) Immobilizations of T4 via the alanine's amino group, (C) direct to the dextrane without a spacer (D), with glycine (Gly) as the bifunctional spacer, (E) with 5-aminovaleric acid (AVA) as spacer, and (F) with two molecules of AVA as spacer. (G) Binding sensorgrams of rTTR (18.2 nM) to the different conjugates.

Optimization of Transport Protein Binding Conditions.

In previous studies [6, 8, 12, 19], the *in vitro* T4-TTR radioligand competitive binding assays were performed at pH 8 in a Tris-HCl buffer

(0.1 M Tris-HCl, 0.1 mM NaCl, 1 mM EDTA). This buffer was found unsuitable for use in the biosensor due to the nonspecific binding of Tris to the sensor chip surface. Borate, phosphate and carbonate buffers were evaluated, and their compositions (pH, NaCl and EDTA concentrations) were optimized.

To evaluate the different T4-modified sensor chip surfaces and the optimum conditions for binding and inhibition, 50 μL of either TTR or TBG (18.2 nM in phosphate buffer pH 8.5) without (blank) or with T4 solution (100 nM) were injected at a flow rate of 25 $\mu\text{L min}^{-1}$. The responses (R) used for comparison were measured 20 s after the injection ended. The surface was regenerated in two steps, first by a 5 μL injection with H_3PO_4 (0.1 M) which was followed by 10 μL of NaOH (0.1 M).

Percentage of inhibition (PI) during these experiments was calculated as $\text{PI} = ((B_0 - B)/B_0) \times 100\%$, where B_0 is the TP response obtained with 0 nM T4 (blank) and B is the TP response in the presence of 100 nM T4.

Direct Capture Assay for the Measurement of the rTTR- T4 Kinetics.

In order to evaluate the nature of the rTTR-T4 kinetic interaction under the chosen conditions, the rTTR was captured on a nickel chelating sensor chip surface (NTA Chip) by means of its His tag. For this purpose, 5 μL of a NiCl solution (100 mM in water) were injected at a flow rate of 10 $\mu\text{L min}^{-1}$ over the sensor surface followed by 10 μL of rTTR (10 $\mu\text{g mL}^{-1}$). Phosphate buffer pH 8.5 (10 mM Na_2HPO_4 , 0.1 M NaCl) was used as the running buffer. A serial (3-fold) T4 dilution (9 μM - 0.1 nM) was injected for 60 s at a flow rate of 100 $\mu\text{L min}^{-1}$ over the captured rTTR and the binding response of T4 was measured 5 s after the injection ended, which was at the beginning of the dissociation phase. Regeneration of the surface was possible in three steps, at a flow rate of 10 $\mu\text{L min}^{-1}$, in which an injection of 10 μL of EDTA (0.35 M) was followed by 5 μL of NaOH (0.1 M) and finally by 5 μL of a BSA solution (2 mg mL^{-1} in phosphate buffer pH 8.5).

A suitable reference surface was constructed by capturing denatured rTTR (heated at 100 $^\circ\text{C}$ for 5 min) following the same protocol as described above. The sensorgrams were double referenced as described elsewhere [20] and the calibration curve obtained was fitted to a suitable model using Scrubber software.

Transport Protein Biosensor Inhibition Assays.

For the evaluation of the RPs of the different compounds, inhibition assay formats were evaluated for rTTR, pTTR and TBG. The principle of the assay is similar to an inhibition immunoassay. In solution, the T4 TP under evaluation is mixed with the analyte of interest and injected over a sensor surface with an immobilized T4-conjugate. If there is no binding of the analyte to the TP, the maximum amount of TP will bind to the sensor surface and a maximum response is obtained. If there is an interaction between the analyte and the TP in solution, the binding of TP to the sensor surface will be inhibited resulting in a lower response. The inhibition of response depends on the concentration of the T4-like analyte as well as on the affinity of this compound for the TP. Therefore, calibration curves (injected concentrations versus responses) of the analyte of interest were compared with a T4 curve and the RP was calculated as the ratio of T4 concentration at 50% inhibition (IC_{50}) versus the IC_{50} of the analyte [IC_{50} (T4)/ IC_{50} (analyte)].

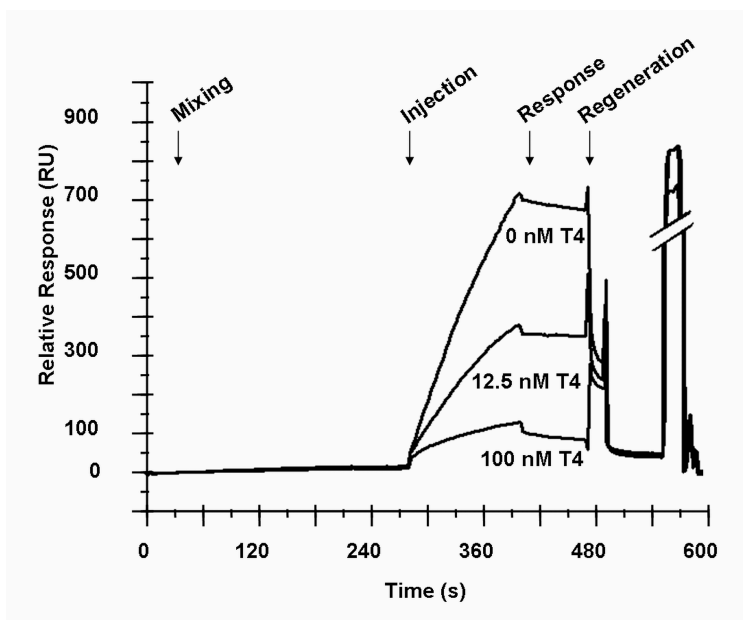


Figure 2. Overlaid sensorgrams showing the binding of rTTR (18.2 nM) mixed (1:9; v/v) with different concentrations of T4 (0 nM, 12.5 nM, 100 nM).

The protocol used was as follows, 10 μL of the TP (182 nM) was mixed in the Biacore with 90 μL of the analyte solution and, immediately after mixing, 50 μL was injected over the sensor chip surface at a flow rate of 25 $\mu\text{L min}^{-1}$ and the response was measured 5 s after the injection ended. The surface was regenerated as described above (Optimization of transport protein binding conditions). Overlaid sensorgrams of the rTTR inhibition assay, corresponding to three different concentrations of T4, are presented in Figure 2. The total run time between samples, including the time for mixing and washing steps in the Biacore, was 10 min. Triplicate injections were performed for each analyte at each concentration.

Results and Discussion

Binding of the TPs to the T4 Sensor Chip Surface.

Table 1 presents the relative responses obtained from the sensorgrams of rTTR and TBG (in phosphate buffer, pH 8.5) binding to the T4 chips coated with the different immobilization chemistries and spacers. The immobilization of T4 via its carboxyl group seriously hindered the binding of the TPs to the sensor chip surface, as shown by the very low responses obtained. This is supported by previous studies where it was found that the side-chain carboxyl group plays a major role in the T4-TTR binding [19].

Table 1. Relative responses obtained with rTTR and TBG binding to the different T4-coated biosensor chips made with different immobilization chemistries (via the carboxyl or the amino group of T4) and with different spacers.

Spacer	Length (atoms)	T4 functional group	Relative responses (%)	
			rTTR	TBG
EDA	4	Carboxyl	0.2	1.5
No	0	Amino	39	64
Glycine	3	Amino	63	76
AVA	6	Amino	100	100
2xAVA	12	Amino	87	68

Immobilization of T4 via its amino group yielded high responses for both TPs, and responses increased with increasing spacer lengths up to a maximum with the six-atoms spacer ((AVA) 5 carbons plus 1 nitrogen). The almost 2-fold higher response obtained with the TBG with the same conjugate could be explained by the previously reported higher affinity of TBG for T4 compared with TTR [21]. Further increase of spacer length did not result in higher responses, therefore the T4-AVA sensor chip surface was used in all the subsequent inhibition experiments.

Optimization of the Inhibition Assay Conditions

Of the three buffers tested, only phosphate was suitable for long term use. The use of borate and carbonate buffers with the T4-AVA sensor chip resulted in an increasing baseline, which was difficult to regenerate and led to a reduced binding capacity of the chip. The results obtained with the phosphate buffer optimization experiments in the rTTR-based assay are shown in Table 2.

Table 2. Results obtained with the phosphate buffer optimization experiments in the rTTR-based assay^a.

pH	rR1	rPI	NaCl (mM)	rR2	EDTA (μM)	rR3
7.5	96	49	0	32	0	100
8	100	81	50	91	1	77
8.5	94	100	100	100	10	42
9	66	74	200	97	100	37
9.5	33	38	500	87	1000	30
-	-	-	1000	45	-	-

^aThe relative Responses (rR = % of the highest obtained response) were measured at different pH (rR1) and the Percentage of Inhibition (PI) during these experiments was calculated as $PI = ((B_0 - B)/B_0 \times 100)$, where B_0 is the rTTR response obtained with 0 nM T4 (blank) and B the rTTR response in the presence of 100 nM T4. The relative PI (rPI) was the percentage of the highest obtained PI. At optimum pH for rPI, various NaCl concentrations were evaluated (rR2) and at optimum pH and NaCl concentrations, different EDTA concentrations were tested (rR3).

The highest response was obtained at pH 8 (700 RU). However, the largest relative percentage of inhibition (rPI, the relative difference in response between a blank and 100 nM of T4) was obtained at pH 8.5 and, as we aimed for maximum sensitivity of the assays, this pH was considered optimum. The addition of NaCl improved the assay with an optimum of 100 mM, and the presence of micromolar levels of EDTA inhibited the rTTR binding to the T4-AVA sensor chip surface with a $IC_{50} = 3.1 \mu\text{M}$. All the following experiments were performed in 10 mM phosphate (Na_2HPO_4) buffer with pH 8.5 and 0.1 M NaCl added, which was found optimal for the TBG assay as well.

Nature of the T4 -Transport Proteins Interaction

The aim of this study was to set up an inhibition assay using rTTR to facilitate large scale screening in the future. Therefore we compared the T4 binding properties of the rTTR with those of pTTR. It has been previously reported that the rTTR used in the present study had the same biochemical characteristics as those found with the pTTR with regard to tetramer formation at neutral pH and fibril formation at acidic pH [22]. TTR has two non cooperative T4 binding sites, meaning that upon binding of the first T4 molecule with high affinity ($K_{a1} \approx 100 - 10 \text{ nM}$), the second T4 molecule binds to the second site with a lower affinity ($K_{a2} \approx 1 \mu\text{M}$) at physiological conditions [19, 23]. We investigated whether both binding sites of the rTTR were able to bind T4 or the AVA-T4 sensor chip surface under the chosen conditions because this would have a direct effect on the geometry of the inhibition curve and therefore on the working range and linearity of the assay.

First, we investigated whether both rTTR binding sites were active for binding T4 at the chosen conditions. Therefore, we evaluated the equilibrium dissociation constants (K_D) of the T4-rTTR interaction using the direct capture assay (see Experimental section). The calibration curve obtained (Figure 3) clearly shows a biphasic binding response indicating that both sites are active for binding T4. The data obtained showed a poor fitting to a non cooperativity model and were fitted to a two independent binding sites model with a K_{D1} of $9.2 \pm 1.2 \text{ nM}$ for the high affinity binding site and a K_{D2} of $5.3 \pm 3.1 \mu\text{M}$ for the low affinity binding site. The second binding site did not show full occupancy because the T4 concentration could not be increased beyond $9 \mu\text{M}$ due to its poor solubility. This fact induced a high uncertainty in the K_{D2} value and gave a poor fit using the negative cooperativity model.

Nevertheless, the present results indicate that, under the assay conditions used, the binding affinity of the second site is found at μM levels of T4.

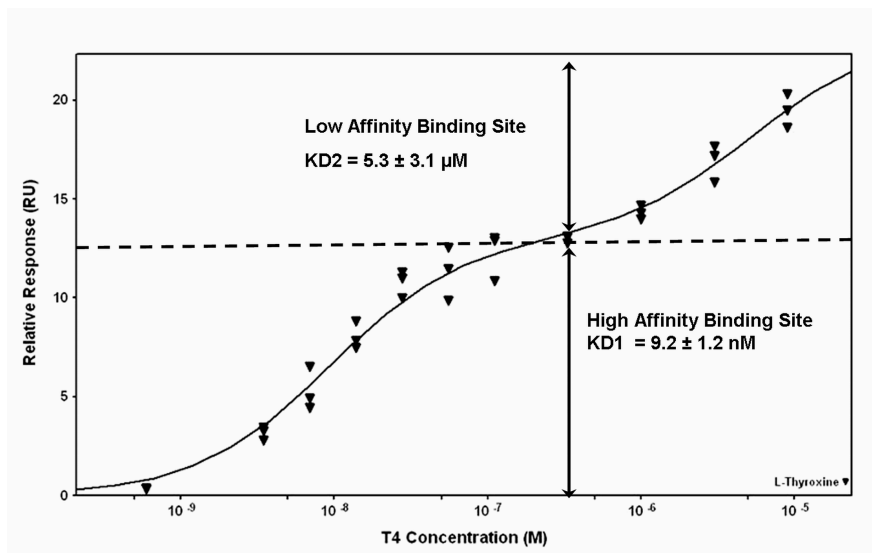


Figure 3. Calibration curve of the binding of T4 to rTTR as obtained in the direct capture assay. The calibration curve shows a biphasic binding response, and the data were fitted to a two independent binding sites model with a K_{D1} of 9.2 ± 1.2 nM for the high affinity binding site and a K_{D2} of 5.3 ± 3.1 μM for the low affinity binding site showing that both sites are active.

Secondly, a T4 calibration curve was measured using the rTTR inhibition assay and it was successfully fitted to a one binding site bimolecular model with a K_D of 13.7 ± 1.3 nM. This affinity constant of rTTR for T4 is in the same range as the K_{D1} obtained for the high affinity binding site using the direct binding assay. These results indicate that with the rTTR inhibition assay setup we are able to measure the inhibition of the high affinity binding site and that if T4 is bound to rTTR, then the T4-rTTR complex is not able to bind the AVA-T4 sensor chip surface with the low affinity binding site in significant amounts due to the approximately 500-fold difference in affinity between the two sites under these conditions. Furthermore the comparable K_D s for T4 in both assays mean that T4 has the same affinity for rTTR when it is immobilized by its amino group as when it is free in solution.

The effect of EDTA on the equilibrium dissociation constants (K_{DS}) was investigated using the direct capture assay in the presence 3 μM of EDTA which was added to the phosphate buffer.

Under the influence of EDTA, the calibration curve was fitted to a one binding site bimolecular model with a K_D of 51.9 ± 1.7 nM and the previously obtained biphasic response was not found (data not shown). These results indicate that the presence of 3 μM EDTA lowered the affinity between T4 and rTTR by a factor of 5 and, in principle, that the affinity of T4 for the low affinity binding site is also lowered by an unknown factor. These results are in good agreement with the low binding observed of rTTR to the AVA-T4 sensor chip surface at increasing concentrations of EDTA.

T4 calibration curves were compared using pTTR and rTTR. The response obtained with the pTTR (18.2 nM) was about six times lower (112 RU) if compared to rTTR at the same concentration. We speculate that this difference is probably due to a loss in T4 binding activity during the pTTR purification procedure. The IC_{50} value for T4 obtained with the rTTR-based assay ($IC_{50} = 13.5$ nM) was comparable to that obtained using the pTTR-based assay ($IC_{50} = 14.9$ nM) and both calibration curves were fitted to a one-binding site model using Graphpad Prism software.

The T4-TBG interaction was also evaluated using the inhibition assay format. The curve fitted to a one-binding site model yielded an affinity constant K_D of 8 nM. All further calibration curves were fitted to a four-parameter equation using BIAevaluation software (Biacore), and the IC_{50} was the parameter used for sensitivity comparison.

Biosensor Thyroid Transport Protein Inhibition Assays for T4 and T3

The rTTR and TBG inhibition assays were tested with the natural ligands T4 and T3 and inhibition curves were determined in triplicate of which the averages are shown in Figure 4. The TBG assay (Figure 4B) was found to be the most sensitive toward the natural ligands with IC_{50} values of 8.6 nM for T4 and 14.2 nM for T3. In comparison, the IC_{50} values with the rTTR assay (Figure 4A) were 13.7 nM for T4 and 216.3 nM for T3. The IC_{50} values obtained for T4 in both assays were used as the reference value for the calculation of the RPs of the EDCs. The RP for T3 using the rTTR inhibition assay ($RP = 0.06$) is consistent with

previous studies where the reported RPs for T3 were 0.036 [24] and 0.08 [25]; however the RP for T3 found in this study using the TBG inhibition assay (RP = 0.6) is higher than the reported RPs of 0.09 [24] and 0.3 [26] (Table 3).

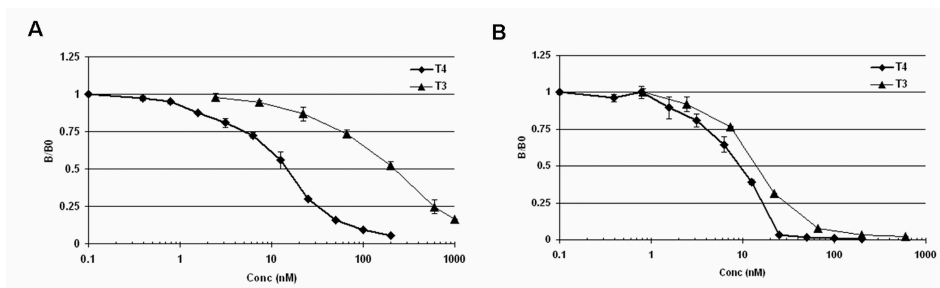


Figure 4. Calibration curves of the natural ligands T4 and T3 in (A) the rTTR-based biosensor inhibition assay and, (B) in the TBG-based biosensor inhibition assay.

Table 3. Structures of the Compounds Tested with the TP Inhibition Assays.

Compound	Structure	R1	R2	R3	R4	R5
Thyroxine	A	I	-	-	-	-
Triiodothyronine	A	H	-	-	-	-
Pentachlorophenol	B	Cl	Cl	Cl	Cl	Cl
Pentabromophenol	B	Br	Br	Br	Br	Br
Bisphenol A	C	H	H	H	H	H
TBrBPA	C	Br	Br	Br	Br	-
TCIBPA	C	Cl	Cl	Cl	Cl	-
4-OH PCB 14	D	Cl	OH	Cl	-	-
PCB 14	D	Cl	H	Cl	-	-

The limit of detection (LOD = concentration at average blank response minus three times the SD) for T4 in buffer was calculated as 0.7 nM in both assays.

To have an impression of the reproducibility (intra day CV%) and accuracy, responses obtained with one T4 standard solution (12.5 nM) were used in both assays to calculate the corresponding concentrations with different calibration curves ($n = 3$) which resulted in an average of 10.8 ± 0.6 nM in the rTTR-based assay (CV = 5%, accuracy = 86%) and 11.0 ± 0.9 nM in the TBG-based assay (CV = 8%, accuracy = 88%).

Compared with previous studies performed with [125 I]T4 binding assays [8, 9], with IC₅₀ values for T4 in the rTTR assay of 62 -138 nM and 52-85 nM in the TBG assay, the rTTR and the TBG biosensor assays were respectively four and six times more sensitive. As a consequence of the simple biosensor assay format, which does not involve the separation of free and bound fractions, the assays were more reproducible and TP consumption was $\sim 30\%$ lower.

Relative Potencies of Model EDCs in the Transport Protein-Based Biosensor Inhibition Assays.

In addition to the natural ligands (T4 and T3) we selected seven chemicals, as model compounds for EDCs belonging to three different structural groups (Table 3). These compounds were evaluated for inhibition in the rTTR- and TBG-based biosensor inhibition assays. The tested EDCs were pentachlorophenol (PCP) and pentabromophenol (PBP), belonging to the halogenated phenols (group B). Bisphenol A (BPA) and its halogenated forms tetrabromobisphenol A (TBrBPA) and tetrachlorobisphenol A (TCIBPA) in group C. Finally, group D is composed of two meta-substituted polychlorinated biphenyls (3,5 dichlorobiphenyl (PCB 14) and its 4-hydroxylated metabolite (4-OH PCB 14).

The calibration curves obtained for the halogenated phenols (Figure 5A) in the rTTR-based assay show that these compounds have lower affinity for TTR than T4 and the calculated RPs were 0.64 ± 0.1 for PBP and 0.53 ± 0.1 for PCP (Table 4). These results differ from those obtained previously using the RLBA where a RP of 7.14 was observed for PBP [14] and 1.74 for PCP [15].

The BPA curve (Figure 5B) showed no inhibition at the highest tested concentration (10 μM) and the halogenated forms (TBrBPA and TCIBPA) showed a comparable or lower inhibition compared to T4 with RPs of 1.5 ± 0.2 for TBrBPA and 0.75 ± 0.2 for TCIBPA. The RP obtained with TBrBPA is significantly lower than the previously reported RP of 10.6 [14]; however the RP for TCIBPA obtained with the biosensor inhibition assay is comparable to the reported value of 0.75 as well as the trend of higher relative potencies of brominated compounds over chlorinated compounds for the bisphenols [14] which is confirmed here using the biosensor inhibition assay.

Table 4. Experimental and literature values of the Relative Potency (RP) of the thyroid disrupting chemicals evaluated using the rTTR and TBG-based biosensor inhibition Assays^a.

Compound	RP values			RP values from lit.	
	TBG	rTTR	pTTR	TBG	pTTR
L-Thyroxine (T4)	1	1	1	1	1
Triiodothyronine (T3)	$0.6 \pm 0.05^*$	$0.06 \pm 0.01^{*d}$	-	0.09 [24] 0.3 [26]	0.036 [24] 0.08 [25]
Pentachlorophenol	<0.001	$0.53 \pm 0.1^*$	0.64 ± 0.13^d	0.001 [15]	1.74 [15]
Pentabromophenol	<0.001	$0.64 \pm 0.1^*$	0.4 ± 0.18^d	-	7.14 ± 1.11 [14]
Bisphenol A (BPA)	<0.001	<0.001 [*]	<0.001 [*]	-	<0.001 [14]
TBrBPA	<0.001	1.5 ± 0.2^d	1.06 ± 0.2^d	-	10.6 ± 1.29 [14]
TCIBPA	<0.001	$0.75 \pm 0.2^{*d}$	$0.66 \pm 0.04^{*d}$	-	0.76 ± 0.07 [14]
4-OH PCB 14	<0.001	$4.36 \pm 0.5^*$	$3.04 \pm 0.25^*$	<0.001 [9]	3.9 [9]
PCB 14	<0.001	<0.001	<0.001 [*]	-	0.59 [25]

^aResults shown are means \pm SD of triplicate measurements performed in different days. Values that differ significantly (Student's *t* test, $P < 0.05$), from T4 are indicated (*), from the following compound with higher RP (^d).

Finally, the polychlorinated biphenyl, PCB 14, showed no inhibition (Figure 5C), but its para-hydroxylated metabolite, 4-OH PCB 14 showed a RP of 4.36 ± 0.5 , confirming the previously reported high interaction with TTR [9]. The ranking of RPs was 4-OH PCB 14 (RP = 4.36 ± 0.5) > TBrBPA (RP = 1.5 ± 0.2) \geq T4 (RP = 1) > TCIBPA (RP = 0.75 ± 0.2) \geq PBP (RP = 0.64 ± 0.1) \geq PCP (RP = 0.53 ± 0.1).

The performance of the rTTR biosensor inhibition assay with the different compounds evaluated shows that the spectrum of detectable compounds is similar to the spectrum of compounds detectable with previously described assays; however, the RPs for PBP and TBrBPA measured are respectively 10 and 7 times lower than the previously reported RPs using RLBA.

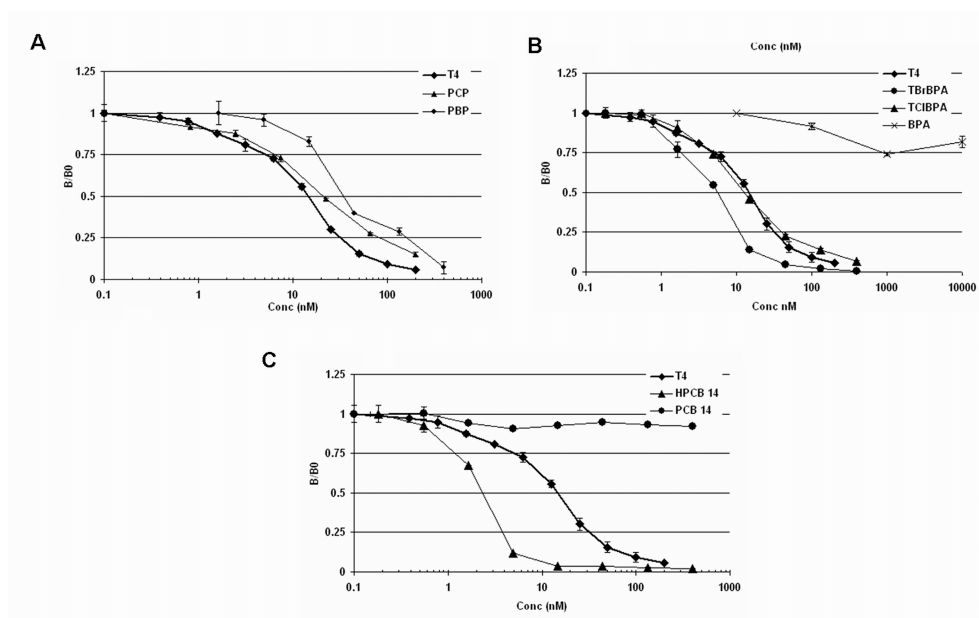


Figure 5. Calibration curves obtained in the rTTR-based biosensor inhibition assay for (A) Halogenated phenols, (B) halogenated bisphenols and (C) (hydroxy-) polychlorinated biphenyls.

To put aside the factor that the rTTR would have affinities different from TTR for the EDCs tested, we performed calibration curves (data not shown) for PBP, PCP, TBrBPA, TCIBPA, 4-OH PCB14 and PCB14 using the pTTR. The results of the biosensor inhibition assay show a similar ranking of affinities as well as absolute RP values (4-OH-PCB 14 (RP=3.04 ± 0.25) > TBrBPA (RP=1.06 ± 0.2) ≥ T4 (RP=1) > TCIBPA (RP=0.66 ± 0.04) ≥ PCIP (RP=0.64 ± 0.13) ≥ PBP (RP=0.4 ± 0.18) indicating that the difference in RP is not caused by the rTTR origin.

The magnitude of the inconsistency in RP values between methods is comparable to the difference in RPs reported by different groups, working with radioligand assays with the estrogen receptor [27] or using

other methods [28]. For example, one study reported 26 parent PCBs binding to TTR with significant RPs (0.05-8.23) using the RLBA [25]. In contrast, a different study selected eight of these parent PCBs and reported that they could only confirm the interaction of two of the PCBs with TTR using an immunoprecipitation-HPLC method [29]. In agreement with the mentioned study, we could not find any interaction between rTTR and PCB14, although an RP of 0.59 was previously reported [25].

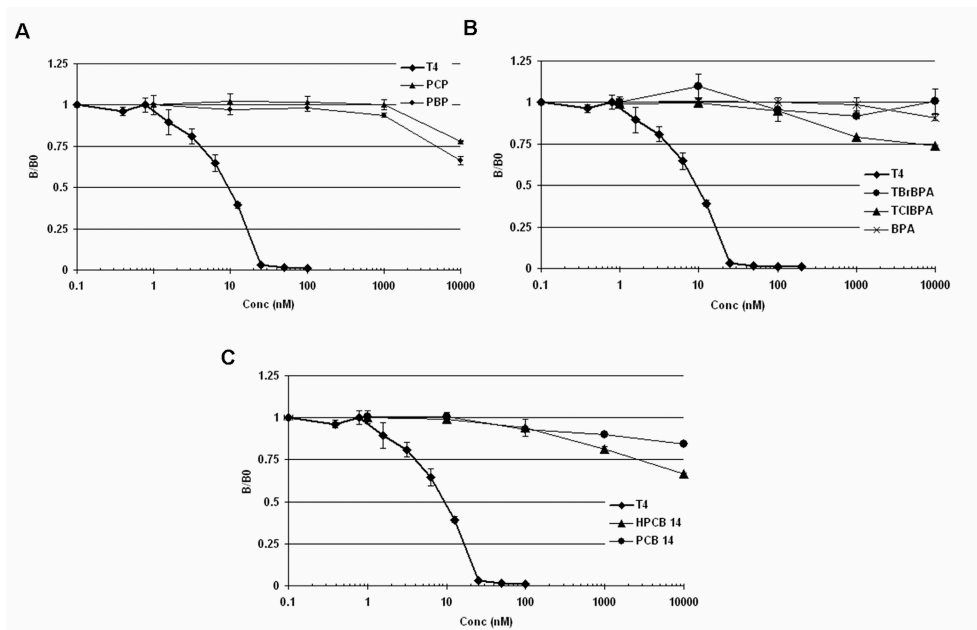


Figure 6. Calibration curves obtained in the TBG-based biosensor inhibition assay for (A) Halogenated phenols, (B) Halogenated bisphenols and (C) (Hydroxy-) polychlorinated biphenyls.

The complex nature of the TTR binding sites and kinetics are a further issue to consider as the source of the RP inconsistency. Dissimilar binding kinetics were reported for TTR ligands depending on their structures, some compounds were able to bind to TTR with negative cooperativity (like T₄), other compounds were found to bind with positive cooperativity (the binding of the ligand to one binding site increases the affinity of the second site for the ligand), and even with non cooperativity (the binding of the ligand is independent in both sites) [30].

Different binding kinetics for some compounds might result in higher or lower dissociation rates of the TTR-ligand complex which, in methods where separation steps are needed, could displace the equilibrium reached during the incubation giving results unrelated among the different ligands. Hence the different RPs obtained with the TP-biosensor inhibition assay are probably due to differences between methods, as well as from the previously suggested sensitivity of TTR to the buffer conditions used [26]. For instance, in our assay the presence of EDTA was shown to specifically inhibit TTR binding to the chip and also significantly alter rTTR-T4 interaction kinetics. Other possible sources of variation are the higher pH (8.5), higher temperature (25 °C), and lower incubation time.

As shown in Figures 6, the TBG-based biosensor inhibition assay was very specific for T4, consistent with previous studies in which diverse groups of compounds and metabolites were tested for competitive interactions and only a few compounds bound to TBG showing in all cases RP values below 0.03 [6, 9, 15]. However, T4 is one of the top 200 most widely prescribed drugs in the United States (top 200 prescribed drugs www.rxlist.com) and it is a potential endocrine disruptor if present in the environment like some other prescribed drugs known to bind TBG [21, 31]. Moreover, and given that TBG plays a major role in T4 transport in humans the biosensor TBG-based assay is a useful complement to the rTTR-based assay for the assessment of potentially new hazardous endocrine disruptors interacting with the thyroid system.

Conclusions

In the present study, we developed novel SPR-based biosensor inhibition assays for the bioeffect-related screening of chemicals with thyroid disrupting activity using the thyroid transport proteins rTTR and TBG as biorecognition elements.

The automated biosensor assays are more sensitive for the natural ligands (T4 and T3) compared with current methods, they are fast (run time between samples is 10 min), easy to perform (no labels), robust (the sensor chip was used for hundreds of cycles) and can be performed with a high reproducibility and accuracy. The rTTR-based biosensor inhibition assay was sensitive toward the model EDC compounds (halogenated phenols and bisphenols and hydroxylated PCB). The spectrum of detectable compounds is comparable to other methods; therefore, the rTTR inhibition assay can be a useful tool for the identification and ranking of the relative potencies of new chemicals with thyroid-disrupting activity and for the screening of samples with potential thyroid activity.

The TBG-based biosensor inhibition assay is suitable for a sensitive and specific detection of T4 and for the assessment of potentially new hazardous endocrine disruptors interacting with the thyroid system. Further research will focus on screening a larger panel of compounds and on validating the TP-based biosensor inhibition assays for the screening of real environmental and food samples for thyroid activity.

Acknowledgments

This study is part of a PhD project supported by a Marie Curie Host Industry Fellowship (Contract EVK1-CT-2001-55002) from the EU funded Marie Curie foundation. Scipac is thanked for his kind gift of the TBG.

References

1. Sonnenschein C, Soto AM (1998) An updated review of environmental estrogen and androgen mimics and antagonists *J. Steroid Biochem. Mol. Biol.* 65, 143-50
2. Amaral Mendes JJ (2002) The endocrine disrupters: a major medical challenge *Food Chem. Toxicol.* 40, 781-88
3. Brouwer A, Ahlborg UG, Van den Berg M, Birnbaum LS, Boersma ER, Bosveld B, Denison MS, Gray LE, Hagmar L, Holene E (1995) Functional aspects of developmental toxicity of polyhalogenated aromatic hydrocarbons in experimental animals and human infants *Eur. J. Pharmac.* 293, 1-40
4. Brouwer A, Morse DC, Lans MC, Schuur AG, Murk AJ, Klasson-Wehler E, Bergman A, Visser TJ (1998) Interactions of persistent environmental organohalogenes with the thyroid hormone system: mechanisms and possible consequences for animal and human health *Toxicol. Ind. Health* 14, 59-84
5. Mills RA, Millis CD, Dannan GA, Guengerich FP, Aust SD (1985) Studies on the structure-activity relationships for the metabolism of polybrominated biphenyls by rat liver microsomes *Toxicol. Appl. Pharmacol.* 78, 96-104
6. Lans MC, Klasson-Wehler E, Willemsen M, Meussen E, Safe S, Brouwer A (1993) Structure-dependent, competitive interaction of hydroxy-polychlorobiphenyls, -dibenzo-p-dioxins and -dibenzofurans with human transthyretin *Chem.-Biol. Interact.* 88, 7-21
7. Hallgren S, Darnerud PO (2002) Polybrominated diphenyl ethers (PBDEs), polychlorinated biphenyls (PCBs) and chlorinated paraffins (CPs) in rats--testing interactions and mechanisms for thyroid hormone effects *Toxicology* 177, 227-43
8. Lans MC, Spiertz C, Brouwer A, Koeman JH (1994) Different competition of thyroxine binding to transthyretin and thyroxine-binding globulin by hydroxy-PCBs, PCDDs and PCDFs *Eur. J. Pharmac.* 270, 129-36
9. Cheek AO, Kow K, Chen J, McLachlan JA (1993) Potential mechanisms of thyroid disruption in humans: interaction of organochlorine compounds with thyroid receptor, transthyretin, and thyroid-binding globulin. *Environ. Health Perspect.* 107, 273-8
10. Schreiber G (2002) The evolutionary and integrative roles of transthyretin in thyroid hormone homeostasis *J. Endocrinol.* 175, 61-73

11. Brouwer A (1991) Role of biotransformation in PCB-induced alterations in vitamin A and thyroid hormone metabolism in laboratory and wildlife species *Biochem. Soc. Trans.* 19, 731-8
12. Darnerud PO, Morse D, Klasson-Wehler E, Brouwer A (1996) Binding of a 3,3',4,4'-tetrachlorobiphenyl (CB-77) metabolite to fetal transthyretin and effects on fetal thyroid hormone levels in mice *Toxicology* 106, 105-14
13. Yamauchi K, Kasahara T, Hayashi H, Horiuchi R (1993) Purification and characterization of a 3,5,3'-L-triiodothyronine- specific binding protein from bullfrog tadpole plasma: a homolog of mammalian transthyretin *Endocrinology* 132, 2254-61
14. Meerts IATM, van Zanden JJ, Luijks EAC, van Leeuwen-Bol I, Marsh G, Jakobsson E, Bergman A, Brouwer A (2000) Potent Competitive Interactions of Some Brominated Flame Retardants and Related Compounds with Human Transthyretin in Vitro *Toxicol. Sci.* 56, 95-104
15. van den Berg KJ (1990) Interaction of chlorinated phenols with thyroxine binding sites of human transthyretin, albumin and thyroid binding globulin *Chem.-Biol. Interact.* 76, 63-75
16. Yamauchi K, Ishihara A, Fukazawa H, Terao Y (2003) Competitive interactions of chlorinated phenol compounds with 3,3',5-triiodothyronine binding to transthyretin: detection of possible thyroid-disrupting chemicals in environmental waste water *Toxicol. Appl. Pharmacol.* 187, 110-17
17. Caelen I, Kalman A, Wahlstrom L (2004) Biosensor-Based Determination of Riboflavin in Milk Samples *Anal. Chem.* 76, 137-43
18. Marchesini GR, Meulenber E, Haasnoot W, Irth H (2005) Biosensor immunoassays for the detection of bisphenol A *Anal. Chim. Acta* 528, 37-45
19. Somack R, Andrea TA, Jorgensen EC (1982) Thyroid hormone binding to human serum prealbumin and rat liver nuclear receptor: kinetics, contribution of the hormone phenolic hydroxyl group, and accommodation of hormone side-chain bulk *Biochemistry* 21, 163-70
20. Myszka DG (1999) Improving biosensor analysis *J. Mol. Recognit.* 12, 279-84
21. Munro SL, Lim CF, Hall JG, Barlow JW, Craik DJ, Topliss DJ, Stockigt JR (1989) Drug competition for thyroxine binding to transthyretin (prealbumin): Comparison with effects on thyroxine-binding globulin *J. Clin. Endocrinol. Metab.* 68, 1141-47

22. Matsubara K, Mizuguchi M, Kawano K (2003) Expression of a synthetic gene encoding human transthyretin in *Escherichia coli* *Protein Expr. Purif.* 30, 55-61
23. Andrea TA, Cavalieri RR, Goldfine ID, Jorgensen EC (1980) Binding of thyroid hormones and analogues to the human plasma protein prealbumin *Biochemistry* 19, 55-63
24. Cody V (1980) Thyroid hormone interactions: molecular conformation, protein binding, and hormone action *Endocr. Rev.* 1, 140-66
25. Chauhan KR, Kodavanti PRS, McKinney JD (2000) Assessing the Role of ortho-Substitution on Polychlorinated Biphenyl Binding to Transthyretin, a Thyroxine Transport Protein *Toxicol. Appl. Pharmacol.* 162, 10-21
26. Tata JR, Widnell CC, Gratzer WB (1961) A systematic study of factors affecting the binding of thyroxine and related substances to serum proteins *Clin. Chim. Acta* 6, 597-612
27. Gurer-Orhan H, Kool J, Vermeulen NPE, Meerman JHN (2005) A novel microplate reader-based high-throughput assay for estrogen receptor binding *Int. J. Environ. Anal. Chem.* 85, 149
28. Cannon MJ, Myszka DG, Bagnato JD, Alpers DH, West FG, Grissom CB (2002) Equilibrium and Kinetic Analyses of the Interactions between Vitamin B12 Binding Proteins and Cobalamins by Surface Plasmon Resonance *Anal. Biochem.* 305, 1-9
29. Purkey HE, Palaninathan SK, Kent KC, Smith C, Safe SH, Sacchettini JC, Kelly JW (2004) Hydroxylated polychlorinated biphenyls selectively bind transthyretin in blood and inhibit amyloidogenesis: rationalizing rodent PCB toxicity *Chem. Biol.* 11, 1719-28
30. McCammon MG, Scott DJ, Keetch CA, Greene LH, Purkey HE, Petrassi HM, Kelly JW, Robinson CV (2002) Screening Transthyretin Amyloid Fibril Inhibitors: Characterization of Novel Multiprotein, Multiligand Complexes by Mass Spectrometry *Structure* 10, 851-63
31. Karami-Tehrani F, Salami S, Mokarram P (2001) Competition of tamoxifen with thyroxine for TBG binding: ligand binding assay and computational data *Clin. Biochem.* 34, 603-6

Chapter 4

Biosensor Discovery of Thyroxine Transport Disrupting Chemicals

In Press: Toxicology and Applied Pharmacology (2008)

Abstract

Ubiquitous chemicals may interfere with the thyroid system that is essential in the development and physiology of vertebrates. We applied a surface plasmon resonance (SPR) biosensor-based screening method for the fast screening of chemicals with thyroxine (T4) transport disrupting activity. Two inhibition assays using the main thyroid hormone transport proteins, T4 binding globulin (TBG) and transthyretin (TTR), in combination with a T4-coated biosensor chip were optimized and automated for screening chemical libraries. The transport protein-based biosensor assays were rapid, high throughput and bioeffect-related. A library of 62 chemicals including the natural hormones, polychlorinated biphenyls (PCBs), polybrominated diphenylethers (PBDEs) and metabolites, bisphenol A (BPA), synthetic fluorinated phenols, pharmaceuticals, pesticides and other potential environmentally relevant chemicals was tested with the two assays. We discovered ten new active compounds with moderate to high affinity for TBG with the TBG assay. Strikingly, the most potent binding was observed with hydroxylated metabolites of the brominated diphenyl ethers (BDEs) BDE 47, BDE 49 and BDE 99, which are commonly found in human plasma. The TTR assay confirmed the activity of previously identified hydroxylated metabolites of PCBs and PBDEs, halogenated BPA and genistein. These results show that the hydroxylated metabolites of the ubiquitous PBDEs not only target the T4 transport at the TTR level, but also, and to a great extent, at the TBG level where most of the T4 in humans is circulating. The optimized SPR biosensor-based transport protein assay is a suitable method for high throughput screening of large libraries of potentially thyroid hormone disrupting compounds.

Introduction

Thyroid Hormones (TH), such as L-thyroxine (T4) and its biologically active metabolite, triiodothyronine (T3), are essential for the modulation of the cellular metabolic rate and for the development, and differentiation of several tissues, specially the brain [1, 2]. The thyroid gland produces and releases T4 in response to the thyroid-stimulating hormone secreted by the pituitary. Once T4 enters the blood stream it is bound to transport proteins and distributed to the target tissues. Thyroxine binding globulin (TBG) is the major T4 transport protein in human plasma and is responsible for 75% of the specific T4 binding activity. Transthyretin (TTR) is the second transport protein carrying about 20% of T4 and finally, human serum albumin (HSA) is the third transport protein carrying about 5% of the total T4. The affinity of the three transport proteins for T4 varies greatly, as well as their plasmatic concentration (0.2 μ M for TBG, 5 μ M for TTR and 600 μ M for HSA) providing a redundant buffer system for free T4 [3]. T4 is specifically transported through the cell membrane into the intracellular compartment and deiodinated to the biologically active T3 metabolite in different tissues [4]. Once inside the cell, T3 is non-specifically transported to the nucleus where it exerts its action by binding to the nuclear thyroid receptors. Several chemical contaminants resembling T4 have been shown to interfere at different levels with the thyroid pathway (for review see [5]). The disruption of the T4 transport has received special attention since several polyhalogenated aromatic hydrocarbons (PHAHs) become bioactivated in vivo upon hydroxylation by the cytochrome P450 monooxygenase system [6]. These hydroxylated PHAHs interact with TTR [7, 8] and some of them, albeit with much lower affinity, interact with TBG [9, 10]. Some studies exclude the dependence of thyroid hormone homeostasis on any transport protein per se [11]. However, TTR is important for maternal to fetal transport of thyroid hormones and for delivery of T4 across the brain barrier [3]. TBG has also been linked to facilitate the iodine supply to the fetus that initially has no iodine reserve [12]. Displacement of T4 from its transport protein complex during the developmental stage could have consequences in fetal development and later in adulthood [13, 14]. For instance, disturbances in the retinoid and TH levels by environmental chemicals during development has been linked with susceptibility to schizophrenia [15], with effects on brain development [16] and with lower IQ levels in adulthood [17]. Moreover, obesity is

increasingly been linked to environmental chemicals and this could be mediated through an impaired TH homeostasis [18-20]. Therefore, the presence and bioaccumulation of these bioactive contaminants in the food chain and finally in humans is a cause of concern. PCBs have been shown to interfere with the TH homeostasis. However, the PCBs concentration in human tissues is gradually declining due to the regulations imposed in the 1970s [21].

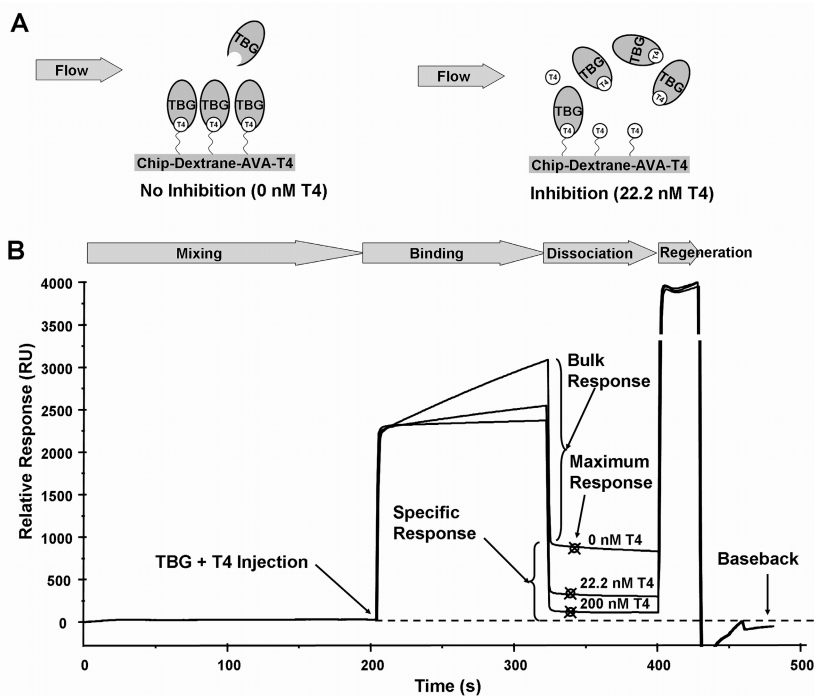


Figure 1. (A) Principle of the biosensor transport protein-based inhibition assay. (B) Overlaid sensorgrams showing the responses in time obtained during a whole cycle (mixing, injection (binding), dissociation and regeneration) and the inhibition of TBG binding to the T4 chip surface when mixed with 0, 22.2 and 200 nM of T4.

On the contrary, the widely used polybrominated diphenyl ethers (PBDEs) flame retardants that were later introduced, have been measured in human adipose tissues from inhabitants of the United States at concentrations of 35 ng/g lipid. This is 10-100 times greater than those reported in European countries and their concentrations have been increasing exponentially for the last 30 years, with a doubling period of about 5 years [21, 22]. Although the influence of PBDEs on

human T4 levels is unknown, one epidemiological study found a significant negative correlation between thyroid stimulating hormone and BDE 47 levels in Scandinavian men [5]. Therefore, there is a rising need for high throughput screening methods to determine whether chemicals are affecting the thyroid system at different levels. In the present study we used two previously developed transport protein-based surface plasmon resonance (SPR) biosensor inhibition assays [23]. The principle of these biosensor assays is similar to an inhibition immunoassay (see Fig. 1 A). If there is no binding of the analyte to the transport protein, the maximum amount of transport protein will bind to the sensor surface and a maximum response is obtained. The binding of transport protein to the sensor surface will be inhibited given an interaction between the analyte and the transport protein in solution, resulting in a lower response. The inhibition of the response depends on the concentration of the T4-like analyte as well as on the affinity of this compound for the transport protein.

The biosensor assays were optimized to endure long periods of automated operation and used to screen a library of 62 chemicals for compounds affecting the T4 transport. This library, shown in Table 1 and Table 2, included the thyroid hormones, polyhalogenated biphenyls, polyhalogenated diphenyl ethers and metabolites, bisphenol A (BPA) and synthetic halogenated derivatives, pharmaceuticals, pesticides and other environmentally relevant chemicals providing a wide range of structural classes.

Experimental

Chemicals and Equipment

The recombinant transthyretin (rTTR) was produced at the Toyama Medical and Pharmaceutical University (Toyama, Japan) [24]. Chemical standards (Tables 1 and 2) had a purity above 95 % and were obtained from AccuStandard (New Haven, CT), LGC Promochem (Teddington, UK), Honeywell Riedel de Haën (Seelze, Germany) or Dr. Ehrenstorfer GmbH (Augsburg, Germany). Thyroxine Binding Globulin (TBG) was obtained from Scipac (Kent, UK). CM5 sensor chips, the amine coupling kit [containing 0.1 M N-hydroxysuccinimide (NHS), 0.4 M 1-ethyl-3-(3-dimethylaminopropyl) carbodiimide hydrochloride (EDC) and 1 M ethanolamine hydrochloride (pH 8.5)] and the Biacore Q biosensor were supplied by GE Healthcare (Uppsala, Sweden). The 5-aminovaleric

acid (AVA), L-thyroxine and the ovalbumin (OVA) and all other reagents were obtained from Sigma-Aldrich Chemie (Zwijndrecht, The Netherlands) unless otherwise stated.

Transport Protein Inhibition Assays

The transport protein assays, of which the principle is shown in Figure 1A, were performed as described previously [23] with some modifications on the conditions to improve the transport protein stability and maximize the unattended operation time. T4 was immobilized to the CM5 biosensor chip surface via the amino group of the alanyl side chain using AVA as spacer. The transport protein assays were performed in a Biacore Q that automatically mixed 20 μL of the transport protein solution (91 nM) with 80 μL of the analyte solution and immediately injected 50 μL of the mixture over the T4-coated sensor chip surface at a flow rate of 25 $\mu\text{L min}^{-1}$. The variation in response over time of each transport protein binding to the T4-coated sensor chip surface under different buffer conditions was used as a parameter of transport protein stability. The response, measured 15 s after the injection ended was used for data comparison and the surface was regenerated by injecting 15 μL of a mixture of 0.1 M NaOH and acetonitrile (ACN) (4:1; v/v). In the final format, a phosphate buffer (NaH_2PO_4 (0.6 g), $\text{Na}_3\text{PO}_4 \cdot 12\text{H}_2\text{O}$ (1.9 g), NaCl (0.59 g) per liter adjusted to pH 8.5) was used as running buffer. The transport protein stock solutions were prepared in running buffer with the addition of OVA (40 $\mu\text{g mL}^{-1}$) to preserve the transport protein stability. A typical maximum response of a blank buffer injection was 750 response units (RU). Stock solutions of the chemical standards (10 mM) were prepared, if possible, in DMSO, or otherwise in the organic solvent recommended by the provider. The T4 stock solution (10 mM) was prepared by dissolving T4 in a solution containing DMSO (94%), chloroform (5 %) and 1 M NaOH (1 %). The buffer used for dilution of the chemical standards was running buffer with the addition of 2% DMSO and ascorbic acid (0.5 g L^{-1}) as antioxidant. At least one T4 calibration curve was included in each set of analyte calibration standards.

Transport Protein Binding Affinity

The binding affinity of a chemical to either rTTR or TBG was expressed as the relative potency (RP) of the compound compared to the natural hormone, T4. Therefore, concentrations inducing 50% inhibition (IC_{50}) were obtained from calibration curves of the compounds and T4. The RP is defined as the ratio between the IC_{50} of T4 and the IC_{50} of the compound [IC_{50} (T4)/ IC_{50} (analyte)]. The mean IC_{50} of all the T4 calibration curves was used for the RP calculations. The mean IC_{50} of T4 in the TTR assay was 18.4 ± 4.4 nM ($n = 15$) and 17.2 ± 1.2 nM ($n = 10$) in the TBG assay. The RPs of the analytes were calculated based on at least two full dose response curves based on six different concentrations. The chemicals were classified either as active or inactive, according to their percentages of inhibition at the highest tested concentrations. Active chemicals were those with an inhibition higher than 50% and were further classified based on their calculated RP. Namely designated as very strong binder (VSB) ($RP > 1$), strong binder (STB) ($1 > RP > 0.1$), moderate binder (MB) ($0.1 > RP > 0.01$), or weak binder (WB) ($RP < 0.01$). Those that did not reach an inhibition of 50 % at the highest tested concentration were differentiated in two groups. Those chemicals inhibiting transport protein binding in the 0-15 % range were designated as "non binders" (NB) and those showing inhibition in the 16-49 % range were designed as "slight binders" (SIB).

Results

Optimization of the Assays

Typical sensorgrams obtained with the TBG assay for three different concentrations of T4 are shown in Figure 1B. There is a relatively large bulk response in the sensorgrams caused by the presence of DMSO in the dilution buffer. After the injection finishes, the specific binding response is measured. The regeneration conditions effectively disrupted the transport protein-T4 interaction without damaging the T4-coated chip surface. The total run time for each cycle was 8 min, including mixing the transport protein stock solution with the sample and the washing steps. The T4-coated chip surface was very stable and could be used for over 1000 cycles. To allow long periods of unattended operation, it is critical that the T4 binding activity of the transport proteins remains stable. One of the factors affecting the stability of TTR

in binding assays is its concentration in solution [25]. rTTR was exposed to different conditions to study the decrease of binding response to immobilized T4. When rTTR was used as previously [23], the response obtained after injection of (18.2 nM) rTTR decreased 43 % after 240 min (30 cycles). At this concentration, the rTTR stability was greatly improved after the addition of (182 nM) OVA as a stabilizing agent and the response decreased only 12 % after 240 min of serial injections. OVA has a reported low affinity for T3 and T4 [26] and is therefore interesting as stabilizing agent because it would have a minor effect on the relative affinities of the analytes to the transport proteins. The stability of rTTR was further improved by preparing a five-fold more concentrated transport protein stock solution. The OVA concentration in this solution was five-fold increased as well. Prior to each injection, the Biacore Q mixed the transport protein stock solution with the analyte solution (1/5; v/v). The measurement of a full set of 7 calibration curves (three analytes in duplicate and T4) took 960 min. Under these conditions, the transport protein stock solutions remained stable and showed minimum response decrease (< 5 % for rTTR and < 2% for TBG). Additional improvements were the presence of 2% DMSO in the dilution buffer, which enhanced the solubility of hydrophobic chemicals allowing the screening of chemicals over a wider range of Log P values, and the presence of 2.8 mM ascorbic acid to prevent oxidation of less stable metabolites [27].

Under the improved conditions, both biosensor transport protein-based assays were more robust than under the conditions used previously [23]. The RP values obtained previously with the same stock solutions of 4-OH PCB14, TBBPA, TCBPA, PBP, PCP and T3 were similar to the RP values under the optimized conditions. The IC₅₀ values for T4 increased in the TTR assay from 13.7 to 18.4 nM, and from 8.6 to 17.2 nM in the TBG assay. However, as other chemicals had concomitant IC₅₀ increases, the RP value was not significantly changed. The only exception was 4-OH PCB14, which showed a significant IC₅₀ increase from 3.1 nM to 16.9 nM, indicating that an interaction of 4-OH PCB 14 with OVA cannot be excluded as the cause. Hence, 4-OH PCB14 was excluded from further analysis.

The TBG assay with improved conditions showed a RP increase for T3 from 0.6 to 0.8 compared to the previous conditions.

A library of 18 chemicals (T4, T3, 4-OH PCB 69, 4-OH PCB 106, 3-OH-BDE 47, 5-OH-BDE 47, 6-OH-BDE 47, 4'-OH-BDE 49, 6'-OH-BDE 49, 6'-OH-BDE 99, TCBPA, TBBPA, DBP, TBP, PCP, PBP, Na Dic, Me Ac) was

tested in the TTR assay with the old and the new conditions, obtaining similar RP values, with a regression equation $RP_{(\text{New Conditions})} = 1.06 RP_{(\text{Old Conditions})} - 0.03$ ($R^2 = 0.86$). These results indicate that the addition of DMSO, OVA and ascorbic acid to the transport protein-based assays had minor effects on the RP values.

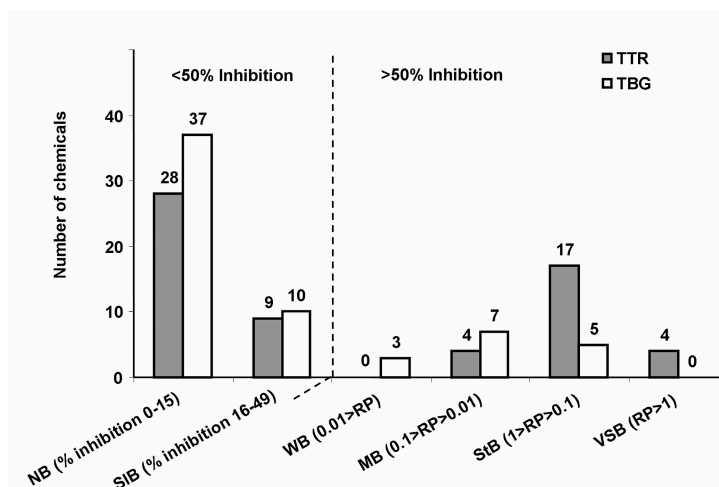


Figure 2. Distribution of the RP values compared to T4 of the 62 tested chemicals determined with the TTR- and TBG inhibition assays. The compounds are classified based on their percentage of transport protein inhibition if they do not reach 50%, or based on their relative binding potency. The categories distinguished are, weak binders (WB, $RP < 0.01$), moderate binders (MB, $0.01 < RP < 0.1$), strong binders (StB, $0.1 < RP < 1$) and very strong binders (VSB, $RP > 1$). Non binders (NB) and slight binders (SIB) inhibited the transport proteins less than 16% and 50 % respectively.

Screening of a 62 Chemicals Library

From the 62 chemicals tested with the two transport protein-based assays, 25 were classified as active for producing more than 50 % inhibition of TTR and 15 for TBG (Figure 2). Of the compounds, 28 were non binders (producing less than 16 % inhibition) to TTR and 37 to TBG. The remaining 9 chemicals for TTR and 10 for TBG, were slight binders (SIB) with more than 15% inhibition but less than 50%. The 25 compounds active towards TTR had RPs ranging from more than 0.01 up to more than 1. For the more specific TBG, 15 compounds were active, but none of them was more potent than T4 itself. The RPs of the TTR active chemicals mostly were centered around the STB category (17

chemicals) and around the MB category for TBG (7 compounds) (Figure 2).

Detailed information about each chemical, i.e., the chemical name, structure, source, CAS number and measured binding affinity, as well as those found in literature (IC_{50} and RP) are presented in Table 1 and Table 2. Structures of the compounds from Table 2 (pharmaceuticals, pesticides and other chemicals), are presented in Figure 3.

The active hormone (T3) is also active for binding the pro-hormone (T4) transport proteins and had an RP compared to T4 of 0.04 in the TTR assay and 0.8 in the TBG assay (Table 1). All tested polychlorinated biphenyls (PCBs) were inactive in both biosensor transport protein-based assays. Even PCBs structurally resembling T4 (PCBs 73, 80, 121, 127), did not interact with TTR nor with TBG. The 5 para-hydroxylated PCBs (OH PCBs) were strong TTR binders (RPs ranging from 0.4 till 2.5). The highly substituted, hydroxylated polyfluorinated biphenyl (4-OH PFB) showed a very strong affinity for TTR (RP = 1.4). The general affinity ranking of this group of chemicals for TTR was 4-OH PCB72 > 4-OH PFB > 4-OH PCB 14 > 4-OH PCB121 > 4-OH PCB 69 > 4-OH PCB 106 > 3-OH PCB 61 (NB) (Table 2). The OH polyhalogenated biphenyls (PHBs) did not bind to TBG, except for the moderate binder 4-OH PCB 72 and the weak binder 4-OH PFB.

All polybrominated diphenyl ethers (PBDEs) tested were inactive in the TTR assay. In the TBG assay, BDE 49 and BDE 99 were weak binders (WB) with RPs of 0.01 and 0.003, respectively. However, all hydroxylated polyhalogenated diphenylethers (OH PHDEs) tested were moderate to strong binders to TTR. The most potent binder to TTR was 3-OH BDE 47 (RP of 0.8), the least potent was Tricl (RP of 0.03). The affinity ranking for the OH-PBDEs for TTR was 3-OH BDE 47 > 5-OH BDE 47 > 6'-OH BDE 49 > 6'-OH BDE 99 = 6-OH BDE 47 = 4'OH BDE 49 followed by Tricl.

The OH PHDEs tested were also slight (6-OH BDE 47 and 6'-OH BDE 99) to moderate binders (including Tricl) in the TBG assay. The TBG affinity ranking was 6'-OH BDE 99 > 6-OH BDE 47 > 6'-OH BDE 49 > 3-OH BDE 47 > 5-OH BDE 47 > 4'OH BDE 49 followed by Tricl. From the two methoxy (MeO) PBDEs tested, only 6-MeO BDE 47 had a slight affinity for both transport proteins and 2'-MeO BDE 68 for TBG only. Although the unsubstituted diphenyl methane (BPA) tested in the transport protein-based assays was inactive, the halogenated congeners were strong binders in the TTR assay with RP values of 0.6 for TCBPA and 1 for TBBPA, but both were inactive in the TBG assay.

None of the fluorinated phenols was active in the transport protein-based assays, of the chlorinated phenols only pentachlorophenol had affinity for binding TTR (RP = 0.6) (Table 1). Interestingly, all the brominated phenols were active TTR binders with RPs up to 0.9 for tribromophenol (TBP). In the TBG assay only DFP, PCP and PBP were slight binders, but showing less than 20 % inhibition.

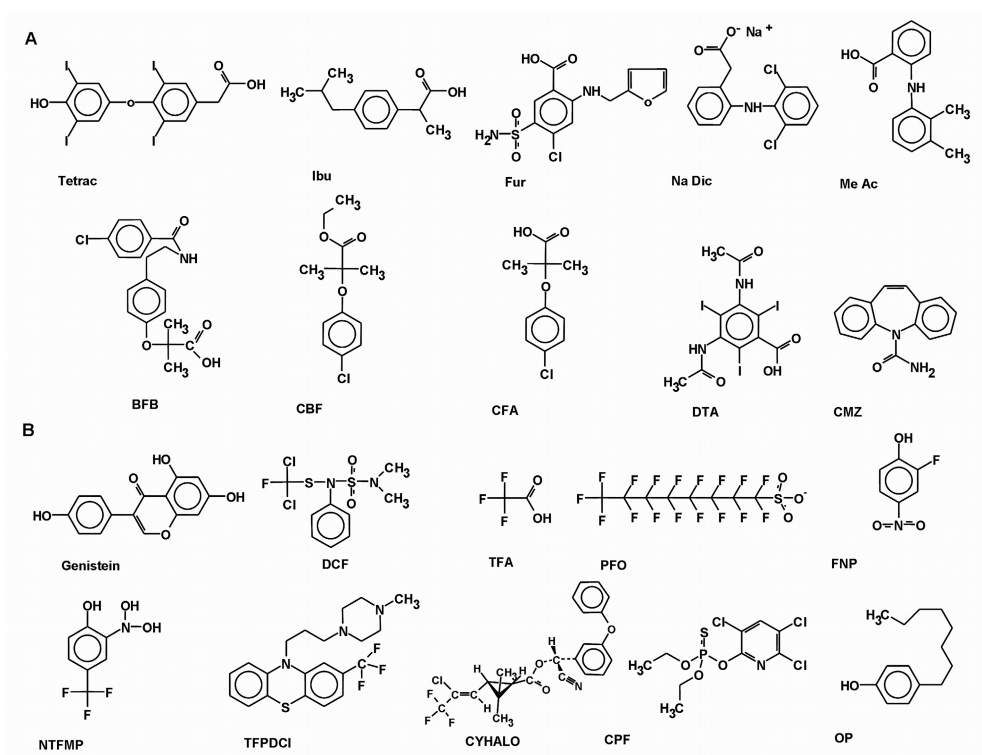
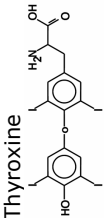
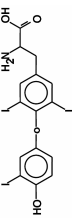
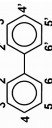
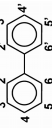
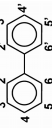
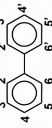


Figure 3. Structures of pharmaceuticals (A) and pesticides and other chemicals (B) presented in Table 2 and tested in the transport protein-based assays.

Three of the ten common pharmaceuticals tested (Figure 3A) were active in the TTR assay (Table 2), with the T4 like Tetrac being the most potent (RP of 1.1). Sodium diclofenac (Na Dic) and mefenamic acid (Me Ac) were less potent (RPs of 0.02). In the TBG assay only Tetrac (RP of 0.6) and NaDic (RP = 0.01) were active.

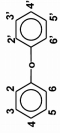
Table 1. Data set of polyhalogenated aromatic hydrocarbons (PHAHs) obtained with the biosensor transport protein inhibition assays.

Compound	Abbreviation (Source)	CAS	TTR			TBG			Cat. Literature RP	Cat. Literature RP			
			HTC (µM)	IC ₅₀ (nM)	RP	HTC (µM)	IC ₅₀ (nM)	RP					
Thyroid Hormones													
Thyroxine		T4 (S-A ¹)	51-48-9	0.2	18.4	1	StB	-	0.2	17.2	1	StB	-
Triiodothyronine		T3 (S-A)	6893-02-3	1.8	419	0.04	MB	0.02 [25], 0.08 [28], 0.09 [29], 0.08 [30], 0.04 [31]	1.8	21.3	0.8	StB	0.09 [32]
Polyhalogenated Biphenyls													
3,5 (Cl)		PCB 14 (AS ²)	34883-41-5	10	n.r.	-	NB	0.6 [33]	10	n.r.	-	SIB	-
2',3,5 (Cl)		PCB 34 (AS)	37680-68-5	10	n.r.	-	NB	0.3 [33]	10	n.r.	-	NB	-
3,4,5 (Cl)		PCB 38 (AS)	53555-66-1	10	n.r.	-	NB	1.9 [33]	10	n.r.	-	NB	-
2,3',5',6 (Cl)		PCB 73 (AS)	74338-23-1	10	n.r.	-	NB	NB ³ [34]	10	n.r.	-	NB	-

HTC. Highest tested concentration. * Categories distinguished, weak binders (WB, RP<0.01), moderate binders (MB, 0.01<RP<0.1), strong binders (StB, 0.1<RP<1) and very strong binders (VSB, RP>1). Non binders (NB) and slight binders (SIB) inhibited the transport protein's less than 16% and 50 % respectively.

¹Sigma Aldrich, ²AccuStandard, n.r. Not reached., ³RP value not available, assay based on immunoprecipitation-HPLC.

Table 1. Continued.

Compound	Abbreviation (Source)	CAS	TTR			TBG						
			HTC (μM)	IC ₅₀ (nM)	RP	Cat.	Literature RP	HTC (μM)	IC ₅₀ (nM)	RP	Cat.	Literature RP
Polyhalogenated diphenyl ethers												
												
2,2',4,4' (Br)	BDE 47 (AS)	5436-43-1	1	n.r.	-	SIB	<2.2E-3 [35] 2.5E-3 [36]	10	n.r.	-	SIB	-
2,2',4,5' (Br)	BDE 49 (AS)	243982-82-3	10	n.r.	-	SIB	<2.2E-3 [35]	16.2	2.5E3	0.01	WB	-
2,3',4,5' (Br)	BDE 68 (AS)	446254-38-2	10	n.r.	-	NB	-	16.2	n.r.	-	SIB	-
2,2',4,4',5 (Br)	BDE 99 (AS)	60348-60-9	10	n.r.	-	SIB	NB [35]	16.2	5685	3E-3	WB	-
Hydroxy polyhalogenated diphenyl ethers												
2-OH-2',4,4' (Cl)	TricI (S-A)	3380-34-5	10	669	0.03	MB	-	10	1182	0.02	MB	-
3-OH-2,2',4,4' (Br)	3-OH BDE 47 (AS)	24949-31-3	0.2	22.3	0.8	StB	4 [36]	1.8	219	0.08	MB	-
5-OH-2,2',4,4' (Br)	5-OH BDE 47 (AS)	602326-30-7	0.2	44.3	0.4	StB	3 [36]	1.8	235	0.07	MB	-
6-OH-2,2',4,4' (Br)	6-OH BDE 47 (AS)	79755-43-4	0.6	87	0.2	StB	0.3 [35] 0.3 [37] 0.4 [36]	0.6	110	0.16	StB	-
4'-OH-2,2',4,5' (Br)	4'-OH BDE 49 (Pr ⁴)	602326-23-8	0.2	107.8	0.2	StB	3.5 [36]	1.8	867	0.02	MB	-
6'-OH-2,2',4,5' (Br)	6'-OH BDE 49 (Pr)	497069-16-6	0.2	66	0.3	StB	-	0.6	191	0.09	MB	-
6-OH-2,2',4,4',5 (Br)	6'-OH BDE 99 (AS)	297742-10-0	0.2	83.6	0.2	StB	-	0.2	100	0.18	StB	-

⁴ Promochem.

Table 1. Continued.

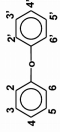
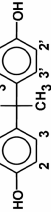
Compound	Abbreviation (Source)	CAS	TTR			TBG			Literature RP	Cat. RP	Literature RP	
			HTC (µM)	IC ₅₀ (nM)	RP	HTC (µM)	IC ₅₀ (nM)	RP				
Methoxy polybrominated diphenyl ethers												
												
6-MeO-2,2',4,4'		102739-99-1	1.8	n.r.	-	SIB	-	10	n.r.	-	SIB	-
2'-MeO-2,3',4,5'		96920-28-4	1	n.r.	-	NB	-	10	n.r.	-	SIB	-
Diphenyl methanes												
												
Bisphenol A	BPA (S-A)	80-05-7	10	n.r.	-	SIB	NB [38]	10	n.r.	-	NB	-
Tetrachlorobisphenol A 2,2',6,6' (Cl)	TCBPA (S-A)	79-95-8	0.2	32.4	0.6	StB	0.8 [38]	10	n.r.	-	SIB	-
Tetrabromobisphenol A 2,2',6,6' (Br)	TBBPA (S-A)	79-94-7	0.2	18.8	1	StB	10.6 [38] 2.3 [37] 1.6 [35]	10	n.r.	-	NB	-

Table 1. Continued.

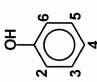
Compound	Abbreviation (Source)	CAS	TTR				TBG					
			HTC (μM)	IC ₅₀ (nM)	RP	Cat.	Literature RP	HTC (μM)	IC ₅₀ (nM)	RP	Cat.	Literature RP
Halogenated phenols												
												
2,4 difluorophenol	DFP (S-A)	367-27-1	10	n.r.	-	NB	-	-	10	n.r.	SIB	-
2,6 difluorophenol	DFP (S-A)	28177-48-2	10	n.r.	-	NB	-	-	10	n.r.	NB	-
2,4,6 trifluorophenol	TFP (S-A)	2268-17-9	10	n.r.	-	NB	-	-	10	n.r.	NB	-
2,4 dichlorophenol	DCP (S-A)	120-83-2	10	n.r.	-	SIB	-	-	10	n.r.	NB	-
Pentachlorophenol	PCP (S-A)	87-86-5	0.2	33.2	0.6	StB	2.5 [39] 1.7 [40]	-	10	n.r.	SIB	0.001 [40]
2,4 dibromophenol	DBP (S-A)	615-58-7	5.4	149.3	0.1	StB	0.06 [38] 1.2 [38]	-	10	n.r.	NB	-
2,4,6 tribromophenol	TBP (S-A)	118-79-6	0.6	20.2	0.9	StB	2 [37] 10.2 [35]	-	10	n.r.	NB	-
Pentabromophenol	PBP (S-A)	608-71-9	0.2	26.6	0.7	StB	7.1 [38]	-	10	n.r.	SIB	-

Table 2. Data set of the 20 pharmaceuticals, pesticides and other compounds tested with the biosensor transport protein inhibition assays (Categories are explained in Table 1, the structures of the compounds are presented in Fig. 3).

Compound	Abbreviation (Source)	CAS	TTR			TBG						
			HTC (μM)	IC50 (nM)	RP	Cat.*	Literature RP	HTC (μM)	IC50 (nM)	RP	Cat.	Literature RP
Pharmaceuticals (Structures in Figure 3A)												
Tetraiodothyroacetic acid	Tetrac (S-A)	67-30-1	10	17.2	1.1	VS		1.8	29	0.6	StB	0.4 [41]
Ibuprofen	IBU (S-A)	15687-27-1	10	n.r.	-	SIB	-	10	n.r.	-	NB	-
Furosemide	Fur (S-A)	54-31-9	10	n.r.	-	NB	NB [42]	10	n.r.	-	NB	1.1E ⁻³ [42]
Sodium Diclofenac	Na Dic (S-A)	15307-79-6	5.4	936	0.02	MB	0.02 [42]	5.4	1360	0.01	MB	3.9E ⁻⁴ [42]
Mefenamic Acid	Me Ac (S-A)	61-68-7	1.8	1.2E ³	0.02	MB	0.3 [42]	10	n.r.	-	NB	2.7E ⁻⁴ [42]
Bezafibrate	BFB (S-A)	41859-67-0	10	n.r.	-	NB	-	10	n.r.	-	NB	-
Clofibrate	CBF (S-A)	637-07-0	10	n.r.	-	NB	-	10	n.r.	-	NB	-
Clofibric acid	CFA (S-A)	882-09-7	10	n.r.	-	NB	-	10	n.r.	-	NB	-
Diatrizoic acid	DTA (S-A)	117-96-4	10	n.r.	-	NB	-	10	n.r.	-	NB	-
Carbamazepine	CMZ (S-A)	298-46-4	10	n.r.	-	NB	-	10	n.r.	-	NB	-

HTC: Highest tested concentration. * Categories. n.r. Not reached. ¹ Sigma Aldrich, ² AccuStandard, ³ Riedel-de Haën, ⁴ Dr. Ehrenstorfer.

Table 2. Continued.

Compound	Abbreviation (Source)	CAS	TTR			TBG						
			HTC (μ M)	IC50 (nM)	Cat. RP	Literature RP	HTC (μ M)	IC50 (nM)	Cat. RP	Literature RP		
Pesticides and Others (Structures in Figure 3B)												
Genistein	Gen (S-A)	446-72-0	10	43.8	0.4	StB	KD=40 nM [43]	10	n.r.	-	NB	-
Dichlofluanid	DCF (S-A)	1085-98-9	10	n.r.	-	NB	-	10	n.r.	-	NB	-
Trifluoroacetic acid	TFAA (S-A)	76-05-1	10	n.r.	-	NB	-	10	n.r.	-	NB	-
Perfluorooctanesulfonate	PFO (S-A)	111873-33-7	1	n.r.	-	SIB	-	10	n.r.	-	NB	-
2-Fluoro-4-nitrophenol	2F-PNP (S-A)	403-19-0	10	n.r.	-	NB	-	10	n.r.	-	NB	-
2-Nitro-4-(trifluoromethyl) phenol	NTFMP (S-A)	400-99-7	1	n.r.	-	NB	-	10	n.r.	-	NB	-
Trifluoperazine dihydrochloride	TFPDCI (S-A)	440-17-5	10	n.r.	-	NB	-	10	n.r.	-	NB	-
l-Cyhalotrin	Cyhalo (AS ²)	91465-08-6	10	n.r.	-	NB	-	10	n.r.	-	NB	-
Chlorpyrifos	CPF (RdH ³)	2921-88-2	10	n.r.	-	NB	-	10	n.r.	-	NB	-
4-OctylPhenol	OP (Dr.E ⁴)	1806-26-4	10	n.r.	-	SIB	-	10	n.r.	-	NB	-

² AccuStandard, ³ Riedel-de Haën, ⁴ Dr. Ehrenstorfer.

Of the 10 pesticides and other compounds with environmental relevance tested (Figure 3B), only the natural isoflavonoid, genistein (Gen), was active in the TTR assay. All these chemicals were inactive in the TBG assay.

To compare the affinity of TTR and TBG toward the chemicals tested, the RP of the active chemicals for TTR was plotted versus the RP of the chemicals active for TBG in Figure 4. Those chemicals that inhibited the transport protein-based assay less than 50 % were plotted using the $-\text{Log}_{10}$ of the percentage of inhibition (PI%) at the highest concentration tested. Inactive compounds showing a PI% for either of the transport proteins below 1 were assigned a Log_{10} value of 0 and are therefore aligned with the axis.

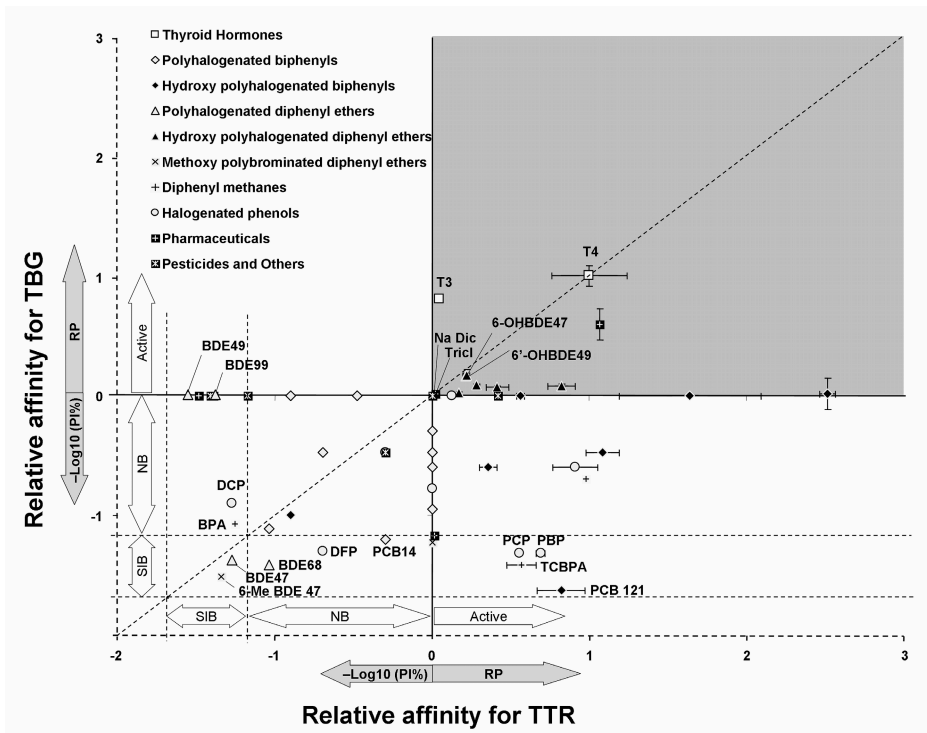


Figure 4. Affinity of the 62 chemicals tested for TTR and TBG binding. The $-\text{Log}_{10}$ of the percentage of inhibition (PI%) was used to plot compounds not reaching 50% inhibition. Compounds for which the relative potency (RP) compared to T4 was calculated were plotted based on their RP. Those compounds in the shaded quadrant have a strong affinity for both TTR and TBG.

The shaded quadrant of the plot contains a group of 13 chemicals that were both active for TTR and TBG. Most of these compounds are located below the T4 diagonal and along the rTTR axis showing in general a higher RP for TTR than for TBG. Four active compounds (TricI, 6-OH BDE47, 6'-OHBDE99 and NaDicI) are aligned with the T4 diagonal indicating similar relative affinity for both TTR and TBG. Only T3, located above the diagonal, was more potent for TBG than for TTR. The following quadrant clockwise depicts 12 compounds active only in the TTR assay, one of them, 4-OH PCB14, being a very strong binder. A subgroup of four compounds (PCP, PBP, TCIBPA and PCB121) all highly substituted and strong binders for TTR are located in the SIB strip for TBG.

The next quadrant clockwise contains 36 compounds showing less than 50 % inhibition in both transport proteins, 24 were non binders for both TBG and TTR, 10 were slight binders with one of the transport proteins. Interestingly, 2 compounds (6-Me BDE47 and BDE47) were slight binders with both transport proteins and were aligned with the T4 diagonal. The last quadrant is virtually empty except for two compounds (BDE49 and BDE99) that had a much higher relative affinity for TBG than for TTR.

Discussion

In our previous study we characterized rTTR and TBG using a SPR-based biosensor and this allowed us to develop two T4 transport protein inhibition assays using this system [23]. In the present study these assays were successfully optimized to endure the conditions needed for screening a large library of 62 chemicals. We discovered, in this library, that several hydroxylated metabolites of commonly used brominated flame retardants have an unexpectedly strong affinity for TBG. All of these compounds also have a strong affinity for binding TTR.

When our results are compared with those reported in literature (Tables 1 and 2), the first issue that arises is the difference in the RPs obtained with those previously reported. One fundamental reason to explain these differences is the TTR source. The classical T4 radioligand binding assay (RBA) uses TTR purified from human serum that is probably less stable than the recombinant TTR used in this study. Additionally, TTR has two allosteric binding sites, a low and a high affinity one. Our TTR assay is only sensitive to the binding of a ligand to the high affinity binding site [23]. On the contrary, the classical TTR RBA reported

measures in principle the displacement of T4 from both binding sites. The structure of the ligands also plays a crucial role in the TTR binding kinetics [44]. This could generate very complex binding kinetics when the isotope-labeled T4 and the ligand are both present during binding in the TTR RBA. When a ligand is bound to one of the binding sites, it influences the binding kinetics of the other ligands. Another important difference between our TTR assay and the TTR RBA is that the latter is performed in a pure aqueous solution, whereas our assay includes ascorbic acid, 2% DMSO and OVA creating more stable conditions for lipophilic compounds.

Furthermore, it has been reported that even in similar experiments using TTR radioligand binding assays, the RP values for a single compound may differ up to 6 fold (i.e. TBBPA) [35, 38]. The RP variations reported confirm previous studies indicating that TTR is very sensitive to slight changes in assay conditions [23, 33]. The dissimilar methods and assay protocols used make quantitative inter method or inter laboratory comparisons unfeasible. However, qualitatively most of the RP values from different studies, including ours, are in accordance with each other.

The RP of T3 (0.04) in our study was comparable with the average RP values (0.06 ± 0.03) reported in literature. The RP for T3 in the TBG assay was 0.8, which is almost ten times higher than previously obtained [32]. This difference could be explained by the pH (7.4-7.8) that was reported as optimum for TBG RBAs [26]. In this study, Korcek and Tabachnick show that the affinity of TBG for T3 increases more at higher pHs than for T4. Therefore, using a pH of 8.5 for the TBG assay, as in the present study, probably increases the RP for T3.

In our transport protein-based assays all the PCBs tested were inactive, in contrast with the results of Chauhan et al., who reported that several of these compounds interacted strongly with TTR using a RBA [33]. Later, Purkey et al. could only confirm an interaction of TTR with only two out of the eight PCBs used by Chauhan, albeit with a method based on immunoprecipitation-HPLC [34]. Most of the previous studies show that parent PCBs were inactive, contrary to their meta or para hydroxylated metabolites of PCBs with one or more adjacent halogens substituents that were potent T4 analogues [8, 25]. Our results with the TTR assay confirmed the TTR binding affinity for OH-PCBs and discovered that 4-OH PFB was a very strong TTR binder.

Of the 4 PBDEs tested, 2 were weak binders, inhibiting TBG more than 50% and 3 were slight binders to TTR, inhibiting TBG less than 50%.

The OH-PBDE metabolites, however, were all active and strong binders in both transport proteins. For TTR, the 3 meta OH group with two adjacent halogens, as present in 3-OH BDE47, provided the optimum structure for binding to TTR, which is in accordance with previously reported results performed with OH PCBs [8, 25]. The presence of the OH group in the 5 meta position with only one adjacent halogen, as in 5-OH BDE47, reduced the RP 2-fold. The RP decreased a further 2-fold when the OH group was in the ortho position without an adjacent halogen group (6-OH BDE 47). This trend in RP decrease is in accordance with the literature (see Table 1), with the exception of 4-OHBDE49 that in our study it had a RP 2-fold lower than 5-OH BDE47 whereas in the literature, the difference was of one order of magnitude lower (Table 1). In contrast with all what has already been reported about compounds binding to TTR, our study is the first to show that environmentally relevant compounds can also bind to TBG. We observe a different structure-related trend for TBG if compared with TTR. The presence of a OH group in the ortho position without an adjacent bromine group seems to favor the binding to TBG, as seen for 6-OH BDE 47 and 6'-OH BDE 99. However, Tricl shows the lowest RP of the group even though it bears a OH group in the ortho position and lacks adjacent chlorines. This suggests that there is a strong effect of the ligand's halogen substituent size for binding TBG and would explain why in the past hardly any TBG binding has been shown for PCBs [10]. The two strongest TTR binders in the group of the OH PHBs were also active in the TBG assay and had the same affinity ranking as for TTR. We could confirm the previously reported inactivity of 4-OH PCB 106, 4-OH PCB 121 and 4-OH PCB14 for TBG, but not the medium affinity of 4-OH PCB 69 for TBG (Table 1).

The number of halogens also plays a role, since all the compounds that were slight binders for TBG were at least tetra-substituted as shown in the second quadrant of Figure 4. The presence of one bromine adjacent to the OH group reduces the RP by about 2-fold, as seen with 6-OH BDE 49. This reduction is also seen with one or two bromines adjacent to the meta positioned OH group with 3-OH BDE 47 and 5-OH BDE 47. The fact that OH PBDEs are medium to strong binders of TTR and TBG is of special interest because of the abundant presence of OH-PBDEs in the in vivo situation. PBDEs are easily hydroxylated and are persistent in blood, contributing to the PBDE mediated toxicity [6, 45]. Of special interest are the OH metabolites of BDE 47 because they are the most common ones in humans [46]. 6-OH BDE 47 showed comparable RPs for

both transport proteins suggesting that high levels of this metabolite in human blood are of health concern because it targets equally T4 displacement from their binding proteins. The strong binding affinity for the transport proteins can explain the persistence of OH-PBDEs in blood because they are protected against secondary metabolism when bound to transport proteins. In addition, it has been reported that OH-PAHs can be transported to the fetus bound to TTR [14, 47].

From the 2 methoxylated PBDEs (MeOPBDEs) tested, only 6-MeO BDE 47 showed a very limited affinity for both rTTR and TBG, much lower than that of the OH-PBDEs. Although MeOPBDEs have been found in the marine environment [48], they seem unlikely to pose a risk based on their limited affinity for the transport proteins according to our results.

Triclosan (Tricl) is a hydroxylated polychlorinated diphenyl ether that, as the OH PBDEs strongly resembles the structure of T4 and equally targeted both rTTR and TBG. Both humans and the environment are exposed to Tricl because it is intensively used as antibacterial agent for example in dishwashing liquid, soap, toothpastes, mouthwashes, etc [49, 50]. This continuous exposure and strong transport protein binding affinities makes Tricl an important candidate for future studies.

BPA hardly inhibited transport protein binding. This widely used weak estrogenic compound contaminant, however, can be transformed into compounds like tetra chlorinated BPA (TCBPA), with thyroid hormone disrupting activity during aqueous chlorination in sewage treatment or in contaminated drinking water hoses [51, 52]. Evidencing the need for future studies were the endocrine disrupting chemicals assessment is performed in a more holistic approach using multi-system assays or multiple assays representing different systems and not only using chemical standards but also real samples were the total bioactive toxicity load is determined. Both TCBPA and the widely used flame retardant tetrabrominated BPA (TBBPA), were strong TTR binders in our studies. TCBPA had a RP (0.6) comparable with literature (0.8) and TBBPA had a RP (1) that could only be compared with one of our previous studies where a RP of 1.6 was found (Table 1).

The RPs we observed for the halogenated phenols in the TTR assay are in accordance with an interesting trend previously reported by Meerts et al. [38]. Given equal structures, the affinity increase with increasing atomic weight of the halogens substituents, for instance, TCBPA < TBBPA, DFP < DCP < DBP, TFP < TBP, PCP < PBP. Apparently, the emerging exclusively fluorine-substituted phenolic compounds are unlikely have an effect as thyroxine transport disruptor.

Several environmentally relevant pharmaceuticals (for review see [53, 54]) were tested with the transport protein assays. In accordance with previous studies Tetrac had a high RP for TTR in the range from 0.8 to 11.5 and Na Dic and Me Ac were moderate binders to TTR. Although MeAc was reported to be one order of magnitude more potent than NaDic, in our study their potency was comparable for TTR (Table 1). In the TBG assay, we found a RP for Tetrac of 0.6, comparable to the RP of 0.4 reported in literature and a RP for NaDic that was 25 times higher (table 1). Previous studies reported an interaction of Furosemide (Fur), NaDic and MeAc with TBG, but in our study Fur and MeAc only were slight binders due to the lower maximum concentration tested compared to the one used in literature.

Of the pesticides and other compounds of environmental relevance tested, only the natural isoflavonoid, genistein (Gen) was active in the TTR assay. The IC_{50} of Gen was 43.8 nM, roughly comparable with the previously reported equilibrium dissociation constant ($KD = 40$ nM) for Gen binding to TTR [43]. This compound also has a weak estrogenic activity and is considered a beneficial nutraceutical for menopausal women. On the other hand, the health implications of the strong TTR binding potency still is unknown and of interest for future research.

Toxicological Relevance of T4 Transport Protein Binding

The T4 binding site of TBG has recently been solved and is located on the surface of TBG [55]. Apparently, TBG is an active T4 carrier specifically adapted to allow triggered and modulated release of T4 to specific tissues including the placentas [55, 56]. Given that the fetus initially has no iodine reserve it is dependent on the iodine transferred by the mother. Consequently, there is an increased concentration of T4-TBG in the mother during pregnancy in order to supply an avid placental uptake [12, 29]. Therefore, one could speculate that during ontogenesis the displacement of the T4-TBG complex by the OH-PBDEs commonly found in humans, could have consequences in fetal development. TTR also mediates the maternal to fetal T4-transport through the placenta, in addition to the delivery of T4 across the blood-brain barrier. It has been shown before that compounds bound to TTR are transported to the fetal compartment and fetal brain, decreasing fetal brain T4 levels [57, 58].

The OH-PBDEs were the most active compounds toward both T4 transport proteins. However, these compounds usually occur in mixtures combined with the OH-PCBs which are more potent toward TTR. This study is the first to show that some OH-PHAHs have a strong binding affinity for TBG and one important requirement for binding is the presence of the bulkier bromine substituents found in OH-PBDEs. Hence, there are good reasons to expect a relevant inhibition of T4 transport to the fetus. In addition to transport protein-binding, T4 and T3-like OH-PBDEs also have been shown to induce T3-dependent cell proliferation in the T-screen and activate the nuclear TH receptors TR α and TR β in specific reporter gene assays [59]. Furthermore, OH-PHAHs, have also been shown to interfere with sulfonotransferases [60, 61] and deiodinases [62]. Apparently especially the OH-metabolites of PHAHs, including the ubiquitous PCBs and PBDEs, have been shown to hamper the TH homeostasis at several physiological levels and via multiple thyroid hormone-related mechanisms. As, in addition, the effects of mixtures of PHAHs not only are additive, but sometimes even synergistic, this could mean a serious risk for thyroid hormone disrupting effects of such mixtures, especially in developing fetuses.

The currently presented fast and reproducible optimized SPR biosensor – based transport protein assay offers a suitable method for high throughput screening of a large library of compounds, their metabolites and even biological samples. As the T4 is immobilized on the chip surface in this method, it could be further expanded to measure binding of compounds to T4 sulfono- and glucuronyltransferases and T4-iodinases. We speculate that the T4 binding sites of these enzymes might share features with those of the transport proteins, allowing their binding to the immobilized T4. For example, Tric1 has been shown to interact strongly with both TBG and TTR in the present study and previous research reported a strong interaction with sulfonotransferases and glucuronyltransferases [63], suggesting a possible predictive value of the transport protein-based assays for other binding assays. Multiple T4- and T3-assays that are currently under study, possibly in combination with multiple SPR biosensing spots [64, 65], would allow a drastic reduction in the number of tests needed for the screening of TH-disrupting potencies of compounds as required for EU regulations of toxic compounds such as REACH [66].

Acknowledgments

The authors thank the EU funded Marie Curie Foundation (Ph.D. project supported by a Marie Curie Host Industry Fellowship (Contract EVK1-CT-2001-55002)) and the Dutch Ministry of Agriculture, Nature and Food Quality for funding this project.

References

1. Yen PM (2001) Physiological and Molecular Basis of Thyroid Hormone Action *Physiol. Rev.* 81, 1097-142
2. Bernal J, Guadano-Ferraz A, Morte B (2003) Perspectives in the study of thyroid hormone action on brain development and function *Thyroid* 13, 1005-12
3. Schreiber G (2002) The evolutionary and integrative roles of transthyretin in thyroid hormone homeostasis *J. Endocrinol.* 175, 61-73
4. Friesema EC, Jansen J, Visser TJ (2005) Thyroid hormone transporters *Biochem. Soc. Trans.* 33, 228-32
5. Boas M, Feldt-Rasmussen U, Skakkebaek NE, Main KM (2006) Environmental chemicals and thyroid function *Eur. J. Endocrinol.* 154, 599-611
6. Hakk H, Letcher RJ (2003) Metabolism in the toxicokinetics and fate of brominated flame retardants--a review *Environ. Int.* 29, 801-28
7. Hallgren S, Darnerud PO (2002) Polybrominated diphenyl ethers (PBDEs), polychlorinated biphenyls (PCBs) and chlorinated paraffins (CPs) in rats--testing interactions and mechanisms for thyroid hormone effects *Toxicology* 177, 227-43
8. Lans MC, Klasson-Wehler E, Willemsen M, Meussen E, Safe S, Brouwer A (1993) Structure-dependent, competitive interaction of hydroxy-polychlorobiphenyls, -dibenzo-p-dioxins and -dibenzofurans with human transthyretin *Chem.-Biol. Interact.* 88, 7-21
9. Cheek A, Kow K, Chen J, McLachlan JA (1993) Potential mechanisms of thyroid disruption in humans: interaction of organochlorine compounds with thyroid receptor, transthyretin, and thyroid-binding globulin. *Environ. Health Perspect.* 107, 273-8
10. Lans MC, Spiertz C, Brouwer A, Koeman JH (1994) Different competition of thyroxine binding to transthyretin and thyroxine-binding globulin by hydroxy-PCBs, PCDDs and PCDFs *Eur. J. Pharmac. Env. Tox. Pharmac.* 270, 129-36
11. Palha JA (2002) Transthyretin as a thyroid hormone carrier: function revisited *Clin. Chem. Lab. Med.* 40, 1292
12. Schussler GC (2000) The thyroxine-binding proteins *Thyroid* 10, 141
13. Koopman-Esseboom C, Morse DC, Weisglas-Kuperus N, Lutkeschipholt IJ, Van der Paauw CG, Tuinstra LGMT, Brouwer A, Sauer PJJ (1994) Effects of

dioxins and polychlorinated biphenyls on thyroid hormone status of pregnant women and their infants *Pediatr. Res.* 36, 468-73

14. Morse DC, Wehler EK, Wesseling W, Koeman JH, Brouwer A (1996) Alterations in rat brain thyroid hormone status following pre- and postnatal exposure to polychlorinated biphenyls (Aroclor 1254) *Toxicol. Appl. Pharmacol.* 136, 269-79

15. Palha JA, Goodman AB (2006) Thyroid hormones and retinoids: A possible link between genes and environment in schizophrenia *Brain Research Reviews* 51, 61

16. Porterfield SP (2000) Thyroidal dysfunction and environmental chemicals--potential impact on brain development *Environ. Health Perspect.* 108 Suppl 3, 433-8

17. Fritsche E, Cline JE, Nguyen NH, Scanlan TS, Abel J (2005) Polychlorinated biphenyls disturb differentiation of normal human neural progenitor cells: clue for involvement of thyroid hormone receptors *Environ. Health Perspect.* 113, 871-6

18. Newbold RR, Padilla-Banks E, Snyder RJ, Phillips TM, Jefferson WN (2007) Developmental exposure to endocrine disruptors and the obesity epidemic *Reprod. Toxicol.* 23, 290-6

19. Grun F, Blumberg B (2006) Environmental obesogens: organotins and endocrine disruption via nuclear receptor signaling *Endocrinology* 147, S50-5

20. Tabb MM, Blumberg B (2006) New Modes of Action for Endocrine-Disrupting Chemicals *Mol. Endocrinol.* 20, 475-82

21. Sjodin A, Jones RS, Focant JF, Lapeza C, Wang RY, McGahee EE, 3rd, Zhang Y, Turner WE, Slazyk B, Needham LL, Patterson DG, Jr. (2004) Retrospective time-trend study of polybrominated diphenyl ether and polybrominated and polychlorinated biphenyl levels in human serum from the United States *Environ. Health Perspect.* 112, 654-8

22. Hites RA (2004) Polybrominated Diphenyl Ethers in the Environment and in People: A Meta-Analysis of Concentrations *Environ. Sci. Technol.* 38, 945-56

23. Marchesini GR, Meulenberg E, Haasnoot W, Mizuguchi M, Irth H (2006) Biosensor Recognition of Thyroid-Disrupting Chemicals Using Transport Proteins *Analytical Chemistry* 78, 1107-14

24. Matsubara K, Mizuguchi M, Kawano K (2003) Expression of a synthetic gene encoding human tranthyretin in *Escherichia coli* *Protein Expr. Purif.* 30, 55-61
25. Rickenbacher U, McKinney JD, Oatley SJ, Blake CC (1986) Structurally specific binding of halogenated biphenyls to thyroxine transport protein *J. Med. Chem.* 29, 641-8
26. Korcek L, Tabachnick M (1976) Thyroxine-protein interactions. Interaction of thyroxine and triiodothyronine with human thyroxine-binding globulin *J. Biol. Chem.* 251, 3558-62
27. van Lipzig MMH, Commandeur JN, de Kanter FJJ, Damsten MC, Vermeulen NPE, Maat E, Groot EJ, Brouwer A, Kester MHA, Visser TJ, Meerman JHN (2005) Bioactivation of Dibrominated Biphenyls by Cytochrome P450 Activity to Metabolites with Estrogenic Activity and Estrogen Sulfotransferase Inhibition Capacity *Chem. Res. Toxicol.* 18, 1691-700
28. Somack R, Andrea TA, Jorgensen EC (1982) Thyroid hormone binding to human serum prealbumin and rat liver nuclear receptor: kinetics, contribution of the hormone phenolic hydroxyl group, and accommodation of hormone side-chain bulk *Biochemistry* 21, 163-70
29. Andrea TA, Cavalieri RR, Goldfine ID, Jorgensen EC (1980) Binding of thyroid hormones and analogues to the human plasma protein prealbumin *Biochemistry* 19, 55-63
30. Cheng SY, Pages RA, Saroff HA, Edelhofer H, Robbins J (1977) Analysis of thyroid hormone binding to human serum prealbumin by 8-anilino-naphthalene-1-sulfonate fluorescence *Biochemistry* 16, 3707-13
31. Cody V (1980) Thyroid hormone interactions: molecular conformation, protein binding, and hormone action *Endocr. Rev.* 1, 140-66
32. Maberly GF, Waite KV, Cutten AE, Smith HC, Eastman CJ (1985) A reappraisal of the binding characteristics of human thyroxine-binding globulin for 3,5,3'-triiodothyronine and thyroxine *J. Clin. Endocrinol. Metab.* 60, 42-47
33. Chauhan KR, Kodavanti PRS, McKinney JD (2000) Assessing the Role of ortho-Substitution on Polychlorinated Biphenyl Binding to Transthyretin, a Thyroxine Transport Protein*1 *Toxicol. Appl. Pharmacol.* 162, 10-21
34. Purkey HE, Palaninathan SK, Kent KC, Smith C, Safe SH, Sacchettini JC, Kelly JW (2004) Hydroxylated polychlorinated biphenyls selectively bind transthyretin in blood and inhibit amyloidogenesis: rationalizing rodent PCB toxicity *Chem. Biol.* 11, 1719-28

35. Hamers T, Kamstra JH, Sonneveld E, Murk AJ, Kester MHA, Andersson PL, Legler J, Brouwer A (2006) In Vitro Profiling of the Endocrine-Disrupting Potency of Brominated Flame Retardants *Toxicol. Sci.* 92, 157-73
36. Hamers T, Kamstra JH, Sonneveld E, Murk AJ, Visser TJ, van Velzen MJM, Brouwer A, Bergman A (2007) Biotransformation of brominated flame retardants into potentially endocrine disrupting metabolites, with special attention to 2,2',4,4'-tetrabromodiphenyl ether (BDE-47) *In Press*
37. Legler J, Cenijn PH, Malmberg T, Bergman A, Brouwer A (2002) Determination of the endocrine disrupting potency of hydroxylated PCB's and flame retardants with in vitro bioassays. *Organohalogen Comp.* 56, 53-56
38. Meerts IATM, van Zanden JJ, Luijckx EAC, van Leeuwen-Bol I, Marsh G, Jakobsson E, Bergman A, Brouwer A (2000) Potent Competitive Interactions of Some Brominated Flame Retardants and Related Compounds with Human Transthyretin in Vitro *Toxicol. Sci.* 56, 95-104
39. den Besten C, Vet JJRM, Besselink HT, Kiel GS, van Berkel BJM, Beems R, van Bladeren PJ (1991) The liver, kidney, and thyroid toxicity of chlorinated benzenes *Toxicol. Appl. Pharmacol.* 111, 69
40. van den Berg KJ (1990) Interaction of chlorinated phenols with thyroxine binding sites of human transthyretin, albumin and thyroid binding globulin *Chem.-Biol. Interact.* 76, 63-75
41. Hao YL, Tabachnick M (1971) Thyroxine-protein interactions. VII. Effect of thyroxine analogs on the binding of 125-I-thyroxine to highly purified human thyroxine-binding globulin *Endocrinology* 88, 81-92
42. Munro SL, Lim CF, Hall JG, Barlow JW, Craik DJ, Topliss DJ, Stockigt JR (1989) Drug competition for thyroxine binding to transthyretin (prealbumin): Comparison with effects on thyroxine-binding globulin *J. Clin. Endocrinol. Metab.* 68, 1141
43. Green NS, Foss TR, Kelly JW (2005) Genistein, a natural product from soy, is a potent inhibitor of transthyretin amyloidosis *Proc. Natl. Acad. Sci.* 102, 14545-50
44. McCammon MG, Scott DJ, Keetch CA, Greene LH, Purkey HE, Petrassi HM, Kelly JW, Robinson CV (2002) Screening transthyretin amyloid fibril inhibitors: characterization of novel multiprotein, multiligand complexes by mass spectrometry *Structure* 10, 851-63

45. Costa LG, Giordano G (2007) Developmental neurotoxicity of polybrominated diphenyl ether (PBDE) flame retardants *NeuroToxicology* 28, 1047-67
46. Letcher RJ, Stapleton HM, Verreault J, McKinney M, Scipione F, Gabrielsen G, Chu S, Valters K 2004; 375-78.
47. Ulbrich B, Stahlmann R (2004) Developmental toxicity of polychlorinated biphenyls (PCBs): a systematic review of experimental data *Arch. Toxicol.* 78, 252
48. Teuten EL, Reddy CM (2007) Halogenated organic compounds in archived whale oil: A pre-industrial record *Environ. Pollut.* 145, 668-71
49. Singer H, Muller S, Tixier C, Pillonel L (2002) Triclosan: Occurrence and Fate of a Widely Used Biocide in the Aquatic Environment: Field Measurements in Wastewater Treatment Plants, Surface Waters, and Lake Sediments *Environ. Sci. Technol.* 36, 4998-5004
50. Gomez MJ, Martinez Bueno MJ, Lacorte S, Fernandez-Alba AR, Aguera A (2007) Pilot survey monitoring pharmaceuticals and related compounds in a sewage treatment plant located on the Mediterranean coast *Chemosphere* 66, 993-1002
51. Gallard H, Leclercq A, Croue JP (2004) Chlorination of bisphenol A: kinetics and by-products formation *Chemosphere* 56, 465-73
52. Yamauchi K, Ishihara A, Fukazawa H, Terao Y (2003) Competitive interactions of chlorinated phenol compounds with 3,3',5-triiodothyronine binding to transthyretin: detection of possible thyroid-disrupting chemicals in environmental waste water *Toxicol. Appl. Pharmacol.* 187, 110-17
53. Halling-Sorensen B, Nors Nielsen S, Lanzky PF, Ingerslev F, Holten Lutzhoft HC, Jorgensen SE (1998) Occurrence, fate and effects of pharmaceutical substances in the environment--a review *Chemosphere* 36, 357-93
54. Jones OA, Voulvoulis N, Lester JN (2001) Human pharmaceuticals in the aquatic environment a review *Environ. Technol.* 22, 1383-94
55. Zhou A, Wei Z, Read RJ, Carrell RW (2006) Structural mechanism for the carriage and release of thyroxine in the blood *Proc. Natl. Acad. Sci.* 103, 13321-26
56. Robbins J (2000) New Ideas in Thyroxine-Binding Globulin Biology *J. Clin. Endocrinol. Metab.* 85, 3994-95

57. Elst JPS-VD, Van Der Heide D, Rokos H, De Escobar GM, Kohrle J (1998) Synthetic flavonoids cross the placenta in the rat and are found in fetal brain *Am. J. Physiol. Endocrinol. Metab.* 274, E253-56
58. Meerts IATM, Assink Y, Cenijn PH, van den Berg JHJ, Weijers BM, Bergman A, Koeman JH, Brouwer A (2002) Placental Transfer of a Hydroxylated Polychlorinated Biphenyl and Effects on Fetal and Maternal Thyroid Hormone Homeostasis in the Rat *Toxicol. Sci.* 68, 361-71
59. Schriks M, Roessig JM, Murk AJ, Furlow JD (2007) Thyroid hormone receptor isoform selectivity of thyroid hormone disrupting compounds quantified with an in vitro reporter gene assay *Environ. Toxicol. Pharmacol.* 23, 302-07
60. Schuur AG, Brouwer A, Bergman A, Coughtrie MW, Visser TJ (1998) Inhibition of thyroid hormone sulfation by hydroxylated metabolites of polychlorinated biphenyls *Chem.-Biol. Interact.* 109, 293-7
61. Schuur AG, Legger FF, van Meeteren ME, Moonen MJ, van Leeuwen-Bol I, Bergman A, Visser TJ, Brouwer A (1998) In vitro inhibition of thyroid hormone sulfation by hydroxylated metabolites of halogenated aromatic hydrocarbons *Chem. Res. Toxicol.* 11, 1075-81
62. Adams C, Lans MC, Klasson-Wehler E, Van Engelen JGM, Visser J, Brouwer A (1990) Hepatic thyroid hormone 5'-deiodinase, another target-protein for monohydroxy metabolites of 3,3',4,4'-tetrachlorobiphenyl *Organohalogen Comp.* 1, 51-54
63. Wang LQ, Falany CN, James MO (2004) Triclosan as a substrate and inhibitor of 3'-phosphoadenosine 5'-phosphosulfate-sulfotransferase and UDP-glucuronosyl transferase in human liver fractions *Drug Metab. Dispos.* 32, 1162-9
64. Steiner G (2004) Surface plasmon resonance imaging *Anal. Bioanal. Chem.* 379, 328-31
65. Chinowsky TM, Soelberg SD, Baker P, Swanson NR, Kauffman P, Mactutis A, Grow MS, Atmar R, Yee SS, Furlong CE (2007) Portable 24-analyte surface plasmon resonance instruments for rapid, versatile biodetection *Biosens. Bioelectron.* 22, 2268-75
66. EEC (2006) Regulation (EC) No 1907/2006 of the European Parliament and of the Council of 18 December 2006 concerning the Registration, Evaluation, Authorisation and Restriction of Chemicals (REACH). *OJEC L* 396, 1-849

Part II. Toward Simple and Portable SPR Biosensor Screening



Chapter 5

Spreeta-based Biosensor Assays for Endocrine Disruptors

Published in: Biosensors and Bioelectronics 528 (2005) 37-45

Abstract

The construction and performance of an automated low-cost Spreeta™ – based prototype biosensor system for the detection of endocrine disrupting chemicals (EDCs) is described.

The system consists primarily of a Spreeta miniature liquid sensor incorporated into an aluminum flow-cell holder, dedicated to support a Biacore chip frame, in combination with a simple pressurized air-driven fluid system.

During the optimization, a monoclonal antibody (MAb)-based immunoassay for the estrogenic compound bisphenol A (BPA) was used as a model. After the optimization, two thyroxine transport protein inhibition assays for thyroid endocrine disruptors were implemented. The average noise of the system for 1 min of baseline was 1.1 μ RIU (Refractive Index Units) and it could be operated in the range of 18-22 °C with a minimum baseline drift (5-10 μ RIU/100 min). Optimum signal to noise ratio (S/N R) was obtained using a flow cell height of 100 μ m and a flow rate of 180 μ L/min. The sensitivity of the Spreeta-based biosensor inhibition assays implemented (50% inhibition concentration (IC_{50}) of 30.2 nM for BPA using MAb 12 and 12.3 and 11.6 nM for thyroxine (T4) using thyroxine binding globulin (TBG) and recombinant transthyretin (rTTR), respectively) was comparable to the sensitivity previously obtained using a Biacore 3000 (IC_{50} of 39.9 nM for BPA and 8.6 and 13.7 nM respectively for T4). The results indicate that the alternative prototype system can be used in combination with ready-to-use biosensor chip surfaces and it is potentially a useful tool for the bioeffect-related screening of EDCs.

Introduction

Contaminants originating from a variety of sources (i.e. industrial waste, pesticides, pharmaceuticals and certain household products) are present in the environment and bio accumulate through the trophic chain posing a threat to human health and wildlife.

Some of these chemicals can mimic or antagonize the effects of endogenous hormones in an organism and are considered endocrine disrupting chemicals (EDCs).

EDCs can be roughly grouped by their biological effect (i.e. estrogenic, androgenic, thyrogenic, etc.) depending on which receptor, enzyme or transport protein they target. However, EDCs might be promiscuous and elicit more than one biological effect.

EDCs can be detected using classic instrumental analytical techniques like high performance liquid chromatography (HPLC), gas chromatography (GC) or, at a lower cost, using immunochemical techniques like enzyme linked immunosorbent assays (ELISA) [1] with the disadvantage that the specificity of the method only allows the detection of a single compound or a group of structurally related compounds [2]. However, the main drawback is that EDCs are structurally diverse and there is a continuous market-driven evolution in the type of compounds produced. Therefore, the discovery and detection of EDCs through their biological effects is a feasible alternative. EDCs usually exert their biological effects by specifically binding to at least one hormone receptor site or a transport protein. Hence, mimicking or antagonizing the effects of the endogenous hormone or disrupting the synthesis or metabolism of endogenous hormones or hormone receptors [3]. Thus, the implementation of a method that uses of the same receptors or transport proteins which are targeted by the EDCs as their biorecognition elements allows a bioeffect-related detection of the total load of endocrine disrupting potency from a chemical or a complex group related to that receptor in a certain sample. This principle has been widely used in radioligand binding assays [4, 5], enzyme linked receptor assays (ELRA)[6-8], and biochemical detection coupled with mass spectrometry [9].

The development of high-throughput, low-cost, bioeffect-related screening methods is of high interest for the detection of the EDCs in certain samples and for the assessment of emerging contaminants like bisphenol A (BPA) and polybrominated compounds (flame retardants), veterinary and human medicines [10] and their metabolites.

Automated surface plasmon resonance (SPR)-based biosensors are capable of monitoring biospecific interactions in real time with no need of labels. This has allowed the widespread use of this technology as a laboratory tool for the qualitative and quantitative assaying of a wide variety of biomolecules to obtain their kinetic constants. This technology, using Biacore SPR biosensors, was previously applied for the bioeffect-related screening of thyroid-disrupting chemicals using the thyroxine (T4) transport proteins (TP) (thyroxine binding globulin (TBG) and recombinant transthyretin (rTTR)) [11].

Further use of SPR biosensors for the assessment of potential EDCs or their detection in fields like food safety or environmental monitoring is challenged by the high costs of the commercially available systems and the lack of portability for in situ analysis [12].

The Spreeta™ TSPR2K11 is a compact, low-cost and commercially available SPR-based sensor manufactured by Texas Instruments. The units consist of a near- infrared diverging LED light source, a polarizer, a gold sensing layer, a reflecting mirror and a photodiode-array detector. The working principle is as follows; first, the polarized light is emitted toward the gold sensing surface and reflected at different angles. At certain angles of light incidence resonance of the gold surface plasmons occurs and the intensity of the reflected light drops dramatically. Second, the light is reflected on a mirror and projected onto the photodiode array where the light intensity is measured. Third, the position of this light intensity minimum is extremely sensitive to changes in refractive index (RI) of the fluid at the sensing area. Therefore the concentration of molecules in solution near to the sensing area changes the local RI which can be measured by monitoring the light intensity minimum shift over time (SPR profile). Hence, if a molecule is immobilized (i.e. hormone, antigen) on the sensing surface and a second molecule with a certain affinity for the immobilized one is introduced (i.e. receptor, antibody). The molecules introduced will accumulate at the sensing surface over time producing a measurable RI change. This principle has been used in Spreeta™ SPR sensors with a proper instrumentation system [13] for the setup of direct and competitive inhibition assays for the detection of toxins [14, 15], food allergens [16], bovine kappa-casein in milk and milk powder [17] and genetically modified organisms [18]. For the detection of EDCs, a model immunoassay for estrone-3-glucuronide has been reported, with a detection range between 20-300 nM and an analysis time of 70 min. [12]. However, the small molecule (hapten) conjugates on the gold

sensor surface had to be stripped and newly physisorpted in each cycle. The Spreeta sensor surface can also be modified for covalent immobilizations [18], nevertheless, in the present work we used the Spreeta sensor in combination with CM5 biosensor chips (Biacore). CM5 biosensor chips are composed of a plastic frame holding a glass slide covered on one side with a gold layer coated with covalently immobilized carboxymethylated dextrane (CMD). The CMD matrix of the CM5 chip enhances the hapten immobilization level due to the higher number of available sites for derivatization in its 3 dimensional structure and blocks non specific binding to the gold surface. These biosensor chips were found suitable and robust in previously described applications in which haptens were immobilized [11, 19].

In the present article we optimized the use of a compact, automated single channel Spreeta biosensor in combination with exchangeable pre-functionalized and commercially available CM5 sensor chips A simple, pressure-driven and pulse-free fluidic system provided low noise and a robust sample delivery method.

In the present study we used an inhibition immunoassay for the specific detection of the estrogenic compound bisphenol A (BPA) as a model for optimization of the system and further implemented two assays for the bioeffect-related screening of thyroxine transport disrupting chemicals using TBG and rTTR.

Experimental

Reagents

Sensor chips (CM5), the amine coupling kit [containing 0.1 M N-hydroxysuccinimide (NHS), 0.4 M 1-ethyl-3-(3-dimethylaminopropyl) carbodiimide hydrochloride (EDC) and 1 M ethanolamine hydrochloride (pH 8.5)], HBS-EP buffer [pH 7.4, consisting of 10 mM 4-(2-hydroxyethyl) piperazine-1-ethanesulfonic acid, 150 mM sodium chloride, 3 mM EDTA, 0.005% (v/v) surfactant polysorbate (P20)] and the BIACORE 3000 were supplied by Biacore AB (Uppsala, Sweden). Ethylenediamine (EDA) was obtained from Merck (Haarlem, The Netherlands). L-Thyroxine ((T4) 3,3',5,5'-tetraiodo-L-thyronine), 3,3',5-triiodothyronine (T3), bisphenol A ((BPA) 2, 2-bis (4-hydroxyphenyl) propane), 4,4 bis (4-hydroxyphenyl) valeric acid, (BVA), 5-aminovaleric acid (AVA), ovalbumin (OVAL), dimethyl sulfoxide (DMSO), acetonitrile (ACN), and all other reagents were obtained from Sigma-Aldrich Chemie

(Zwijndrecht, The Netherlands) unless otherwise stated. Aqua regia was prepared by mixing 100 μ l concentrated nitric acid with 300 μ l concentrated hydrochloric acid.

The T4 stock solution (10 mM) was prepared by dissolving T4 in a solution containing DMSO (94%) chloroform (5%) and 1 M NaOH (1%). The monoclonal antibody 12 (MAb 12) was originally raised toward a BVA conjugate and it strongly cross-reacted with BPA [19].

The recombinant his-tagged transthyretin (rTTR) was a kind gift from the Toyama Medical and Pharmaceutical University (Toyama, Japan). Thyroxine Binding Globulin (TBG) was obtained from Scipac (Kent, UK).

Apparatus

The scheme of the Spreeta-based automated prototype biosensor system is presented in Figure 1. The system consists of an aluminum holder which combines a SpreetaTM Miniature liquid sensor (TSPR2K11, Texas Instruments, USA) with a Biacore CM5 chip frame (removed from its holder) and an aluminum flow cell. The sensor is controlled by a digital signal processor (DSP)-controller box and pc-based evaluation software (Box version 16, software version 5.21, Nomadics, Inc., USA).

The removal of the gold sensor surface with aqua regia from the Spreeta sensor left a transparent glass-like surface available for coupling with a CM5 sensor chip. The two glass surfaces were optically coupled with a glass-like refractive index film of poly (vinyl chloride) (PVC) [20]. The refractive index matching polymer (RIMP) interface was brought in contact with the glass side of a CM5 biosensor chip and the sliding flow cell pressed the system together and allowed the contact of the fluid with the CM5 sensor chip surface (see insert Figure 1). In the final system setup, the gold surface present in the CM5 sensor chip is used as the sensing surface of the SpreetaTM sensor, with the advantage of an easy exchange of the sensor chip surface for different applications.

The flow system is connected via Teflon tubing (diameter 0.5 mm) and based on a pressurized air-fluid supply, driven by a 12 V dc miniature membrane pump (Nater, The Netherlands). The buffer container has a capacity of 50 ml and the flow is controlled by using capillaries of various diameters as flow restrictors. The liquid sensor, controller box and fluid system were built in an isolated hard case incorporating a Maxim MAX1978 integrated temperature controller (Getronics, The Netherlands) and a Marlow Industries thermoelectric cooler (Farnell In One, The Netherlands).

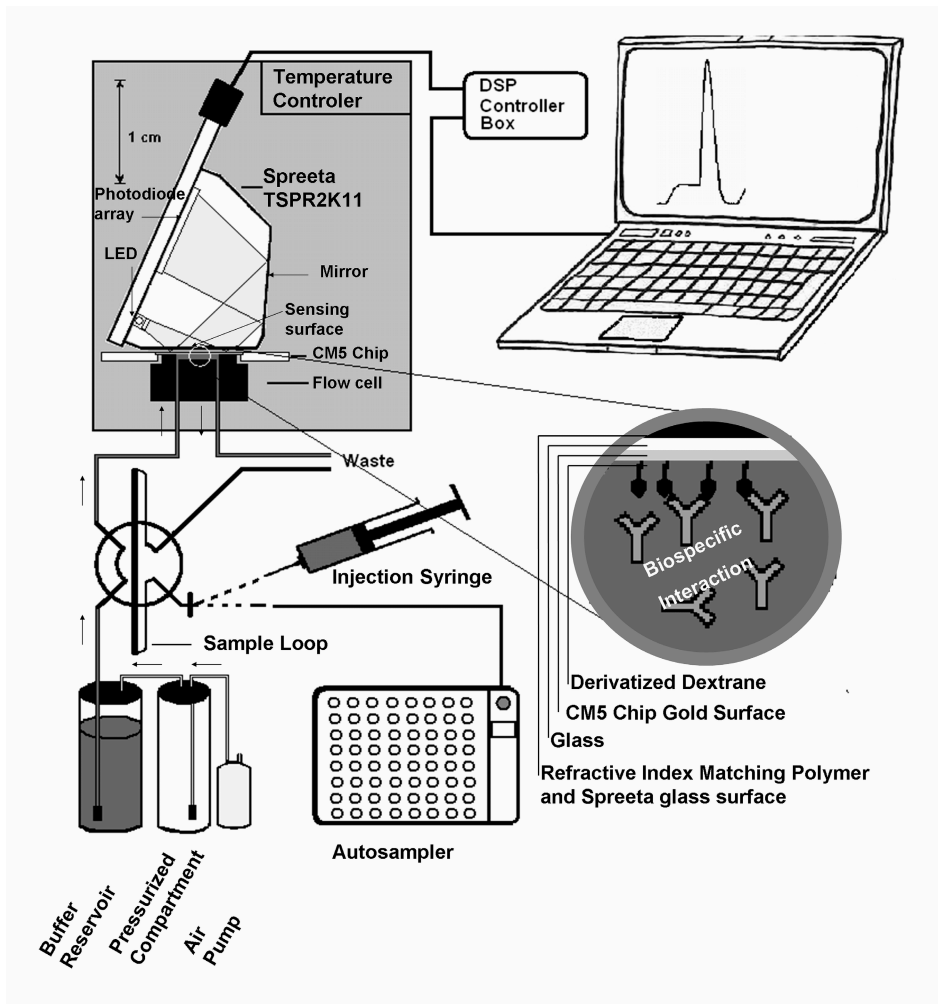


Figure1. Schematic illustration of the Spreeta™-based automated prototype biosensor system. The sample can either be injected using an autosampler or a syringe. The pressurized air-driven fluidic system delivers the sample to the biosensor chip surface where the biospecific interaction takes place (see insert). The system scheme is not at scale except for the Spreeta TSPR2K11 sensor unit.

During the evaluation study the system was connected to a Perkin-Elmer ISS-100 auto injector with a 200 μl sample loop. The system can also be operated manually by means of a stainless steel injection valve (Instrument Solutions, The Netherlands) equipped with a sample loop. The three flow cells evaluated had a flow path of 1 mm width, 4 mm long and heights of 100 μm (small volume = 0.4 μl), 400 μm (medium

volume = 1.6 μ l) and 1000 μ m (large volume = 4 μ l). BIAevaluation 3.1 (Biacore AB, Sweden) software was used to evaluate and handle the sensorgrams generated with the Spreeta-based biosensor.

Biosensor Chip Immobilization Methods

The CM5 sensorchip surfaces are prefunctionalized with a dextrane layer that contains free carboxy groups for the formation of amide bonds with the molecule immobilized for the assay. Two different CM5 sensor chip surfaces were prepared on the bench top. For the BPA inhibition immunoassay, BVA was immobilized to the CMD sensor chip surface. For the T4 transport protein inhibition assays (rTTR and TBG), T4 was immobilized using a spacer (AVA).

In both cases the CM5 sensorchip surface was activated by directly pipetting 100 μ l of a mixture of 0.4 M EDC and 0.1 M NHS (1:1; v/v). The activated carboxylated dextran surface was washed with water and 100 μ l of the corresponding spacer were added and left to react for 30 min.

Preparation of the BVA Sensorchip Surface

Ethylenediamine (2 M solution, pH 10) was used as the bifunctional spacer. BVA (2.1 mg/ml in ethanol (35%) and 10 mM sodium acetate coupling buffer (pH 4.5) (65%)) was activated by mixing with 0.4 M EDC and 0.1 M NHS (2:1:1; v/v/v) and incubated for 30 min with the previously derivatized ethylenediamine-sensorchip surface. The activated BVA solution on the chip surface was changed every 10 min or when a white deposit was observed.

Preparation of the AVA-T4 Sensorchip Surface

AVA (20 mM in carbonate buffer pH 9.6) was used as bifunctional spacer for the immobilization of T4. Once immobilized, the AVA surface was washed and its carboxyl groups were re-activated with 100 μ l of a mixture of 0.4 M EDC and 0.1 M NHS (1:1; v/v) for 30 min. T4 (2 mM in carbonate buffer pH 9.6) was incubated for 30 min with the activated AVA surface and the amino group present in the alanyl side chain of T4 created an amide bond with the activated AVA carboxyl group immobilizing T4 to the chip surface.

Competitive inhibition assays

The assays were based on the competitive inhibition format in which the absence of a compound binding to the biospecific molecule (BSM) (i.e. receptor or antibody) results in maximum BSM binding to the derivatized sensor chip surface. Increasing concentrations of compounds binding to the BSM will compete for binding with the hapten immobilized on the sensor surface and the signal will drop proportionately. One might ask why the direct detection of the compounds was not evaluated where the BSM would be immobilized on the sensor chip surface and the binding of the compounds directly measured. Given the small molecular mass of the present compounds, the refractive index change produced by these compounds binding to the immobilized antibodies would be around the detection limit of the present system. In a previous study we evaluated the direct assay approach for BPA [19] and it was found that although it was possible to measure directly BPA responses using the BIACORE 3000 system, the signal was limited and the stability of the immobilized BSM was not satisfactory.

The inhibition assay procedure was as follows, the corresponding biospecific molecule at appropriate concentrations were mixed (1:5 v/v) with analyte dilution series. The mixture was injected for 1 min at a flow rate of 180 $\mu\text{l}/\text{min}$ in the biosensor system over the corresponding sensor chip surface (BVA for MAb 12 and T4 for TBG and rTTR). In order to prepare the chip for the following injection cycle, 180 μl of regeneration solution (0.2 M NaOH 20% Acetonitrile) were injected. Calibration curves of BPA and T4 were generated with the MAb 12 and T4-transport protein inhibition assays respectively. To evaluate the reproducibility of the assays, at least two calibration curves were measured with each assay in different days, and the IC_{50} was used to calculate the Inter assay CV%.

Results and Discussion

Sensor System

In the present system we removed the original gold sensing surface and added a RIMP film of about 5 μm thick and a CM5 sensorchip (including glass slide). Figure 2 depicts the shift of the SPR dip for distilled water with the original gold layer (SPR minimum at pixel 91.86 ± 0.003) and after the gold was removed and the RIMP was used in combination with

the CM5 sensor chip (SPR minimum at pixel 75.62 ± 0.005). The SPR dip shift is due to two reasons. First, the polarized light has to travel a longer optical path until it reaches the sensing surface, this shifts the position of the sensing surface as well as the position from where the light is projected, which finally shifts the pixel where the SPR minimum is detected [21]. Second, to the change in RI induced by the carboxymethylated dextrane on the CM5 sensor chip surface.

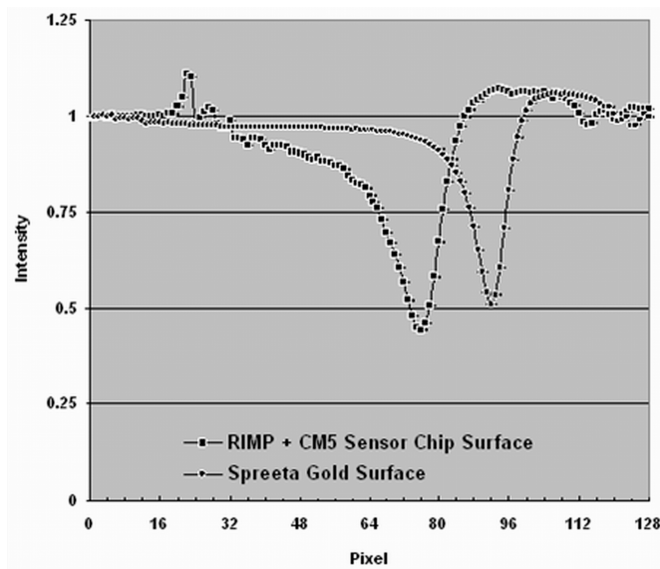


Figure 2. SPR profiles in water measured with the original gold sensor surface and the modified sensor surface using the RIMP film and a CM5 chip. Each profile is an average of 3 consecutive measurements. If error bars are not visible, they were smaller than the data marker.

Given that a SPR minimum shift of one pixel is equivalent to a $500 \mu\text{RIU}$ change, the shift due to the RIMP film is equivalent to $8120 \mu\text{RIU}$, or a loss of only 12% of the dynamic range ($70,000 \mu\text{RIU}$) above the RI of water. The expected responses in inhibition immuno- and receptor assays are in the order of $10\text{--}10,000 \mu\text{RIU}$, therefore well within the dynamic range left in the sensor.

The SPR curve is analyzed by the software and the SPR minimum shift is expressed as refractive index change (ΔRI) and plotted over time. A ΔRI of 1×10^{-6} ($1 \mu\text{RIU}$) is comparable to about 1 pg/mm^2 of proteins bound to the chip surface [22] and to one response unit (RU) in the Biacore

3000 system. For convenience the RI change in all sensorgrams will be expressed in μ RIU.

The optimization of the RI noise is crucial for obtaining maximum sensitivity in the system. Hence, we compared the noise (as the standard deviation of the RI monitored in one minute) in the bare gold sensor surface and the CM5 sensor surface modified with the RIMP film and the CM5 chips. Fitting of the SPR profiles with polynomial functions from second to ninth order were evaluated for both sensors and the noise obtained with both systems was very similar across the polynomials functions. The minimum noise (1.1 μ RIU) was obtained using a 4th order polynomial function at 1.22 Hz acquisition rate with both the bare gold sensor surface and the CM5 sensor surface modified with the RIMP film. These results indicate that the introduction of the RIMP film does not introduce measurable noise at this magnitude and that the same polynomial fitting functions used with the bare gold sensor can be used with the RIMP film. It should be noted that the noise can be further lowered to sub μ RIU levels by spectral averaging and sum normalization. Both have proven effective ways of further noise reduction in Spreeta™ systems [13].

Temperature drift was evaluated and, once the system was stabilized (30min), it could be operated in the range of 18-22 °C and compensated by the software with a minimal baseline drift (5-10 μ RIU/100 min). Given the inherent sensitivity of SPR biosensors to temperature change, a portable device should include strong temperature compensation [23]. If otherwise, the assays should be designed to be as fast as possible to minimize the effects of baseline drift due to temperature change during the measurement.

Fluidic System Optimization

The pressurized air-driven fluidic system was first tested using the BVA-derivatized sensor chip by injecting a two-fold dilution series of MAb 12 (48-6 nM). As shown in Figure 3A, each MAb 12 concentration was injected for 1 min (in duplicate) at a flow rate of 180 μ l/min and was followed by a 1 min injection of regeneration solution (0.2 M NaOH with 20% ACN). The binding of MAb 12 to the BVA-derivatized sensor surface has a linear phase and a non-linear phase repeatable among duplicates in each binding cycle. This non-linear phase is due to the dilution of the sample plug tail in the dead volume between the sample loop and the

flow cell and it does not affect the maximum responses measured after each binding cycle.

The maximum responses obtained decreased linearly with decreasing MAb 12 concentrations and the average CV% for all the duplicate injections of MAb 12 was 3.9% indicating a robust and repeatable sample delivery using the pressurized air-driven fluidic system. The pressurized air-driven fluidic system was pulse-free and it could be used for up to 4.5 hours without buffer change.

Given the strong influence that flow cell height has on mass transport in surface-based binding assays [24], the fluidic system was first optimized with three flow cells of different height and volume and three different flows (48, 78 and 180 $\mu\text{l}/\text{min}$) using the BVA-derivatized sensor chip in combination with MAb 12 (12 nM). Figure 3B shows the signal to noise ratios (S/N R) obtained after 1 min injections of MAb 12. The noise in these measurements remained constant within different flow cells and flow rates therefore the average was used (1.1 μRIU) for the S/N R calculations. The bar graph clearly illustrates the dramatic effect of flow cell height on the maximum antibody binding response achievable at a fixed time.

Applying the small flow cell at a flow rate of 180 $\mu\text{l}/\text{min}$ provided the maximum signal to noise ratio (S/N R) which decreased geometrically with increasing flow cell heights. In contrast, in the small flow cell, a flow rate decrease of 74% resulted in a S/N R reduction of only 37%. These results agree in general terms with the mass transport theory for continuous flow biosensors which only applies under laminar flow regimes. The theory briefly states that; the higher the flow and the lower the height of the flow compartment the higher the mass transport and therefore the signal obtained.

Although the small flow cell at 180 $\mu\text{l}/\text{min}$ provided the highest S/N R, at this flow it also consumed the highest amount of biospecific molecule and therefore had the lowest binding efficiency (E ($\mu\text{RIU}/\text{fmol}$) = (biospecific molecule bound (μRIU)/biospecific molecule injected (fmoles))*100). The binding efficiency of MAb 12 increased from 0.25 $\mu\text{RIU}/\text{fmol}$ at 180 $\mu\text{l}/\text{min}$ to 0.6 $\mu\text{RIU}/\text{fmol}$ at 48 $\mu\text{l}/\text{min}$.

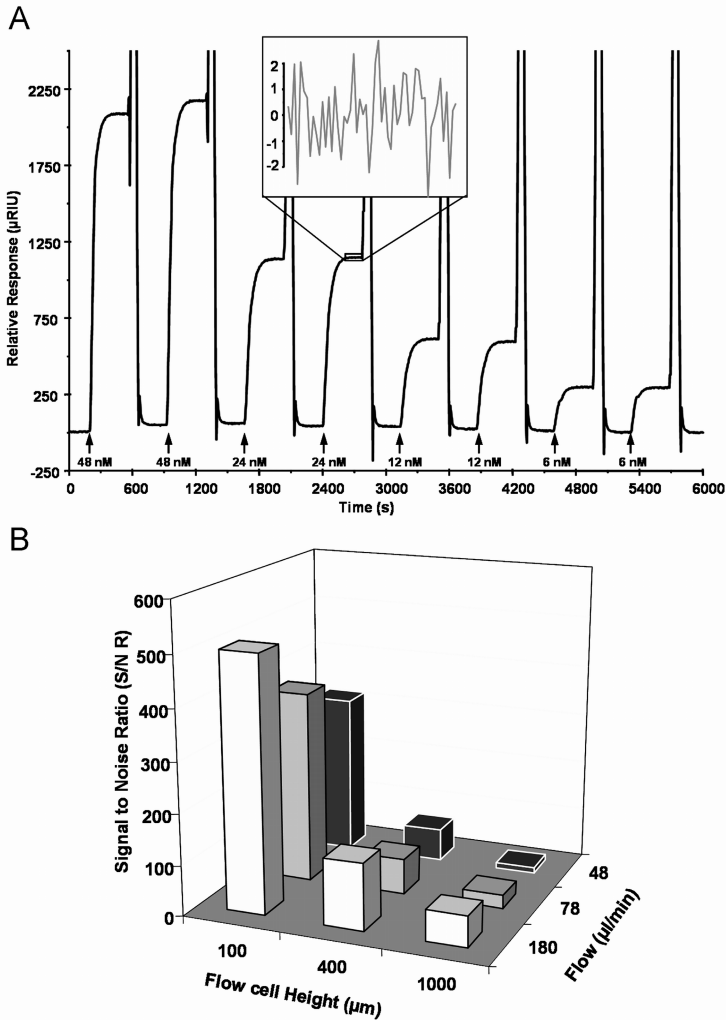


Figure 3. (A) Sensorgrams of duplicate injections of a two-fold dilution series of MAb 12 over the BVA-sensor chip surface. Each 1 min injection (flow rate of 180 μ l/min) was followed by a 1 min injection of regeneration solution (0.2 M NaOH with 20% ACN). The insert shows a zoomed view of the noise of the sensorgram monitored at 1.22 Hz. (B) Signal to noise ratios obtained for 1 min injections of MAb 12 (12 nM) in the Spreeta-based BPA inhibition assay using flow cells of different heights at three flow rates.

BPA calibration curves were generated at the three mentioned flows using the small flow cell to evaluate the effect of the flow on the future sensitivity of the assay (data not shown). Decreasing flow rates lowered

the sensitivity of the assay (180 $\mu\text{l}/\text{min}$ IC_{50} =30.2 nM, 78 $\mu\text{l}/\text{min}$ IC_{50} =52.7 nM, 48 $\mu\text{l}/\text{min}$, IC_{50} = 496.6 nM). We also observed incomplete inhibition at maximum BPA concentrations (1000 nM) in the calibration curves obtained at flow rates 78 $\mu\text{l}/\text{min}$ and 48 $\mu\text{l}/\text{min}$ indicating that non specific binding of MAb 12 to the BVA-sensor chip surface occurs. Probably, this relatively large flow cell (i.e. compared to a Biacore 3000 flow cell of 20 μm height) with a geometry which should still be optimized, does not allow an efficient sample removal at low flow rates. Hence, the small flow cell at a flow rate of 180 $\mu\text{l}/\text{min}$ was used for all further experiments. However, it should be noted that flow cell height can be easily decreased down to 16 μm using soft photolithographic techniques in poly (dimethylsiloxane) [25]. If these micro fabrication techniques are implemented, considerably higher S/N R, binding efficiency and lower flow rates can be achieved consequently lowering biospecific molecule consumption.

Given that short time injections are preferred in portable sensor subjected to temperature change to minimize the temp drift within a single measurement we chose to make 1 minute injections in all further measurements.

Implementation of Competitive Inhibition Assays for Endocrine Disruptors

In the Spreeta prototype, the specific MAb 12-based inhibition assay for the estrogenic compound BPA yielded a comparable sensitivity (IC_{50} = 30.2 nM) to that previously obtained in the Biacore 3000 (IC_{50} = 39.9 nM) (Table 1) [19]. However, due to the larger flow cell in the Spreeta-based biosensor system, the concentration of MAb 12 required to obtain a comparable signal with a 1 min injection had to be increased 5 times. TBG and TTR are responsible for the transport of T4 (75 and 20% respectively) in human plasma and are potential targets for chemicals contaminants affecting the endocrine system. Therefore, they were previously used to develop two T4 transport protein inhibition assays for bioeffect-related screening of such chemicals in a Biacore 3000 SPR-based biosensor [11]. In the present study we implemented both T4 transport protein inhibition assays in the Spreeta-based biosensor (as described in section 2.3.1) to compare the system's performance with the Biacore.

Table 1. Comparison of sensitivity between assays implemented in the Biacore 3000 and the Spreeta™ -based biosensor.

Inhibition Assay		Spreeta (180 μ l at 180 μ l/min)			Biacore 3000 (50 μ l at 25 μ l/min)	
Biospecific Molecule	Analyte	B0 Response \pm SD (μ RIU)* (n= 3)	IC ₅₀ (nM)	Inter assay CV%	IC ₅₀ (nM)	Inter assay CV%
MAB 12 (150 Kd)	BPA	546.9 \pm 34 (12 nM)	30.2	18	39.9 **	3
TBG (54 Kd)	T4	108.6 \pm 8.8 (18.2 nM)	12.3	9	8.6	8
rTTR (55 Kd)	T4	36.2 \pm 3.7 (18.2 nM)	11.6	24	13.7	9

* Response of the biospecific molecule at 0 nM of analyte.

**The concentration of MAB 12 in the Biacore 3000 inhibition assay for BPA was 2.4 nM.

The response obtained after a 1 min injection of TBG (18.2 nM) was about 7-fold lower than that obtained in the Biacore 3000. However, the overlaid sensorgrams of TBG mixed with increasing concentrations of T4 (Figure 4) show a strong inhibition of TBG binding to the AVA-T4 sensor chip surface and are very repeatable (average CV% for all T4 concentrations = 0.7%). The calibration curve for T4 with the TBG inhibition assay is shown in Figure 5B, the sensitivity (IC₅₀ = 12.3 nM) (Table 1.) is slightly lower than the one previously obtained with the Biacore 3000 (IC₅₀ = 8.6 nM). Inter assay CV% was comparable in both systems for this inhibition assay.

The response obtained with the Spreeta-based biosensor system using rTTR (18.2 nM) was about 18-fold lower than previously obtained with the Biacore 3000. Despite the low response obtained we generated a calibration curve for T4 to evaluate the limit of the system with regard the minimum response required for an inhibition assay. The calibration curve for T4 in Figure 5C clearly shows that the magnitude of the response (36 μ RIU for 0 nM T4) was still sufficient to generate a calibration curve for T4 and a sensitivity comparable to the Biacore 3000 (Table 2) was obtained. However, the inter assay associated error increased significantly (CV = 24%) at these low signals. An increase in rTTR concentration (182 nM) greatly increased the signal (455 μ RIU) with minimum effect on the sensitivity (IC₅₀ = 17.6 nM) however at the expense of higher rTTR consumption.

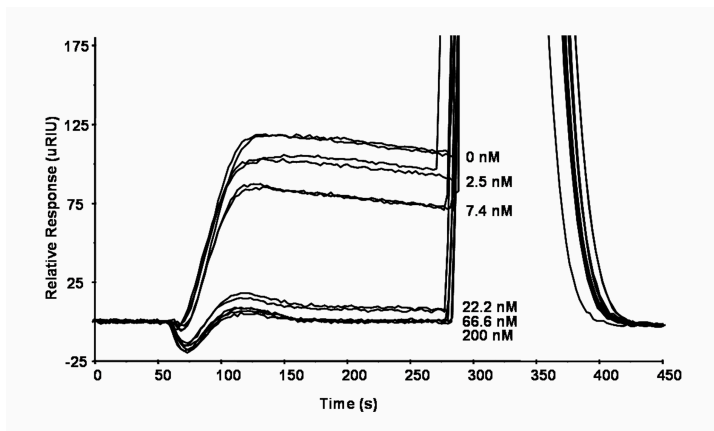


Figure 4. Overlaid sensorgrams showing the TBG binding inhibition to the AVA-T4 sensorchip surface at increasing concentrations of T4.

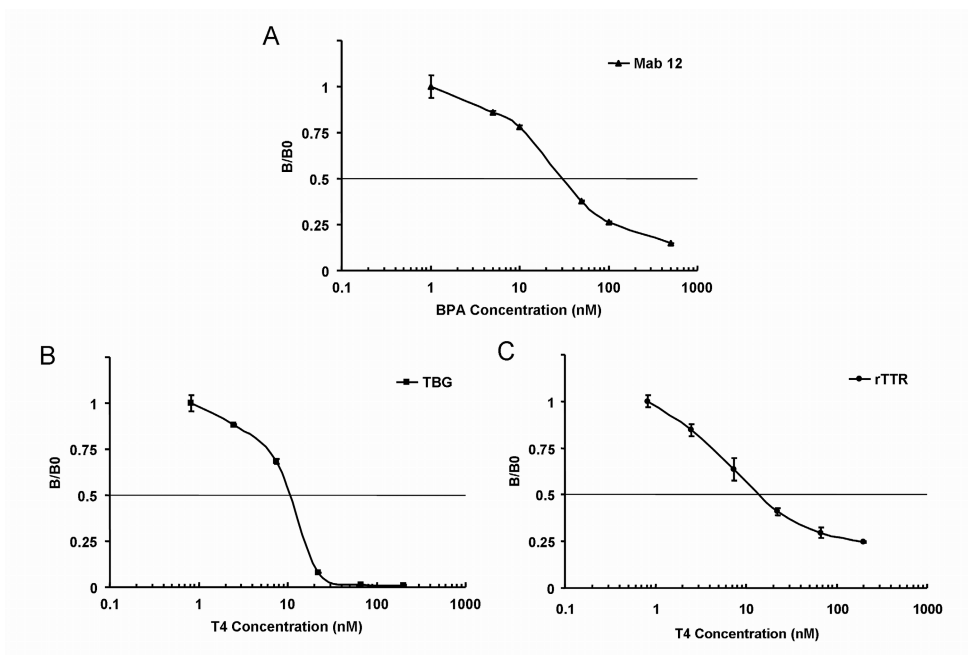


Figure 5. Representative normalized calibration curves obtained with the Spreeta™-based biosensor system for (A) BPA using the MAb 12 inhibition assay (Average relative standard deviation (RSD) 1.4%), (B) T4 using the TBG inhibition assay (Average RSD 0.7%) and (C) T4 using the rTTR inhibition assay (Average RSD 3%). Each concentration was measured at least in duplicate. If error bars are not visible, they were smaller than the data marker.

The throughput of the system for these inhibition assays was 8 cycles/hour. Although not currently in the market, the three channel Spreeta SPR biosensor under development by Texas Instruments [26] seems a very promising tool for further throughput increase or multiple analyte detection.

Conclusions

We have optimized and tested the performance of an automated low-cost Spreeta™ -based prototype biosensor system in combination with commercially available CM5 sensor chips.

The system was successfully used to setup assays previously used for EDCs, an inhibition immunoassay for BPA and two T4 transport protein inhibition assays. The sensitivities obtained are comparable to those previously obtained with the Biacore 3000, moreover the sensitivity of the rTTR and TBG inhibition assays in this system are comparable to that of competitive radioligand binding assays [27, 28]. To the best of the author's knowledge, this is the first time that human biospecific molecules are successfully combined with a fast, simple and affordable SPR biosensor, which is a promising tool for the bioeffect-related screening of compounds with endocrine disrupting activity.

References

1. De Meulenaer B, Baert K, Lanckriet H, Van Hoed V, Huyghebaert A (2002) Development of an enzyme-linked immunosorbent assay for bisphenol a using chicken immunoglobulins *J. Agric. Food Chem.* 50, 5273-82
2. Cliquet P, Cox E, Haasnoot W, Schacht E, Goddeeris BM (2003) Generation of group-specific antibodies against sulfonamides *J. Agric. Food Chem.* 51, 5835-42
3. Sonnenschein C, Soto AM (1998) An updated review of environmental estrogen and androgen mimics and antagonists *J. Steroid Biochem. Mol. Biol.* 65, 143-50
4. Lans MC, Spiertz C, Brouwer A, Koeman JH (1994) Different competition of thyroxine binding to transthyretin and thyroxine-binding globulin by hydroxy-PCBs, PCDDs and PCDFs *Eur. J. Pharmacol.: Environ. Tox. and Pharmacol.* 270, 129-36
5. Yamauchi K, Ishihara A, Fukazawa H, Terao Y (2003) Competitive interactions of chlorinated phenol compounds with 3,3',5-triiodothyronine binding to transthyretin: detection of possible thyroid-disrupting chemicals in environmental waste water *Toxicol. Appl. Pharmacol.* 187, 110-17
6. Seifert M, Haindl S, Hock B (1999) Development of an enzyme linked receptor assay (ELRA) for estrogens and xenoestrogens *Anal. Chim. Acta* 386, 191-99
7. Oosterkamp AJ, Hock B, Seifert M, Irth H (1997) Novel monitoring strategies for xenoestrogens *Trends Anal. Chem.* 16, 544-53
8. Garrett SD, Lee HA, Morgan MR (1999) A nonisotopic estrogen receptor-based assay to detect estrogenic compounds *Nat Biotechnol* 17, 1219-22
9. van Elswijk DA, Schobel UP, Lansky EP, Irth H, van der Greef J (2004) Rapid dereplication of estrogenic compounds in pomegranate (*Punica granatum*) using on-line biochemical detection coupled to mass spectrometry *Phytochemistry* 65, 233-41
10. Rodriguez-Mozaz S, Marco M-P, Lopez de Alda MJ, Barceló D (2004) Biosensors for environmental applications: Future development trends *Pure Appl. Chem.* 76, 723-52
11. Marchesini GR, Meulenberg E, Haasnoot W, Mizuguchi M, Irth H (2006) Biosensor Recognition of Thyroid-Disrupting Chemicals Using Transport Proteins *Anal. Chem.* 78, 1107-14

12. Sesay AM, Cullen DC (2001) Detection of hormone mimics in water using a miniturised SPR sensor *Environ Monit Assess* 70, 83-92
13. Chinowsky TM, Quinn JG, Bartholomew DU, Kaiser R, Elkind JL (2003) Performance of the Spreeta 2000 integrated surface plasmon resonance affinity sensor *Sens. Actuators B: Chem.* 91, 266-74
14. Naimushin AN, Soelberg SD, Nguyen DK, Dunlap L, Bartholomew D, Elkind J, Melendez J, Furlong CE (2002) Detection of Staphylococcus aureus enterotoxin B at femtomolar levels with a miniature integrated two-channel surface plasmon resonance (SPR) sensor *Biosens. Bioelectron.* 17, 573-84
15. Spangler BD, Wilkinson EA, Murphy JT, Tyler BJ (2001) Comparison of the Spreeta(R) surface plasmon resonance sensor and a quartz crystal microbalance for detection of Escherichia coli heat-labile enterotoxin *Anal. Chim. Acta* 444, 149-61
16. Mohammed I, Mullett WM, Lai EPC, Yeung JM (2001) Is biosensor a viable method for food allergen detection? *Anal. Chim. Acta* 444, 97-102
17. Haasnoot W, Marchesini GR, Koopal K (2006) Spreeta-based biosensor immunoassays to detect fraudulent adulteration in milk and milk powder *J. AOAC Int.* 89, In press
18. Wang R, Tombelli S, Minunni M, Spiriti MM, Mascini M (2004) Immobilisation of DNA probes for the development of SPR-based sensing *Biosens. Bioelectron.* 20, 967-74
19. Marchesini GR, Meulenber E, Haasnoot W, Irth H (2005) Biosensor immunoassays for the detection of bisphenol A *Anal. Chim. Acta* 528, 37-45
20. Masadome T, Asano Y, Imato T, Ohkubo S, Tobita T, Tabei H, Iwasaki Y, Niwa O, Fushinuki Y (2002) Preparation of refractive index matching polymer film alternative to oil for use in a portable surface-plasmon resonance phenomenon-based chemical sensor method *Anal. Bioanal. Chem.* 373, 222-26
21. Owega S, Poitras D, Faid K (2006) Solid-state optical coupling for surface plasmon resonance sensors *Sens. Actuators, B* 114, 212
22. Jung LS, Campbell CT, Chinowsky TM, Mar MN, Yee SS (1998) Quantitative Interpretation of the Response of Surface Plasmon Resonance Sensors to Adsorbed Films *Langmuir* 14, 5636-48

Spreeeta-based Biosensor Assays for Endocrine Disruptors

23. Naimushin AN, Soelberg SD, Bartholomew DU, Elkind JL, Furlong CE (2003) A portable surface plasmon resonance (SPR) sensor system with temperature regulation *Sens. Actuators, B* 96, 253-60
24. Myszka DG, He X, Dembo M, Morton TA, Goldstein B (1998) Extending the Range of Rate Constants Available from BIACORE: Interpreting Mass Transport-Influenced Binding Data *Biophys. J.* 75, 583-94
25. Wheeler AR, Chah S, Whelan RJ, Zare RN (2004) Poly(dimethylsiloxane) microfluidic flow cells for surface plasmon resonance spectroscopy *Sens. Actuators B: Chem.* 98, 208-14
26. Soelberg S, Chinowsky T, Geiss G, Spinelli C, Stevens R, Near S, Kauffman P, Yee S, Furlong C (2005) A portable surface plasmon resonance sensor system for real-time monitoring of small to large analytes *J. Ind. Microbiol. Biotechnol.* 32, 669
27. van den Berg KJ (1990) Interaction of chlorinated phenols with thyroxine binding sites of human transthyretin, albumin and thyroid binding globulin *Chem. Biol. Interact.* 76, 63-75
28. Lans MC, Klasson-Wehler E, Willemsen M, Meussen E, Safe S, Brouwer A (1993) Structure-dependent, competitive interaction of hydroxy-polychlorobiphenyls, -dibenzo-p-dioxins and -dibenzofurans with human transthyretin *Chem. Biol. Interact.* 88, 7-21

**Part III. Strategies for Coupling SPR
Biosensor Screening with Liquid
Chromatography Electrospray Time-of-
Flight Mass Spectrometry Identification**



Chapter 6

Dual Biosensor Immunoassay-Directed Identification of Fluoroquinolones in Chicken Muscle by Liquid Chromatography Electrospray Time-of- Flight Mass Spectrometry

Published in: *Analytica Chimica Acta* 586 (2007) 259-268

Abstract

Fluoroquinolones (FQs) are synthetic antibiotics of broad-spectrum antibacterial activity widely used to treat infections in farmed fish, turkeys, pigs, calves and poultry. Monitoring these substances residues is therefore regulated by law. For the detection of FQs, we studied the feasibility of coupling the simultaneous screening of several FQs, using a dual surface plasmon resonance (SPR) biosensor immunoassay (BIA), in parallel, with an analytical chemical methodology for their identification. Six FQs were simultaneously screened at or below their maximum residue level (MRL) in chicken muscle using a multi-FQ BIA for norfloxacin, ciprofloxacin, enrofloxacin, difloxacin and sarafloxacin, and a specific BIA for flumequine. The two BIAs were serially coupled in a multi-channel SPR biosensor featuring a dual BIA in a competitive inhibition format. The samples noncompliant during the screening with the dual BIA were further concentrated and fractionated with gradient liquid chromatography (LC). The effluent was splitted towards two 96-well fraction collectors resulting in two identical 96-well plates. One was re-screened with the dual BIA to identify the immunoactive fractions and direct the identification efforts toward the relevant fractions in the second well-plate with high resolution LC-Electrospray Time-of-Flight Mass Spectrometry (ESI-TOF-MS). The system not only allows the possibility to screen and identify known FQs, but also to discover unknown chemicals of similar structure which show activity in the dual BIA.

Introduction

Profitability of livestock is often hampered by infectious diseases, therefore the use of veterinary antibacterial drugs is expected for treatment and prophylaxis. Fluoroquinolones (FQ) belong to a new generation of broad-spectrum antibiotics capable of inducing bacterial death by inhibiting DNA gyrase [1]. FQs are active against Gram negative and Gram positive bacteria [2] and are widely used to treat infections, as prophylactic and growth promoters in farmed fish, turkeys, pigs, calves and poultry [3]. Therefore raising public health concerns relating to allergic reactions and the generation of antibiotic resistant bacterial strains [4, 5]. In consequence, a national veterinary residue monitoring plan for these and other groups of substances should be established by the EU member countries in accordance to EC Council Directive 96/23/EC [6]. Consequently, there is a rising need for rapid, robust, multi residue screening assays coupled to identification methods for these low molecular weight compounds. Several methods have been described for the determination of quinolone residues using liquid chromatography (LC) with fluorescence detection [1, 7, 8], with Ultra Violet (UV) detection [1, 9, 10] and LC-Mass Spectrometry (MS) [11]. Alternative methods like a microbiological assay [12, 13], specific and multi-FQ immunoassays have also been reported [14-17]. Within the scope of the EU project BioCop (www.biocop.org) several biosensor-based screening methods are being developed for chemical contaminants in food. Our challenge within this project is to evaluate strategies for coupling the biosensor screening methods with MS for confirmation of identity and/or the identification of unknowns having activity in the biosensor assays. In the present study we coupled a dual inhibition biosensor immunoassay (BIA) in a multi-channel surface plasmon resonance (SPR) biosensor for the screening of FQs in chicken muscle samples in parallel with high resolution LC/MS identification. This concept was previously evaluated using yeast bioassay-directed identification of estrogen and androgen residues in urine [18, 19]. In the dual BIA for the FQs, a multi-FQ BIA was developed for the detection of norfloxacin (Nor), ciprofloxacin (Cipro), enrofloxacin (Enro), difloxacin (Diflo) and sarafloxacin (Sara) was coupled to a specific BIA for flumequine (Flu). Samples considered positive during the screening with the dual BIA were concentrated with solid phase extraction (SPE) and separated with a standard HPLC of which the effluent was splitted toward two identical 96-well fraction collectors. The fractions in the 96-

well plate were re-screened for immunoactivity using the dual BIA, this generated an immunoaffinity chromatogram or immunogram [20]. In the immunogram the immunoactive fractions positions were clearly distinguished and this the immunoactive wells positions were used in the second 96-well plate for immunoactive oriented identification using high resolution HPLC, electrospray ionization (ESI) time-of-flight mass spectrometry (TOF MS).

Experimental

Materials

Sensor chips (CM5), HBS-EP buffer [pH 7.4, consisting of 10 mM 4-(2-hydroxyethyl) piperazine-1-ethanesulfonic acid, 150 mM sodium chloride, 3 mM EDTA, 0.005% (v/v) surfactant polysorbate (P20)] and an amine coupling kit [containing 0.1 M N-hydroxysuccinimide (NHS), 0.4 M N-ethyl-N'-(3-dimethylaminopropyl) carbodiimide hydrochloride (EDC), and 1 M ethanolamine hydrochloride-NaOH (pH 8.5)] were supplied by Biacore AB (Uppsala, Sweden). Ethylene diamine (EDA) was obtained from VWR International (Amsterdam, The Netherlands). ELISA microtitre plates were supplied by Greiner (Frickenhausen, Germany). Polyclonal antisera were raised in rabbits against a Flu conjugate (PAb MH41) [16] and a Nor-COOH derivative (see Figure 2) conjugated to a carrier protein (PAb CA65) [17, 21]. Acetonitrile HPLC far-UV grade was from Lab-Scan Ltd. (Dublin, Ireland). Water was purified using a Milli-Q gradient A10 system (Millipore, Bedford, MA). Solid Phase Extraction (SPE) (20 mg N-vinylpyrrolidone/ divinylbenzene based sorbent) OASIS HLB cartridges were from Waters (Milford, MA, USA). The 0.45 μ m Durapore and 30 kD cutoff Amicon filters were from Millipore (Amsterdam, The Netherlands). Cipro and Enro were from Fluka Chemie (Zwijndrecht, The Netherlands). Diflo was from Abbott Laboratories (North Chicago, Illinois, USA). Sara was from Dr. Ehrenstorfer (Augsburg, Germany). Nor, Flu, 5-aminovaleric acid (AVA) and all other reagents were obtained from Sigma-Aldrich Chemie BV (Zwijndrecht, The Netherlands) unless otherwise stated.

Solutions and samples

The FQs mixture (FQs mix) was prepared using standards of Nor, Cipro, Enro, Diflo, Sara and Flu in methanol (10 mg L⁻¹). Muscle samples from

blank broilers and broilers treated with Enro were obtained from an animal experiment performed at the Animal Sciences Group (ASG; Lelystad, The Netherlands). The spiked blank chicken muscle samples were prepared by adding 100 μl of a FQs mix (1 mg L^{-1}) to 1 g of chicken muscle, achieving a level of 100 ng g^{-1} for each of the FQs before extraction. To prepare the incurred chicken muscle samples, chickens were dosed with Enro at 30 mg kg^{-1} total body weight through the drinking water for five consecutive days. This resulted in $2700\text{--}6800 \text{ }\mu\text{g kg}^{-1}$ levels, far above the MRL levels, hence the samples were diluted with blank chicken samples until a level of 0.5 MRL ($50 \text{ }\mu\text{g kg}^{-1}$) was reached. The official Dutch committee for ethics on animal experiments (DEC) approved these animal experiments.

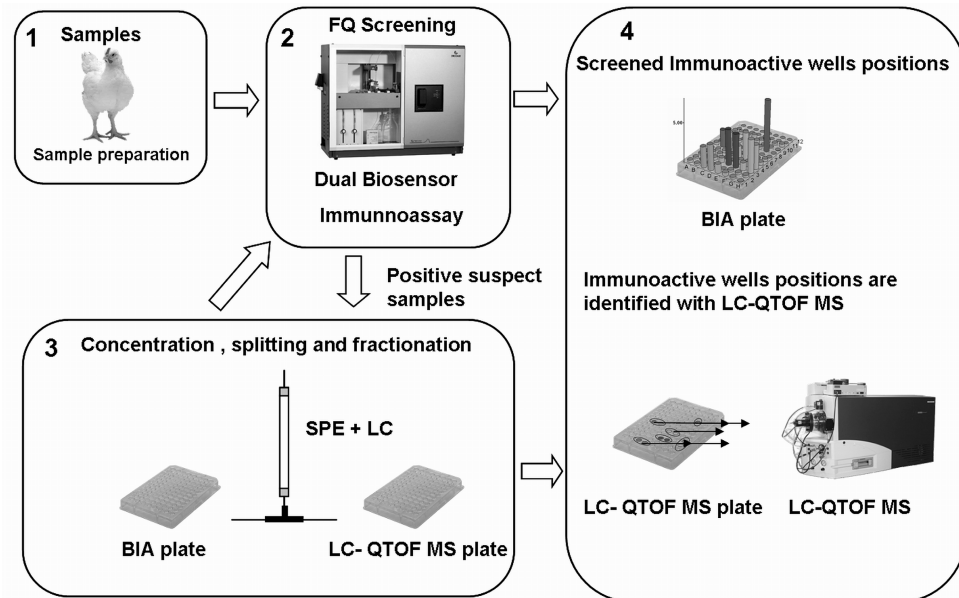


Figure 1. Scheme of the analysis procedure for FQ in chicken muscle samples. (1) Screening using a dual BIA (2), separation and fractionation using gradient LC (3) and BIA /LC/TOFMS for oriented identification (4).

Equipment

The experimental system setup (Figure 1) consisted of a dual SPR-based inhibition BIA, a gradient LC, an autosampler, a dual 96-well fraction collector and a high resolution LC QTOF MS. The BIACORE 3000 was

supplied by Biacore AB (Uppsala, Sweden). The gradient LC system consisted of two Knauer (Berlin, Germany) model WellChrom K-1001 pumps, a Knauer high pressure dynamic mixing chamber, a GasTorr model 154 membrane degasser, and an autosampler model Endurance from Spark Holland (Emmen, The Netherlands). Liquid chromatography was performed using a Waters (Milford, MA) 150 x 3 mm i.d. Symmetry column packed with 5 μm C18 material. The column effluent was split toward two identical Gilson (Villiers-le-Bel, France) model FC203B 96-well fraction collectors. Identification was performed using a Waters Acquity UPLC system equipped with a 50 x 2.1 mm i.d. column packed with 1.7- μm BEH C18 material. The LC column was directly interfaced with a Micromass (Manchester, U.K.) model QTOF micro MS system.

Procedures

Sample Preparation and Solid Phase Extraction

Chicken muscle samples were extracted by homogenizing 1 g of chicken breast tissue with 10 mL of water. The homogenate was centrifuged and the supernatant was filtered through a 0.45 μm filter. 2 mL of the filtrate were ultrafiltrated with a 30 kD cutoff filter and the filtrate was measured with the dual BIA. The chicken extracts were concentrated using SPE cartridges, conditioned with 2 mL of methanol, equilibrated with 2 mL of water and washed with 2 mL of water/methanol (9.5/0.5). After that, 2 mL of a mixture of chicken extract/formic acid (99.8/0.2; v/v) were loaded on to the cartridge, the cartridge was washed with 2 mL of water, dried and eluted with 1 mL of methanol/acetonitrile (8:2; v/v). The eluate was evaporated to dryness and resuspended in 250 μl of water/formic acid (99.8/0.2; v/v).

Biosensor Chip Preparation and BIAs

The Biacore 3000 biosensor allows the possibility to immobilize and measure in four serially connected flow channels (Fc). Therefore up to four different assays can be simultaneously performed. We combined two BIAs in a competitive inhibition format, a multi-FQ BIA for the detection of five FQ (Nor, Cipro, Enro, Diflo and Sara), and a specific BIA for Flu. For the multi-FQ BIA we immobilized a Nor-NH₂ derivative (see Figure 2) to the carboxymethylated sensor chip surface in Fc2. The Nor-NH₂ derivative was prepared by coupling Nor with ethylenediamine as

follows. Oxalyl Chloride (164 μL) was added dropwise to a solution of Nor (20 mg mL^{-1} (15 mL)) in DMF and stirred for 2 h. DMF excess was evaporated by reduced pressure, the residue was redissolved in pyridine (10 mL) and 200 μL ethylenediamine were added.

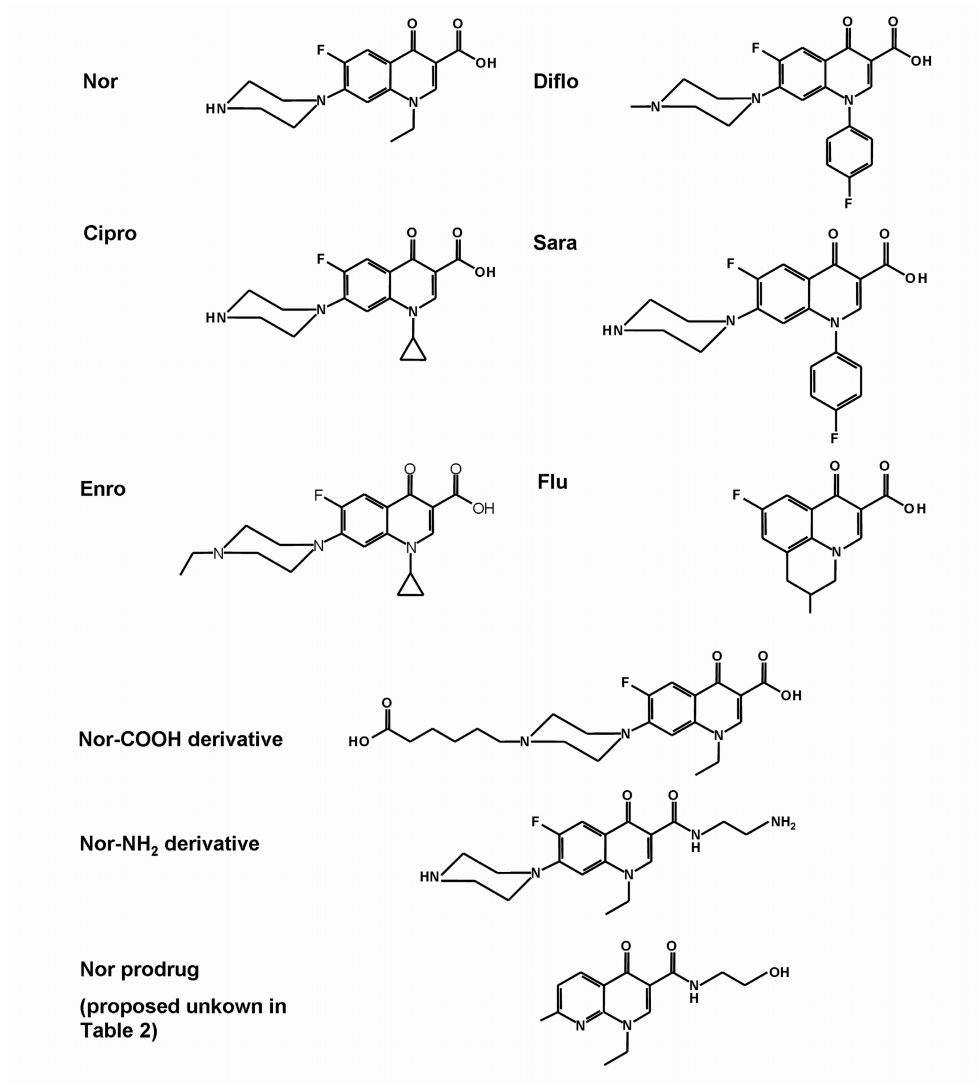


Figure 2. Structures of the FQs, the Nor-COOH and Nor-NH₂ derivatives used in this study and of the Nor prodrug.

The solution was stirred overnight at room temperature and pyridine was evaporated under a stream of nitrogen. The residue was washed three times with 10 mL ether. The procedure to immobilize the Nor-NH₂ derivative was as follows. The CM5 sensor chip surface was activated by injecting 100 μ l of a mixture of 0.4 M EDC and 0.1 M NHS (1:1; v/v) at a flow rate of 5 μ l min⁻¹, followed by the injection of 40 μ l of 0.5 mg ml⁻¹ Nor-NH₂ in borate buffer pH 8.5 at a flow rate of 2 μ L min⁻¹. After several short injections of 50 mM NaOH, about 2400 RU of Nor-NH₂ remained immobilized. For the specific Flu BIA, we immobilized Flu using its carboxylic group with a double spacer consisting of AVA and EDA. Briefly, the whole immobilization procedure was performed at a flow rate of 5 μ L min⁻¹, the sensor chip surface in Fc4 was activated with NHS/EDC as previously described followed by a 140 μ L injection of 20 mM AVA in carbonate buffer pH 9.6 and a further EDC/NHS activation step followed by a 140 μ L injection of EDA, the second bifunctional spacer. Finally, Flu was activated by mixing 150 μ L of a 0.01 M Flu in carbonate buffer pH 9.6 with 0.4 M EDC and 0.1 M NHS (1:1:1; v/v/v) and the mixture was injected over the sensor chip surface. The activated carboxyl group of Flu formed an amide bond with the free amines provided by the EDA spacer on the chip surface and 2200 RU could be immobilized. It should be noted that using a single di-amine spacer is also a feasible alternative which would lower the amount of immobilization steps of Flu.

The assay is based on the inhibition immunoassay format in which the absence of FQ (or other compounds complexing with the antibody) results in maximum antibody binding to the derivatized sensor chip surface. Increasing concentrations of the cross-reacting FQ will compete for antibody binding with the hapten immobilized on the sensor surface and the signal will drop proportionately. The assay procedure was as follows; sample or standard solutions in HBS-EP buffer and a mixture of the antibodies (antiserum PAb CA65 (dilution factor (d.f.) 160) and antiserum PAb MH41 (d.f. 50)) were mixed (4/1; v/v) by the Biacore 3000 and 50 μ L were injected over the four Fcs at a flow rate of 25 μ L min⁻¹. The sensor chip surface was regenerated with 15 μ L of 0.2 M NaOH/ACN (4/1; v/v). Fc 1 and 3 were left unmodified to monitor the non-specific binding of the sample matrix to the carboxymethylated dextrane surface, the responses obtained were used as a reference for subtraction of Fcs 2 and 4 respectively. The results obtained with the dual-BIA are always the mean of at least duplicate measurements

except for the screening of the immunoactive well positions where one measurement/well is performed.

Instrumentation

Gradient LC fractionation and splitting

Liquid chromatography was performed using a mobile phase consisting of (A) water/formic acid (99.8/0.2) and (B) acetonitrile. Gradient elution was performed at a flow rate of 0.4 mL min^{-1} , starting at 10% B isocratically for 18 min and linearly increasing up to 55% B in 7 min, to 80% B in 5 min, to 10% B in 3 min and finally conditioning isocratically for 7 min. The column effluent was split and the fractions were collected every 30s ($100 \text{ }\mu\text{l/well}$) with two identical 96-well fraction collectors. One well-plate was used for FQs immunoactivity detection. These fractions were evaporated overnight at room temperature and the residues re-dissolved in $100 \text{ }\mu\text{l}$ of HBS-EP buffer. Only the immunoactive wells in the duplicate well plate were subjected to identification with high-resolution LC/TOFMS.

High Resolution LC-TOF MS Identification

Gradient LC separation was performed using a mobile phase consisting of (A) water/formic Acid (99.8/0.2) and (B) acetonitrile. Gradient elution was performed at a flow rate of 0.75 mL min^{-1} , starting at 10% B isocratically for 2.5 min and linearly increasing up to 40% B in 1.5 min, to 80% B in 1 min and decreasing to 10% B in 1 min. The effluent from the LC column was splitted 1:1 and interfaced with a QTOF micro MS system equipped with a dual electrospray ionization (ESI) probe and operated in the positive ion mode at a resolution of 5000 (fwhm), source temperature $150 \text{ }^\circ\text{C}$, desolvation temperature $400 \text{ }^\circ\text{C}$, and a cone voltage of 30 V. The second LockSpray ESI probe provided an independent flow of the lock mass calibrant consisting of 0.1% phosphoric acid in acetonitrile/water (1/1; v/v), at $10 \text{ }\mu\text{L min}^{-1}$. The lock calibrant data were acquired at a frequency 0.2 S^{-1} and using a cone voltage of 5 V. Data were acquired in the continuum mode from 100 to 600 Da with a scan time of 0.44 s and processed using Masslynx v. 4.0 software.

Results and Discussion

BIAs Performance

The biosensor chip surfaces in the different Fcs were first evaluated with the separate injection of PAb CA65 (d.f. 800) and PAb MH41 (d.f. 250) in the biosensor. No binding was observed of PAb CA65 to the Flu conjugate (AVA-EDA-FLU) immobilized in Fc4 or of PAb MH41 to the Nor conjugate immobilized in Fc2, indicating that the antibodies are specific for their respective conjugates. A mixture of the two antibodies injected over the 4 Fcs resulted in maximum relative responses of 700 Response Units (RU) in Fc2 minus Fc1 and 890 RU in Fc4 minus Fc3 (Figure 3A).

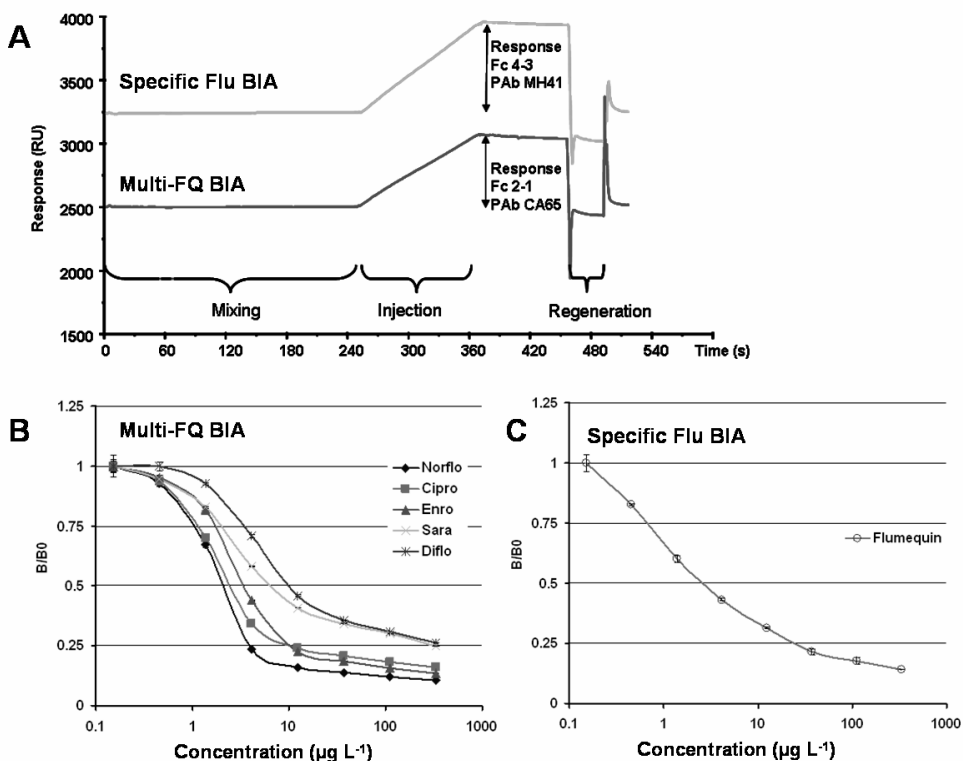


Figure 3. BIAs for FQs. (A) Reference-subtracted sensorgrams of a 50 μl injection of PAb CA65 (d.f. 250) and PAb MH41 (d.f. 800) at 25 $\mu\text{L min}^{-1}$ (B) Calibration curves obtained in buffer with different FQ with the multi-FQ BIA and (C) with Flu in the specific Flu BIA.

Fc1 and Fc3 were left unmodified and were further used for reference subtraction of non specific binding (NSB). After regeneration with a mixture of 0.2 M NaOH/acetonitrile (4/1; v/v), the responses in both Fcs returned to baseline and a new sensorgram could be produced with similar binding responses indicating repeatable sensor chip surface binding capacities in both Fcs. The assay time including mixing the reagents, sample injection and the regeneration of the surface was 8.5 min per sample.

The following step to evaluate the dual BIA performance was the measurement of the sensitivity, cross-reactivity and matrix effects. Injections of a mixture (1:4; v/v) of the antibodies and chicken muscle extract (prepared according to section 2.4.1) diluted in HBS-EP buffer (up to 50%) showed a NSB of less than 50 RU in the reference Fcs. This indicates that for this specific application with low NSB, the two Fcs could be omitted and potentially used for the setup of other simultaneous BIAs for the detection of additional compounds. Calibration curves for the six FQ (for the structures see Figure 2) were prepared in buffer (Figure 3B-C) and in a solution containing 50% chicken muscle extract and were measured with the dual BIA. Full inhibition of the multi-FQ BIA was observed with Nor, Cipro, Enro, Diflo and Sara at concentrations in the range of 10-300 $\mu\text{g L}^{-1}$ in buffer and in chicken muscle extract. The specific Flu BIA only showed inhibition with Flu.

The 50% inhibition concentration (IC_{50}) values and the crossreactivities are presented in Table 1 show that the assay was more sensitive toward Nor ($\text{IC}_{50} = 2 \mu\text{g L}^{-1}$) in buffer and the affinity ranking for the other crossreacting FQs was Nor > Cipro > Enro > Diflo > Sara. This ranking is similar to that previously obtained with this antibody in an enzyme linked immunosorbent assay (ELISA) [17] except for Enro which showed the highest affinity in the ELISA. The assay setup and the immobilization of the hapten to the sensor chip surface probably played a role in the affinity ranking differences because previous FQ affinity ranking with this antibody in a competitive assay format strongly depended on its affinity for the tracer-hapten conjugate used in the ELISA [17].

Table 1. Sensitivity and cross-reactivity of the multi-FQ and specific Flu BIAs for six FQ in HBS-EP buffer and in chicken muscle extract diluted in HBS-EP (1:1; v/v).

Compound	Multi-FQ BIA				Specific Flu BIA			
	IC ₅₀ (µg L ⁻¹)		Crossreactivity (%)		IC ₅₀ (µg L ⁻¹)		Crossreactivity (%)	
	Buffer	Extract	Buffer	Extract	Buffer	Extract	Buffer	Extract
Norfloxacin	2	2.8	100	100	n.d.	n.d.	n.d.	n.d.
Ciprofloxacin	2.4	3.7	83	79	n.d.	n.d.	n.d.	n.d.
Enrofloxacin	3.4	3.4	58	85	n.d.	n.d.	n.d.	n.d.
Difloxacin	10	5.9	20	48	n.d.	n.d.	n.d.	n.d.
Sarafloxacin	6.6	2.7	30	108	n.d.	n.d.	n.d.	n.d.
Flumequine	n.d.	n.d.	n.d.	n.d.	2.7	3.8	100	100

n.d. = not detected

As shown in Table 1, the calibration curves in 50% spiked blank chicken muscle extract showed higher IC₅₀ values for Nor and Cipro, equal values for Enro and lower values for Diflo and Sara therefore changing the affinity ranking to Sara > Nor > Enro > Cipro > Diflo. The ratios between the IC₅₀ values from the calibration curves in buffer and those in chicken extract for the different FQs seem to increase with decreasing FQ polarity. One might consider that the differences found in IC₅₀ could be a matter of solubility of the FQs and that small soluble proteins present in the chicken extract matrix are acting as a surfactant improving the solubility of the less polar FQs and therefore improving the sensitivity of the multi-FQ BIA toward those compounds. However, this explanation does not apply to the specific Flu BIA which showed an IC₅₀ value for Flu 40% higher in chicken muscle extract than in buffer. Further experiments evaluating different sample dilution buffers might solve this issue. No cross-reactivity was found with the other FQs tested in the specific Flu BIA.

Although the initial concentration of the FQs in the chicken muscle samples are diluted ten times during the extraction method, the sensitivities of these BIAs are well suited for the detection of FQs below the MRLs established by the EU for FQs in poultry (100 µg kg⁻¹ for Sara (only set for chicken liver and 10 µg/kg for skin and fat) and up to 400 µg kg⁻¹ for Flu) [22]. The multi-FQ BIA was able to detect Enro in chicken muscle samples incurred with Enro at 0.5 MRL (100 µg kg⁻¹,

MRL set as the sum of Enro and Cipro) in 50% of the extract and the recovery was 82% compared with the LC-MS/MS confirmatory method previously used to determine the concentration of Enro in the incurred chicken samples [13]. To evaluate the average recovery of the six FQs, blank chicken muscle samples were spiked with a FQ mixture (100 ng g⁻¹ each). The samples were extracted as described above and measured with the dual BIA. The concentration was calculated using a calibration curve prepared with the six FQs mixture in a solution containing 50% chicken muscle extract. The average recovery of the Nor, Enro, Cipro, Diflo, Sara, and Flu mixture was 74% in the Multi-FQ BIA and 88% in the specific Flu BIA.

BIA-directed identification of FQs

Reporter gene bioassays in yeast have been used for screening the presence of bioactive chemicals like estrogens and androgens [18, 19]. These bioassays were used after the screening phase to direct the MS identification efforts of known and unknown chemicals showing bioactivity. In this bioassay format the starting point is a biospecific interaction, a biospecific molecule (i.e. estrogen receptor or androgen receptor) present in the genetically modified yeast binds a hormone (i.e. estradiol or testosterone) or a similar bioactive compound and following a series of interactions of the hormone-receptor complex with responsive elements in the yeasts engineered DNA, a reporter gene is activated and a fluorescent probe is expressed and measured.

Likewise, in the present study the starting point is the immuno specific interaction between antibodies and antibiotics. The yeast and the fluorescent probe were replaced by a SPR-based biosensor system where the dual BIA was used for FQ screening and to direct the identification efforts of chemicals cross-reacting with the antibodies due to structural similarities with the antigen conjugate used to raise the antibodies. This approach was evaluated with the chicken muscle extracts, previously measured with the dual BIAs (blank, blank spiked with the FQ mixture and incurred with Enro at 0.5 MRL). The samples were further concentrated using SPE (see 2.4.1), the concentrated extracts were fractionated using gradient LC, the effluent of the column was splitted in two and the fractions were collected by identical fraction collectors in 96-well plates featuring a resolution of 30 s/well. The fractions were evaporated overnight at room temperature and the

residues redissolved in 100 μL HBS-EP buffer for the immunoactivity screening with the dual-BIA.

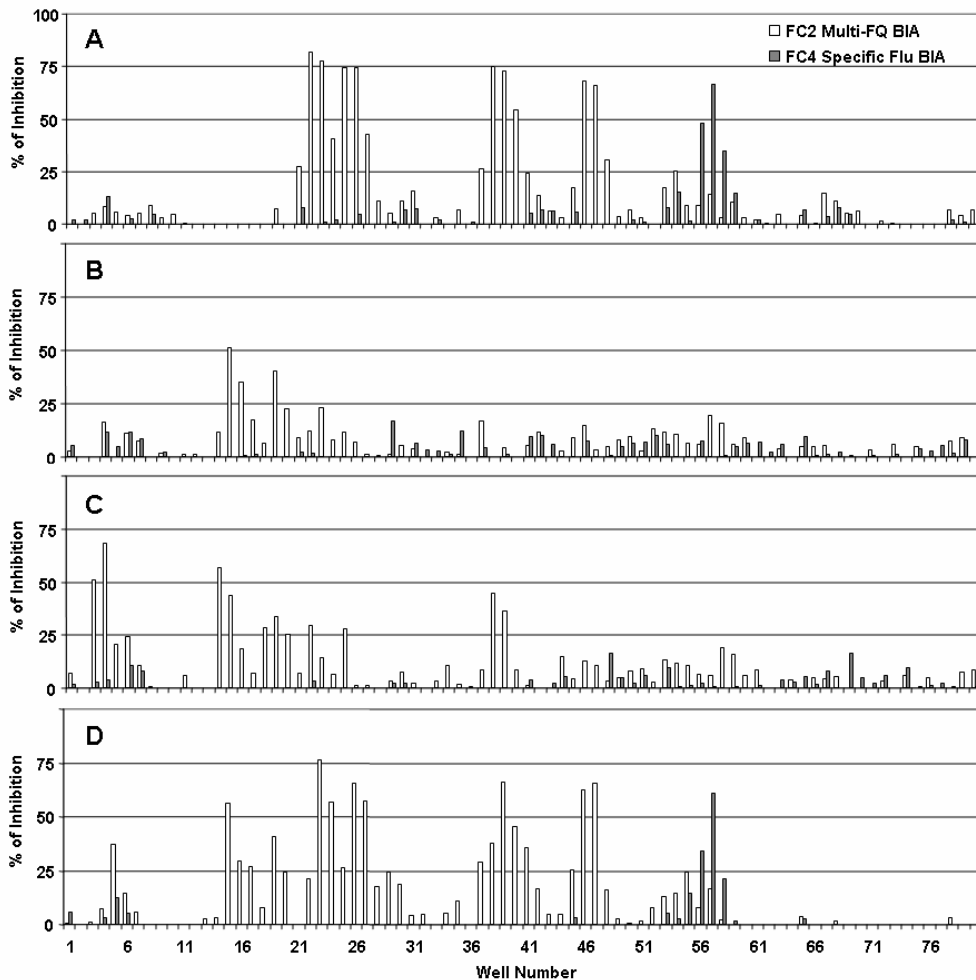


Figure 4. Immunograms of (A) mixture of Nor, Cipro, Enro, Diflo, Sara and Flu standards ($100 \mu\text{g L}^{-1}$ each in buffer). (B) Blank chicken muscle sample, (C) Chicken muscle sample incurred with Enro ($50 \mu\text{g kg}^{-1}$) and (D) Blank chicken muscle sample spiked (before extraction) with Nor, Cipro, Enro, Diflo, Sara and Flu ($100 \mu\text{g kg}^{-1}$ each). The ordinate axis represents the percentage of inhibition of the measured wells on the abscissa axis in the multi-FQ BIA (white bars) or the specific Flu BIA (filled bars).

The second 96-well plate fractions were kept at $-20\text{ }^{\circ}\text{C}$ after evaporation until the immunoactive fractions were redissolved in water/formic acid for chemical identification with high-resolution LC/TOFMS. The bar graph shown in Figure 4A is an immunogram of the gradient LC effluent from a FQ mixture injection. The peak width in this immunograms is determined by several factors, the quality of the gradient LC chromatography, the final concentration of the FQ in the well and the crossreactivity of the dual BIA toward the specific fractions. Immunoactivity is therefore expected in more than one well per FQ, in consequence adjacent wells showing high immunoactivity (i.e. belonging to the same chromatographic peak) are pooled for the chemical identification with high-resolution LC/TOFMS.

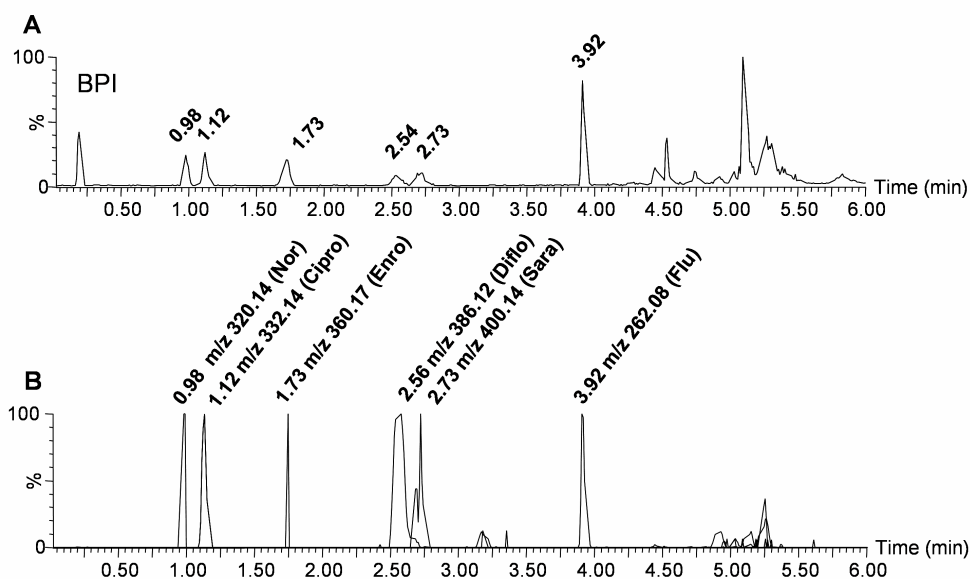


Figure 5. BIA-directed identification of a chicken muscle blank sample spiked with a mixture of the six FQs standards ($100\text{ }\mu\text{g kg}^{-1}$ each). (A) Base peak intensity (BPI) of a mixture of the six FQs standards ($100\text{ }\mu\text{g L}^{-1}$ each Nor, Cipro, Enro, Diflo, Sara and Flu in solvent). (B) Overlaid reconstructed ion chromatograms (0.05-Da mass window) obtained with high-resolution LC/QTOFMS from pooled immunoactive wells belonging to the same chromatographic peak present in the spiked blank chicken muscle sample (see Figure 4D) that matched the immunoactive wells positions obtained with the chemical standards immunogram (see Figure 4A).

The immunogram of the mixture of the six FQ shows four peaks in the multi-FQ BIA and one peak in the specific Flu BIA. The accurate mass measurement with high-resolution LC/TOFMS and elemental composition calculation showed that wells 22 + 23 corresponded to the Nor fraction, wells 25 + 26 to Cipro, wells 38 + 39 + 40 to Enro and wells 46 + 47 to Diflo and Sara which were coeluting in those fractions. Wells 56 + 57 were immunoactive only in the specific Flu BIA and corresponded to Flu as expected. The base peak intensity (BPI) chromatogram (Figure 5A) of the six FQ shows that they could be fully separated in a short analysis time (6 min) with high-resolution LC/TOFMS.

Although the column chemistry of the gradient LC was not identical to that of the high-resolution LC, a similar elution order for the FQs was found (Figure 5A-B).

Even though the blank chicken muscle sample was found negative during the dual BIA screening phase, the immunograms obtained with the blank chicken muscle extract showed two immunoactive peaks (Figure 4D). The presence of these peaks could be explained by the presence of compounds from the sample extract which cross-reacted in the multi-FQ BIA after the SPE concentration and splitting step. These sample extracts had a concentration 8-fold higher than in the dual BIA screening. The immunogram of the chicken sample incurred with Enro (Figure 4C) showed three immunoactive peaks, one of them in coincidence with the first peak position found in the blank chicken sample, a second immunoactive peak in front and a third immunoactive peak corresponding to the position of Enro. Finally, the immunogram of the chicken sample spiked with the six FQ showed three unknown immunoactive wells matching the other unknown positions (see Table 2 and Figure 4D) in addition to the same immunoactive well positions present in the immunogram of the chemical standards.

All the immunoactive well positions of the different chicken samples were measured in the second 96-well plate with high-resolution LC/TOFMS. The peaks of the reconstructed ion chromatograms (0.05 Da mass window) obtained from the immunoactive wells with the spiked blank chicken sample matching those of the chemical standards (Figure 5B) showed similar retention times (Rt) and errors in the order of 0.01 s. These peaks matching those of the chemical standard were background subtracted and mass measured with the lock mass provided by the second electrospray probe. The accurate masses of the $[M + H]^+$ ions were used to calculate the elemental composition and the following restrictions were applied: the mass accuracy window was set to ± 5

mDa, the ring and double-bond equivalents number (DBE) was set in the range of 5.5-20 and the elements were restricted to C₀₋₃₀, H₀₋₄₀, N₀₋₅, O₀₋₅, F₀₋₃ because no evident isotope pattern originating from chlorine, bromine or sulfur atoms was seen beyond the [M+H]⁺ ion. The accurate masses of the [M + H]⁺ ions of the peaks from Figure 5B were 320.1416, 332.1404, 360.1725, 386.1283, 400.1423, 262.0876 corresponding to the elemental compositions C₁₆H₁₉N₃O₃F, C₁₇H₁₉N₃O₃F, C₁₉H₂₃N₃O₃F, C₂₀H₁₈N₃O₃F₂, C₂₁H₂₀N₃O₃F₂, C₁₄H₁₃NO₃F respectively. These elemental composition corresponded with Nor, Cipro, Enro, Diflo, Sara and Flu respectively, indicating that it was possible to confirm the identity of the known immunoactive compounds in chicken muscle samples.

Table 2. BIA-directed identification of immunoactive wells with high resolution LC/QTOFMS* of (A) Chemical standard of a Nor, Cipro, Enro, Diflo, Sara and Flu mixture (100 µg L⁻¹ each). (B) Blank chicken muscle sample, (C) Chicken muscle sample incurred with Enro at 0.5 MRL (50 µg kg⁻¹) and (D) Blank chicken muscle sample spiked with Nor, Cipro, Enro, Diflo, Sara, Flu (100 µg kg⁻¹ each). Shaded cells indicate immunoactivity of those wells in that specific sample.

Immunoactive wells	Sample				[M+H] ^a (m/z)	Element composition	DBE	Error (mDa) ^b	Compound Proposed
	A	B	C	D					
3-5					123.0493	C ₆ H ₇ N ₂ O	4.5	6.4 ± 0	Vitamin B3
14-16					276.1317	C ₁₄ H ₁₈ N ₃ O ₃	7.5	-3.1 ± 1	Prodrug
19-20					-	-	-	-	-
22-24					320.1416	C ₁₆ H ₁₉ N ₃ O ₃ F	8.5	0.6 ± 0.5	Norfloxacin
25+26					332.1404	C ₁₇ H ₁₉ N ₃ O ₃ F	9.5	0.6 ± 0.6	Ciprofloxacin
38-40					360.1725	C ₁₉ H ₂₃ N ₃ O ₃ F	9.5	2.6 ± 1.4	Enrofloxacin
46+47					386.1283	C ₂₀ H ₁₈ N ₃ O ₃ F ₂	12.5	3.3 ± 0.3	Difloxacin
					400.1423	C ₂₁ H ₂₀ N ₃ O ₃ F ₂	12.5	5.0 ± 1.5	Sarafloxacin
56+57					262.0876	C ₁₄ H ₁₃ NO ₃ F	8.5	1.5 ± 0.9	Flumequine

^a Restrictions used for elemental composition calculation; Mass accuracy window ± 5 mDa (except for m/z 123.0493 where 7 mDa was used), ring and double-bond equivalents number (DBE) range 0.5-20, elements C₅₋₃₀, H₅₋₄₀, N_{(0 or 1)-3}, O₀₋₅, F₀₋₃.

^b Average of the absolute error ± SD of all the immunoactive fractions were the specific mass was present.

The unknown compounds in the immunoactive wells from the chicken muscle extracts eluting before Nor during the fractionation should also have shorter retention times (Rts) than Nor in the high-resolution LC/TOFMS. Hence, the mass spectra of the time window between 0 and 0.98 min (before the RT for Nor) were combined, the adjacent time window (1-2 min) was used for subtraction. The mass spectra obtained were compared between similar well positions showing immunoactivity in the different sample immunograms looking for coincident high intensity $[M + H]^+$ ions which might be responsible for immunoactivity. The elemental composition search of the $[M + H]^+$ ions was restricted considering the common piperazinyl moiety and oxoquinoline core structure of the Nor conjugate used as antigen for raising PAb CA65 and the FQs cross-reacting in the multi-FQ BIA (Figure 2). We considered that the structure of any chemical showing immunoactivity in the Nor BIA immunograms should at least contain one ring structure with at least 5 carbon atoms. The number of nitrogen atoms was always restricted by the maximum number present in crossreacting FQs (N=3) and the nitrogen rule was applied. The proposed elemental compositions were used for formula search in SciFinder and the number of hits was refined to compounds with calculated Log P values below that of Nor.

The main $[M + H]^+$ ion found in the mass spectra from the immunoactive wells 3-5 after background subtraction had an accurate mass of 123.0494. The reconstructed ion chromatogram (0.05 Da mass window) showed that this ion had a peak Rt of 0.25.

The element composition search was performed with a 7 mDa mass tolerance restriction because at lower m/z, a lower accuracy is expected in the TOF MS system. The double bond equivalent (DBE) number was set in the range of 0.5 to 20 and the elements were restricted to C_{5-10} , H_{5-40} , N_{0-3} , O_{0-5} , F_{0-3} . Four chemical formulas were obtained for this ion, however only two of them yielded matches in SciFinder after the restrictions described above were applied. The chemical formulas were $C_7H_6O_2$ and $C_6H_6N_2O$ with mass errors of 4.8 and -6.4 mDa respectively. The search of the $C_7H_6O_2$ yielded 123 matches of which only 13 contained an aromatic ring as part of the structure and 3 were benzaldehydes with references to biological activity like antibacterial agents or insecticides. However, no resemblance of these structures with any part of the crossreacting FQs was found.

The search of the chemical formula $C_6H_6N_2O$ in SciFinder yielded 229 compounds, no partial homology of the piperazinyl moiety was found with any these compounds. Therefore, a further search was performed

looking for homology with the oxoquinoline core by restricting the formula search only to heterocyclic aromatic compounds containing at least one nitrogen in the ring structure. This yielded 30 matches of which only 20 are commercially available including several pyridine derivatives, the most notorious one was nicotinamide (Niacin, vitamin B3), a compound commonly found in chicken muscle [23].

The immunoactive wells 14-16 in the different samples showed one main $[M + H]^+$ ion in common with a mass of 276.1317 and a peak Rt of 0.73 min in the reconstructed ion chromatograms (0.05 Da mass window). The elemental composition search was restricted to a 5 mDa mass error tolerance, the DBE number range was set to 0.5-20, the compounds and the elements were restricted to C_{5-30} , H_{5-40} , N_{1-3} , O_{1-5} , F_{0-3} . Four element composition possibilities were obtained $C_{15}H_{16}N_3F_2$, $C_{11}H_{19}N_3O_4F$, $C_{12}H_{17}N_3O_3F_3$ and $C_{14}H_{18}N_3O_3$ with mass errors 0.5, -4.3, -0.7 and -3.1 mDa respectively. Database search with SciFinder yielded no hits for $C_{15}H_{16}N_3F_2$ after the search was refined as described above and the search of $C_{11}H_{19}N_3O_4F$ yielded 5 very saturated ring structures without any partial homology with the FQs.

The search for $C_{12}H_{17}N_3O_3F_3$ yielded 12 compounds after the LogP restriction, none with an homology to the piperazinyl or oxoquinoline group. About 9 compounds were obtained with the formula $C_{14}H_{18}N_3O_3$ in the SciFinder database, these compound structures fulfilled the piperazinyl homology restrictions imposed using the rationale described above. From these compounds, only 2 had biological references but none was related to antibacterial activity. However, when the search for this formula was restricted to substructure homology with the oxoquinoline group present in all the FQs, 8 matches were obtained with high structural similarity to the FQs core structure. Four of these compounds had references to antimicrobial activity and one of them as a prodrug of norfloxacin and nalixidic acid [24] (see Figure 2). Ordering or synthesizing the compounds suspected for immunoactivity and further testing in the system in addition to MS/MS experiments of the standards and the chicken sample extracts might confirm the presence of these compounds in chicken muscle in the near future.

The immunoactive wells 19 + 20 (see table 2) did not show any high abundance $[M + H]^+$ ions in common. It is therefore possible that this specific compound was not detected with the TOF MS because it did not ionize in the electrospray in positive mode.

Conclusions

A fast dual BIA screening method for FQ was coupled in parallel with high resolution LC/QTOF MS identification of known and unknown compounds in noncompliant chicken muscle samples. A simple sample preparation of the chicken muscle samples was necessary prior to the dual BIA screening which was very sensitive allowing the detection of the FQs below MRL levels and therefore saving time during the screening process of known compounds. However, it was shown that the measurement of concentrated muscle samples with the dual BIA resulted in three unknown immunoactive peaks, showing the potential applicability of the system for finding unknown structurally related compounds. Further work will focus in testing the best candidate compounds with the Dual-BIA and with the high resolution LC-TOF MS system for the elucidation of the unknown immunoactive compounds origin present in these samples.

Acknowledgements

We thank our partner Dr Sheryl Tittlemier (Health Canada, Ottawa) for the supply of the Nor-NH₂ derivative.

This project was financially supported by the European Commission, project New technologies to screen multiple chemical contaminants in foods (acronym BioCop), contract FOOD-CT-2004-06988

References

1. Carlucci G (1998) Analysis of fluoroquinolones in biological fluids by high-performance liquid chromatography *J. Chromatogr. A* 812, 343-67
2. Wolfson JS, Hooper DC (1991) Overview of fluoroquinolone safety *Am. J. Med.* 91, 153-61
3. Steffenak I, Hormazabal V, Yndestad M (1991) Reservoir of quinolone residues in fish *Food Addit. Contam.* 8, 777-80
4. Aarestrup FM (1999) Association between the consumption of antimicrobial agents in animal husbandry and the occurrence of resistant bacteria among food animals *Int. J. Antimicrob. Agents* 12, 279-85
5. Bower CK, Daeschel MA (1999) Resistance responses of microorganisms in food environments *Int. J. Food Microbiol.* 50, 33-44
6. EEC (1996) Council Directive 96/23/EC On measures to monitor certain substances and residues thereof in live animals and animal products and repealing Directives 85/358/EEC and 86/469/EEC and Decisions 89/187/EEC and 91/664/EEC *OJEC L125*, 10-31
7. Ramos M, Aranda A, Garcia E, Reuvers T, Hooghuis H (2003) Simple and sensitive determination of five quinolones in food by liquid chromatography with fluorescence detection *J. Chromatogr. B Analyt. Technol. Biomed. Life. Sci.* 789, 373-81
8. Horie M, Saito K, Nose N, Nakazawa H (1994) Simultaneous determination of benfloxacin, danofloxacin, enrofloxacin and ofloxacin in chicken tissues by high-performance liquid chromatography *J. Chromatogr. B* 653, 69-76
9. Maraschiello C, Cusido E, Abellan M, Vilageliu J (2001) Validation of an analytical procedure for the determination of the fluoroquinolone ofloxacin in chicken tissues *J. Chromatogr. B* 754, 311-18
10. Hermo MP, Barron D, Barbosa J (2005) Determination of residues of quinolones in pig muscle: Comparative study of classical and microwave extraction techniques *Anal. Chim. Acta* 539, 77-82
11. Schneider MJ, Donoghue DJ (2002) Multiresidue analysis of fluoroquinolone antibiotics in chicken tissue using liquid chromatography-fluorescence-mass spectrometry *J. Chromatogr. B* 780, 83-92

12. Giles JS, Hariharan H, Heaney SB (1994) A microbiological assay for determining sarafloxacin and oxolinic acid concentrations in Atlantic salmon plasma *New Microbiol.* 17, 155-8
13. Pikkermaat MG, Elferink JAW, Mulder PPJ, de Cocq A, Nielen MWF, Egmond HJ (2007) An improved microbial screening assay for the detection of quinolone residues in egg and poultry muscle *Food Addit. Contam.* 24,842-50
14. Van Coillie E, De Block J, Reybroeck W (2004) Development of an indirect competitive ELISA for flumequine residues in raw milk using chicken egg yolk antibodies *J. Agric. Food Chem.* 52, 4975-8
15. Bucknall S, Silverlight J, Coldham N, Thorne L, Jackman R (2003) Antibodies to the quinolones and fluoroquinolones for the development of generic and specific immunoassays for detection of these residues in animal products *Food Addit. Contam.* 20, 221-28
16. Haasnoot W, Gerçek H, Cazemier G, Nielen MW (2007) Biosensor immunoassay for flumequine in broiler serum and muscle *Anal. Chim. Acta*, 586, 312-18
17. Huet AC, Charlier C, Tittlemier SA, Singh G, Benrejeb S, Delahaut P (2006) Simultaneous Determination of (Fluoro)quinolone Antibiotics in Kidney, Marine Products, Eggs, and Muscle by Enzyme-Linked Immunosorbent Assay (ELISA) *J. Agric. Food Chem.* 54, 2822-27
18. Nielen MWF, van Bennekom EO, Heskamp HH, van Rhijn JA, Bovee TH, Hoogenboom LAP (2004) Bioassay-directed identification of estrogen residues in urine by liquid chromatography electrospray quadrupole time-of-flight mass spectrometry *Anal. Chem.* 76, 6600-08
19. Nielen MWF, Bovee TH, van Engelen MC, Rutgers P, Hamers AM, van Rhijn JA, Hoogenboom LAP (2006) Urine testing for designer steroids by liquid chromatography with androgen bioassay detection and electrospray quadrupole time-of-flight mass spectrometry identification *Anal. Chem.* 78, 424-31
20. EEC (2002) Commission Decision 2002/657/EC 2002/657/EC: implementing Council Directive 96/23/EC concerning the performance of analytical methods and the interpretation of results
Off. J. Eur. Communities L221, 8-36
21. Tittlemier SA, Gelinat J, Cleroux C, Menard C, Delahaut P, Singh G, Benrejeb S (2007) Development of a direct competitive enzyme linked immunosorbent assay for the detection of fluoroquinolone residues in shrimp. *Food Annal. Methods*, DOI 10.1007/s12161-007-9004-1

22. EEC (1990) Council Regulation No 2377: laying down a Community procedure for the establishment of maximum residue limits of veterinary medicinal products in foodstuffs of animal origin *Off. J. Eur. Communities* L224, 1-8
23. Lombardi-Boccia G, Lanzi S, Aguzzi A (2005) Aspects of meat quality: trace elements and B vitamins in raw and cooked meats *J. Food Compos. Anal.* 18, 39
24. Khan MM (2001) Prodrugs of nalidixic acid and norfloxacin *Indian J. Chem.* 40B, 530-36

Chapter 7

Nanoscale Affinity Chip Interface for Coupling Inhibition SPR Immunosensor Screening with nano-LC TOF MS

Published in: Analytical Chemistry 80 (2008) 1159 -1168

Abstract

The on-line nanoscale coupling of a surface plasmon resonance (SPR)-based inhibition biosensor immunoassay (iBIA) for the screening of low molecular weight molecules with nano-liquid-chromatography electrospray ionization time-of-flight mass spectrometry (nano-LC ESI TOF MS) for identification is described. The interface is based on a reusable recovery chip (RC) that contains a nanoscale biosorbent composed of a hydrogel layer modified with antibodies raised against the analyte featuring the unique possibility of performance characterization using the SPR biosensor. Various hydrogel chemistries were evaluated, and the standard Biacore CM5 chip showed the highest capture capacity in combination with affinity-purified polyclonal antibodies. The procedure has four stages: the samples are prepared (1) and screened using a screening chip (SC) in the iBIA (2). Suspected noncompliant samples are reinjected over the RC, and the analyte is captured at subnanogram level (3). The captured analyte is released, and the eluate is analyzed with nano-LC ESI TOF MS via a loop-type interface (4). The coupling of the technologies proved effective for screening enrofloxacin, a model compound, in incurred chicken muscle samples followed by identity confirmation in suspected noncompliant samples. Ciprofloxacin, a known metabolite of enrofloxacin, was identified as well in incurred chicken samples. This demonstrates the potential of the technologies coupled by means of a RC for the rapid screening and identification of known as well as unknown compounds. Finally, we demonstrate the feasibility of combining the two biosensor chips (SC and RC) with a robust chip-based nano-LC chip TOF MS system, thus providing a robust alternative triple-chip system.

Introduction

A wide variety of surface plasmon resonance (SPR)-based biosensor applications have been reported during the last decade [1, 2]. These applications exploit biorecognition events of (at least) two binding partners that interact at the sensor chip surface where one of them is immobilized. The binding of the partners increases the total mass and the density of the molecules at the chip surface, hence resulting in a local refractive index change that is proportional to the SPR biosensor signal output. A major advantage is that the interaction can be monitored in real time allowing the determination of the kinetic parameters. The concentrations of interacting biomolecules can be quantitatively estimated either by the direct binding of the analyte to the chip surface (direct binding assay (DBA)), or by constructing an inhibition (competitive binding) assay. Since the signal output depends directly on the mass of the interacting analyte, the DBA format is widely used for fishing high molecular weight biomolecules out of complex biological matrices. Nevertheless, with the proper experimental forethought, this approach has also proven effective for the determination of kinetic parameters of low molecular weight molecules binding to antibodies or receptors [2, 3]. Such antibody-based DBAs were developed for the direct detection of low molecular weight drug residues (aminoglycosides with molecular weights of 466 and 583 Da) in milk of dairy cows [4, 5]. However, for low molecular weight compounds the inhibition assay format is generally preferred in biosensor immunoassays (BIAs) because of its flexibility, higher response and robustness [4, 6]. In this format, the sample (containing the analyte/s) is mixed with the high molecular weight affinity biomolecule (i.e., antibody, receptor, etc) and injected over the chip surface previously coated with the analyte. The signal drop due to the inhibition of the binding of the biomolecule to the immobilized analyte on the chip surface will be proportional to the analyte concentration in the sample. The robustness of such a low molecular weight compound coated chip has been proven with a sulfamethazine derivative coated chip which was used for approximately 1100 cycles and no significant change in performance was observed [6].

The main drawback of the biosensor screening technology is the lack of information about the identity of the interacting analyte. Hence, its combination with mass spectrometry is a powerful approach that already yielded a number of successful attempts in the field of proteomics [7, 8],

where the presence of proteins retained during the direct assay interaction analysis can be unambiguously confirmed by coupling the SPR biosensor with matrix-assisted laser desorption ionization time-of-flight mass spectrometry (MALDI-TOF MS) [9]. The SPR-MALDI-TOF MS analysis has evolved from the direct measurement of the interacting biomolecules from the chip surface (yielding the chip unusable after one binding cycle) to the further deposition of the biomolecules on MALDI plates for analysis upon elution [10, 11] to a small volume elution using automated commands [12-14] and lately to a bifunctional SPR/MS flow cell with removable MS probes [15]. Alternatively to MALDI-TOF MS analysis, the analysis of the chip eluate using liquid chromatography electrospray ionization MS (LC-ESI-MS) has been reported [16, 17]. Although these interfacing concepts have proven well suited for the identification of high molecular weight molecules in conjunction with DBAs, they are not functional for the screening of compounds of low molecular weight.

Within the scope of the EU project BioCop (www.biocop.org), several inhibition biosensor immunoassays (iBIAs) are being developed as screening methods for chemical contaminants in food. Our challenge within this project is to couple the iBIA with MS for confirmation of identity and/or the identification of unknowns having activity in the iBIAs. We have recently reported a method for the parallel coupling of these technologies using a dual wellplate LC fractionator [18]. In the present study we demonstrate the proof of principle, using enrofloxacin (Enro) as the model analyte, for the serial coupling concept between the iBIA and nano-LC-ESI-TOF MS. Enro is an antibiotic widely used in cattle and poultry that should be monitored and is regulated in accordance to EC Council Directive 96/23/EC [19]. The proposed system is composed of the Biacore 3000 SPR biosensor that carries out the screening using a robust iBIA. When a suspected noncompliant sample is found, the system stops the screening procedure and an aliquot of the sample without antibody is reinjected into the accessory surface preparation unit (SPU) that accommodates a recovery chip (RC) containing anti-Enro antibodies. This RC contains a 100-200 nm thick porous polymer (hydrogel) layer modified with antibodies. The antibodies in the biosorbent specifically capture the analyte while the sample matrix flows through. The chip surface is washed and next, the captured analytes are eluted into a loop from where they enter the nano-LC system and routed toward a precolumn followed by an analytical column and finally electrosprayed in the TOF MS for mass analysis. Both an iBIA and a DBA

were developed for Enro (the latter for RC characterization). The hyphenated system was tested with standard solutions and with chicken muscle extracts in a regulatory-relevant concentration range. The detection of unknown compounds was addressed along with the viability of using high-capacity RC surfaces. Finally, a more robust chip-nano LC TOF MS alternative to the standard nano-LC Chip TOF MS set up was briefly studied in combination with the SC and RC to create a triple-chip approach.

Experimental Section

Chemicals and Materials

Sensor chips (CM5), HBS-EP buffer [pH 7.4, consisting of 10 mM 4-(2-hydroxyethyl) piperazine-1-ethanesulfonic acid, 150 mM sodium chloride, 3 mM EDTA, 0.005% (v/v) surfactant polysorbate (P20)], an amine coupling kit [containing 0.1M *N*-hydroxysuccinimide (NHS), 0.4 M *N*-ethyl-*N*-(3-dimethylaminopropyl) carbodiimide hydrochloride (EDC), and 1 M ethanolamine hydrochloride NaOH (pH 8.5)], CNBr-activated Sepharose™ 4B and the SPR-based biosensor systems Biacore 3000 and Q, the SPU accessory as well as the AKTA purifier and HI Trap protein G columns (1 mL) were supplied by GE Healthcare (Uppsala, Sweden). Sensor chips featuring other hydrogel chemistries were purchased from XanTec bioanalytics GmbH (Muenster, Germany). Ethylene diamine (EDA) was obtained from VWR International (Amsterdam, The Netherlands). Acetonitrile (ACN) HPLC far-UV grade was from Lab-Scan Ltd. (Dublin, Ireland). Water was purified using a Milli-Q gradient A10 system (Millipore, Bedford, MA). The 0.45 µm Durapore filters and the 30 kDa and 50 kDa Amicon cutoff filters were from Millipore. Ciprofloxacin (Cipro) and enrofloxacin (Enro) were from Fluka (Zwijndrecht, The Netherlands). All other reagents were obtained from Sigma–Aldrich (Zwijndrecht, The Netherlands) unless otherwise stated. The AKTA purifier and HiTrap protein G columns (1 mL) were provided by Amersham Biosciences (Uppsala, Sweden). Mouse anti-Enro/Cipro monoclonal IgM antibody (clone 72FIG1F7#1) (MAb72F) was obtained from Abcam (Cambridge, U.K.). The preparation and purification of the polyclonal antiserum (PAb MH40) is described in the Supporting Information at the end of this chapter.

Equipment

The system (Figure 1) consists of the Biacore 3000 SPR biosensor containing both a CM5 chip coated with Enro for the iBIA screening (inset 2) and a SPU accessory containing the RC, a CM5 chip coated with antibodies, for analyte capture (inset 3). The flow cell carrier type 2 (FCT2) on top of the RC features a serpentine-like flow cell (area ≈ 16 mm², height of 50 μ m and volume of 800 nL). The SPU is connected to a 10 μ L loop-type interface with a Micro Tight® tubing sleeve (i.d. 535 μ m) and Peek™ tubing (i.d. 255 μ m, 510 μ m o.d., 9.6 cm). The inlet of the loop interface is connected to the Waters (Milford, MA) model Acquity UPLC pump. The outlet of the loop-type interface is connected to the tee of a nano-LC switching system adapted from Meiring *et al.* [20] using 1/16 in. connections having short (0.02 in. i.d.) Peek™ sleeves and fused silica capillary tubing (360 μ m o.d., 200 μ m i.d., 60 cm). The flow is split ($\approx 1/2000$), with this switching system, between the restrictor (360 μ m o.d., 50 μ m i.d., 50 cm) and the trapping column (Biosphere C18 120 Å 5 μ m 50 μ m i.d., 360 μ m o.d., 2 cm length) between the first and the second tee. Following the second tee, the analytical column (Biosphere C18 120 Å 3 μ m 50 μ m i.d., 360 μ m o.d., 20 cm) is directly butt-connected with the Nanoease emitter (Waters) through the universal NanoFlow™ Sprayer mounted on the Waters model QTOF-micro MS system. The nano-LC gradient separation was performed using a mobile phase consisting of (A) water/formic acid (99.8:0.2; v/v) and (B) ACN/water/formic acid (89.8:10:0.2; v/v/v). Sample loading through the trapping column is performed at 10 μ L min⁻¹ for 5 min with 100% solvent A. Upon valve switch, the precolumn split is activated and the restrictor back pressure allows a flow in the order of 300 nL min⁻¹ through the analytical column. Details concerning nano-LC columns, capillaries, connectors, valves, solvent composition- and flow gradient and the MS settings can be found in the Supporting Information.

The feasibility of the triple chip approach was carried out using the nano-LC chip TOF MS system of Agilent Technologies (Waldbronn, Germany) previously described elsewhere [21]. The chip trapping column had a volume of 40 nL and was packed with Zorbax 300SB C18 5 μ m particles. The nano-LC chip column had a 75 x 50 μ m cross section, length of 43 mm and was packed with Zorbax 300SB C18 3.5 μ m. Mobile phases were similar to those used with the capillary nano-LC TOF MS system described above. The electrospray voltage was set to

2400 V at the MS inlet capillary. Nitrogen drying gas at 350 °C and 4 L min⁻¹ was used for spray desolvation.

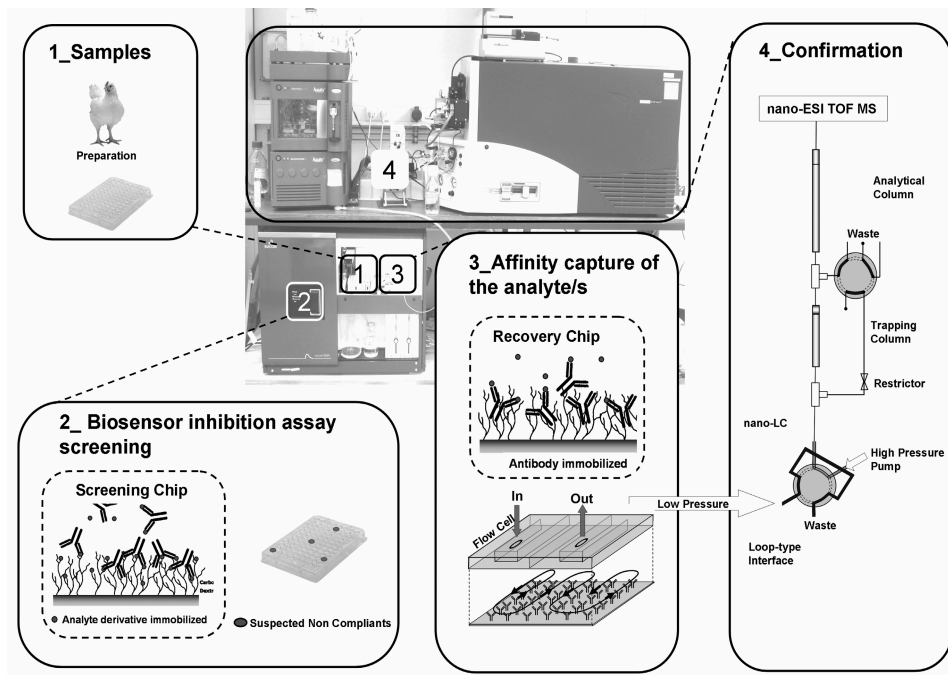


Figure 1. System setup overview with exploded view of key components. Muscle extracts (inset 1) are screened in the SPR Biosensor with the Enro iBIA using the screening chip (SC) (inset 2). The analytical efforts are focused only on the suspected noncompliant samples that are re-injected as they are detected over a recovery chip (RC) with immobilized antibodies (inset 3). Enro is captured on the RC surface and eluted into a loop-type interface (inset 4). The first valve is switched to the high-pressure side and the analyte is transferred from the loop-type interface to the trapping column. Once the analyte is trapped, the second valve is switched and the nano-LC gradient is started. Dashed frames in insets 2 and 3 depict the mirror-image immunochemistry nature between the SC and RC.

Screening Chip Preparation and iBIA Procedure

Enro was immobilized via its carboxyl group to the carboxymethylated chip surface using EDA as a bifunctional spacer. The SC surface was preconditioned by consecutive duplicate injections of 10 μ L of HCl (10 mM), NaOH (50 mM), sodium dodecyl sulfate (0.1% w/v) and water at 100 μ L min⁻¹ in one flow channel (Fc2) of the Integrated μ -fluidic

cartridge (IFC) in the biosensor. Then, the surface was activated with 150 μL of a mixture of 0.4 M EDC and 0.1 M NHS (1:1; v/v) and then coated with 100 μL of 2 M EDA in water (pH 10), both at 10 $\mu\text{L min}^{-1}$. Then, all remaining activated groups were blocked with 100 μL of EA (1 M). The SC surface and the IFC were cleaned by two injections of 10 μL of a mixture of 0.2 M NaOH, ACN and water (1:1:3; v/v/v) using the "Wash needle" and "Wash IFC" wizards in the biosensor software.

Meanwhile, the carboxyl group of Enro was activated by adding 10 μL of an Enro solution (10 mg mL^{-1} in methanol) to one vial containing 115 μL of 0.4 M EDC and to another vial containing 115 μL of 0.1 M NHS. Both freshly prepared vials were mixed (1:1; v/v) in the biosensor before the injection of 150 μL at 2 $\mu\text{L min}^{-1}$ over the EDA-modified SC surface. Finally, the SC was washed with 0.05 M NaOH and HBS-EP.

For the iBIA procedure, the sample extracts or standard solutions in HBS-EP buffer were mixed (4:1; v/v) with the antibodies (diluted antiserum PAb MH40 or its purified IgG fraction (SpMH40)) in the biosensor and 50 μL was injected at a flow rate of 25 $\mu\text{L min}^{-1}$. The SC surface was regenerated with 15 μL of a mixture of 0.2 M NaOH and ACN (4:1; v/v).

Recovery Chip Preparation

Antibodies (SpMH40 or MAb72F) were immobilized onto the entire carboxymethylated surfaces of the sensor chips (Biacore CM5 or XanTec chips assembled in Biacore frames as described by the manufacturer). Preconditioning was the first step and the second step involved the activation of the sensor chip surface and the immobilization of the antibodies. For the preconditioning step, 100 μL aliquots of the preconditioning solutions (HCl (10 mM), NaOH (50 mM), and sodium dodecyl sulfate (0.1% v/v)) were successively pipetted over the chip surface. The chip surface was thoroughly rinsed with distilled water and activated with 100 μL of a mixture of 0.4 M EDC and 0.1 M NHS (1:1; v/v) for 20 min. Finally, SpMH40 antibody was diluted (1:10; v/v) in acetate buffer (pH 5) and 100 μL was placed onto the activated chip surfaces, left to react for 90 min, and the remaining active groups were deactivated by pipetting 100 μL of 1 M EA. The immobilization levels were evaluated by measuring the relative responses of the chips in the biosensor before and after immobilization. The characteristics of the sensor chip hydrogel chemistries used for preparing the RCs (Table 2) are presented in Table 1.

Table 1. Evaluation of screening chips with different hydrogel properties in the inhibition SPR biosensor immunoassay (iBIA) for Enro .

Chip	Hydrogel		Inhibition BIA		
			Immobilized	Bound	Sensitivity
Code	Lenght (nm)	Chain density	Enro (RU)	PAb MH40 (RU)	IC ₅₀ (pg μL^{-1})
A ^a	100 - 200	Low	600	11700	7.1
B ^b	150	High	300	3800	4.8
C ^b	200	Low	800	10000	5.3
D ^b	200	High	700	4000	3.3
E ^c	500	High	400	6400	5.5
F ^c	1000	Medium	1400	6700	6.6

^a Carboxymethylated dextran chip from Biacore

^b Carboxymethylated dextran chip from XanTec

^c Linear carboxylated hydrogel matrix from XanTec

Samples and Standards

Muscle samples from untreated broilers and broilers treated with Enro were obtained from an animal experiment that is described elsewhere [22]. The chicken breast samples (1 g) were extracted by homogenizing with 10 mL of water. The homogenate was centrifuged and the supernatant was filtered through a 0.45 μm filter. Two milliliters of the filtrate were passed through a 30 kDa cutoff filter and diluted (1:1; v/v) in HBS-EP buffer for further experiments. Enro and Cipro standard solutions were prepared by dissolving 10 mg in 10 mL of a mixture of methanol and formic acid (99.9:0.1; v/v) and subsequently diluted with HBS-EP buffer to relevant concentrations.

Results and Discussion

Screening Chip Performance

Different screening chips (SCs) were prepared by immobilizing Enro on sensor chips having different hydrogel properties (see Table 1). The amount of immobilized Enro is proportional to the increase in response units (RU) measured on the different chip surfaces and these varied from 300 RU in SC B to 1400 RU in SC F. To assess the maximum

binding capacity of the Enro-modified chips, high amounts of antibodies (raw antiserum PAb MH40 diluted in HBS-EP buffer (1:10; v/v)) were injected (50 μL at 25 $\mu\text{L min}^{-1}$) over each chip, and the maximum response varied from 3800 RU for SC B to 11700 RU for chip A. After regeneration with a mixture of 0.2 M NaOH and ACN (4:1; v/v), the responses returned to baseline and a new sensorgram could be produced with similar binding responses.

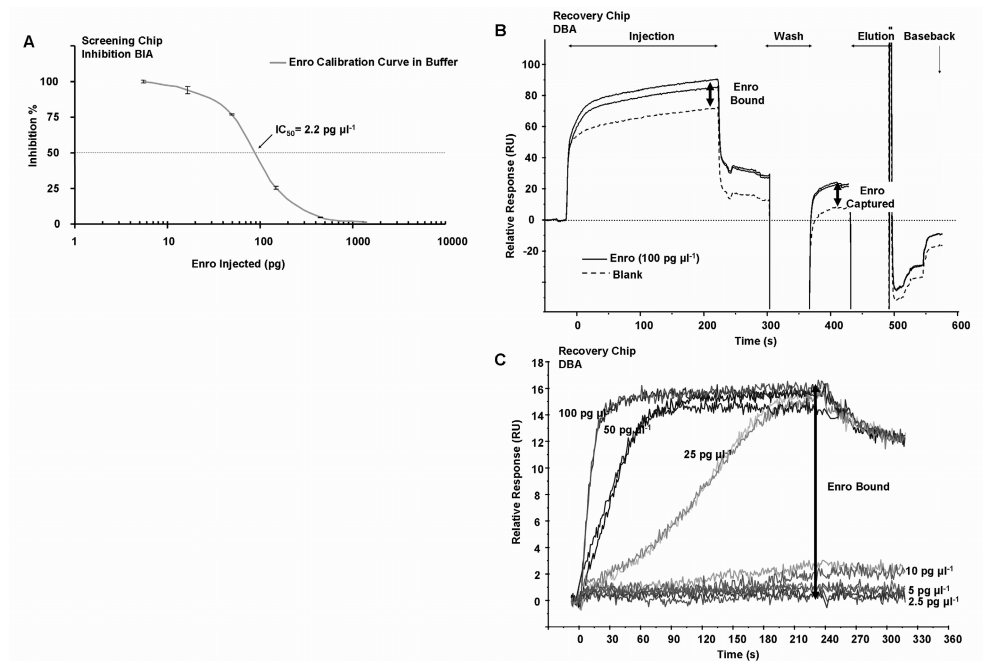


Figure 2. (A) Calibration curve of Enro in the iBIA with SC A (see Table 1 and the Screening Chip Performance section). (B and C) Evaluation of the direct binding of Enro to SpMH40 immobilized on the RC A (see Table 2 and the Recovery Chip Performance section). (B) Overlaid sensorgrams of complete ligand/wash/regeneration cycles obtained in the direct binding assay (DBA) format measured with the Biacore Q. (C) Blank-subtracted (i.e., dashed line in B subtracted from the Enro sensorgrams) sensorgrams of duplicate injections of Enro at various concentrations to evaluate the maximum capacity and saturation time of RC A.

A calibration curve for Enro was measured for each chip (data not shown) as described in the iBIA procedure using diluted raw antiserum PAb MH40 (1:40; v/v). More than 2-fold difference in sensitivity (defined as the concentration at 50% inhibition (IC_{50})) was observed between SC A ($IC_{50} = 7.1 \text{ pg } \mu\text{L}^{-1}$) and SC D ($IC_{50} = 3.3 \text{ pg } \mu\text{L}^{-1}$). However, the high

maximum response obtained for the blank ($B0 = 1950$ RU) with SC A allowed a further 3-fold PAb MH40 antiserum dilution with a concomitant maximum response decrease for the blank (670 RU) and a 2-fold increase in sensitivity ($IC_{50} = 3.7$ pg μL^{-1}). The measurement of a calibration curve (see Figure 2 A) using the purified antiserum fraction (SpMH40) (1:50; v/v) in SC A resulted in an additional increase in sensitivity (Enro $IC_{50} = 2.2$ pg μL^{-1}) with a robust maximum response of 750 RU. All further iBIA experiments were performed using SpMH40 in combination with SC A. The sensitivity of the iBIA for Cipro, a known Enro metabolite, was lower ($IC_{50} = 85.4$ pg μL^{-1}), and the cross-reactivity (CR) was 3%. The iBIA assay time, including mixing the reagents, sample injection, the regeneration of the surface and washing steps, was 8.5 min per sample.

Development of the Recovery Chip Procedure

The Biacore 3000 software was modified by GE Healthcare to allow the development of a method for the injection of suspected noncompliant samples over the RC mounted in the SPU, followed by washing steps and analyte forward-elution. The procedure for the recovery of the analyte from samples suspected as being noncompliant in the iBIA started with the injection of 40 μL of sample without antibody over the RC at 10 $\mu\text{L min}^{-1}$. The RC was washed for 2 min with water, then 10 μL of formic acid (1%) were injected to disrupt the interaction of the analyte with the biosorbent followed by the injection of a transfer volume (water) to position the eluate in the loop-type interface leading toward the nano-LC TOF MS. In order to reduce carryover issues, two washing steps were added in the RC controlling software after the elution step. The first one was the elution solvent (i.e., formic acid 1%) and the second one was water to condition the antibodies for the next recovery cycle.

The transfer volume required to position the 10 μL RC eluate plug from the SPU into the loop-type interface was optimized using a glass chip (instead of a functionalized RC) that was fitted in the SPU and connected to the loop-type interface and the nano-LC TOF MS system. Injections of 10 μL of a standard solution of Enro (100 pg μL^{-1}) in 1% formic acid were followed by increasing transfer volumes. A transfer volume of 13 μL showed that the area counts of the Enro peak in the chromatogram matched the area counts of an injection of Enro from the nano-LC TOF MS autosampler. With the same procedure, a calibration curve injected

from the SPU and the loop-type interface was constructed by measuring increasing concentrations of Enro standards (0- 500 pg) with the nano-LC TOF MS system. The Enro calibration curve was used for all further estimations of the RC capacity.

Recovery Chip Performance

If compared with traditional affinity extraction columns, the RC concept features the unique advantage of being able to characterize the affinity sorbent using the SPR biosensor. Using the DBA format we can study the performance of the RC in detail and obtain useful information to select the biomolecule best suited for each application. Robust biomolecules, with high affinity, low dissociation rate, and an interaction with the analyte that can be disrupted with MS-compatible buffer, are desired. The optimal density of immobilized biomolecules, capacity, affinity constants and saturation time can also be evaluated. Additionally, the non-specific binding of matrix components to the RC and the wash and elution steps can be scouted without compromising the nano-LC TOF MS system. As a model, the interaction between Enro and the antibodies (SpMH40) immobilized in RC A (see Table 2) was evaluated using a Biacore Q SPR biosensor. This biosensor features a flow cell height of 50 μm , comparable to the FCT2 flow cell used with the RC in the SPU. Figure 2B depicts the representative sensorgrams obtained with the injection of 40 μL of (100 $\text{pg } \mu\text{L}^{-1}$) Enro standard solution. The bulk response jump upon injection caused by the blank and the Enro standard solution are due to the lack of a reference channel in the Biacore Q for subtraction. The maximum response of Enro binding to the immobilized antibodies was 16 RU as observed from the difference between the Enro and the blank buffer injection. The Enro response decays when the dissociation of the lower strength interactions occurs after the injection ends. About 12 RU of Enro remain captured on the RC A surface after the dissociation and the 1 min washing step. The interaction can be disrupted for elution purposes using a 1 min injection of MS compatible solvent (formic acid 1%, pH 2). The response returns close to its baseline values with a loss of <20 RU (<0.1%) of immobilized SpMH40 after each cycle. Figure 2C depicts sensorgrams of duplicate injections of standards solutions with increasing concentration of Enro after the subtraction of sensorgrams of blank injections (at least one for each concentration). The SpMH40-based biosorbent in RC A

showed to be robust and preserved its binding properties for more than 50 cycles under these wash-elution conditions.

In Biacore SPR measurements an equivalence of 1 RU to 1 pg mm⁻² is assumed for proteins [23]. Hence, the 19000 RU of SpMH40 immobilized in RC A are roughly equivalent to 2 pmol on the complete surface of 16 mm².

Table 2. Evaluation of chips with different hydrogel properties for the production of Enro recovery chips. ^a

Chip	DBA Biosensor	Nano-LC TOF MS	
	Immobilized	Captured	Captured
Code	Antibody (RU) ^a	Enro (RU)	Enro (pg mm ⁻²)
A	19600	12	31
A1	18900	0	3
B	16400	10	-
D	4800	4	-
E	8200	0	13
F	9200	9	14

^a The chips having a surface of 16 mm² were evaluated using both the direct binding assay format in the SPR biosensor and the nano-LC TOF MS system.

^b PAb SpMH40 immobilized except in chip A1 where monoclonal antibody (MAb72F) was immobilized.

- not measured

The maximum theoretical response of a ligand ($RU_{L\ MaxPred}$) binding to immobilized macromolecules (RU_M , response of the macromolecule immobilized) is predicted for proteins using: $RU_{L\ MaxPred} = RU_M n (Mw_L / Mw_M)$. With n being the number of binding sites in the macromolecule (2 for antibodies), Mw_L being the molecular weight of the ligand (359 Da for Enro), and Mw_M being the molecular weight of the macromolecule (150 kDa for antibodies). Hence, given the immobilization level of SpMH40 in RC A (see Table 2), one would expect to measure a response of about 90 RU upon saturation of all binding sites with Enro (4 pmol on the 16 mm²). Nevertheless, Figure 2, parts B and C, show that about 16 RU of Enro are bound and 12 RU remain captured after the washing step. Nano-LC TOF MS measurements of Enro actually eluted from RC A (Table 2 and Figure 3) revealed that the

maximum Enro capture capacity of the chip after dissociation and wash step is approximately 500 pg (≈ 1.4 pmol of Enro), which is 34% of the theoretical maximum. This lower capacity is partly due to the nonspecific immobilization method used, that renders many binding sites inactive because it couples primary amines (N-terminal and possibly lysine groups) of the macromolecule with the dextran surface [24]. The actual maximum capacity of the RC as measured with nano-LC TOF MS is approximately 500 pg (30 RU), higher than the 190 pg (12 RU) expected from the SPR measurement. This underestimation of the maximum capacity arise possibly from two erroneous presumptions. The first is the correlation of $\text{RU} = 1 \text{ pg mm}^{-2}$. This correlation cannot be applied to small molecules because the SPR response depends on the molecular structure as well as the molecular weight [25]. Second, the distribution of the antibodies in the hydrogel is homogeneous. Instead, the antibodies in this highly packed affinity biosorbent probably form a gradient perpendicular to the sensor surface, as previously suggested [26, 27]. This influences the SPR response because the evanescent wave intensity has a strong exponential decay within a few hundred nanometers next to the surface [23]. Hence, highly concentrated antibodies binding Enro in the distal regions of the hydrogel would contribute little to the final Enro SPR response and also limit the transport to the lower density layers under a higher evanescent wave intensity.

The linear binding curves of Enro to the antibodies in the sensorgrams of Figure 2C show that the reaction is strongly limited by mass transport under the conditions of low flow rate ($10 \mu\text{L min}^{-1}$) and a high flow cell height ($50 \mu\text{m}$), in accordance with expectation [28]. The sensorgrams also suggest a further diffusion limitation at Enro concentrations below $25 \text{ pg } \mu\text{L}^{-1}$ where very low responses are obtained indicating low capture levels. An attempt to obtain the kinetic constants by fitting the Enro sensorgrams of Figure 2C to a simple 1:1 bimolecular model with mass transport, using CLAMP software [29], resulted as inconclusive, indicating a complex kinetic system influenced by additional diffusion limitations and a heterogeneous kinetic behavior of the polyclonal antibodies. SPR experiments using a lower capacity RC (8900 RU of immobilized antibodies) showed an Enro binding response of 15 RU. This binding response is comparable to the response obtained with the high-capacity RC A and suggests either that a higher proportion of binding sites are active or that they are distributed more homogeneously at lower densities.

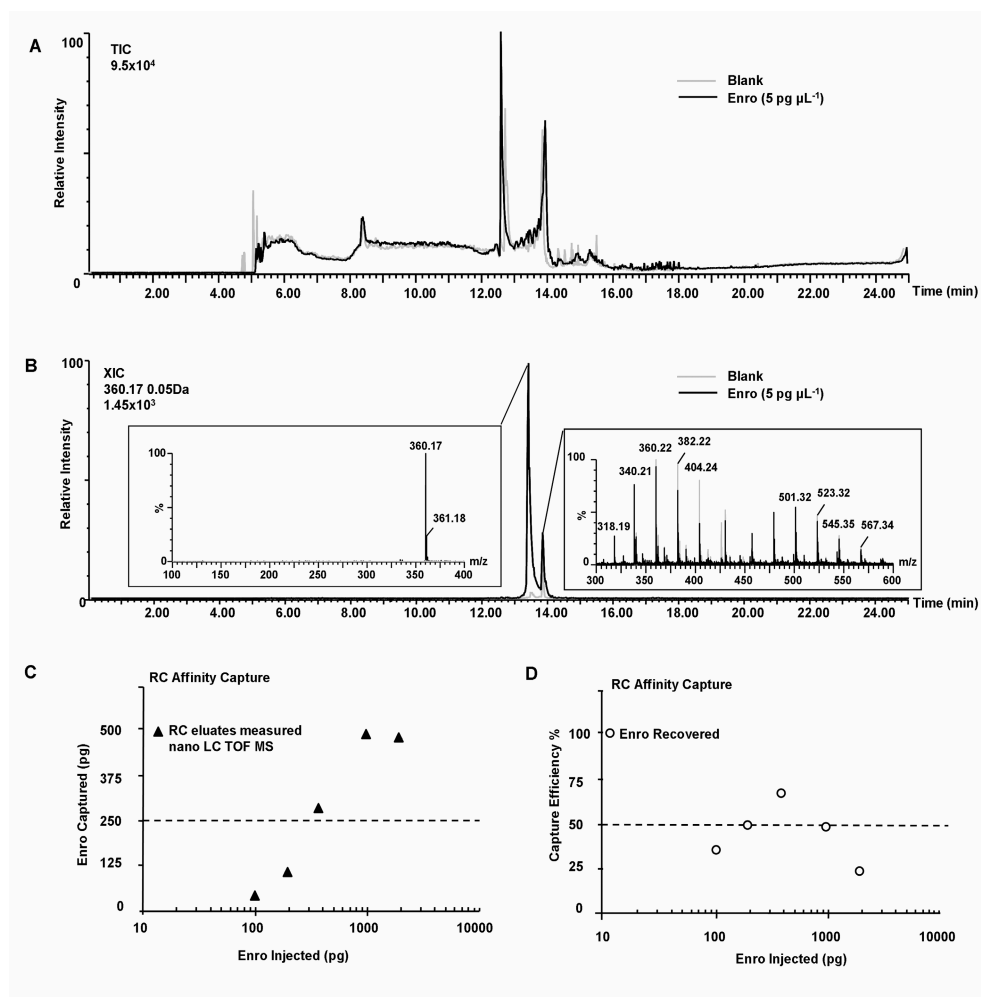


Figure 3. Overlaid chromatograms and mass spectra (see insets) of relevant peaks of RC eluates analyzed on-line by nano-LC TOF MS. Reagent blank (gray) and Enro standard solution ($5 \text{ pg } \mu\text{L}^{-1}$) (black) in HBS-EP buffer were injected ($40 \text{ } \mu\text{L}$, $10 \text{ } \mu\text{L min}^{-1}$) over RC A and eluted with $10 \text{ } \mu\text{L}$ of formic acid (1%). (A) Total ion current (TIC) (B) extracted ion chromatogram (0.05 Da mass window). Enro (360.17) elutes in the first peak. The second peak corresponds to a buffer interference (360.22) also present in the blank. (C) Nano-LC TOF MS analysis of RC eluates after injections with increasing Enro concentrations. (D) Recovery efficiency of the RC A at different concentrations of Enro injected over the RC.

The nano-LC TOF MS analysis of RC A eluates from injections of Enro below $25 \text{ pg } \mu\text{L}^{-1}$ shown in Figure 3 demonstrates that Enro is indeed captured at levels that should be measurable with the biosensor. An increase in the concentration of Enro injected over RC A correlates with increasing amounts of Enro captured on the RC as shown in Figure 3C yielding a curve that mirrors the calibration curve obtained in the iBIA (Figure 2A). The analysis of the RC capture efficiencies shown in Figure 3D clearly shows that there is an optimal concentration of Enro that maximizes the capture.

Knowing the kinetic constants could have an additional analytical value in the characterization of the biosorbent since they predict the RC behavior and would correlate the estimated analyte concentration values of the suspected noncompliers selected with the iBIA screening with a binding rate and capture efficiency when injected in the affinity chip interface. This would facilitate an automated adjustment of the sample concentration and volume needed in the RC to maximize the capture efficiency. The results presented show the potential insight to which the RC affinity sorbent can be studied using the present system. Last but not least, the predicted RC performance from the SPR measurements represents just a worst case (i.e. SPR can be exploited as a QA/QC check). More considerations about RC hydrogel immobilization capacity can be found in the Supporting Information section of this chapter. Future research will focus first on optimizing the immobilization chemistry and using recombinant antibodies that allow an oriented immobilization, a higher efficiency and a simpler estimation of the kinetic constants. The nano-LC TOF MS analyses presented in Figure 3 demonstrate that the amount of Enro captured onto the RC is more than sufficient, even when Enro is injected onto the RC at low concentrations of $5 \text{ pg } \mu\text{L}^{-1}$.

The Enro capture capacities of sensor chips of different hydrogel lengths and branching densities (see Table 2) were studied. Again, the SPR biosensor and the on line biosensor-RC-nano-LC TOF MS system were used for measuring the amount of captured Enro. The standard Biacore chip, RC A showed the highest antibody immobilization capacity (19.6 ng mm^{-2}) and Enro capture capacity (12 RU). A shorter hydrogel of higher density (RC B) lowered 16% the immobilization capacity and proportionally decreased the Enro capture capacity. However, a small increase in length of this high-density hydrogel (RC D) dramatically lowered the antibody immobilization capacity by 75%. RC E and RC F had a linear polymer hydrogel (undisclosed polymer chemistry by the

manufacturer) and showed 59% and 53% lower immobilization capacities, respectively. Nevertheless, these hydrogels exceeded the evanescent wave sensing region and more antibodies than probed by SPR measurement were expected. The Enro capture capacities of RC E (high-density hydrogel) and RC F (lower density hydrogel) were 0 and 9 RU, respectively, according to the biosensor. In contrast, the nano-LC TOF MS eluate analysis showed that Enro could be captured in RC E and RC F at a similar level of 13 and 14 pg mm^{-2} respectively. This suggests that the diffusion of Enro in chip E was limited by the high-density hydrogel and that the SpMH40 interaction took place too far from the chip surface. Given the potential of a 5-10 fold higher hydrogel volume featured in RC F, this seems as a suitable candidate for a high capacity chip still allowing characterization using the biosensor. However, RC A was used throughout this study due to its high capacity and robustness. Further research will focus in optimizing the antibody immobilization procedure for this chip combined with recombinant antibodies currently under development.

Multianalyte Capture

In order to test the feasibility of capturing more than one analyte on the RC surface, a monoclonal antibody IgM (MAb72F) with high CR for Enro and Cipro was immobilized on a chip (RC A1). The level of immobilization (Table 2) was similar to that of RC A with the SpMH40 although the IgM molecules have a molecular weight of 900 kDa. The SPR measurements resulted in a lack of Enro response. The nano-LC TOF MS analysis of eluates from RC A1 after the injection of a mixture of Enro and Cipro ($100 \text{ pg } \mu\text{L}^{-1}$) showed that about 3 pg mm^{-2} of Enro (CR 100%) and 1.6 pg mm^{-2} of Cipro (CR 53%) were captured. Comparatively, 30.6 and 1.8 pg mm^{-2} , respectively, were obtained (CR 6%) when the same experiment was repeated using the PAb SpMH40-based RC A described above. These results prove that more than one analyte can be captured and measured with the RC nano-LC TOF MS system, even with an RCA1 based on MAb72F that is an unstable MAb isotype where few binding sites remained active after immobilization.

Nanoscale Affinity Chip Interface for Coupling SPR with nano-LC TOF MS

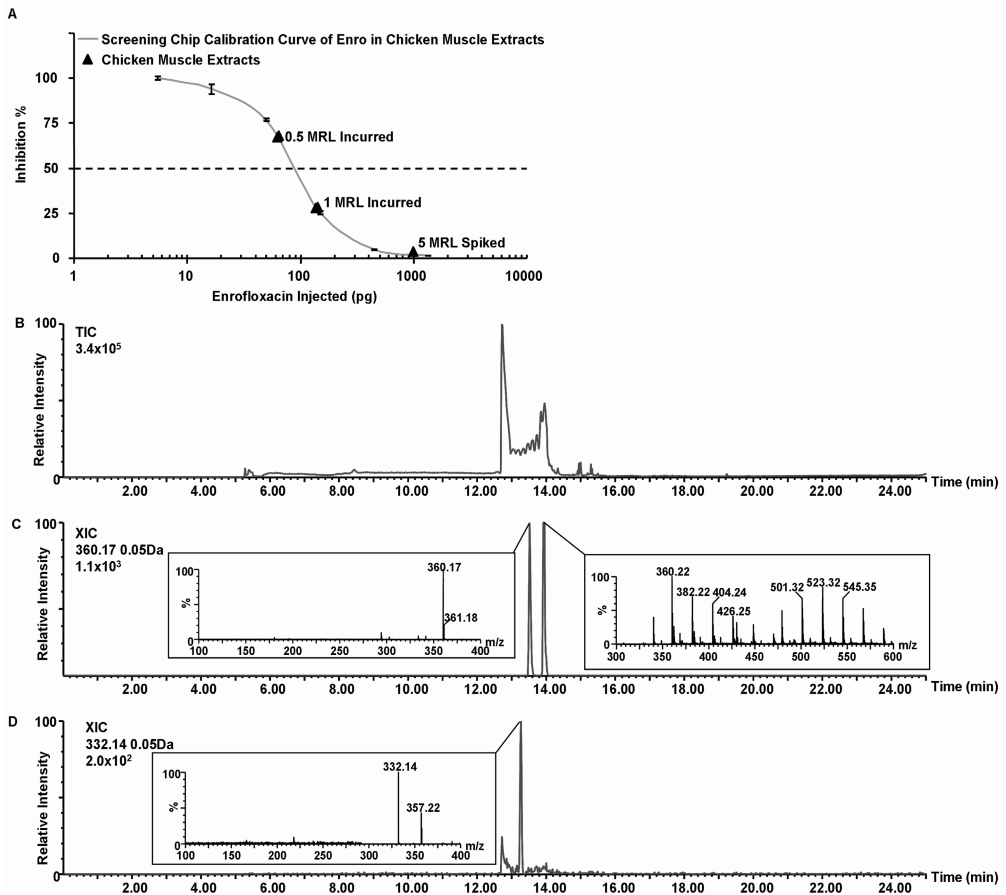


Figure 4. (A) iBIA calibration curve obtained with chicken muscle extract spiked with Enro using SC A. Black triangles show the muscle extract samples from chicken samples either incurred or spiked with Enro. Following the iBIA screening, 40 μL of muscle extract was reinjected into the RC A for affinity extraction and the eluate is used for nano-LC TOF MS analysis. (B-D) Chromatograms and mass spectra (see insets) of relevant peaks of an RC A eluate obtained from muscle extract incurred with Enro at 1 MRL (5 $\text{pg } \mu\text{L}^{-1}$ in the extract). (B) TIC and (C) XIC (0.05 Da mass window) of Enro (360.17). The second peak corresponds to a buffer interference (360.22) also present in the blank. (D) XIC (0.05 Da mass window) of Cipro (332.14), a Enro metabolite.

Screening, Recovery and Identification of Enro in Chicken Samples

The applicability of this iBIA for the screening of Enro in chicken muscle extracts was further evaluated by measuring a calibration curve of Enro in chicken muscle extracts diluted (1:1; v/v) in HBS-EP buffer (Figure 4 A). Similar sensitivity (Enro $IC_{50} = 2.4 \text{ pg } \mu\text{L}^{-1}$) was obtained compared to the calibration curve in buffer (Figure 2A), and no nonspecific binding of the sample matrix to the SC surface was observed.

Extracts of chicken samples incurred or spiked with Enro at regulatory-relevant levels (maximum residue level (MRL) $100 \text{ } \mu\text{g kg}^{-1}$ for the sum of Enro and Cipro) were measured with the iBIA in conjunction with SC A. Although, due to dilution during the extraction procedure of the chicken muscle samples, the concentration of the sample extract is lowered 20 times, all the chicken muscle extracts (at 0.5, 1 and 5 MRL) could be measured with the iBIA. These samples were considered as suspected noncompliant and were reinjected into the SPU containing RC A for analyte capture and further analyzed with nano-LC TOF MS. Figure 4, parts B and C, shows the total ion current (TIC) and extracted ion current (XIC) chromatogram obtained during the analysis of the incurred chicken sample at 1 MRL. The mass spectra of some peaks between 12.6 and 14.2 min (see second inset in Figures 3B and 4B), display peaks separated by 44 and 22 Da. These correspond to single- and double-charged ethylene oxide residues of the polyethylene glycol used as surfactant in the HBS-EP buffer used to dilute the extracts, suggesting that the washing steps implemented after the injection of the sample through the RC surface were not sufficient to completely remove the surfactant. Surfactant removal from the buffer would invariably increase nonspecific binding issues. However, ongoing efforts will further optimize the buffer conditions. Nevertheless, even with these surfactant interferences, the XIC chromatogram clearly displays a peak corresponding to the mass of the $[M+H]^+$ ion of Enro (360.17) at 13.4 min. The second peak at 14 min corresponds to the elution of one of the surfactant isomers having a similar m/z (360.22). We considered the possibility that Cipro might be captured in this sample using RC A with PAb SpMH40. The XIC chromatogram in Figure 4D shows a peak with a mass that corresponds to the $[M+H]^+$ ion of Cipro (332.14) that elutes shortly (13.3 min) before Enro. This finding implies that Cipro, an Enro metabolite, is present at a low concentration in the incurred chicken muscle sample. This result was independently confirmed by an

LC/MS/MS confirmatory analysis method (data not shown). These results strongly suggest the potential use of the serial SPR RC nano-LC TOF MS coupling concept for the identification of biologically relevant, but yet unknown, analytes in the samples. Optimization of the buffer surfactant interferences and the use of accurate masses will allow an untargeted analysis of relevant peaks, facilitated by the biosorbent featured on the RC that provides a selective cleanup, greatly reducing the number of irrelevant peaks in the mass spectra and minimizing ion suppression.

Triple-Chip Feasibility

The common drawbacks of the classical capillary nano-LC setup described above are nano-ESI spray positioning, blocking of capillaries, dead volumes, etc.

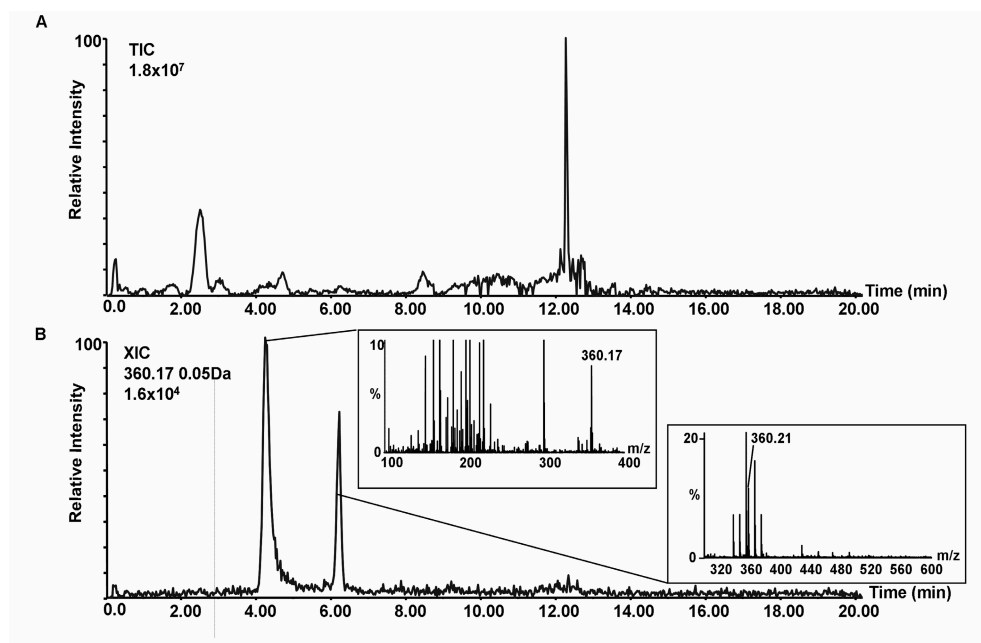


Figure 5. Triple-chip system. Chromatograms and mass spectra (see insets) of an RC A eluate obtained from the injection of 10 μL of muscle extract from chicken incurred with 0.5 MRL level of Enro ($2.5 \mu\text{g} \mu\text{L}^{-1}$ in the extract) and analyzed of-line by chip-LC TOF MS. (A) TIC and (B) XIC (0.05 Da mass window) of Enro (360.17). The second peak in B corresponds to a buffer interference (360.21) also present in the blank.

Due to these issues, specific skills of the operator are required for troubleshooting. Recently a microfluidic nano-LC chip TOF MS system was introduced which overcomes these traditional nano-LC limitations [21]. We briefly evaluated the feasibility of introducing such a third chip into the system aiming for a more robust overall setup.

Chicken muscle samples spiked and incurred with Enro at levels as low as 0.5 MRL were injected over the RC A, and the eluates were analyzed (off-Line) with the chip LC TOF MS system as described in the Experimental Section. As a typical example, Figure 5 shows the TIC (Figure 5A) and XIC (Figure 5B) of the SpMH40 RC eluate from a chicken muscle sample incurred with Enro at 0.5 MRL. The XIC clearly displays two peaks, the first one ($R_t = 4.3$ min) corresponding to the $[M+H]^+$ ion of Enro (m/z 360.1723), and the second one of lower intensity corresponding to the buffer impurity discussed above. The high mass accuracy of TOFMS allowed elemental composition calculation of the analyte of interest. Within the restrictions of $m/z \pm 5$ mDa, ring plus double bond equivalent number 5-20, atoms $C_{0-30}H_{0-40}N_{0-5}F_{0-5}$ nine elemental composition options remain, $C_{19}H_{23}N_3O_3F$ being on top of the list having the smallest difference between the theoretical and experimentally determined accurate mass. Subsequent data mining for $C_{19}H_{22}N_3O_3F$ using the comprehensive SciFinder database confirmed the presence of Enro in the incurred sample. Such a robust chip format nano-LC ESI system would be probably the only realistic option for routine food analysis laboratories. It should be emphasized that no theoretical limitation would limit the integration of the RC and the nano-LC ESI chip.

Conclusions

A new concept for coupling an iBIA screening of low molecular weight analytes with nano-LC ESI TOF MS for confirmation of identity using an affinity chip interface has been presented. The interface features the unique advantage of allowing an in depth characterization of the biosorbent and its interaction with the analyte and sample matrix components. This interface provides a highly selective sample cleanup which greatly reduces the number of irrelevant peaks in the subsequent nano-LC TOF MS analysis. For the application selected, the optimal hydrogel thickness for the RC interface was 100-200 nM. With this RC the interfaced system was able to detect our model analyte in noncompliant samples below the regulatory limits during the screening in incurred chicken muscle samples. Reinjection of relevant samples in the affinity chip interface provided a good recovery and a concentration step of the analyte to be identified in the nano-LC MS analysis, even with a minor biosorbent crossreactivity for a bioactive metabolite of Enro present in the non-compliant sample. The metabolite was captured in the RC at a suitable level for nano-LC TOF MS analysis.

This is a promising outcome that shows the potential of designing multianalyte affinity chips for multianalyte inhibition BIAs followed by multi analyte recovery. Finally, a more robust triple chip approach seems feasible. The concept presented can be easily extended to other applications requiring both a fast bioactivity-based screening and accurate mass assessment with subsequent elemental composition calculation, for example in the fields of natural toxin analysis and security applications.

Acknowledgments

This project is part of the EU-project "New technologies to screen multiple chemical contaminants in foods (acronym BioCop)" and is financially supported by the European Commission, contract FOOD-CT-2004-06988 and the Dutch Ministry of Agriculture, Nature and Food Quality. We are also thankful to Dr. Shaun Bilsborough from Agilent Technologies for his support with the evaluation of the nano-LC chip TOF MS system.

Supporting Information

Experimental details about the preparation of PAb MH40 antiserum and the preparation of the specific fraction of PAb MH40 antiserum necessary to produce the recovery chip (RC) are described in this section. In addition, we present details relevant to the Nano-LC Equipment setup and some considerations about the RC hydrogel immobilization capacity.

Preparation of PAb MH40 Antiserum

The polyclonal antiserum was raised in a rabbit against an Enro-keyhole limpet hemocyanin (KLH) conjugate. The immunization was performed at the Laboratory of Hormonology (Marloie, Belgium) according to their standard protocol. The sera obtained were stored at -80°C until further use.

Preparation of the PAb MH40 Antiserum Specific Fraction

The total IgG fraction (2 mL) from 20 mL of raw antiserum (PAbMH40) was obtained using a protein G column (1 mL) according to the manufacturer's instructions. The specific anti-Enro IgG fraction (SpMH40) was isolated from this total IgG fraction using an Enro-sepharose column (1.25 mL). Enro was coupled to CNBr-activated Sepharose™ 4B using ethylene diamine as a bifunctional spacer. After loading the total IgG (diluted 10 times in PBS) at a flow rate of 1 mL min^{-1} , the chromatography continued using two mobile phases consisting of (A) PBS buffer (pH 7.4) and (B) 1% formic acid (pH 2). The SpMH40 fraction was eluted with a gradient starting at 0% B isocratically for 5 min, followed by a linear increase to 100% B in 2 min and then step-wise to 0% B and conditioning for 5 min. This affinity chromatography was repeated with the pooled effluent until total depletion of SpMH40. The SpMH40 eluates were pooled, buffer exchanged to PBS and concentrated to 1 mg mL^{-1} (total end volume was 0.5 mL) using a 50 kDa Amicon cutoff filter and stored at $-20\text{ }^{\circ}\text{C}$ until use.

Nano-LC Equipment Details

The pump flow during the gradient was steadily increased to $375\text{ }\mu\text{L min}^{-1}$ and 20% of solvent B until 5.5 min, linearly increased to flow $400\text{ }\mu\text{L min}^{-1}$ and 25% of B at 9 min, to flow $600\text{ }\mu\text{L min}^{-1}$ and 70% of at 12

min, decreased to flow $500 \mu\text{L min}^{-1}$ and 30% B at 14 min, to flow $550 \mu\text{L min}^{-1}$ and 0% B at 18 min, then isocratically until 24.5 min for preconditioning and finally to flow $10 \mu\text{L min}^{-1}$ at 25 min. Thus the split flow in the nano LC column was on average in the order of 300 nL min^{-1} . The Nano ESI probe was operated in the positive ion mode, source temperature $90 \text{ }^\circ\text{C}$, a cone and capillary voltage of 30 V and 2.8 kV respectively. Data were acquired in the continuum mode from 100 to 1200 Da with a scan time of 0.44 s at a resolution of 5000 (fwhm) and processed using Masslynx v. 4.0 software.

The polyimide coated fused silica capillaries were obtained from Polymicro (Phoenix, Arizona, USA). Tubing connections were made with Micro Tight® fittings, unions, tees and sleeves were provided by Upchurch (Oak Harbor, Washington, USA). Two six ports-two position valves were used. One with a manual actuator for the loop type interface fitted with a PEEK $10 \mu\text{L}$ loop, provided by VICI AG International (Schenkon, Switzerland) and a Lab Pro (PR-700-100-01) with an electric actuator obtained from Rheodyne (California, USA). The nano LC columns were provided by Nano Separations (Nieuwkoop, The Netherlands).

Considerations About the RC Hydrogel Immobilization Capacity

Considering that the dextran hydrogel layer contains flexible polymer chains of nonuniform length between 100 to 200 nm long [23], the hydrogel volume in the RC flow cell would be $1.9 \times 10^{15} - 3.8 \times 10^{15} \text{ nm}^3$. Hence, the estimated number of SpMH40 IgG molecules immobilized on on the 16 mm^2 of RC A would be 1.2×10^{12} , or one IgG molecule per 1500 - 3000 nm^3 of dextran. Assuming an ideal cubical and homogeneous distribution, the average distance between every two IgG molecules would be 12 -15 nm. As a reference, the IgG dimensions are 10 nm long, 7 nm wide and 2 nm thick, therefore suggesting a densely packed biosorbent. In consequence, future efforts to increase the capture capacity of the RC should focus on increasing the hydrogel volume and on the antibody immobilization chemistry.

References

1. Malmqvist M (1993) Biospecific interaction analysis using biosensor technology *Nature* 361, 186
2. Rich RL, Myszka DG (2006) Survey of the year 2005 commercial optical biosensor literature *J. Mol. Recognit.* 19, 478-534
3. Rich RL, Hoth LR, Geoghegan KF, Brown TA, LeMotte PK, Simons SP, Hensley P, Myszka DG (2002) Kinetic analysis of estrogen receptor/ligand interactions *Proc. Natl. Acad. Sci.* 99, 8562-67
4. Haasnoot W, Loomans EEMG, Cazemier G, Dietrich R, Verheijen R, Bergwerff AA, Stephany RW (2002) Direct Versus Competitive Biosensor Immunoassays for the Detection of (Dihydro)Streptomycin Residues in Milk *Food Agric. Immunol.* 14, 15
5. Haasnoot W, Verheijen R (2001) A Direct (Non-Competitive) Immunoassay for Gentamicin Residues with an Optical Biosensor *Food Agric. Immunol.* 13, 131
6. Haasnoot W, Bienenmann-Ploum M, Kohen F (2003) Biosensor immunoassay for the detection of eight sulfonamides in chicken serum *Anal. Chim. Acta* 483, 171
7. Nedelkov D, Nelson RW (2003) Surface plasmon resonance mass spectrometry: recent progress and outlooks *Trends Biotechnol.* 21, 301
8. Nedelkov D (2007) Development of Surface Plasmon Resonance Mass Spectrometry Array Platform *Anal. Chem.*
9. Nelson RW, Krone JR, Jansson O (1997) Surface Plasmon Resonance Biomolecular Interaction Analysis Mass Spectrometry. 1. Chip-Based Analysis *Anal. Chem.* 69, 4363-68
10. Gilligan JJ, Schuck P, Yergey AL (2002) Mass Spectrometry after Capture and Small-Volume Elution of Analyte from a Surface Plasmon Resonance Biosensor *Anal. Chem.* 74, 2041-47
11. Nedelkov D, Nelson RW (2001) Analysis of native proteins from biological fluids by biomolecular interaction analysis mass spectrometry (BIA/MS): exploring the limit of detection, identification of non-specific binding and detection of multi-protein complexes *Biosens. Bioelectron.* 16, 1071

12. Borch J, Roepstorff P (2004) Screening for Enzyme Inhibitors by Surface Plasmon Resonance Combined with Mass Spectrometry *Anal. Chem.* 76, 5243-48
13. Lopez F, Pichereaux C, Burlet-Schiltz O, Pradayrol L, Monsarrat B, Esteve JP (2003) Improved sensitivity of biomolecular interaction analysis mass spectrometry for the identification of interacting molecules *Proteomics* 3, 402-12
14. Zhukov A, Schurenberg M, Jansson O, Areskoug D, Buijs J (2004) Integration of Surface Plasmon Resonance with Mass Spectrometry: Automated Ligand Fishing and Sample Preparation for MALDI MS Using a Biacore 3000 Biosensor *J. Biomol. Tech.* 15, 112-19
15. Grote J, Dankbar N, Gedig E, Koenig S (2005) Surface Plasmon Resonance/Mass Spectrometry Interface *Anal. Chem.* 77, 1157-62
16. Bouffartigues E, Leh H, Anger-Leroy M, Rimsky S, Buckle M (2007) Rapid coupling of Surface Plasmon Resonance (SPR and SPRI) and ProteinChipTM based mass spectrometry for the identification of proteins in nucleoprotein interactions *Nucl. Acids Res.* 35, 1-10
17. Font MP, Cubizolles M, Dombret H, Cazes L, Brenac V, Sigaux F, Buckle M (2004) Repression of transcription at the human T-cell receptor V[β]2.2 segment is mediated by a MAX/MAD/mSin3 complex acting as a scaffold for HDAC activity *Biochem. Biophys. Res. Commun.* 325, 1021
18. Marchesini GR, Haasnoot W, Delahaut P, Gercek H, Nielen MWF (2007) Dual biosensor immunoassay-directed identification of fluoroquinolones in chicken muscle by liquid chromatography electrospray time-of-flight mass spectrometry *Anal. Chim. Acta* 586, 259
19. EEC (1996) Council Directive 96/23/EC on measures to monitor certain substances and residues thereof in live animals and animal products and repealing Directives 85/358/EEC and 86/469/EEC and Decisions 89/187/EEC and 91/664/EEC *Off. J. Europ. Comm.* L125, 10-31
20. Meiring HD, van der Heeft E, ten Hove GJ, de JongA PJM (2002) Nanoscale LC-MS(n): technical design and applications to peptide and protein analysis *J. Sep. Sci.* 25, 557-68
21. Yin H, Killeen K, Brennen R, Sobek D, Werlich M, vandeGoor T (2005) Microfluidic Chip for Peptide Analysis with an Integrated HPLC Column, Sample Enrichment Column, and Nanoelectrospray Tip *Anal. Chem.* 77, 527-33

22. Pikkermaat MG, Elferink JAW, Mulder PPJ, de Cocq A, Nielen MWF, Egmond HJ (2007) An improved microbial screening assay for the detection of quinolone residues in egg and poultry muscle *Food Addit. Contam.* 24, 842-50
23. Stenberg E, Persson B, Roos H, Urbaniczky C (1991) Quantitative determination of surface concentration of protein with surface plasmon resonance using radiolabeled proteins *J. Colloid Interface Sci.* 143, 513
24. Howell S, Kenmore M, Kirkland M, Badley RA (1998) High-density immobilization of an antibody fragment to a carboxymethylated dextran-linked biosensor surface *J. Mol. Recognit.* 11, 200-3
25. Davis TM, Wilson WD (2000) Determination of the Refractive Index Increments of Small Molecules for Correction of Surface Plasmon Resonance Data *Anal. Biochem.* 284, 348
26. Svitel J, Boukari H, Van Ryk D, Willson RC, Schuck P (2007) Probing the Functional Heterogeneity of Surface Binding Sites by Analysis of Experimental Binding Traces and the Effect of Mass Transport Limitation *Biophys. J.* 92, 1742-58
27. Zacher T, Wischerhoff E (2002) Real-Time Two-Wavelength Surface Plasmon Resonance as a Tool for the Vertical Resolution of Binding Processes in Biosensing Hydrogels *Langmuir* 18, 1748-59
28. Myszka DG, He X, Dembo M, Morton TA, Goldstein B (1998) Extending the Range of Rate Constants Available from BIACORE: Interpreting Mass Transport-Influenced Binding Data *Biophys. J.* 75, 583-94
29. Myszka DG, Morton TA (1998) CLAMP: a biosensor kinetic data analysis program *Trends Biochem. Sci.* 23, 149-50

Part IV: Summary, Conclusions and Future Perspectives



Chapter 8

Summary, Conclusions and Future Perspectives

Summary

The term bioactive contaminant refers to chemicals introduced in to a given system at levels above a certain frame of reference causing adverse effects to living matter due to their inherent biological activity. Bioactive contaminants are ubiquitous in the environment and in food, nevertheless, they can have very different origins. Those from industrial sources may enter the food chain through the environment or from their use in household products. Chemicals used for pharmacological purposes may, on the other hand, enter the food chain as drug residues in treated livestock or through contaminated drinking water. Screening the environment and food for the presence of multiple bioactive contaminants simultaneously and in a short time, whilst obtaining data about their biological potency, is a challenge. If, confirmation of the identity of these bioactive chemicals is required, the challenge grows exponentially.

The general introduction presented in **chapter one** of this thesis puts in perspective the importance of the bioactive contaminants studied as well as the background of screening methods within the greater context of analytical chemistry. Some historic and basic concepts of biosensors are described with a special emphasis on optical biosensors, specifically those SPR-based biosensors considered in this thesis. Background and challenges concerning the different strategies for interfacing biosensors with mass spectrometric identification is included at the end of the introduction.

Part I deals with the development of various biosensor screening assays for bioactive contaminants.

The first biosensor screening assay developed was against the ubiquitous estrogenic compound Bisphenol A (BPA) and is described in **chapter two**. Several polyclonal and monoclonal antibodies were characterized as biorecognition elements. The monoclonal antibody showing the best kinetic parameters was selected and tested using direct and indirect (inhibition) assay formats. Although the direct assay was the most sensitive, the inhibition assay was the most robust. Using the latter in combination with solid phase extraction (SPE) allowed the determination of BPA in tap water at the ppt (ng L^{-1}) level.

Even though antibody-based screening assays were sensitive and robust, they were very specific and provided no clue of the total biological potency when a mixture of bioactive contaminants is measured in a complex sample. In consequence, an alternative

biorecognition element was sought in **chapter three**. Two human thyroxine (T4) transport proteins; T4 binding globulin (TBG) and transthyretin (TTR), were selected as biologically relevant biorecognition elements to screen for compounds with T4-like activity. An inhibition assay was developed by immobilizing T4 with a spacer to the biosensor chip surface. The use of recombinant TTR was validated by measuring the equilibrium dissociation constants of both binding sites for T4 with the biosensor. The application was further evaluated by analyzing a small library of nine known bioactive chemicals and comparing their relative potencies to T4 using both recombinant and purified TTR. Both T4 transport proteins provided suitable biosensor assays with a higher sensitivity and shorter analysis time than radioligand binding assays using comparable biorecognition elements.

Further optimization of the assay conditions, as described in **chapter four**, provided the correct working conditions for long unattended operation of the biosensor assays. The robustness and short analysis time were suitable for high throughput screening of the relative potencies of a sixty two chemicals library. This library included important bioactive contaminants like polychlorinated bisphenyls (PCBs), polybrominated diphenyl ethers (PBDEs), their hydroxylated metabolites, bisphenol A and its halogenated congeners, pharmaceuticals and other environmentally relevant compounds. Ten new bioactive compounds were identified to bind to TBG with a high affinity and were also confirmed to bind to TTR. Strikingly these bioactive compounds were hydroxylated metabolites of PBDEs (BDE 47, 49, 99) and polyhalogenated biphenyls, usually present in human blood. Suggesting that these hydroxylated metabolites of halogenated diphenyl ethers not only are disrupting T4 transport at the transthyretin level, but also at the T4 binding globulin level, responsible for most of the T4 transport. The toxicological relevance of these findings remains to be determined, nevertheless this biosensor technology proved very applicable and promising for toxicological research.

The drawbacks of the technology used in **part I** concern the high cost the of the SPR systems and the lack of portability. Therefore, **part II** deals with the implementation of the assays previously developed in **part I** to evaluate a similar SPR technology having a low-cost instrumentation and potential portability. In **chapter five**, a miniature Spreeta SPR sensor was combined with a simple fluidic system and adapted to function with commercial biosensor chips. The assays were quickly implemented in this low-cost prototype system with a comparable sensitivity to the commercial systems used in **part I**.

The fast, online and (potentially) bioeffect related information provided by the biosensor technology can be synergistically coupled with traditional analytical techniques such as liquid chromatography (LC) and mass spectrometry (MS). These hyphenated techniques are able to separate the analytes based on their physico-chemical properties and unequivocal structural information can be obtained using MS. Such a coupling would be applicable for the discovery of unknown bioactive compounds interacting with the biorecognition element in complex samples. Additionally, the confirmation of identity of known analytes, regulated by law could be achieved in a short time because all the analytical efforts are focused only on samples pinpointed during the screening as suspected non-compliance.

The main challenge of such hyphenation is to find a suitable strategy for coupling inhibition biosensor assays with MS. Consequently, **part III** of this thesis deals with the strategies investigated for interfacing SPR inhibition biosensor assays with mass spectrometric detection. Fluoroquinolone antibiotics were selected as model analytes because the monitoring of these antibiotics are regulated by law because they are widely used for the treatment of bacterial infections in farm animals.

In **chapter six**, a parallel interfacing strategy is presented. The feasibility of this strategy was proven by coupling the simultaneous screening of six fluoroquinolones using a dual SPR biosensor immunoassay with ultra high resolution LC- electrospray ionization (ESI) Time-of-Flight (ToF) Mass Spectrometry (MS) for their identification.

The dual SPR biosensor immunoassays enabled the screening of norfloxacin, ciprofloxacin, enrofloxacin, difloxacin, sarafloxacin and flumequine at, or below, their maximum residue levels in chicken muscle. The biorecognition elements used in these assays were polyclonal antibodies, a specific antibody against flumequine and a generic antibody recognizing the other five structurally related fluoroquinolones.

Samples considered noncompliant during the biosensor screening were concentrated using solid phase extraction and fractionated with gradient LC. The effluent was split and fractionated in two identical 96-well plates. One was re-screened with the biosensor to identify the immunoactive fractions and directed the identification efforts with high resolution LC-ESI-ToF-MS only toward the relevant fractions in the second well-plate. The system could screen and identify known fluoroquinolones and also discover unknown chemicals of similar structure cross-reacting with the antibodies used as biorecognition elements in the biosensor assays.

The main limitations of such an interfacing strategy were; the requirement of a relatively large sample volume, the extensive sample handling required, which increased the chances of sample contamination, and the limited fractionation resolution.

As a result and considering these limitations, an online strategy physically coupling the systems was studied in **chapter seven**. The biosensor and a nano-LC- ESI ToF MS systems were coupled through a reusable affinity capture interface (recovery chip).

The full procedure has four main stages. First, the samples are prepared. Second, the samples are screened using a screening chip with the inhibition biosensor immunoassay. Third, only those samples suspected of being noncompliant are reinjected over the recovery chip, and the analyte is captured at subnanogram level. Fourth, the analyte is released from the recovery chip into a loop-type interface and analyzed with nano-LC- ESI ToF MS system.

The screening chip and the recovery chip both featured a similar hydrogel where mirror chemistries were immobilized. On the screening chip, the analyte was immobilized to implement the inhibition assay and on the recovery chip the complementary biorecognition elements were immobilized (affinity-purified polyclonal antibodies). The recovery chip operated as an immuno affinity column. The main differences were, first that the nanoscale biosorbent is immobilized in one of the walls of a flow cell. Second, the interaction of the biosorbent with the analyte and sample matrix were rapidly characterized using the biosensor. This advantage was particularly useful for optimizing the elution conditions and assessing the biosorbent robustness without engaging the complete hyphenated system.

The strategy was tested for screening the fluoroquinolone antibiotic enrofloxacin in incurred chicken muscle samples as a model compound and matrix. Using the online strategy, we were able to detect and confirm the identity of enrofloxacin in noncompliant samples below the regulatory limits. A known metabolite of enrofloxacin, ciprofloxacin, was identified in incurred chicken samples. This demonstrated the potential of the online interfacing strategy for the rapid screening and identification of known as well as unknown compounds with an affinity for the biorecognition element.

Additional advantages of interfacing with the recovery chip were a highly selective sample cleanup, a good recovery and concentration step.

Finally, the feasibility of combining the biosensor with a robust chip-based nano-LC- ESI ToF MS was tested offline and provided a robust alternative triple-chip system.

Conclusions and Future Perspectives

The main goals in this thesis were three-fold. First, to develop screening assays for bioactive industrial contaminants with hormonal activity using SPR-based biosensor technology and various biorecognition elements. Second, to study the feasibility of implementing screening assays for bioactive industrial contaminants in a lower cost and potentially portable SPR biosensor system. Third and final, to evaluate different interfacing strategies for the hyphenation of inhibition assays in a SPR biosensor with liquid chromatography-mass spectrometry for the confirmation of analyte identity using bioactive pharmaceuticals as model analytes.

In **part one** of this thesis three SPR biosensor inhibition assays were successfully developed and applied for the screening of bioactive industrial contaminants. A specific inhibition biosensor immunoassay (iBIA) was developed in **chapter two** for the ubiquitous estrogenic contaminant BPA. For a generic and bioeffect related screening, two inhibition biosensor T4 transport protein assays for contaminants with T4 transport disruption potential were developed in **chapter three**.

In **part III**, previously developed iBIAs against fluoroquinolone pharmaceutical contaminants were quickly implemented with some modifications.

Although using the direct assay format was evaluated, in general it was not suitable for the screening of bioactive contaminants due to the inherently low signals generated by these analytes of low molecular weight. Nevertheless, the kinetic parameters of the biorecognition element-analyte interactions obtained in the direct assay format were useful for predicting assay sensitivity and characterizing the immobilized or captured biorecognition elements.

The inhibition biosensor assays were robust due to the high responses generated by the binding of the high molecular weight biorecognition elements and due to the extreme resistance of the sensor chip with a low molecular weight molecule immobilized which could resist over 1500 measurements. Above 400 unattended measurements could be made in a single experiment if the reagents were premixed manually. The throughput of the inhibition biosensor assays was as high as 6 min per sample if the reagents were premixed manually, 8-10 min if the reagents were mixed by the biosensor and 15 min if combined with solid phase extraction.

The inhibition biosensor immunoassays (iBIAs) could be easily multiplexed as shown in **chapter six** where a specific iBIA was combined with a group-generic iBIA detecting six different fluoroquinolones in a single measurement of 8.5 min.

Further throughput improvement can be obtained with currently commercially available SPR biosensor systems with higher multiplexing and parallelization capabilities.

In the near future, imaging SPR in a microarray-type of format seems to be best suited for such purposes in combination with advanced microfluidic systems.

The iBIA for BPA performed very good for measuring surface water samples with a minimum sample cleanup, showing the potential of this technology to rapidly screen environmental water samples. If concentrations of the analyte in the order of low ng L⁻¹ need to be detected, the inhibition biosensor assays can be combined with solid phase extraction for sample concentration as shown in **chapter two**.

Both inhibition biosensor T4 transport protein assays developed in **chapter three** were optimized and applied in **chapter four** to screen a library of chemicals. It was shown that both human purified and recombinant TTR can be used as robust biorecognition elements in inhibition biosensor assays. If compared with radioligand assays previously used [1, 2], the inhibition biosensor T4 transport protein assays provide comparable results at a much higher throughput and sensitivity. Thus, showing the potential of SPR biosensor technology for in-vitro toxicological research. As a matter of fact in **chapter four**, several hydroxylated metabolites of polyhalogenated diphenyl ethers and biphenyls were discovered to bind with strong affinity to TBG, the main T4 transport protein in humans.

Most of the compounds previously tested using the radioligand binding assay and considered strong TTR binders were confirmed with the TTR-based inhibition biosensor assay.

All in all, from the chemicals tested in **chapter four**, the hydroxylated metabolites of the ubiquitous brominated flame retardants polybrominated diphenyl ethers (PBDEs) were the most active compounds toward both T4 transport proteins. The toxicological relevance of these results is of concern given that the human fetus initially has no iodine reserve and depends on the iodine transferred by the mother. Such an avid placental uptake is compensated by the mother during pregnancy with an increased concentration of T4-TBG [3, 4]. TTR, on the other hand, mediates the maternal to fetal T4-transport through the placenta and the delivery of T4 across the blood-brain

barrier. Hence, compounds bound to TTR are transported to the fetal compartment and fetal brain decreasing fetal brain T4 levels [5, 6]. Altogether, these results suggest that the displacement of the T4-TTR and T4-TBG complex by the OH-PBDEs during ontogenesis may have consequences in fetal development.

The inhibition biosensor T4 transport protein assays are valuable tools for the discovery and relative affinity ranking of bioactive chemicals with T4 transport disrupting activity.

Focusing future research in multiplexing or parallelization of these bioeffect related assays with other human transport proteins and receptors for screening, will provide a wealth of information for the toxicological screening of compounds as required for EU regulations of toxic compounds such as REACH [7]. Furthermore, combining these assays with an in-vitro metabolization step will provide more toxicological relevance to the screening of environmental and food samples with potential thyroid activity.

There is a tendency to switch from specific assays to generic or bioeffect related assays for the screening of food, environmental or biological samples. It is the author's opinion that bioeffect-related assays are unlikely to replace specific assays, but on the contrary, they will merge into the same platform and provide highly complementary information. If bioeffect-related assays as those described in this thesis are multiplexed with specific assays such as those based on antibodies against regulated chemicals or those analytes considered of natural origin, the information obtained from the specific assays could provide a very useful frame of reference and become a very valuable complement to the bioeffect-related assays.

Future research should focus in more in understanding the physicochemistry of the hydrogel and how the macromolecules behave in such an environment. A deep understanding of the surface chemistry will also support the development of more challenging applications where matrix interferences are high.

As shown in **part two**, is possible and relatively simple to transfer the inhibition biosensor assays developed in **part one** to a simple and potentially portable SPR biosensor platform. The Spreeta™ -based prototype biosensor system, optimized and tested in **chapter five** had a low cost instrumentation and was combined with commercially available sensor chips. The assays developed in the Biacore 3000 in **chapters two** and **three** were easily implemented with comparable sensitivities. Combining this human biorecognition elements with a fast, simple and

affordable SPR biosensor is a novel approach for the bioeffect-related screening of compounds with endocrine disrupting activity.

Recent developments of systems achieving portability are very promising for on site deployment for the detection of bioactive contaminants [8, 9]. Considerable sensitivity increase of SPR biosensors is necessary to achieve on-site measurement of environmental bioactive contaminants. Such sensitivity increase can be obtained by engineering the biorecognition elements for higher analyte affinity in combination with the ten-fold increase in sensitivity that can be obtained using noble metal nanoparticles [10].

Advances in micro and nano fabrication and the adoption of localized SPR will aid mass production possibilities of the optical and microfluidic parts and provide further reduction of SPR biosensor costs.

The synergy of combining SPR biosensor screening with analytical techniques like LC-MS was explored in **part three** of this thesis. A parallel coupling strategy was explored in **chapter six** where a duplex inhibition biosensor immunoassay for screening six fluoroquinolones was coupled with high resolution LC TOF MS for identification of analyte identity. Known and unknown compounds having affinity for the biorecognition element were identified in chicken muscle samples evidencing the potential of this approach for screening regulated bioactive compounds in food.

The use of antibodies as biorecognition elements in these assays allows for the detection of unknown compounds structurally related to the target analyte. A bioeffect related detection and identification of compounds with biological activity could be achieved in the future if biologically relevant biorecognition molecules are used instead of antibodies.

The dual iBIA screening was compatible with a simple sample preparation and allowed the detection of fluoroquinolones below MRL in a complex matrix like chicken muscle extract.

It was also shown that the identity of potential bioactive contaminants can be detected using the concentration, fractionation and re-screening steps in this parallel strategy.

Further work should be focused on validating this parallel interfacing strategy for the elucidation of unknown immunoactive compounds.

Concerns regarding the extensive sample handling required in the parallel interfacing strategy led to the development of a serial strategy in **chapter seven**. The serial iBIA-MS coupling strategy was achieved

by using a recovery chip interface. This interface had the biorecognition element immobilized on its surface and was able to capture the relevant analyte(s). The analyte(s) was (were) further eluted and analyzed online with nano-LC TOF MS and the recovery chip could be reused.

Advantages of the recovery chip are; a highly selective sample cleanup, in depth characterization of the biosorbent including its interaction with the analyte and sample matrix components.

Using the serial interfacing strategy we were able to detect our model analyte, enrofloxacin and even ciprofloxacin, a bioactive metabolite, in noncompliant samples below the regulatory limits during the screening in incurred chicken muscle samples.

The serial interfacing strategy can be further improved by using a more robust nano-LC ESI on a chip as shown in **chapter seven**.

Ongoing work focuses on multianalyte recovery chips for multi-analyte iBIAs for screening, identifying and potentially discovering natural toxins.

In conclusion, the results presented in this thesis demonstrate various aspects of the SPR biosensor technology applied to the screening of bioactive contaminants of small molecular weight. First, versatility for developing screening assays using either antibodies or human transport proteins. Second, the feasibility of transferring these assays to other low-cost and potentially portable SPR biosensor platforms. Third, the hyphenation potential. i.e. with SPE, with (high resolution or nano-) LC and MS.

The SPR biosensor screening-MS interfacing concepts presented can be easily extended to other applications requiring both, a fast bioactivity-based screening and accurate mass assessment.

Such hyphenated systems would be of interest not only for national inspection laboratories in the fields of food analysis, forensics and biosecurity, but also for drug discovery and toxicology research.

MS technology is becoming a standard instrument in most laboratories and a must in bioanalytical laboratories. The cost-effectiveness of SPR biosensor screening and MS coupling will very likely grow for most laboratories together with the increase of labour costs and the decrease in the cost of SPR biosensor technology.

References

1. van den Berg KJ (1990) Interaction of chlorinated phenols with thyroxine binding sites of human transthyretin, albumin and thyroid binding globulin *Chem.-Biol. Interact.* 76, 63-75
2. Lans MC, Klasson-Wehler E, Willemsen M, Meussen E, Safe S, Brouwer A (1993) Structure-dependent, competitive interaction of hydroxy-polychlorobiphenyls, -dibenzo-p-dioxins and -dibenzofurans with human transthyretin *Chem.-Biol. Interact.* 88, 7-21
3. Schussler GC (2000) The thyroxine-binding proteins *Thyroid* 10, 141
4. Andrea TA, Cavalieri RR, Goldfine ID, Jorgensen EC (1980) Binding of thyroid hormones and analogues to the human plasma protein prealbumin *Biochemistry* 19, 55-63
5. Elst JPS-VD, Van Der Heide D, Rokos H, De Escobar GM, Kohrle J (1998) Synthetic flavonoids cross the placenta in the rat and are found in fetal brain *Am. J. Physiol. Endocrinol. Metab.* 274, E253-56
6. Meerts IATM, Assink Y, Cenijn PH, van den Berg JHJ, Weijers BM, Bergman A, Koeman JH, Brouwer A (2002) Placental Transfer of a Hydroxylated Polychlorinated Biphenyl and Effects on Fetal and Maternal Thyroid Hormone Homeostasis in the Rat *Toxicol. Sci.* 68, 361-71
7. EEC (2006) Regulation (EC) No 1907/2006 of the European Parliament and of the Council of 18 December 2006 concerning the Registration, Evaluation, Authorisation and Restriction of Chemicals (REACH). *OJEC L* 396, 1-849
8. Chinowsky TM, Soelberg SD, Baker P, Swanson NR, Kauffman P, Mactutis A, Grow MS, Atmar R, Yee SS, Furlong CE (2007) Portable 24-analyte surface plasmon resonance instruments for rapid, versatile biodetection *Biosens. Bioelectron.* 22, 2268-75
9. Fu E, Chinowsky T, Nelson K, Johnston K, Edwards T, Helton K, Grow M, Miller JW, Yager P (2007) SPR imaging-based salivary diagnostics system for the detection of small molecule analytes *Ann. N. Y. Acad. Sci.* 1098, 335-44
10. Hu WP, Chen SJ, Huang KT, Hsu JH, Chen WY, Chang GL, Lai KA (2004) A novel ultrahigh-resolution surface plasmon resonance biosensor with an Au nanocluster-embedded dielectric film *Biosens. Bioelectron.* 19, 1465-71

Biosensoren voor Bioactieve Contaminanten

Test Ontwikkeling en Koppeling met Massaspectrometrie

Samenvatting

De term bioactieve verontreinigingen verwijst naar chemicaliën die in een bepaald systeem worden ingebracht in concentraties boven een bepaald referentiekader waarbij negatieve effecten worden uitgeoefend op levend materiaal als gevolg van hun inherente biologische activiteit. Bioactieve verontreinigingen komen overal in het milieu en in voedsel voor, maar ze kunnen van een zeer verschillende oorsprong zijn. Die uit industriële bronnen kunnen de voedselketen binnenkomen via het milieu of als gevolg van hun gebruik in huishoudproducten. Aan de andere kant kunnen chemicaliën die gebruikt worden voor farmacologische doeleinden, de voedselketen binnenkomen als geneesmiddelresten in behandeld vee of via verontreinigd drinkwater.

Het tegelijkertijd kunnen screenen van materiaal uit het milieu en voedsel op de aanwezigheid van meerdere bioactieve verontreinigingen in een korte tijd, terwijl ook gegevens worden verkregen over hun biologische potentie, is een uitdaging. Indien bevestiging van de identiteit van deze chemicaliën vereist is, neemt de uitdaging exponentieel toe.

De algemene inleiding die gepresenteerd is in hoofdstuk één van dit proefschrift, plaatst het belang van de onderzochte bioactieve verontreinigingen in perspectief, alsook de achtergrond van de screeningswerkwijzen binnen de grotere context van de analytische chemie. Enkele historische en basale concepten van biosensoren worden beschreven met speciale nadruk op optische biosensoren en dan vooral de op SPR-gebaseerde biosensoren die in dit proefschrift gebruikt worden. Achtergronden en uitdagingen betreffende de verschillende strategieën voor het verbinden van biosensoren met massaspectrometrische identificatie zijn beschreven aan het einde van de inleiding.

Deel I gaat over de ontwikkeling van diverse op biosensoren gebaseerde screeningsmethoden voor bioactieve verontreinigingen.

De als eerste ontwikkelde screeningsmethode was tegen de alom voorkomende estrogene verbinding Bisfenol A (BPA) en wordt

beschreven in hoofdstuk twee. Verscheidene polyklonale en monoklonale antilichamen werden gekarakteriseerd als biologische herkenningselementen. Het monoklonale antilichaam dat de beste kinetische parameters vertoonde, werd geselecteerd en getest met behulp van directe en indirecte (gebaseerd op remming) methoden. Hoewel de directe methode het gevoeligst was, was de indirecte methode het meest robuust. Het gebruik van deze laatste in combinatie met vastefaseëxtractie (SPE) maakt de bepaling van BPA in kraanwater mogelijk in de orde van grootte van ng/liter.

Zelfs al waren de op antilichamen gebaseerde screeningsmethoden gevoelig en robuust, ze waren zeer specifiek en ze verschaften geen uitsluitel over de totale biologische potentie, wanneer een mengsel van bioactieve verontreinigingen wordt gemeten in een complex monster. Dientengevolge werd gezocht naar een alternatief biologisch herkenningselement in hoofdstuk drie. Twee humane thyroxine- (T4) transporteiwitten, T4-bindend globuline (TBG) en transthyretine (TTR) werden geselecteerd als biologisch relevante herkenningselementen om te screenen op verbindingen met T4-achtige activiteit. Er werd een indirecte methode ontwikkeld door T4 met behulp van een spacer te immobiliseren op het biosensorchippoppervlak. Het gebruik van recombinant TTR (rTTR) werd gevalideerd door het meten van de evenwichtsdissoctatieconstanten van beide bindingsplaatsen voor T4 met de biosensor. De toepassing van TTR werd verder geëvalueerd door het analyseren van een kleine bibliotheek van negen bekende bioactieve chemicaliën en het vergelijken van hun relatieve potenties ten opzichte van T4 met behulp van zowel recombinant als uit plasma gezuiverd TTR. Beide T4-transporteiwitten verschaften geschikte biosensorbepalingen met een hogere gevoeligheid en kortere analysetijd dan de op radioliganden gebaseerde methoden, waarin gebruik wordt gemaakt van vergelijkbare biologische herkenningselementen.

Verdere optimalisering van de bepalingomstandigheden, zoals beschreven in hoofdstuk vier, verschaftte de correcte werkomstandigheden voor langdurige en onbemande uitvoeringen van de biosensormethoden. De robuustheid en korte analysetijd waren geschikt voor het met hoge doorloop screenen van de relatieve potenties van een bibliotheek van 62 chemicaliën. Deze bibliotheek omvatte belangrijke bioactieve verontreinigingen zoals gepolychlorineerde bisfenylen (PCB's), gepolybromineerde difenylethers (PBDEs), hun gehydroxyleerde metabolieten, BPA en gehalogeneerde soortgenoten, farmaceutica en andere voor het milieu relevante verbindingen. Er werden tien nieuwe bioactieve verbindingen geïdentificeerd die met hoge affiniteit binden aan TBG en ook werd

bevestigd dat ze binden aan TTR. Opvallend was, dat deze bioactieve verbindingen gehydroxyleerde metabolieten van PBDE's (BDE 47, 49, 99) en bifenylen waren die gewoonlijk aanwezig zijn in menselijk bloed. Dit suggereert dat deze gehydroxyleerde metabolieten van gehalogeneerde difenylethers niet alleen het T4-transport verstoren op het niveau van transthyertine, maar ook op het niveau van het T4-bindend globuline, dat verantwoordelijk is voor het grootste gedeelte van het T4-transport. De toxicologische relevantie van deze bevindingen moet nog bepaald worden, maar niettemin bleek deze biosensortechnologie zeer toepasbaar en veelbelovend voor toxicologisch onderzoek.

Enkele van de nadelen van de in deel I gebruikte technologie hebben betrekking op de hoge kosten van de SPR-systemen en de zeer beperkte mobiliteit. Daarom gaat deel II over de implementatie van de eerder in deel I ontwikkelde methoden in een goedkoop alternatief instrument met grotere mobiliteitsmogelijkheden. In hoofdstuk vijf werd een miniatuur Spreeta SPR-sensor gecombineerd met een eenvoudig vloeistoftransportsysteem en aangepast om te functioneren met commerciële biosensorchips. In dit prototype systeem werden de eerder ontwikkelde methoden snel geïmplementeerd en met een vergelijkbare gevoeligheid.

De snelle, on-line en (potentieel) bio-effectgerelateerde informatie verkregen met de biosensortechnologie kan synergetisch worden gekoppeld met traditionele analytische technieken zoals vloeistofchromatografie (LC) en massaspectrometrie (MS). Met deze geavanceerde technieken kunnen de analieten worden gescheiden op basis van hun fysisch-chemische eigenschappen en eenduidige structurele informatie kan worden verkregen met behulp van MS. Een dergelijke koppeling zou toepasbaar kunnen zijn bij de ontdekking van onbekende bioactieve verbindingen die interageren met het biologisch herkenningselement in complexe monsters. Daarnaast zou de bevestiging van de identiteit van bekende analieten, gereguleerd in de wet, in een korte tijd bereikt kunnen worden, omdat alle analytische inspanningen alleen gefocust hoeven te zijn op monsters die tijdens de screening als verdacht naar voren komen.

De belangrijkste uitdaging van een dergelijke koppeling is om een geschikte strategie te vinden voor het koppelen van indirecte biosensorbepalingen met MS. Derhalve gaat deel III van dit proefschrift over de strategieën die werden onderzocht om op SPR-biosensor

gebaseerde indirecte screeningsmethoden te verbinden met massaspectrometrische detectie. Fluoroquinolonen-antibiotica werden gekozen als modelstoffen, omdat het meten van deze antibiotica in de wet geregeld is en omdat ze wijdverbreid worden gebruikt voor de behandeling van bacteriële infecties in landbouwhuisdieren.

In hoofdstuk zes wordt een parallelle koppelingsstrategie gepresenteerd. De haalbaarheid van deze strategie werd bewezen door het koppelen van een op SPR-biosensor gebaseerde duplex immunoassay, voor het gelijktijdig screenen van zes fluoroquinolonen, met ultra hoge resolutie-LC-electrospray-ionisatie (ESI) Time-of-Flight (ToF) Massaspectrometrie (MS) voor hun identificatie. Met deze duplex biosensorimmunoassay kon gescreend worden op norfloxacin, ciprofloxacin, enrofloxacin, difloxacin, sarafloxacin en flumequine op of onder hun maximale residuconcentratie in spierweefsel van kippen. De in deze bepalingen gebruikte biologische herkenningselementen waren polyklonale antilichamen, een specifiek antilichaam tegen flumequine en een generiek antilichaam tegen de andere vijf structureel gerelateerde fluoroquinolonen.

Monsters die beschouwd werden als verdacht tijdens de biosensorscreening, werden geconcentreerd met behulp van vastefaseextractie en gefractioneerd met gradiënt-LC. Het effluent werd gesplitst en gefractioneerd in twee identieke 96-wells microtiterplaten. De ene werd opnieuw gescreend met de biosensor om de immuunactieve fracties te identificeren en de identificatie-inspanningen met hoge resolutie-LC-ESI-ToF-MS alleen te richten op de relevante fracties in de tweede microtiterplaat. Met het systeem konden bekende fluoroquinolonen worden gescreend en geïdentificeerd en ook onbekende chemicaliën worden ontdekt met vergelijkbare structuur kruisreagerend met de antilichamen die gebruikt werden als biologische herkenningselementen in de biosensorbepalingen.

De belangrijkste beperkingen van een dergelijke koppelingsstrategie waren: de vereiste van een relatief groot monstervolume, de uitgebreide monsteropwerking die vereist was en die de kansen op monsterverontreiniging verhoogde, en de beperkte scheiding in de fractionering.

Deze beperkingen in ogenschouw nemend werd een on-line strategie, waarbij de systemen fysiek gekoppeld werden, onderzocht in hoofdstuk zeven. De biosensor en een nano-LC-ESI-ToF-MS-systeem werden gekoppeld via een herbruikbare op immunoaffiniteit gebaseerde interface (recoverychip).

De volledige werkwijze heeft vier hoofdstadia. Als eerste worden de monsters voorbereid. Als tweede worden de monsters gescreend met behulp van een screeningschip met de biosensorremmingsimmunoassay. Als derde werden alleen de verdachte monsters opnieuw geïnjecteerd over de recoverychip, en de analiet wordt ingevangen op subnanogramniveau. Als vierde wordt de analiet van de recoverychip losgemaakt en via een loop gebracht naar en geanalyseerd met het nano-LC-ESI-ToF-MS-systeem.

De screeningschip en de recoverychip waren beide voorzien van een vergelijkbare hydrogel, waarop verschillende chemicaliën werden geïmmobiliseerd. Op de screeningschip werd de analiet geïmmobiliseerd, om de indirecte bepaling uit te voeren, en op de recoverychip werden de complementaire biologische herkenningselementen geïmmobiliseerd (affiniteitsgezuiverde polyklonale antilichamen). De recoverychip werkte als een immunoaffiniteitskolom. De belangrijkste verschillen waren, ten eerste dat het affiniteitsmateriaal op nanoschaal wordt geïmmobiliseerd aan één van de wanden van een vloeistofstroomcel. Ten tweede dat de interacties van het affiniteitsmateriaal met de analiet en de monstermatrix snel werden gekarakteriseerd met behulp van de biosensor. Dit voordeel was bijzonder bruikbaar voor het optimaliseren van de elutieomstandigheden en het bepalen van de robuustheid van het affiniteitsmateriaal zonder het complete gekoppelde systeem daarbij te hoeven betrekken.

De strategie werd getest voor het screenen van het fluoroquinolon-antibioticum enrofloxacin in verontreinigde kippenspiermonsters als modelverbinding en matrix. Met behulp van de on-line strategie waren we in staat de identiteit van enrofloxacin in verdachte monsters te detecteren en te bevestigen onder de regulatoire grenzen. Een bekende metaboliet van enrofloxacin, ciprofloxacin, werd geïdentificeerd in verontreinigde kippenmonsters. Hiermee werd het potentieel van de on-line koppingsstrategie voor de snelle screening en identificatie van bekende alsook onbekende verbindingen met een affiniteit voor het biologisch herkenningselement aangetoond.

Additionele voordelen van de koppeling met behulp van de recoverychip waren een zeer selectieve opschoning van het monster, een goede recovery en een concentreringsstap.

Tenslotte werd de haalbaarheid van het combineren van de biosensor met een robuuste chipgebaseerde nano-LC-ESI-ToF-MS off-line getest en dit verschaftte een alternatief systeem met drie chips.

Samenvatting

List of Publications

Marchesini GR, Meimaridou A, Haasnoot W, Meulenberg E, Albertus F, Mizuguchi M, Takeuchi M, Irth H, Murk AJ (2008) **Biosensor Discovery of Thyroxine Transport Disrupting Chemicals**. *Tox. and App. Pharm.* In Press.

Marchesini GR, Buijs J, Haasnoot W, Hooijerink D, Jansson O, Nielen MWF (2008) **Nanoscale Affinity Chip Interface for Coupling Inhibition SPR Immunosensor Screening with Nano-LC TOF MS** *Anal. Chem.* 80, 1159-68

Marchesini GR, Haasnoot W, Delahaut P, Gercek H, Nielen MWF (2007) **Dual Biosensor Immunoassay-Directed Identification of Fluoroquinolones in Chicken Muscle by Liquid Chromatography Electro spray Time-Of-Flight Mass Spectrometry** *Anal. Chim. Acta* 586, 259

Marchesini GR, Koopal K, Meulenberg E, Haasnoot W, Irth H (2007) **Spreeta-Based Biosensor Assays for Endocrine Disruptors** *Biosens. Bioelectron.* 22, 1908-15

Haasnoot W, **Marchesini GR**, Koopal K (2006) **Spreeta-Based Biosensor Immunoassays to Detect Fraudulent Adulteration in Milk and Milk Powder** *J. AOAC Int.* 89, 849-55

Marchesini GR, Meulenberg E, Haasnoot W, Mizuguchi M, Irth H (2006) **Biosensor Recognition of Thyroid-Disrupting Chemicals Using Transport Proteins** *Anal. Chem.* 78, 1107-14

Marchesini GR, Meulenberg E, Haasnoot W, Irth H (2005) **Biosensor Immunoassays for the Detection of Bisphenol A** *Anal. Chim. Acta* 528, 37-45

List of Publications

Cannon MJ, Papalia GA, Navratilova I, Fisher RJ, Roberts LR, Worthy KM, Stephen AG, **Marchesini GR**, Collins EJ, Casper D, Qiu H, Satpaev D, Liparoto SF, Rice DA, Gorshkova, II, Darling RJ, Bennett DB, Sekar M, Hommema E, Liang AM, Day ES, Inman J, Karlicek SM, Ullrich SJ, Hodges D, Chu T, Sullivan E, Simpson J, Rafique A, Luginbuhl B, Westin SN, Bynum M, Cachia P, Li YJ, Kao D, Neurauter A, Wong M, Swanson M, Myszka DG (2004) **Comparative Analyses of a Small Molecule/Enzyme Interaction by Multiple Users of Biacore Technology** Anal. Biochem. 330, 98-113

Perez MF, Maglio LE, **Marchesini GR**, Molina JC, Ramirez OA (2002) **Environmental Changes Modify the Expression of Diazepam Withdrawal** Behav. Brain Res. 136, 75-81

Perez MF, Nasif FJ, **Marchesini GR**, Maglio LE, Ramirez OA (2001) **Hippocampus and Locus Coeruleus Activity on Rats Chronically Treated with Diazepam** Pharmacol., Biochem. Behav. 69, 431-8

Curriculum Vitae

Gerardo R. Marchesini was born on May 9th 1978 in Villa Allende, Cordoba, Argentina. After two years in the local technical highschool, Paula Albarracin de Sarmiento, he went to Instituto Saul A Taborda from where he graduated in 1995. Subsequently, in March 1996, he started studying biology at the Universidad Nacional de Cordoba. After following specialization courses in natural products, advanced mathematics, biophysical chemistry, embryology and physiology of the endocrine and nervous system, he chose to finish his studies with a two-year thesis in brain electrophysiology. The main purpose of the research was to correlate behavioral patterns of rats addicted to the drug diazepam with neuronal learning (long term potentiation). Many rats later, in the middle of the riots, strikes and demonstrations due to the socioeconomic meltdown at the end of 2001 he finished his exams. Soon, in March 2002 he graduated with the degree of Biologist with a few PhD position applications sent. In July of the same year he arrived to the Netherlands with an Industry Host Marie Curie Fellowship to initiate PhD studies (which is described in this thesis from chapter 1 to 5). The research was a collaborative effort and was carried out under the supervision of Dr. E. Meulenberg from Elti-Support, Mr. W. Haasnoot from the Rikilt Institute of Food Safety and Prof. Dr. Irth from the Vrije Universiteit Amsterdam. Until July 2005 the project was carried out at Rikilt and aimed at developing methods for the detection and discovery of endocrine disrupting chemicals using human transport proteins. Following this period he started working at Rikilt as a Junior researcher under the supervision of Prof. Dr. Nielen, for the European project Biocop. In this function Gerardo was responsible for developing strategies for coupling biosensor screening with (nano) LC TOF MS for confirmation of drug residues in food (chapters 6 and 7 in this thesis). Currently he still holds this position and is working on setting up a system for the screening and confirmation of marine toxins.

Curriculum Vitae

Acknowledgments

I would like to express my most sincere gratitude to those who supported me to make this thesis possible. First, to the EU funded Marie Curie Foundation (Marie Curie Industry Host Fellowship (Contract EVK1-CT-2001-55002)). Second, to the RIKILT Institute of Food Safety through the Dutch Ministry of Agriculture, Nature and Food Quality and lately the EU-project BioCop ("New technologies to screen multiple chemical contaminants in foods" (contract FOOD-CT-2004-06988)) gave me the opportunity to engage and finish in this PhD.

There were many people behind these contracts to whom I would like to express my most sincere gratitude. To my copromotor, Dr. Eline Meulenberg and her company, who ultimately created an opportunity that enabled me to begin this PhD. To my promotor, Prof. Dr. Irth, for his supervision, guidance and support throughout this years. To my other copromotor, Willem Haasnoot. Willem, thanks for understanding the difficulties of working far from university, for the motivation, helpful discussions, suggestions and for keeping your door always open to hear new ideas, even the wild ones. I am especially grateful to Prof. Dr. Michel Nielen, my second promotor since 2005. For his patience and flexibility, his motivation, expertise and interest in engaging in scientific discussions. Overall, I really appreciate from my four supervisors the freedom, openness and strong sense of self-sufficiency that I have acquired in these years.

I am also grateful with my colleagues from biomolecular detection at RIKILT, Both Moniques , Nathalie, Anniek, Dick and specially Geert Cazemier for his coaching and patience at the beginning.

It is also a pleasure to thank the people in ACAS that were nice hosts during my visits to Amsterdam.

I would also like to thank the students Faywell Albertus and Anastasia Meimaridou who worked very hard on the assays. Prof. Dr. Tinka Murk from Toxicology with whom I had very fruitful discussions and advice.

I also want to thank my newer colleagues and friends, Sabina and Anastasia for the great discussions and lunches we have shared.

A number of people supported me throughout these years in one way or another.

Acknowledgments

My whole family was always there when I needed them with a supportive and empathic word for me at the end of a phone call or a visit. My parents, Osvaldo (bobby) and Silvia (vieja), Ernesto, Paula and Sandra brother and sisters in Cordoba and the Netherlands were an essential companionship these years and all the previous ones...

I would like to express my deepest gratitude to Aldana, my life partner, beloved girlfriend and best friend. For always being there, for your unconditional support and love. Together, we have enjoyed and endured the experience of living abroad; growing together these years has been fantastic.

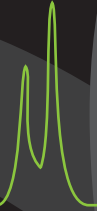
Adele, my Dutch Tante in Amsterdam, always knew what to say, how to support and encourage me to keep going. Dank Uw Tante. I also had great pleasure in keeping my Dutch Oma, back in Cordoba, updated every Sunday with the latest news of my work and her country. Special thanks, to my grandma (Abuela) in Buenos Aires who always encouraged us to study more and always go beyond average.

Luckily, Wageningen brought us many friends that have come and gone, creating the right environment to share the daily discoveries, the joys of success and the frustrations. Just across the street we had our heaven of Argentinean culture in the Seghezzo's place. Mate was always ready to be "cebado" and good talk about anything and everything was always waiting. Lucas, Adriana, Natalia and Mateo, muchisimas gracias por todos esos momentos y por su apoyo. Clarita, Gus, Marzia, Jorge, Lidia, Edinson, Sabina, Ishay, Ben, Bacci, Marga, Felipe we shared the most amazing barbecues, dinners, moments and even vacations you all were very important to this thesis.

Pato, you were here for a long year, it was amazing to have you around and share the "Dutch experience" for a while. Jose Luis Vera, was here at the very beginning, always with a smile and a funny story.

Outside the Netherlands I am very thankful to all my friends back in Cordoba and those scattered around the world for keeping close contact. I had the luck of keeping my best friends nearby, in Europe. Ivan, "brother of life" (and I quote you) in Osnabrueck it was awesome to share and go through the PhD process in parallel, just separated by a phone call or a two hour drive. Diego, another "brother of life" in Madrid and my very good friends Mauri and Leo. I knew I could always count on you people for a visit to Madrid when I needed a brake from my PhD.

LC



SPR

MS

